

Sarah Maguire

**Natural and Anthropogenic Radionuclides
in Organic and Mineral Soils**

Thesis submitted for Ph.D October 1993

Glasgow University

c . Catrin Sarah Maguire 1993

ProQuest Number: 11007862

All rights reserved

INFORMATION TO ALL USERS

The quality of this reproduction is dependent upon the quality of the copy submitted.

In the unlikely event that the author did not send a complete manuscript and there are missing pages, these will be noted. Also, if material had to be removed, a note will indicate the deletion.



ProQuest 11007862

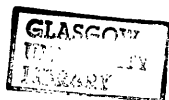
Published by ProQuest LLC (2018). Copyright of the Dissertation is held by the Author.

All rights reserved.

This work is protected against unauthorized copying under Title 17, United States Code
Microform Edition © ProQuest LLC.

ProQuest LLC.
789 East Eisenhower Parkway
P.O. Box 1346
Ann Arbor, MI 48106 – 1346

Thesis
10268
C971



CONTENTS

TABLE OF CONTENTS	pi
ILLUSTRATIONS	pviii
ACKNOWLEDGEMENTS	pxvi
SUMMARY	pxvii

	Page Number
CHAPTER 1 INTRODUCTION	1
1.1 Introduction	1
1.1.1 Radionuclides in the Terrestrial Environment	2
1.1.2 The U.K. Nuclear Industry	4
1.1.3 Radioactive Waste	5
1.1.4 Radiological Implications of Nuclear Waste Generation	7
1.2 Radiocaesium	11
1.2.1 The Chemistry of Caesium	11
1.2.2 The Radiochemistry of Caesium	13
1.2.3 Radiocaesium in the Environment	17
1.3 ^{210}Pb	22
1.3.1 The Chemistry of Lead	22
1.3.2 Lead Isotopes	23
1.3.3 ^{210}Pb Dating	24

1.4	The Interactions of Metal Ions in Soil	30
1.4.1	The Clay Fraction	30
1.4.2	The Oxide Fraction	33
1.4.3	The Organic Fraction	34
1.4.4	Clay-Humic Interactions	37
1.4.5	Metal Retention	39
1.4.6	The Mathematical Interpretation of Metal Retention on Soil Surfaces	41
1.5	Literature Review	47
1.5.1	Laboratory Based Experiments	47
1.5.2	Radiocaesium in the Environment - literature review	54
1.6	Thesis Aims	70
CHAPTER 2 MATERIALS AND METHODS		71
2.1	Samples used in Laboratory Experiments	71
2.1.1	Soils and Peats	71
2.1.2	Reference Clays	73
2.2	Sample Collection and Preperation	74
2.2.1	Bulk Soil Samples	74
2.2.2	Core Collection	75

2.3	Characterisation of Soils	77
2.3.1	Gravimetric Moisture Content	77
2.3.2	Loss on Ignition	77
2.3.3	pH	77
2.3.4	Cation Exchange Capacity	78
2.3.5	Available Potassium	78
2.3.6	Particle Size Distribution	79
2.4	Radionuclide Detection -	
	Gamma Spectroscopy	81
2.4.1	Analysis	81
2.4.2	The Principles of Gamma Detection	82
2.4.3	Experimental Work	86
2.5	Sorption/Desorption Methods	99
2.5.1	Sorption Isotherms	100
2.5.2	Desorption Isotherms	102
2.5.3	Method Modifications	103
2.6	Organic Matter Analysis	109
2.6.1	The Isolation and Characterisation of Humic and Fulvic Acids	109
2.6.2	Infra Red Spectroscopy Analysis of Humic Acid/Metal Interactions	111
2.6.3	Potentiometric Titrations of Humic Acid	113

2.6.4	The Effects of Humic Acid/Clay Interactions upon Caesium Sorption and Desorption	118
CHAPTER 3	SAMPLE CHARACTERISTICS	121
3.1	Soil Core Samples	121
3.2	Characterisation of Soil Samples	129
3.3	Characterisation of Humic and Fulvic Acids	133
CHAPTER 4	RADIONUCLIDE MOBILITY IN PEAT AND SOIL CORES	142
4.1	Introduction	142
4.2	Results of the Gamma Analysis of Sample Set 1	144
4.2.1	^{210}Pb	144
4.2.2	Radiocaesium	145
4.3	Discussion of the Analyses of Sample Set 1	178
4.3.1	^{210}Pb	178
4.3.2	Radiocaesium	181
4.4	Gamma Analysis of Sample Set 2 - Inverness'90 Peat Transect	187
4.4.1	Results	187
4.4.2	Discussion	211

4.5	Radiocaesium Mobility - a proposed model	215
4.6	Summary	225
CHAPTER 5	LABORATORY EXPERIMENTS EXAMINING THE SORPTION OF CAESIUM AND LEAD BY SOILS AND CLAYS	226
5.1	Introduction	226
5.2	Sorption Experiments	228
5.2.1	Caesium Adsorption Isotherms	228
5.2.2	K_d Calculations	238
5.2.3	The Application of the Langmuir Equation	242
5.2.4	Correlation Analysis	245
5.3	Caesium Adsorption/Desorption Isotherms	254
5.4	Long Term Adsorption Experiment	264
5.5	Effect of Background Electrolyte	267
5.6	Adsorption/Desorption Isotherms at Low Solution Concentrations	271
5.6.1	Caesium	271
5.6.2	Lead	278

5.7	The Development of a Method to Measure Desorption of Added Metal From Soil	286
5.8	Summary	302

CHAPTER 6 SOIL ORGANIC MATTER AND ITS INFLUENCE

	ON SOIL-METAL INTERACTIONS	304
6.1	Introduction	304
6.2	Infra Red Analysis of Metal Humate Binding	307
6.3	Potentiometric Titrations of Humic Acid	318
6.3.1	Titration Curves of Humic Acids	318
6.3.2	Potentiometric Titrations in the Presence of Metal Ions	318
6.4	Caesium Sorption/Desorption by Clay/Humic Acid Mixtures	330
6.4.1	Caesium Sorption by Clays	330
6.4.2	Caesium Sorption by Clay/ Humic Acid Mixtures	331
6.4.3	Desorption of Caesium from Clay/ Humic Acid Mixtures	332
6.4.4	Distribution Coefficients (K_d)	333
6.5	Summary	342

CHAPTER 7	CONCLUSIONS	343
7.1	Conclusions	343
7.2	Recommendations for Further Work	345
APPENDIX 1		347
REFERENCES		356

ILLUSTRATIONS

FIGURES

	TITLE	PAGE
1.1	The Natural Decay Series	29
3.1	Infra-red Spectra of Humic Acids	136
3.2	Infra-red Spectra of Fulvic Acids	137
4.1	^{210}Pb Profiles for Sample Set 1	157-158
4.2-	Radiocaesium Profiles for	
4.6	Sample Set 1	169-173
4.7	Inverness'90 Transect Sampling Plan	189
4.8	^{210}Pb Profiles for Inverness'90 Transect Cores	196
4.9-	Radiocaesium Profiles for	
4.13	Inverness'90 Transect Cores	205-209
4.14	Predicted Removal of Radiocaesium from the Mixing Zones of Peat Soils	224

5.1.1-	Caesium Adsorption Isotherms	230-237
5.1.13		
5.2.1-	Langmuir Maxima Correlations	247-248
5.2.6		
5.3-	K_d Correlations	249-251
5.5		
5.6-	Caesium Adsorption/Desorption	
5.9	Isotherms	258-262
5.10	Long Term Caesium Adsorption	266
5.11-	The Effect of Background	
5.12	Electrolyte upon Caesium	
	Adsorption and Desorption	269-270
5.13-	Low Level Caesium Adsorption/	
5.15	Desorption Isotherms	272-275
5.16	The Effect of Increasing the	
	Degree of Dilution upon the	
	Percentage of Caesium held	
	after Desorption	276
5.17-	Low Level Lead Adsorption/	
5.19	Desorption Isotherms	281-284
5.20	The Effect of Increasing the	
	Degree of Dilution upon the	
	Percentage of Lead held after	
	Desorption	285

5.21-	Caesium Desorption Isotherms	292-298
5.26		
5.27-	Lead Desorption Isotherms	299-301
5.29		
6.1.1-	Infra-red Spectra Illustrating	
6.1.7	Humic Acid/Metal Interactions	310-317
6.2	Base Titration Curves for Humic Acid	326
6.3	Consumption of Base by Sequential Additions of M^{n+} to Humic Acid	327-328
6.4	Base Consumption vs Amount of M^{n+} Added to Humic Acid	329
6.5-	Clay/Humic Acid Sorption Isotherms	
6.7		338-340
6.8	Effect of Dilution Factor on the Percentage Caesium Desorbed	341

TABLES

	TITLE	PAGE
1.1	Radii(\AA) of the alkali metal ions	12
1.2	Radionuclides emitted during the Chernobyl accident	20
1.3	Lewis acid/base classification	39
1.4	Migration rates of radiocaesium in a forest soil	61
1.5	Migration rates of radiocaesium in German soils	62
2.1	Background gamma radiation levels recorded for the Ge-detectors used from 12/88-10/90	90
2.2	Detection Efficiencies in Gamma Spectroscopy	91-93
2.3	Descriptions of Counting Geometry Containers	94
2.4	Operating conditions for the Perkin Elmer 1100B Spectrophotometer	100

3.1	Dry density and moisture contents in Sample Set 1	122
3.2	Dry density and moisture contents in the Inverness'90 Transect cores	123
3.3.1-	Chemical and physical analysis of	
3.3.5	Sample Set 1	124-128
3.4	Chemical and physical analysis of soil 'A' horizons	130
3.5	Chemical and physical analysis of soil 'B' horizons	131
3.6	Particle size fractionation of a selected sub-set of soils	132
3.7	Infra-red analysis of Fenwick Moor peat humic and fulvic acid extracts	138-139
3.8	Ultra-violet analysis of humic and fulvic acids	140
3.9	Microanalysis of humic and fulvic acids	141
4.1	^{210}Pb specific activities for Sample Set 1	150-154
4.2	Excess ^{210}Pb Inventories and Fluxes	155

4.3	Sedimentation rates calculated from graphs of $\ln(\text{excess}^{210}\text{Pb})$ vs depth	155
4.4	Sedimentation rates calculated from graphs of $\ln(\text{excess}^{210}\text{Pb})$ vs cumulative weight to mid-section (gcm^{-2})	156
4.5-	Radiocaesium activities for	
4.9	Sample Set 1	159-168
4.10	^{137}Cs Inventories for Sample Set 1	174-175
4.11	Average annual rainfall data for the sample sites	176
4.12	Correlation coefficients for linear regression of total inventories with average rainfall for Sample Set 1	177
4.13	^{210}Pb specific activities in the Inverness'90 transect	190-193
4.14.1	^{210}Pb inventories and flux values for Inverness'90 transect	194
4.14.2	Sedimentation rates calculated from ^{210}Pb data for the Inverness'90 transect	195

4.15-	Radiocaesium activities in the	
4.18	Inverness'90 transect	197-204
4.19	Radiocaesium total inventories	
	for the Inverness'90 transect	210
4.20	Coefficients characterising	
	the downward movement of	
	radiocaesium	217
4.21.1	Mixing zone constants	222
4.21.2	Projected times in years for	
	mixing zone concentrations of	
	^{137}Cs to be reduced	223
5.1	K_d values for caesium sorption	241
5.2	Langmuir maxima for caesium	
	sorption	244
5.3-	Correlation data between Langmuir	
5.4	Maxima, K_d values and the pH, CEC	
	and the organic matter content of	
	the soils	252-253
5.5	Langmuir maxima for caesium	
	adsorption/desorption isotherms	263

6.1	Lead stability constants	
	-literature review	323
6.2	Conditional stability constants	
	of Fenwick Moor Peat humic acid	324
6.3	Percentage caesium sorbed at pH 5	
	in clay/humic acid mixtures	335
6.4	K_d values at pH 7 for caesium	
	adsorption and desorption at	
	given solution concentrations of	
	Cs at equilibrium, with and without	
	humic acid addition	336

ACKNOWLEDGEMENTS

The research for this thesis was made possible through a studentship awarded by the Natural Environment Research Council (Ref:GT4/88/AAPS/20).

I wish to acknowledge the help of all those who have in any way contributed to my research work. Particular thanks to the technical staff of the Scottish Research and Reactor Centre, Glasgow University Chemistry Department, and especially to Michael Beglan of the Agricultural, Food and Environmental Chemistry Department for his patience and support.

I am grateful for the support and advice provided by the staff and students of both the AFE chemistry department and SURRC. Above all, I wish to acknowledge the guidance and motivation given by my supervisors; Dr Ian Pulford, Dr Gordon Cook and Dr Gus MacKenzie.

Finally, I wish to thank Tom, for his patient support, and our children Anna and Sam whose timely arrivals were the best reasons for the late submission of this thesis.

SUMMARY

In 1986 anthropogenic radionuclides were released into the atmosphere as a direct result of the nuclear reactor accident at Chernobyl. Radiocaesium deposited on the U.K has undergone a considerable amount of recycling with areas of high plant concentrations being found above soils of high organic matter content. This was contrary to the expected behaviour of radiocaesium as it was expected to fix rapidly to mineral soils and to leach rapidly from organic soils and thus be unavailable to plants and animals.

This thesis examines the mobility of radiocaesium in organic rich and mineral soils from selected sites in Scotland using gamma spectroscopy and ^{210}Pb dating in an attempt to correlate the observed behaviour with the soils properties and local topography.

Laboratory methods such as adsorption/desorption isotherms are used to examine the sorption of caesium and lead in a selected range of fully characterised soils and clays in order to understand further the environmental behaviour of the radionuclides.

As the behaviour of radiocaesium and other radionuclides is of interest this thesis takes both a

qualitative and quantitative view of the binding of a range of metal ions to soil humic acid using techniques such as infra-red spectroscopy and potentiometric titrations. In addition, the influence of clay/humic acid interactions upon caesium sorption are examined.

The main findings of this thesis support the observed long term availability of radiocaesium in soils of high organic matter content. Radiocaesium appears to undergo lateral movement in peatlands resulting in the enrichment of layers fed by surface water run-off. Little evidence was found to support the downwards diffusion of radiocaesium in peats. The presence of humic acid in clay/humic acid systems depressed the sorption of caesium and enhanced the desorption of caesium from bentonite and kaolinite. For both sorption and desorption, the presence of humic acid resulted in lower K_d values thus causing caesium to be more mobile.

CHAPTER 1 - INTRODUCTION

1.1 Introduction

As a direct consequence of the nuclear reactor accident at Chernobyl in 1986 anthropogenic radionuclides, including radiocaesium, were released into the atmosphere. This led ultimately to their precipitation in rainfall onto the earth's surface. The deposition of radiocaesium in the United Kingdom correlated closely with rainfall, with the highest areas of deposition being north Wales, Cumbria and the west of Scotland (Horrill et al, 1990). These regions contain areas of vegetation overlying soils of low pH and high organic matter content which are subject to seasonal or permanent waterlogging (Beresford et al, 1987; Livens and Loveland, 1988; Horrill et al, 1990). Since the accident at Chernobyl, a considerable amount of radiocaesium recycling has been found with high plant concentrations being found, on damp peats, bogs and peaty grasslands, especially in radioactive 'hot-spots' where deposition was particularly high (Frissel et al, 1987, 1990; Livens and Loveland, 1988). It was apparent that models designed to predict the mobility and fate of radiocaesium in mineral soils, based on the premise that the uptake of caesium occurs rapidly due to ion exchange reactions onto clay surfaces,

with some sorption being irreversible, were inappropriate for this situation (McKinley and Haddermann, 1984; Cremers et al, 1988). Radiocaesium deposited on soil was expected to fix rapidly to mineral soils and to leach rapidly from organic soils and thus be unavailable to plants and animals (Coughtry and Thorne, 1983).

It therefore became necessary to develop a greater understanding of the interaction of radiocaesium and other radionuclides in order to predict their mobility and fate following a pollution incident of this kind. This thesis aims to contribute to this undertaking; to examine the mobilization and binding of radiocaesium within organic soils in the environment, utilizing ^{210}Pb chronometry and laboratory experiments with the stable isotope of caesium.

1.1.1 Radionuclides in the Terrestrial Environment

Radionuclides have been present since the Earth's formation some four and a half billion years ago. Some of these can be used for dating purposes and measuring the rates of environmental processes: for example investigation of the abundances of the decay products of ^{235}U , ^{238}U and ^{232}Th can be used to date rocks many millions of years old, while at the other extreme of the time scale ^{210}Pb can be used to

establish chronologies for sediments and soils of ages up to about 150 years, (Swan et al, 1982).

Since the first discoveries about radioactivity made by Becquerel in 1896, man has learnt to manipulate radionuclides and to induce nuclear fission for the benefit or the detriment of mankind. Natural and anthropogenic (man-made) radionuclides have been used successfully in medicine for the treatment of cancers (^{60}Co , ^{57}Ge), to produce electricity (^{235}U , ^{239}Pu) and to produce the nuclear weaponry of the twentieth century (Santschi and Honeyman, 1989). Due to the persistence of long half life radionuclides the uses of radiation have provided us with an environmental legacy for thousands of years to come.

In order to examine the distribution of radionuclides within the terrestrial environment it is necessary to have a degree of understanding of both their natural and anthropogenic sources, such as the production of waste from the nuclear industry and as a result of global fallout from weapons testing and nuclear accidents. Sections 1.1.2-1.1.4 give an outline of the historical development of the British nuclear industry, the generation of radioactive wastes and the radiological implications caused by the release of waste to the environment. The specific case of radiocaesium will be discussed in greater

depth in Section 1.2, which examines the chemistry of caesium and its presence within the terrestrial environment.

1.1.2 The UK Nuclear Industry

Research and development in the nuclear industry has flourished in the post-war era, leading to the rapid development of nuclear power generating stations. At present, 19.3% of total UK electricity output is generated by nuclear power; in Scotland this rises to 50%. Worldwide a total of 16% of annual electricity output is generated by nuclear reactors, (U.K Parliament, 1990). UK nuclear reactors are mainly gas-cooled and at present nine are of the older Magnox type which are due for decommissioning and seven are the more modern advanced gas-cooled reactors. One pressurised water reactor at Sizewell B is due to be commissioned in 1994/5 to replace the Magnox reactors at that site.

The policy of the present UK government is to support the development of nuclear power if its production can become more economic and if high safety and environmental protection standards can be achieved. The advantages of nuclear power lie in the lack of gaseous emissions such as NO_x and SO_2 (acid rain forming) and CO_2 (a greenhouse gas) and the protection of non-renewable energy resources. The

disadvantages of nuclear power include the production of low level waste pollution and the problems involved in high and intermediate level waste storage and disposal.

Due to the possible consequences of nuclear accidents, rigorous licensing procedures have been established by the Health and Safety Executive's Nuclear Installations Inspectorate of all plant construction, commissioning, operation and decommissioning.

The inevitable consequence of the operation of nuclear power stations and the use of radionuclides in research, medicine and defence is the generation of radioactive waste. If Britain is to follow EC Directive 85/337/EEC which obliges member states to add to, or modify, national legislation regarding environmental impact assessment, reports which analyse the environmental impact of radioactive waste disposal must be prepared. The following elements of the environment which must be considered when preparing these reports were specified in the directive: human beings, flora and fauna, soil, water, air and climate, landscape, any interactions between the previous categories, material assets and the cultural heritage, (Stone and Walker, 1992).

1.1.3 Radioactive Waste

Radioactive waste can be categorized as low,

intermediate and high level. The Sellafield (formerly Windscale) nuclear fuel reprocessing plant on the Cumbrian coast is one of three major sources of nuclear waste in a global context, the others being at Trombay, India and Cap de la Hague, France (MacKenzie and Scott, 1984). Sellafield discharges more low level liquid radioactive waste than all other UK sources combined. Discharges from Sellafield started in 1952, peaked in the mid 1970's and declined more recently due the introduction of technological improvements, for example the use of ion-exchange resins to remove radionuclides from waste liquids (BNFL, 1981). The liquid effluent contains radionuclides from two sources; the storage ponds where spent Magnox fuel elements are flushed with water prior to reprocessing, and the sea tanks where reprocessing wastes are held. After storage the effluents are monitored, neutralised with alkali and discharged to sea at high tide via a pipeline (BNFL; 1982,1984; Pentreath et al, 1985). Nuclear fuel reprocessing allows the recovery of uranium and plutonium isotopes including ^{239}Pu (BNFL, 1982). The bulk of the fission products are stored (in an aqueous form) as high level waste. ^{137}Cs and ^{90}Sr are major constituents of the beta/gamma fraction of the waste. Plutonium isotopes and ^{241}Am produce the main alpha activity. The quantities of ^{137}Cs released to the environment peaked at 5236 TBq in 1975, dropping

to a level of 12 TBq in 1987 (1 Bq = 1 disintegration per second, 1TBq = 10^{12} Bq). The total activity of ^{137}Cs released by 1987 was 40505 TBq (BNFL, 1981-1988; Cambray, 1982). Plans are underway to establish a plant at Sellafield which will deal with high level waste by vitrification to reduce the total volume of waste after a greater than 50 year cooling time to reduce the total activity. There is a need to provide methods of permanent disposal for intermediate and high level waste. NIREX UK is currently contracted to develop a deep underground repository for intermediate level waste. Only after suitable and safe methods of disposal have been established for nuclear waste will the 'cradle to grave' requirement of an environmental impact assessment have been accomplished. This, in hindsight, should have been carried out prior to the development of our first nuclear power station at Calder Hall in 1956.

1.1.4 Radiological Implications of Nuclear Waste Generation

Guidelines have been established by the International Commission on Radiological Protection (ICRP) to regulate and minimise the harm caused by the production and use of radioactive substances. Advice on issues of radiological protection is given to the U.K Government by the National Radiological

Protection Board (the official Government body responsible for radiological protection) and the Medical Research Council. This enables the Government to introduce legislation to empower the appropriate bodies to act upon them e.g Her Majesties Inspectorate of Pollution. The recommendations of the International Commission on Radiological Protection in the ICRP Publication 26 are that:

- no practice shall be adopted unless its introduction produces a net positive benefit.
- all exposures shall be kept as low as reasonably achievable, economic and social factors being taken into account.
- the dose equivalent to individuals shall not exceed the limits recommended for the appropriate circumstances by the Commission.

(Vennart, 1983)

Despite these regulations there have been numerous incidents which have resulted in the exposure of the Earth's population to enhanced levels of radiation during the past half century.

It is essential to assess the radiation detriment of routine activities and abnormal events (e.g accidents) which result in the release of radioactive materials to the

environment, to assist those who are responsible for authorizing the discharge of radioactive materials and setting limits for such discharge, and to improve the scientific basis of environmental monitoring programs.

(Myttenaere, 1983)

In order to do this it is first necessary to accumulate data which allow us to predict the behaviour of the radionuclides in the environment. To evaluate radiological impact requires the development of dynamic models where the thermodynamics and kinetics of transfer processes are known. An important aspect in this context is that many models used in environmental modelling are based upon thermodynamics and assume steady state equilibrium, but by their very nature accidents do not give rise to such conditions.

Within the terrestrial environment it is of fundamental importance to understand the behaviour of radionuclides in soil systems. Soil provides the medium for plant growth, and radionuclides contained within the soil have the potential to undergo transfer via plant uptake through the food chain and ultimately to humans. The distribution and retention of radionuclides within the terrestrial environment varies greatly due to its diversity and the geochemical behaviour of the radionuclides. The

soil's physico-chemical characteristics influence element retention and mobility, in conjunction with the biological processes which control the dynamics of the labile fraction of most elements (Heal and Horrill, 1983). It is possible to combine the major physico-chemical properties of environmental systems with chemical information to predict element speciation. Modelling programs have been developed, for example GEOCHEM which contains data on more than 2000 aqueous species, many containing organic ligands (Sposito and Mattigod, 1979). However, complex organic ligands are usually treated as mixtures of simple organic acids with functional groups, whose formation constants for interaction with metals are known e.g salicylic acid, acetic acid (Wild, 1988). This approach, due to the lack of available thermodynamic data and the absence of data for most organic ligands, is therefore of limited value (Livens and Rimmer, 1988).

1.2 Radiocaesium

The main body of this thesis is concerned with the fate of radiocaesium within the terrestrial environment as a consequence of the nuclear accident at Chernobyl (Section 1.2.3). It has therefore been necessary to gain an understanding of the chemical behaviour of caesium, the generation of its radioisotopes and their radiochemistry and the sources of radiocaesium input to the terrestrial environment. These are covered in the following sections.

1.2.1 The Chemistry of Caesium

The following summary of the chemical behaviour of caesium is derived mainly from Cotton and Wilkinson (1972).

Caesium is a member of the alkali metal group of the periodic table with an electronic configuration;



Its properties are similar to those of sodium and potassium. The alkali metals readily lose the single electron in their outermost shell to adopt the stable configuration of an inert gas, therefore their chemistry is that of the 1+ ions. The M^+ ions are

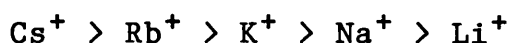
spherical and of low polarizability, no other oxidation state is known or expected due to the very high second ionization potentials of the alkali metals. Although caesium is predominantly ionic, Cs_2 gas is a diatomic covalent molecule. The structures and stabilities of caesium salts are determined by lattice energies and by radius ratio effects. Cs^+ is large enough to accommodate eight near neighbour Cl^- ions differentiating its structure from Na^+ which can accommodate only six near neighbours. Caesium salts have high melting points and are highly soluble in water, hence the behaviour of Cs^+ in the terrestrial environment is usually that of a hydrated ion.

Table 1.1 Radii (nm) of the alkali metal ions

	Cs^+	Na^+	K^+
Metal Radius	0.265	0.186	0.227
Ionic Radius	0.184	0.112	0.144
Hydrated Radius	0.228	0.276	0.232

(after Cotton and Wilkinson, 1972)

Measurements of cation exchange preference of resins for alkali cations usually follow the order;



because of the electrostatic nature of the binding force and because the ion with the smallest hydrated radius will be able to approach more closely and form stronger coulombic attractions.

It is known that Na^+ and K^+ form essentially ionic organometallic compounds and it is reasonable to assume that Cs^+ would behave similarly when in contact with soil organic matter, forming simple organic salts.

Caesium's metabolism in humans resembles that of potassium. Compounds are rapidly absorbed from the gastro-intestinal tract and transported throughout the body in a uniform manner. The biological half-time of caesium is approximately 30 days (time for 50% of ingested compound to be excreted) which corresponds to 2 days for removal of 10% of any given intake and 110 days for removal of 90% of an intake, (Fry and Summerling, 1984).

1.2.2 The Radiochemistry of Caesium

Caesium, atomic number 55, has fourteen isotopes with atomic weights ranging from 116 - 146; ^{133}Cs (100% natural abundance) being stable, while the remainder are radioactive. The majority of these isotopes are not of importance due to their half-lives ($t_{1/2}$ - the time required for an initial number of atoms to be reduced on the average to half that number by

transformations) ranging from seconds to days, (Friedlander et al, 1981). The two radioisotopes of interest in this study are ^{137}Cs and ^{134}Cs , which have half-lives of 30.17 years and 2.062 years respectively (Friedlander et al, 1981).

1.2.2.1 ^{137}Cs

This isotope of caesium is a fission product resulting from the fission of ^{235}U or ^{239}Pu in a nuclear reactor or in a nuclear weapon. ^{137}Cs has too many neutrons for stability and decays by beta minus particle emission.

Beta minus decay: when the ratio of neutrons to protons in a nucleus is too high, a neutron (n) is converted into a proton (p^+) and an electron (e^-) which is emitted at high speed. The emission of the electron, or beta particle, is accompanied by the emission of another particle, the neutrino, which has no charge and almost no mass. This results in a daughter element with an atomic number one higher than that of the parent but which has the same atomic mass number as the parent, (Friedlander et al, 1981).

As a result of the sub-atomic disturbance undergone to emit a beta particle, the excited product nuclei undergo spontaneous rearrangements and the excess energy is emitted as electromagnetic radiation of short wavelength known as gamma rays. The gamma rays emitted are characteristic of the

nuclei of origin. The gamma rays emitted by ^{137}Cs have an energy of 661.6 keV.

Gamma rays interact with matter in three ways;

a) The Photoelectric Effect - this occurs when a high energy gamma photon transfers all of its energy to one of the inner bound orbital electrons of an atom of the absorber. Absorption of the gamma photon energy (E_γ) causes ejection of the electron as a photoelectron with energy (E_e). The effect decreases in probability with photon energy but increases with the atomic number (z) of the absorber approximately in proportion to z^5 . Energy is conserved during the interaction according to the equation:

$$E_\gamma = E_e + E_b$$

where E_γ = gamma photon energy

E_e = photoelectron energy

E_b = the binding energy of the electron

b) Compton Effect - this occurs with the partial transfer of photon energy to either a bound or free electron leaving a scattered gamma photon of reduced energy.

$$E_\gamma = E_i + E_e + E_b$$

where E_γ = gamma photon energy

E_e = photoelectron energy

E_b = the binding energy of the electron

E_i = energy of the scattered gamma photon

c) Pair Production - photons of energy greater than 1.02 MeV, can disappear in the process of creating a positron-electron pair of energy equivalent to the residual photon energy. The recombination of these particles results in the emission of two gamma photons of energy 0.511 MeV.

(Friedlander et al, 1981)

1.2.2.2 ^{134}Cs

This isotope of caesium is an activation product resulting from the bombardment of neutrons on stable ^{133}Cs , which is both naturally occurring and is a fission product. The direct production of ^{133}Cs is small, the concentration building up as a consequence of a succession of beta decays in the mass 133 chain. ^{134}Cs is therefore not produced in weapons testing since irradiation is over too short a time period. Also, the ^{134}Cs fission chain ends at ^{134}Xe (i.e. ^{134}Cs is a 'shielded' nuclide). It is present in waste from spent fuels in amounts dependent upon irradiation and cooling times (MacKenzie and Scott, 1984). This isotope decays primarily by beta emission with associated gamma rays of characteristic

energies: 569.3 keV, (14.4%); 604.7 keV, (97.6%); 795.8 keV, (85.4%) and to a lesser degree by electron capture.

1.2.3 Radiocaesium in the Environment

The presence of radiocaesium in the environment can be attributed to three major sources;

- a) fallout from nuclear weapons testing
- b) routine emissions from nuclear installations
- c) accidental emissions from nuclear installations.

Major inputs of radionuclides due to atmospheric explosions of nuclear bombs occurred in the late 1950s and early 1960s. Following the Atmospheric Test Ban Treaty of 1963, inputs from this source have been reduced significantly. However, some countries are continuing these activities as they develop their own nuclear capabilities, (Bertell, 1985). Due to weapons testing, low-level contamination of the environment on a global scale was produced. It has been estimated that 1.26×10^6 TBq of ^{137}Cs had been introduced to the environment prior to 1970 by weapons testing, (Joseph et al, 1971; Santschi and Honeyman, 1989), as a result of a total of 200 megatons of atomic and H-bomb tests. In addition, 10^8 MBq of ^{131}I , 10^8 MBq of

^3H , 10^6 MBq of $^{89,90}\text{Sr}$ and 10^5 MBq of $^{239,240}\text{Pu}$ were released, (Santschi and Honeyman, 1989). The activation product ^{134}Cs was not released in significant amounts during this time due to the reasons outlined above.

Radionuclides released to the stratosphere during weapons testing underwent mixing and transport to the lower atmosphere prior to deposition. Deposition on the terrestrial environment is due mainly to the scavenging of radionuclides by rainwater. The average depositions of weapons testing fallout ^{137}Cs in relation to rainfall was found to be $2.75 \text{ Bq m}^{-2}\text{mm}^{-1}$, (Cawse, 1983). Details of the interactions of radiocaesium within the terrestrial environment are given in section 1.5.2.

The second major source of radiocaesium to the UK environment is from routine discharges from Sellafield in Cumbria where aqueous low level waste is discharged into the Irish Sea (see section 1.1.3). Due to the transport of radioactive material from sea to land in marine spray or resuspended marine sediment, enhanced levels of radiocaesium are found in Cumbrian soils (Cawse, 1980). Studies which examined the radionuclide distribution in the northern Solway coastal zone of south-west Scotland indicate evidence of on-land transfer of Sellafield waste radionuclides through tidal inundation in

riverine systems. The airborne transfer of material was found to be of negligible significance at this location (McDonald et al, 1992a). In addition, an accidental release of fission products to the atmosphere occurred at Sellafield in 1957 including 46 TBq of ^{137}Cs (Cawse, 1983; Sumner, 1987).

The third source of radiocaesium in the environment was from the nuclear accident which took place on April 26th 1986 when the No. 4 reactor at the Chernobyl plant in the Ukraine exploded and a plume of radioactive gases and fragments of hot reactor fuel were emitted. This emission continued for ten days as a series of fires burned. The fires were finally extinguished by dropping sand, clay and dolomite onto them from helicopters. It is estimated that 3.5% of the reactor's total radionuclide content was released (2×10^6 TBq) of which radiocaesium in the form of ^{134}Cs , ^{137}Cs made up more than one third. The levels of individual radionuclides emitted at one and ten days after the explosion are shown in Table 1.2.

Contaminated air travelled over the south of England on the morning of Friday May 2nd, moving over the north of the UK in the ensuing days. Due to the heavy rainfall experienced in Cumbria and South West Scotland, high fallout activities were recorded in these areas. Levels of ^{137}Cs in Cumbria increased

from approximately 100 Bq m⁻² before this incident to approximately 7000 Bq m⁻² afterwards. Levels of up to 38000 Bq m⁻² have been recorded in south west Scotland which can be compared with Sellafield inputs of up to 40000 Bq m⁻² (McDonald et al., 1992b).

Table 1.2 - Radionuclides emitted during the Chernobyl accident

Radionuclide	Activity after	Activity after
	1 day	10 days
	PBq	PBq
¹³¹ I	170	440
¹³⁷ Cs	10	50
¹³⁴ Cs	5	25
⁹⁰ Sr	0.5	9
^{239,240} Pu	0.01	0.07

N.B 1 PBq = 10¹⁵Bq

(Smith and Clark, 1986; Sumner, 1987).

In the days after Chernobyl, the NRPB issued guidelines establishing the maximum permissible level of radiocaesium in meat to be 1000 Bq kg⁻¹. This superceded their previous generalised derived limit of 10000 Bq kg⁻¹, set in March 1986, in order to take into account the elevated levels of radioactivity

(Linsley et al, 1986). The lower level of 1000 Bq kg^{-1} was selected to ensure an annual dose of less than 1 mSv to an average adult of the UK population, assuming no reduction in the consumption of meat and increased radiation levels in other food types. A government ban on sheep movement was set, based on this limit, in the expectation that it would last for a short period of time only. However, it has remained in force for longer than expected due to high levels of contamination remaining in upland sites. In August of 1987, 500000 sheep and lambs were still under restrictions on upland pastures (Sumner, 1987).

Now, in the early 1990's, some sheep are still under restriction, emphasising the need for research into the mobility of radiocaesium in upland soils. These soils are dominantly highly organic and acidic. The chemistry of such soils is discussed in detail in section 1.4 together with their ability to interact with metal ions.

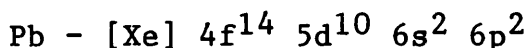
1.3 ^{210}Pb

The behaviour of ^{210}Pb within the terrestrial environment has been used within this study to allow a chronology to be applied, where suitable, to soil cores. The following sections give an outline of the chemistry of lead, its radioisotopes and an explanation of ^{210}Pb dating.

1.3.1 The Chemistry of Lead

The following summary of the chemistry of lead is derived mainly from Cotton and Wilkinson (1972).

Lead has an electronic configuration;



The divalent state dominates the chemistry of lead which has a well defined cationic chemistry. Most lead salts, with the exception of lead nitrate and lead acetate, are sparingly soluble or insoluble in water. Lead has an extensive organometallic chemistry and is present in the environment as $(\text{CH}_3)_4\text{Pb}$ and $(\text{C}_2\text{H}_5)_4\text{Pb}$, the covalent antiknocking additives to petrol and their combustion product PbBrCl which undergoes conversion to PbSO_4 , PbO and PbS in the environment. Lead is retained in soils by adsorption on hydrous oxides, notably ferric hydroxide. Lead can

also be retained by binding to soil organic matter (Evans, 1989). The principles governing this are discussed in section 1.4.

The principal chemical species of lead in acid and alkaline soil solutions are:

Acid - Pb^{2+} , Pb organic complexes, PbSO_4 , PbHCO_3^+
Alkali - PbCO_3^0 , PbHCO_3^+ (Pb^{2+} species)
 $\text{Pb}(\text{CO}_3)^{2-}$ (Pb^{4+} species)
(Wild, 1988)

1.3.2 Lead Isotopes

Lead has an atomic number of 82 and has isotopes with atomic weights ranging from 185 to 214. The stable isotopes of lead are given below together with their average abundances for the earth in percentages of atoms;

^{204}Pb	- natural abundance 1.42%
^{206}Pb	- natural abundance 24.1%
^{207}Pb	- natural abundance 22.1%
^{208}Pb	- natural abundance 52.3%

(Friedlander et al., 1981)

The stable isotopes ^{206}Pb and ^{207}Pb are the end products of the ^{238}U and ^{235}U natural decay series, ^{208}Pb is the end product of the third natural decay series which has ^{232}Th as its initial nuclide. The

current concentrations of parent radionuclides and lead daughter isotopes can be used for dating purposes when applied to closed systems, for example certain minerals, (Geyh and Schleicher, 1990).

The lead isotope of significance in this study is ^{210}Pb , a member of the ^{238}U natural decay series (Fig. 1.1). ^{226}Ra a descendant radionuclide of ^{238}U decays to the gas ^{222}Rn which diffuses continually from soil into the atmosphere. ^{222}Rn decays via several short lived daughter products to ^{210}Pb which settles out in less than 30 days onto soil surfaces. The ^{210}Pb is incorporated into the soil as 'unsupported' or 'excess' ^{210}Pb . This phenomenon can be utilised to determine chronologies for young sediments and rapidly accumulating peats, (Robbins and Edgington. 1975; Geyh and Schleicher, 1990).

1.3.3 ^{210}Pb Dating

Goldberg and Koide (1963) used ^{210}Pb of atmospheric origin to establish a chronology for snow fields in Greenland. It was found that the flux of excess ^{210}Pb and the rate of accumulation of the ice had been fairly constant over the time interval studied. Robbins and Edgington (1975) developed a mathematical model to calculate sedimentation rates from excess ^{210}Pb profiles in sediments from Lake Michigan. The model involves four assumptions:

- a) that there has been a constant flux of excess ^{210}Pb to the sediment,
- b) that there has been a constant rate of sediment accumulation,
- c) that there has been no post-depositional migration of ^{210}Pb within the sediment,
- d) that supported ^{210}Pb activity is constant with depth.

Under these conditions for an ideal sediment the ^{210}Pb concentration decreases exponentially with depth. This can be described by the equations:

$$A_t = A_0 \cdot e^{-\lambda t}$$

where,

A_0 = excess ^{210}Pb activity at time = 0 (at the surface)

A_t = the activity of excess ^{210}Pb at time t , corresponding to an accumulation depth D of sediment.

λ = the characteristic decay constant for the radionuclide.

As, $t = D/s$

where,

D = the depth (cm)

s = the sedimentation rate in cm yr^{-1}

A plot of $\ln A$ against depth should give a linear

graph with gradient equal to $-\lambda/s$. Thus a value for the sedimentation rate can be calculated.

Problems occur with this model if a constant activity of ^{210}Pb with depth is found over the upper portion of the profile. This phenomenon is attributed to the surface layers being homogeneous due to physical or biological mixing, (MacKenzie and Scott, 1979; Robbins and Edgington, 1975; Swan et al, 1982). However, it is possible to apply the mathematical model to the lower section of the profile in order to calculate sedimentation rates.

The majority of ^{210}Pb dating has been carried out on sediments but it can be applied to certain soils. Profiles of peatland soils are thought to preserve a historical record of atmospheric deposition, and ^{210}Pb dating has been used with some success for peats (Appleby et al, 1988; Oldfield et al, 1978; 1979; Schell et al, 1989). However, it is now recognised that profiles of concentration with depth are usually distorted by compaction and decomposition (Urban et al, 1990). Urban et al (1990) questions the validity of the assumption which is a basis for the continuous rate of supply model most commonly used for dating recently deposited sediments. The model assumes that ^{210}Pb , once deposited, is immobile in peat and is not subject to post-depositional diagenesis.

Research workers have made three observations which question this assumption:

1. Profiles of ^{210}Pb concentration with depth in peat often appear anomalous, with sub-surface maxima in the zone of water table fluctuations, indicating the physical transport of lead or redox transformations (Pakarinen and Tolonen, 1977). However, the concentration profile can also be affected by processes unrelated to lead mobility such as rates of primary production, decomposition and vegetation change.

2. The inventories of ^{210}Pb have been observed to differ significantly between adjacent hummocks and hollows. Aaby and Jacobsen (1979) measured 50% more lead in peat above a common depth horizon in a hummock than in an adjacent hollow in a Danish bog. However, both El-Daoushy (1988) and Oldfield et al. (1979) recorded larger inventories in hollows compared to hummocks. These local differences may be due to differential deposition or post-depositional mobility.

3. Dates derived from ^{210}Pb chronology do not agree in all cases with dates based on other methods such as radiocarbon dating, moss increment dates and pollen horizons. Oldfield et al (1979) found that the ^{210}Pb profile from a hummock and pool environment at Bolton Fell Moss, Cumbria underestimated the profile's age compared to pollen horizon dates, and

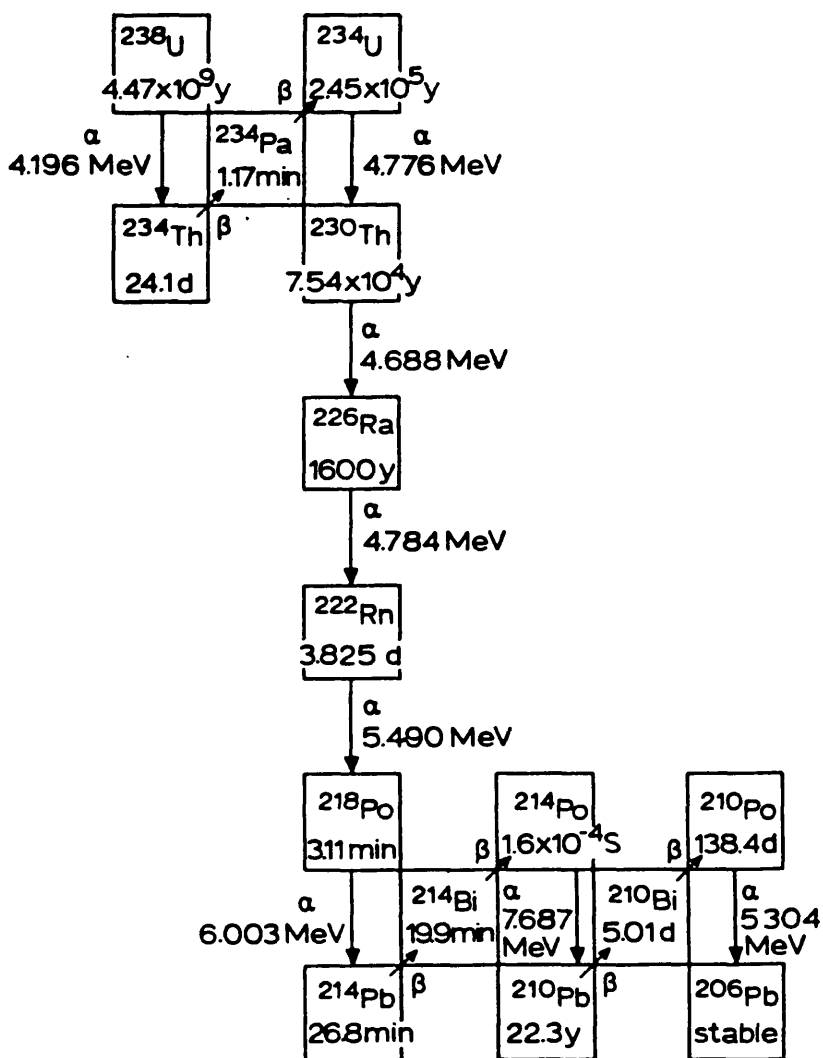
that this was possibly due to the diffusion of unsupported ^{210}Pb within the profile.

By comparing ^{210}Pb dates with dates obtained by alternative methods for several peat cores, Urban et al (1990) concluded that there is clear evidence for ^{210}Pb mobility in peatlands and that lead can be transported out of peatlands in the lateral flow of water. The retention of ^{210}Pb is governed by two factors. Firstly, the hydrology of the area is of importance and it has been suggested that where the water table is high a greater loss of lead will occur. Secondly, the amount of dissolved organic matter present in the soil water has a major chemical control on lead mobility due to the complexation of lead by organic matter (Heinrichs and Mayer, 1977; Tyler, 1981).

From these findings Urban et al (1990) recommended that dates based on ^{210}Pb profiles should be verified by independent techniques especially if ^{210}Pb inventories appear to be lower than expected.

Fig. 1.1 The Natural Decay Series

- The Uranium Series



1.4 The Interaction of Metal Ions with Soil

The interaction of metal ions in solution with the three major components of the soil matrix: clays, oxides and organic matter, has been described using mathematical models (Wild, 1988). However, it is necessary to understand the composition and nature of each fraction in order to predict the principal binding mechanisms controlling the interactions of metal ions with the surface sites of these soil components.

1.4.1 The Clay Fraction

The clay fraction is composed predominantly of minerals formed as a result of weathering of the soil's parent rock material. Clay minerals consist of silica tetrahedra (SiO_4^{4-}) and aluminium hydroxide octahedra ($\text{Al}(\text{OH})_6^{3-}$). The tetrahedral layer is formed when the three basal oxygens of the silicon tetrahedra are shared with adjacent tetrahedra. This forms a sheet structure with hexagonal holes. The octahedral layer is composed of two layers of hydroxyl ions with the octahedral holes being filled with cations such as aluminium or magnesium. The tetrahedral and octahedral layers combine together to form the aluminosilicate unit lattice layer of the clay mineral.

The linking of these units in various formations

leads to the development of:

a) 1:1 clay minerals e.g kaolinite - $\text{Si}_2\text{Al}_2\text{O}_5(\text{OH})_4$

These clays exhibit a low level of isomorphous substitution of Al for Si in the tetrahedral layer, resulting in the clay mineral having an overall negative electric charge which is balanced by exchangeable cations attracted electrostatically from the soil solution. The lattice layers are strongly bound together by hydrogen bonding between oxygen atoms on the tetrahedral surface and hydroxyl groups from the octahedral layer.

b) 2:1 non-expanding clay minerals e.g illite - $(\text{Al}_{1.3}\text{Si}_{6.7})\text{Al}_4\text{O}_{20}(\text{OH})_4$

Isomorphous substitution of mainly Al for Si occurs in the tetrahedral layer. The negative charge created is almost satisfied by the presence of interlamellar K^+ ions which, due to their size, fit into the hexagonal holes formed by the tetrahedral arrangement. This enables the lattice layers to come close together forming a strongly bonded crystal.

c) 2:1 expanding clay minerals e.g bentonite $(\text{K},\text{Na},\text{Ca})^{0.7+}[\text{Si}_8(\text{Mg}_{0.7}\text{Al}_{3.3})\text{O}_{20}(\text{OH})_4]^{0.7-}$

A low degree of isomorphous substitution of divalent cations for Al in the octahedral layer occurs. The cation bonding between lattice layers is weak, enabling the lattice to expand and the free exchange of cations to occur.

In addition to isomorphous substitution within

the clay lattice providing a permanent charge to the clay, the electric charge on clays can also vary with pH. This is due to the loss of hydrogen ions from frayed clay edges at pH values above the clay's point of zero charge (pzc) which alters the clay's total cation exchange capacity (CEC). This charge is of primary importance for clays such as kaolinite where the lattice layers are bound together forming a crystal with a low surface area. Due to this, the charges at the edge sites become significant.

The manner in which cations interact with clay surfaces is determined by the physical properties of the cation. For example when a sodium ion approaches a clay surface it retains its hydration shell due to its high charge density, thus forming an outer sphere cation complex. However, caesium ions lose their weakly-held water molecules to form inner sphere complexes, permitting the caesium ions to be more closely held to the clay surface (Wild, 1988). The retention of metals by clays is further discussed in 1.4.5.

1.4.2 The Oxide Fraction

The oxides of primary significance in soils are the hydrated oxides of iron, aluminium and manganese. These compounds have electrical properties influenced by pH, with a net positive charge at pH values below the point of zero charge (pzc) and a net negative charge above the pzc. The pzc for oxides is dependent upon the affinity for electrons of the metal ions present in the oxide. The pzc for Al_2O_3 occurs at $\text{pH} = 7.5 - 9.5$, whereas for SiO_2 the pzc occurs at $\text{pH} = 2$.

Chemisorption occurs when an ion forms a covalent bond with the surface of the oxide. This process is of primary importance with respect to oxide surfaces, as their pzc can be affected by the chemisorption of species such as phosphates or silicates. This is in contrast to the ion exchange processes which dominate the reactions of metals with clays. The pH of the system in which the oxide is present can affect chemisorption reactions taking place, firstly the pH dependent charge on the oxide surface will determine the ease or difficulty in approach of ions; secondly the affinity of an oxide will be affected by the species of the metal ion present at that pH.

In addition, the substitution of metal ions within the oxide will move the pzc towards the pzc of

the oxide of the impurity hence affecting the pH dependent charge.

1.4.3 The Organic Fraction

Organic matter in soils consists of a series of products formed from the decay of plant and animal material, ranging from fresh material through partially decomposed matter to humic material. The decomposed brown/black material that forms is named 'humus' and is composed of carbon, hydrogen, oxygen, nitrogen, sulphur and phosphorus. The extraction of fractions of 'humus' can be carried out using alkalis resulting in the operationally defined fractions of :

'humic' - the insoluble residue

'humic acid' - extracted by alkali and acid precipitated.

'fulvic acid' - extracted by alkali and acid soluble

Soils can also contain traces of sugars, amino acids, organic acids and lipids.

Humic acid is of interest as it consists of a large colloidal polyelectrolyte of as yet unconfirmed formulation, with many pH dependent sites for adsorption of cations and anions. Humic acid is known to contain the following functional groups:

basic groups - -NH_2 (amino),
 =O (carbonyl),

-OH (alcohol),
-S (thioether)
acidic groups - -COOH (carboxyl),
-OH (enolic or phenolic)
(Evans, 1989)

The acidity of humic acid depends upon the proportion and type of reactive groups present and also the nature of the structures associated with the colloid. The acidic nature of humic acid is attributed mainly to the ionization of acid carboxyl and phenolic hydroxyl groups although structures such as keto-enol tautomers may also be involved (Stevenson, 1982).

Potentiometric base titrations of aqueous solutions of humic acid can be used to examine the polyelectrolytic nature of the sample and to provide an estimate of its acid content. A typical titration curve of humic acid is illustrated in Figure 6.2. Stevenson (1982) divided the curve into three zones:

Zone I - the lower acid region where -COOH groups are known to dissociate

Zone II - an intermediate area where the ionization of weak COOH and very weak acid groups overlap.

Zone III - the area which probably represents

the dissociation of phenolic -OH groups and other very weak acid types

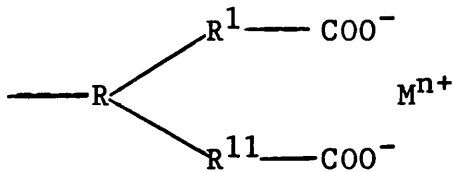
A problem that occurs when interpreting these titration curves is where to select the end-point. One favoured point is the area of maximum rate of change of pH with added alkali, however, the concept of a fixed end-point at pH 8.0 is also used.

Data from the titration curves can be used to calculate ionization constant values and to determine ' A_t '; the number of free acid sites in the sample. The mathematical calculation of these values is given in Chapter 2.

The reaction of humic and fulvic acids with metals can lead to increased metal solubility hence affecting their mobility within the soil, however, it is more likely that precipitation will occur due to a decrease in solubility. For example, the binding of ferric ions to low molecular weight fulvic acids maintains their solubility at pH values higher than those at which precipitation of ferric ions would normally occur (Wild, 1988). In comparison, the adsorption of metal ions to higher molecular weight humic acid leads to the formation of less soluble metal complexes and hence to precipitation.

Metal ions can interact with soil organic matter to form inner sphere complexes with strong covalent bonds due to the ability of functional group sites on

humic acid to act as complexant organic ligands. If it is sterically possible, due to the number and positions of these functional groups, chelated complexes may also form, (Evans, 1989).



Steric constraints usually result in the 1:1 complex forming.



1.4.4 Clay-Humic Interactions

Organic material can interact with clay particles, the resultant surfaces being of major significance with regard to the soil's interaction with metal ions. Interactions occur when polyvalent cations are present, allowing the co-ordination of the organic anion to the cation via water molecules in the hydration shell of the cation which is also bound to the clay via a water bridge (Theng, 1979). Another binding mechanism is by short range Van der Waals forces. This mechanism becomes important when humus polymers are in close proximity to the clay surface.

Extensive studies have shown that much of the humified material in soil is firmly bound to

colloidal clay (Kublena,1953; Stevenson, 1982). Clays retain organic matter as:

1. substances held on clay mineral surfaces by one or more of the following mechanisms; physical adsorption, chemical adsorption, hydrogen bonding and in co-ordination complexes.
2. organic substances held within the interlayers of expanding type clay minerals and which can be released only by destruction of the clay with HF.

The latter mechanism has not been fully established as occurring naturally, however, fulvic acids have been shown to be adsorbed on inter-lamellar surfaces of bentonite at $\text{pH} < 5$ (Schnitzer and Kodama, 1967; Tan and McCreery, 1975; Theng, 1976). Humic and fulvic acids contain various functional groups capable of interacting with clay minerals and providing an active organic surface for exchange with cations in the soil solution (Greenland, 1971; Theng, 1979).

For clay minerals containing 2:1 type lattices e.g bentonite and illite, adsorption of organic acids at their negatively charged surfaces can occur only in the presence of divalent cations which act to form bridges (Stevenson, 1982).

1.4.5 Metal Retention

Metals in soil solution exist either as free cationic ions or as complexes with inorganic or organic ligands' in which case the complexes can be cationic, anionic or neutral. Metal ions can interact with the solid phases of the soil by the formation of ion pairs between hydrated cations and complexant ligands held together by weak electrostatic forces or by the formation of inner sphere complexes held together by strong covalent bonds (Evans, 1989).

In the soil, metal ions act as Lewis Acids or electron acceptors interacting with ligands which are Lewis bases or electron donors. Small metal ions with no unshared electron pairs and/or high charge are known as HARD acids and will react selectively with HARD bases. Conversely large metal ions with unshared electron pairs and smaller charges are known as SOFT acids and will interact selectively with SOFT bases. Some common soil solution constituents are classified in table 1.3.

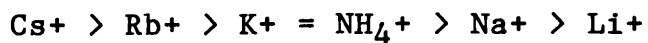
Table 1.3 Lewis Acid/Base Classification

	Acids	Bases
Hard	Na ⁺ , Cs ⁺ , Al ³⁺ , Mg ²⁺ , Sr ²⁺	O, N, Cl
Soft	Ag ⁺ , Pb ²⁺ , Co ²⁺ , Cd ²⁺	S

(Sposito, 1989)

Metal retention in soils depends on the concentration of the specific metal ion in solution and the nature of the mineral and humic surfaces associated with it.

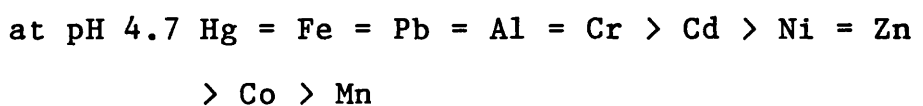
Caesium adsorbs on constant charge surfaces of clay minerals such as montmorillonite, illite and kaolinite in direct competition with other monovalent ions in the order:



(Kinniburgh & Jackson, 1981)

Due to the size of caesium's hydrated ionic radius (Table 1.1) it can fit into the frayed edge sites of clay minerals. Caesium ions can also form exchangeable ion pairs with soil organic matter.

Lead ions are retained in soils by adsorption on hydrous oxides, particularly ferric oxide. The adsorption is pH dependent and increases with increasing pH (Wild, 1989). Lead can also form inner sphere complexes with organic matter, becoming strongly retained in the process. Experiments reported by Evans (1989) in his review of metal/soil interactions show the relative retentions of a number of metals by humic acid:



at pH 5.8 Hg = Fe = Pb = Al = Cr = Cu > Cd > Zn
> Ni > Co > Mn

The interaction of metals with soil surfaces can be described both quantitatively (1.4.6) and qualitatively.

A qualitative approach to elucidating the nature, degree and strength of metal-humate linkages can be achieved by the use of infra-red spectroscopy to study the gradual conversion of a fully protonated sample of humic acid to the metal humate complex by the incremental addition of a metal salt solution. Using Fourier Transform Infra-Red Spectroscopy, it is possible to obtain spectra illustrating the sequence of transformations which occur as the metal becomes bound. This provides information allowing the contribution of functional groups to the binding of metal ions to be determined, and also the nature of the binding sites to be ascertained. Results obtained using this method are presented in Chapter 6.

1.4.6 The Mathematical Interpretation of Metal Retention on Soil Surfaces

Mathematical models have been developed to enable the calculation of metal sorption and retention from the results of laboratory experiments (Stevenson, 1982; Wild, 1988). Two concepts used will be considered in

this section:

- i) sorption theory
- ii) stability constants

1.4.6.1 Sorption Theory

The sorption of a metal ion from solution on to a solid phase can be described in terms of the distribution of metal ions between the solution and the solid phase at equilibrium. The graphical plot of the amount adsorbed by the solid versus the equilibrium solution concentration is termed an adsorption isotherm.

These plots can provide a great deal of mechanistic information purely by their shapes. These can fall into one of four categories:

H-type - surfaces with an initial high affinity for the sorbate which decreases rapidly at high concentrations.

S-type - surfaces with a low initial affinity for the sorbate due to the greater affinity of the sorbate to interact with the solution phase or components of it i.e organic ligands.

C-type - a constant and continual degree of sorption per unit change in equilibrium concentration.

L-type - the solid adsorbs the solute to give an initial slope which is independent of solute concentration but decreases with higher surface

coverage.

Several well known equations have been developed to describe the isotherm curves (Wild, 1988).

Langmuir Equation - this equation is based upon three assumptions:

- a) constant energy of adsorption that is independent of the extent of surface coverage;
- b) adsorption on specific sites, with no interaction between adsorbate molecules;
- c) maximum adsorption equal to a complete monomolecular layer on all reactive adsorbant surfaces.

(Bohn et al., 1985)

The equation can be expressed as;

$$c/x = c/x_m + 1/kx_m$$

c = equilibrium concentration of adsorbing compound ($\mu\text{g cm}^{-3}$)

x = amount of sorbate adsorbed ($\mu\text{g g}^{-1}$)

k = a constant relating to bonding ($\mu\text{g}^{-1} \text{cm}^{-3}$)

x_m = maximum sorbate capable of being adsorbed - the Langmuir Maxima ($\mu\text{g g}^{-1}$)

A linear plot of ' c/x ' versus ' c ' allows for the calculation of the Langmuir Maxima.

However, this model has its limitations as the

initial assumption of constant free energy rarely occurs in nature. Commonly, the energy of adsorption decreases with increasing surface coverage but increased interactions with molecules already adsorbed at greater surface coverage results in increases in the energy of adsorption. The net effect is a constant energy of adsorption.

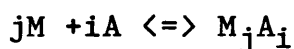
It is possible for the Langmuir equation to be used to describe adsorption over a portion of a data range even if it cannot be used to describe the adsorption behaviour observed as a whole. The equation can then be used to estimate the adsorption capacity of the system for the sorbate.

1.4.6.2 Stability Constants

Metal binding capacities of humic acids can be determined based on the premise that the maximum amount of metal ion that can be bound to humic acids is approximately equal to the content of acidic functional groups (-COOH) as measured by base titration, (see Sections 1.4.3 and 2.6.3). Stevenson (1982) quotes the average COOH content of humic acids to fall within the range 1.5 - 5.0 meq g⁻¹. The quantity of metal that binds to the humic acid can be influenced by factors such as pH, ionic strength and molecular weight of the humic acid as well as its functional group content.

The measurement of metal-organic complex

formation or stability constants, 'K', provides a quantitative measurement of the affinity of the metal (M) for the ligand (A) where for the reaction:



where 'j' is the number of metal ions and 'i' the number of ligands taking part in the reaction. The overall formation constant, K, is defined as:

$$K = \frac{(M_jA_i)}{(M)^j(A)^i}$$

Two approaches are utilized in investigating metal-humic complexes leading to two different constants:

- i) the metal ion is regarded as the central group resulting in the formation of MA_i complexes.
- ii) the humic acid is regarded as the central group resulting in the formation of M_jA complexes.

One popular method for determining stability constants is by base titration which is based upon the competition of metal ions and protons for complexing sites on the ligand, (Stevenson, 1982). The mathematical treatment of this approach is given in Chapter 2.

A modified method was devised by Stevenson (1977) in order to alleviate a problem he had experienced in his earlier research (Stevenson 1976a and b). The titration curves obtained in these

studies featured horizontal displacement in the presence of metal ions due to the release of protons from an otherwise non-titratable weak acid group. The modified experimental method involved sequential additions of metal ions to solutions of humic acid at constant pH. The resultant drop in pH was due to the release of protons from participating reactive groups. Base titration was carried out under N₂ with CO₂ free potassium hydroxide in order to return the solution to its initial pH. The initial pH was varied by mixing, in a range of proportions, the fully protonated humic acid and the neutralised potassium humate salt allowing the effect of pH on stability to be studied. Results obtained using this modified method are presented in Chapter 6.

Another method for obtaining stability constants is by ion exchange equilibrium which assumes that the metal ion is the central group and that the concentration of the metal ion in solution is negligible in comparison with the ligand. The method is based upon the competition between the ligand and a cation exchange resin for the metal ion resulting in the calculation of the stability constant K_j. The stability constant, B_j, resulting from base titration methods can be converted to K_j using the equation:

$$B_j = K_i \cdot K_j$$

where k_i is the ionization constant of the acidic functional group.

1.5 Literature Review

In order to understand fully the areas under study and to ascertain the research that was needed a literature review was required.

1.5.1 Laboratory Based Experiments

The input of the fission product ^{137}Cs to the environment in the 1950's and 1960's from nuclear weapons testing fallout stimulated an interest amongst research workers in the chemistry of caesium in soils and clays. Studies were predominantly laboratory based and examined the behaviour of caesium at both macro (greater than 1mM Cs-salt concentrations) and micro concentrations (less than 1mM), (Coleman et al., 1963a).

Experiments using caesium concentrations greater than 1mM showed that caesium appeared to be the most strongly adsorbed of the alkali metal ions, (Krishnamoorthy and Overstreet, 1950). It was found that caesium is able to exchange reversibly with some cations and in the case of some clays, notably vermiculite, and in many soils caesium can become fixed in interlayer spaces, (Schulz et al., 1960).

Trace concentrations of caesium have been shown to undergo fixation by soils and clays. Experimental work by Schulz et al. (1960) recorded 11-96% fixation

of caesium which was not removed by extraction with 1 molar ammonium acetate for a range of soil types. However, work carried out by Tamura and Jacobs (1960) suggested that caesium can undergo ion exchange with montmorillonite but not with micas or collapsed montmorillonite.

Coleman et al. (1963b) carried out work to determine the extent to which caesium was bound in non-exchangeable forms on clays. The study found that caesium was sorbed onto montmorillonite, illite and kaolinite in quantities corresponding to the saturation of the cation exchange sites. The sorbed caesium was readily displaced by leaching with KCl or CaCl₂. Vermiculite and heated, potassium saturated montmorillonite bound caesium tightly against displacement by CaCl₂ and AlCl₃ but not by KCl or NH₄Cl, with KCl removing 97.5% of sorbed caesium from K-montmorillonite. This behaviour suggests that the sorption of caesium in interlayer spaces by these clays leads to interplanar distances which prevent the exchange of caesium ions with larger ions such as Ca²⁺.

Sawhney (1966) extended these studies of caesium chemistry by researching the kinetics of caesium sorption by clays. Using 0.1 mM CsCl, it was found that equilibrium was achieved quickly by montmorillonite but that the caesium sorbed by vermiculite had not reached equilibrium after 500

hours. These observations were explained as follows:

a) Caesium sorption on illite occurs at external planar surfaces and at inter-lattice edges so equilibrium is reached quickly. Selective sorption of caesium by illites has been shown and this has been explained by edge fixation by minerals with an approximate basal spacing of 1nm, (Jacobs and Tamura, 1960). A model proposed to further explain this behaviour (Gaudette et al., 1966) attributes the selectivity to the competitive behaviour of caesium in contrast with other ions with respect to potassium or potassium-depleted sites of the skeletal, outer rind portion of the illite;

b) In montmorillonite, rapid exchange occurs due to the expanded lattice making all sites equally available;

c) The sorption of caesium by vermiculite is controlled by two processes, initial fast exchange onto external surfaces and edges followed by slow diffusion into interlayer sites.

Klobe and Gast (1967; 1970) showed that over 90% of caesium sorbed by a natural hydrobiotite of vermiculite origin was fixed irreversibly. They also determined that trace levels of ^{137}Cs were fixed to a much lesser extent, indicating a greater availability to plants. Investigations to determine the nature and occurrence of the lattice collapse associated with caesium fixation showed that caesium saturation

levels below 40% of exchange capacity resulted largely in interstratified Cs-rich layers with little edge collapse. Higher caesium saturations increased edge collapse. Formation of interstratified layers and edge collapse of the particles tend to be associated with smaller and larger clay particles, respectively.

Isotherm studies carried out on soils and clays allow qualitative evaluation of their adsorption and desorption trends. Erten et al. (1988a and b) examined the sorption/desorption behaviour of caesium on montmorillonite and kaolinite using a concentration range of 10^{-1} - 10^{-5} mM. Both clays exhibited non-linear isotherms, with montmorillonite sorbing more caesium than kaolinite due to structural differences. These were explained by two different sorption processes, adsorption onto sites at low concentrations and ion-exchange at higher concentrations ($> 10^{-5}$ meq Cs g^{-1}). The amount of caesium sorbed by the clays increased with clay particle size suggesting that sorption is primarily a surface phenomenon governed by the amount of surface sites available for sorption. Caesium sorption on soils was high. This was explained by the possible sorption of caesium onto organic components such as humic acid present in the soil. In addition, the sorption processes for the soils were only partially reversible.

Filipovic-Vincekovic et al. (1989) carried out studies on the sorption behaviour of montmorillonite and kaolinite over a concentration range of 10^{-1} - 10^{-7} M CsCl. In agreement with Erten et al. (1988a and b) the sorption of caesium on montmorillonite was found to be higher than for kaolinite due to differences in cation exchange capacities. Sorption was concentration dependent and could be described by the Freundlich Isotherm ($x = a.c^n$, where 'x' is the amount of ion adsorbed at an equilibrium solution concentration 'c', 'a' and 'n' represent constants) for a range of initial CsCl concentrations of 10^{-3} - 10^{-7} M. K_d (distribution coefficient, see section 2.5.1) values were also calculated, these were found to decrease with increasing caesium ion concentration with a range of values of 800 ml g⁻¹ at 10^{-7} M and 500 ml g⁻¹ at 10^{-3} M for montmorillonite and 700 ml g⁻¹ at 10^{-7} M and <50 ml g⁻¹ at 10^{-3} M for kaolinite.

When investigating the sorption of radionuclides onto rocks and minerals, Torstenfelt et al. (1982) found it to be a two stage process, in agreement with early investigations by Sawhney (1966).

Column experiments have been used to determine the migratory behaviour of caesium through clays and soils. Ohnuki and Tanaka (1989) and Ohtsuka and Takabe (1990) illustrated that for a sandy soil layer, very little migration of ¹³⁷Cs occurred, with

<0.3% migrating readily through the soil. This can be explained by the suggestion that most of the caesium sorption occurs in the uppermost part of the layer by sorption onto the soil matrix by ion exchange. The small fraction that migrates readily is in the form of neutral particles which are carried through the column by the flow of water leaching through it. These neutral particles form by the sorption of caesium onto very fine silt particles.

In summary, caesium sorption can be thought of as a two stage process consisting of a short initial period of sorption by ion exchange onto external accessible sites, followed by a slower, diffusion controlled process into internal exchange sites.

Caesium sorption relates to cation exchange capacity, pH and the cation concentration of the background solution. Caesium fixation occurs due to edge collapse and the formation of interstratified caesium-rich layers in vermiculite clays and by selective sorption on the frayed edge sites of illitic clays. Fixation may also occur due to the collapse of expanding clays due to heating or be induced by cation sorption. In certain cases, caesium sorption can be described using the Freundlich equation. The migration of caesium in soil profiles is governed by two processes, the migration of the

ionic form and the migration of caesium adsorbed onto very fine particulate matter.

In order to obtain a thorough understanding of the migratory behaviour and retention mechanisms of radiocaesium in soils it is necessary to extend laboratory experiments to the wider and more varied conditions found in the environment and to whole soils rather than mineral separates. This would take into account the contribution of soil fractions such as oxides and organic matter, as well as the clay fraction, to caesium sorption. Fahad et al. (1989) found that 28 - 57% of ^{137}Cs applied to loam and clay soil columns was retained by the clay fraction and 13 - 27% by the silt fraction. A lesser but significant fraction was held by iron oxides.

The results of these laboratory experiments must then be reviewed in parallel with recorded measurements of the observed behaviour of radiocaesium in the environment. This will enable the evaluation of whether laboratory models can be used successfully to explain observed behaviour and hence predict future behaviour. The following section deals with literature reports of radiocaesium present in the terrestrial environment.

1.5.2 Radiocaesium in the Environment - literature review

1.5.2.1 Pre - 1986

Prior to the Chernobyl accident, inputs of radiocaesium to the terrestrial environment occurred in the form of the fission product ^{137}Cs during the testing of nuclear weapons and in discharges from the nuclear industry (see section 1.2.2).

Nuclear weapons testing resulted in global contamination with radiocaesium, with releases from nuclear industries providing localised areas of enhanced activity. The cumulative activity released by Sellafield between 1957 and 1981 corresponds to 5% of the global fallout budget for ^{137}Cs (MacKenzie and Scott, 1984). However, in the immediate vicinity of the plant, radiocaesium concentrations in environmental materials can exceed weapons testing fallout concentrations as a consequence of the point source nature of the discharge. These elevated concentrations decrease rapidly to concentrations below fallout levels with increasing distance from source.

Onshore transfer of discharged radionuclides occurs due to direct transport of wind blown spray, aerosol transfer and the transport of contaminated particulate material from exposed intertidal deposits or from sea water suspended particulates (Mackenzie

and Scott, 1984).

Intensive surveys have been carried out, looking at the impact of Sellafield on Cumbrian soils. Away from the immediate vicinity of the site the main component of the ^{137}Cs content was due to weapons testing fallout. Cawse (1983) measured levels of 7.26 kBq m^{-2} of ^{137}Cs in soils from the highest rainfall areas of the west of Britain, with samples being taken to 15cm depth. Caesium deposition was found to correlate positively with rainfall, indicating that wet deposition was the main method of contamination. ^{137}Cs was found to be retained mainly in the top 0-15cm layer of soils, with 75% of the total inventory in the sample retained on grassland soil; 73% under coniferous woods and 76% under deciduous woodland, (Cawse, 1980; Cawse and Horrill, 1986). This observation was in good agreement with field experiments carried out by Gale et al. (1964) where a brown calcareous soil was treated with one acute addition of ^{137}Cs . After 4.8 years, 53% was retained in the uppermost 5cm and 95% in the top 20cm. This compared with a core of untreated soil containing only ^{137}Cs of weapons testing origin, which retained 22% in the upper 5cm and 62% in the top 20cm, suggesting a difference in mobility between one acute addition and continuous addition via rainfall. This is possibly due to differences in the chemical form of the radionuclide or in the nature of any

associated cations. In comparison, in a peat from Garvauld in Sutherland, 83% of fallout ^{137}Cs was contained in the top 20cm but the ^{137}Cs inventory in the peat was only 50% of that present to a depth of 30cm in a mineral soil from an adjacent site. These relative levels suggest that runoff of caesium is more efficient in the peat soil (Cawse, 1983). Cline and Rickard (1971) reported retention of 70% of ^{137}Cs in the upper 2.5cm of untilled field plots eight years after application. From these experimental reports radiocaesium could be expected to fix rapidly to mineral soils and to leach from organic soils due to their low content of 'caesium fixing' minerals. This would prevent caesium from being taken up by plants and entering the food chain.

1.5.2.2 Post-1986, after the Chernobyl accident

Radiocaesium resulting from the Chernobyl accident, in the form of the isotopes ^{137}Cs and ^{134}Cs , was recorded in the terrestrial environment. It is possible to calculate the contribution of Chernobyl ^{137}Cs in a soil total inventory, as the ^{134}Cs contribution is solely of Chernobyl origin and the $^{134}\text{Cs}/^{137}\text{Cs}$ ratio in Chernobyl fallout at the time of deposition was found to be 0.47-0.62, with values of 0.55 being recorded for the west of Scotland (Cambray et al., 1987; McDonald et al., 1992). Therefore, the ^{134}Cs content can be used to calculate the ^{137}Cs

contribution from Chernobyl and subtraction then provides an estimate of the weapons testing component.

McCauley and Moran (1992) measured ^{137}Cs inventories in soils in Ireland of up to 12 kBq m^{-2} . They found a correlation between ^{137}Cs levels and rainfall indicating that wet deposition was the primary route for Chernobyl fallout to enter the terrestrial environment. Using the equation:

$$W_r = W/CR$$

where W_r is the washout ratio for a given radionuclide, W the concentration of radionuclide per square metre deposited by R metres of rainfall scavenging an average rainfall concentration C , they calculated a national mean air concentration of ^{137}Cs of 0.4 kBq m^{-3} . McGee et al. (1992), again in Ireland, measured soil ^{137}Cs levels of $3.5\text{--}7.4 \text{ kBq m}^{-2}$ across a valley and were able to show a positive correlation between Chernobyl activity and altitude.

Chernobyl ^{137}Cs activity levels in soils range across Europe from 28.2 kBq m^{-2} in Germany, 12 kBq m^{-2} in Ireland, 5.5 kBq m^{-2} in the Netherlands and greater than 4 kBq m^{-2} in Britain (Frissel et al., 1987; Livens and Loveland, 1988; Bunzl et al., 1992; MacNeil et al., 1992; McCauley and Moran, 1992; McGee et al., 1992).

Chernobyl radiocaesium was expected either to fix to mineral soils or to leach from organic soils and therefore to rapidly become unavailable for plant uptake. Several years after the accident, levels of radiocaesium in sheep grazing on organic soils remained elevated, implying that some types of soil retain caesium in an available form for much longer than expected (Coughtry and Thorne, 1983; Livens and Loveland, 1988).

1.5.2.3 Plant availability of radiocaesium

The transfer of radiocaesium to plants has been the subject of extensive studies, both before and after Chernobyl. Studies consisted of both simulated inputs of activity onto field plots or pots and measurements of transfer rates after incidents such as the Chernobyl accident.

Garten and Paine (1977) found that caesium uptake by plants increased with: increasing soil ammonium content and a decrease in soil potassium content; decreasing clay content and organic matter content. However, D'Souza (1980) measured an increase in ^{134}Cs uptake with increased organic matter and also uptake was greater from kaolinite than from bentonite.

Increases in soil organic matter contents by greater than 15% caused an increase in uptake of caesium to grass, whereas increases in contents of

less than 15% had no effect upon caesium uptake (Frissel et al., 1987 and 1990). Soils with a very high organic matter content such as peats were found to hold ^{137}Cs , but in a form more available to plants than ^{137}Cs fixed by illitic soils. Cremers et al. (1990) found that for peaty soils, of organic matter content greater than 80%, the plant availability of radiocaesium was governed by the ammonium-potassium status of the soil and that the bulk of the caesium was reversibly associated with ion-exchange sites. In soils of lower organic matter content (20-50%), caesium availability was controlled by the specific sites on the micaceous clay fraction and the ammonium-potassium status. Andolina and Guillitte (1990) found that radiocaesium availability in a forest soil was closely related to the fulvic and humic fractions and caesium was strongly bound to the lignin fraction in the soil.

Dahlman (1975) measured ^{137}Cs transfer ratios for plant/soil of 0.01-1.0 for most soils with values of <1 for productive agricultural soils and >1 for acid weathered soils. A short time after contamination incident the uptake of radionuclides by plant roots becomes the most important method of contamination, relative to foliar uptake, with the transfer factor (TF) being defined as:

$$\text{TF} = \frac{\text{radioactivity/unit dry weight of plant}}{\text{radioactivity/unit dry wt of soil in root zone}}$$

Factors which can affect soil to plant transfer of radionuclides include: plant type; the chemical nature, sorption behaviour and migratory behaviour of the radionuclide; the depth of the rooting zone; time since deposition and soil type (Bell et al., 1988). Frissel et al. (1987; 1990) measured caesium transfer factors at pH 6 for grass shoots, of 0.14 for a sandy soil, 0.12 for a clay soil and 0.011 for a loam soil. The uptake of caesium by grass, cereals and other crops was found to decrease with increasing pH and increasing soil moisture content. MacNeil et al. (1992) measured equivalent transfer factors of 0.033 for a brown earth and 0.49 for a gley soil in April 1987, and values of 0.11 and 0.02 in October 1988 respectively. In general, transfer factors decrease with time as the caesium becomes less available, due to fixation or leaching.

1.5.2.4 The mobility of radiocaesium in soils

The mobility of caesium has a strong influence on its availability to plants. Bunzl et al. (1992) found that in a podzolic brown earth forest soil, of pH 2.9-3.8; organic matter content 49% in the organic horizon and 0.9-2.8% in the mineral horizon, that the major portion of Chernobyl caesium was present in the

upper 5cm of the organic layer 4 years after deposition, with only small amounts penetrating to greater depths. This compared with weapons testing fallout which was concentrated in the top 2cm of the mineral layer but with some penetration to 20cm depth. The data were used to calculate residence times and migration rates for ^{137}Cs of weapons testing and Chernobyl origin (see Table 1.4).

Table 1.4 Migration rates of radiocaesium in a forest soil

	residence time years	migration rate cm y^{-1}
^{137}Cs weapons testing		
upper organic layer	<3	0.5
lower organic layer	4	0.4
mineral layer	45	0.04
^{137}Cs Chernobyl		
organic layer	0.7	2.0
mineral layer	4	0.5

(Bunzl et al., 1992)

Residence times in the upper organic layer are short due to the rapid transport of organic material to the

lower organic layer and bioturbation by earthworms. Chernobyl derived caesium showed a greater mobility than the weapons testing component, possibly due to the gradual fixation of caesium by diffusion into the clay mineral layer.

Kirchner and Baumgartner (1992) used a compartment model to calculate the migration rates of radionuclides deposited after Chernobyl in a range of north German soils. The three soils had a range of characteristics summarised in Table 1.5 together with the calculated migration rates.

Table 1.5 Migration rates of radiocaesium in German soils

Soil	pH	organic content %	^{137}Cs migration rates cm y^{-1}	
			weapons	Chernobyl
Cambisol	7	low	0.47	0.66
Podsol	3	low	0.40	0.32
Histosol	4-5	40	0.30	0.60

(Kirchner and Baumgartner, 1992)

Taking into account errors of 5-30%, it was found that after 1150 days there was no significant difference between the migration rates of ^{137}Cs from different sources, although increased migration of caesium immediately after Chernobyl was observed.

This is due to the caesium from Chernobyl having undergone slow fixation to the soil matrix after this length of time (1150 days).

The diffusion coefficient of ^{137}Cs has been measured in mineral soils, and in general found to lie between 4.5×10^{-9} and $1.9 \times 10^{-8} \text{ cm}^2 \text{ s}^{-1}$ (Polyakov et al., 1973).

To summarise this section, caesium is more likely to be immobilised rapidly in soils of pH 4-7 that are: dominated by micaceous minerals; contain free carbonates; contain little organic matter; contain little montmorillonite or kaolinite and contain free potassium (Livens and Loveland, 1988).

1.5.2.5 ^{210}Pb and radiocaesium in peats

The migration of radionuclides in ombrogenous peats, where all radionuclide input is due to atmospheric precipitation, is of particular interest due to the possible application of ^{210}Pb dating techniques to determine a chronology.

Base metals such as lead show little or no downwards translocation in soils, this enables ^{210}Pb deposited from the atmosphere to be used to determine the sedimentation rates and age of the peat under study (Zoltai, 1988; Section 1.3.3). However, under acid conditions lead deposited on peat from an adjacent smelter has been remobilised, showing limited downward migration (Dumontet et al., 1990).

Clymo (1983) considered biological cycling to be an active process involved in the relocation of lead resulting in regions of the soil core having uniform activity. Schell et al. (1989) postulated that there are five major mechanisms involved in the vertical transport of ions in soils: chemistry of the ion; gravity; precipitation; infiltration and evapotranspiration. In addition, it is necessary to consider the effects of diffusion, solution-surface interactions and bioturbation.

Lead binds tightly to the complexing functional groups present in peat soils. Lead speciation may be as oxides near the surface and as sulphides in the lower reducing zone, the latter compounds being insoluble, so that their formation would limit transport (Schell and Tobin, 1990).

^{137}Cs was observed to have migrated to depths of at least 16cm in a peat bog over the last 30 years. This mobility was explained by advection and diffusion. Mixing of ^{137}Cs between layers occurred by both infiltration during precipitation and upward transport by capillary action on evapotranspiration (Schell and Tobin, 1990). This agreed with the findings of Oldfield et al. (1979) who found ^{137}Cs migration in peat cores was affected by diffusion and that the activity profiles were unusable for dating. In one peat core there was evidence that ^{210}Pb had undergone diffusion, resulting in an underestimation

of the peat's age. Schell et al. (1989) stated that ^{210}Pb can be used as a time determinant in peat and wetland ecosystems but that ^{137}Cs diffuses both upward and downward, due to weak chemical bonding between ^{137}Cs and organic ligands. Therefore, caesium data are unsuitable for use in dating.

1.5.2.6 Organic matter/radionuclide interactions

From the review of the literature in the previous section, it is apparent that the interaction of radionuclides with natural organic materials is relatively poorly understood, despite the potential importance of such processes in the transport and retardation of radionuclides.

It is generally assumed that humic substances contain at least two important classes of acidic binding sites, namely carboxylic and phenolic functional groups. The carboxylic type ligand represents an abundant source of metal binding sites in the natural environment. Complexation of metal ions can often alter the solubility of metallic elements, providing a source of rapid and efficient geochemical transport (see Section 1.4.3).

Many studies have been carried out to determine the stability of metal-organic complexes using a variety of methods. Schnitzer and Skinner (1966) using an ion-exchange technique measured stabilities

in the sequence:



contrasting with the results obtained by titration data of:



(Beckwith, 1959; Khanna and Stevenson, 1962).

Mantoura et al. (1978), using a gel-filtration method, obtained a comparable sequence of metal-humate stabilities. In addition, it was found that the origin of the organic acid affected the metal-organic acid stability constant. The stability constants of copper complexes followed the sequence:

soil FA < soil HA < peat FA < peat HA < sea water HM
< lake HM < river HM < marine sedimentary FA < marine
sedimentary HA

where HA - humic acid, FA - fulvic acid and HM -
humic material.

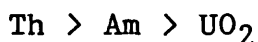
Studies examining the binding of lead with humic materials found that lead-fulvic complexes precipitated out of solution before the fulvic acid complexing capacity for the metal ion had been reached. This removal of lead from solution may influence the mobility of lead in organic rich soils (Saar and Weber, 1980). A review of stability constants measured for lead is given in Chapter 6.

Stevenson (1976 a and b, 1977, 1982) found that

the stability of metal-humate complexes increased with increasing pH due to the greater ionization of functional groups, especially -COOH. It is possible for humic material to influence the oxidation state of metals, for example PuO_2^{2+} is reduced to Pu^{4+} by humic material (Clark and Choppin, 1990). It is apparent that there is a high degree of variability in measured stability constants due to: the method of determination used; the sample of humic material; experimental conditions such as pH, temperature and ionic strength.

Caesium, being monovalent, is assumed to form a simple salt with organic ligands. More complex radionuclides will bind by complexing and redox reactions to form a series of complexes of the general formula $\text{M}_r \cdot \text{A}_x \cdot \text{H}_y \cdot (\text{OH})_z$, where M^{n+} is the simple metal ion which reacts with the polybasic acid H_LA (Jensen and Jensen, 1988).

Choppin (1978) recorded data for the actinides using a solvent extraction method illustrating the variation in stability with degree of ionisation of the humic acid. The actinides follow the stability sequence:

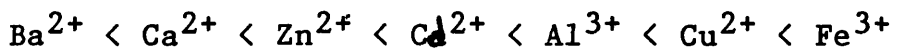


Maes et al. (1988) measured the stability of europium organic complexes at pH 9 using an ion-exchange method. It was found that a 1:1 complex was formed with concentrations of soil organic matter in the

range $< 10^{-3}M$. Log K values of 13.2 - 14.6 were obtained, reflecting the strongly bound nature of the complex formed. Esteban and Choppin (1978) measured stability constants for europium and americium of log K 7.4 and 6.8 respectively at pH 4.5. It was possible that there was a secondary stability constant which corresponds to the reaction $M + 2Y = MY_2$. This was explained by the simultaneous binding of a metal ion to two adjacent carboxylate groups. Clark and Choppin (1990) examined the kinetics of the complexation of europium by humic acid. It was found to be a rapid reaction with initial strong binding of only a fraction of the metal. This increased over a period of two days, probably due to cation migration to interior sites of the humic molecule and the contraction and folding of the molecule trapping surface bound cations. Thus, if the flow of water through a soil is fast, there may be insufficient contact time for strong binding to occur. However, with slower movement, the metals can become retained by the humic material and their migration slowed or stopped.

The interaction of organic colloids with the clay fraction of soils may affect the structural condition of the humus and hence its interaction with metals. Evans and Russell (1959) found that the adsorption of humic and fulvic acids was less by kaolinite than by bentonite. The adsorption of the

organic matter was found to be rapid (90% in the first hour). The main mechanisms for interaction being: physical adsorption; chemical adsorption; hydrogen bonding and the formation of co-ordination complexes (Greenland, 1971; Stevenson, 1982). Theng (1976) examined the effect of adsorbing fulvic acid from aqueous solutions containing different exchangeable cations by montmorillonite. At pH 7, greater adsorption occurred in the order of metal ions:



The fulvic acid binds to the clay by hydrogen bonding between an anionic group of the acid and a water molecule in the hydration shell of the exchangeable cation.

Further research is required to study the influence of humic or fulvic acid sorption onto clay surfaces and the subsequent binding of metal ions, in order to understand more fully the interactions which occur in soils of high organic and clay content.

1.6 Thesis Aims

1. To examine the mobility of radiocaesium in organic rich and mineral soils from selected sites in Scotland using ^{210}Pb dating where appropriate, in an attempt to correlate the observed behaviour with the soil's properties and local topography.

2. To use laboratory methods to study the adsorption/desorption behaviour of caesium and lead in a selected range of soils and clays.

3. To characterise extracts of humic acid from the study sites and to describe both quantitatively and qualitatively the binding of a range of metals to the extract.

4. To elucidate the influence of clay/humic acid interactions on the subsequent binding of caesium to the solid phase.

CHAPTER 2 - MATERIALS AND METHODS

2.1 Samples used in laboratory experiments

2.1.1 Soils and Peats

Samples of soils were necessary for analysis of radionuclide inventories and vertical distributions and for use in laboratory experiments. Care was taken to choose sites where comparisons could be made both between soils of similar characteristics and soils of variable origin. In order to obtain a data set covering a wide spectrum of soil properties, samples were collected from the four different sites described below.

South Drumboay - Grid Reference NS 502 482

This site is located on a hill situated on Fenwick Moor to the South of Glasgow and was selected because a diverse range of soil types is found within a small area and the sheep grazing on the pastures overlying organic soil were known to have a high Chernobyl radiocaesium burden.

Drumboay hill (altitude 220m) experiences a climate with moderate winters and an average rainfall of approximately 1400mm per annum. The underlying geology of the area consists of Carboniferous age basaltic bedrock overlain by a deep layer of clay textured till. The impermeability of the till, combined with high

rainfall and the gentle contours of the area have led to the formation of areas of blanket peat coverage.

The five soils studied at this site, from the Darleith Association, were:

- (1) Fenwick Moor Peat, a highly humified soil with an organic content of >90% and a surface coverage of reeds and sphagnum moss;
- (2) Darleith Series, a freely drained brown earth with an organic content of approximately 20% and a high clay content, the A horizon being approximately 20 cm deep;
- (3) Dunlop Series, an imperfectly drained brown earth with a gleyed B and C horizon, the A horizon being approximately 20 cm deep;
- (4) Myres Series, a surface water gley with a humose/peaty top-soil;
- (5) Dunwan Series, a humic ground water gley.

(Mitchell and Jarvis, 1956)

Cores of Fenwick Moor Peat and Darleith were collected in addition to bags of loose soil (see Section 2.2).

Auchincruive - Grid Reference NS 383 232

Average rainfall 940 mm y^{-1} , altitude 24 m.

The sampling site here was in the grounds of the West of Scotland Agricultural College near Ayr which comprise several raised beaches and areas of Carboniferous sandstone and glacial till, providing a series of freely and imperfectly draining sandy soils.

The two main soil types are:

(1) Dreghorn Association, Dreghorn Series, a freely drained brown earth;

(2) Bargour Association, Bargour Series, an imperfectly drained brown earth.

(Grant et al, 1962)

A core of Dreghorn was collected.

Aachmor Farm, near Inverness

- Grid Reference NH 480 500

Average rainfall 953 mm y^{-1} , altitude 300 m.

This site of ombrotrophic blanket peat, near Inverness, has developed at high altitude and was selected to provide a sample relatively free of industrial pollution in an area of known Chernobyl contamination. The Inverness Peat was a highly humified, dense soil with an organic content >90%, overlain with a cover of coarse grass.

Over-Rig, Borders - Grid Reference NY 245 935

Average rainfall 889 mm y^{-1} .

This site at Over Rig, Eskdalemuir in Dumfries, provided a peat sample of a totally different nature to the other samples. The Borders Peat was a lightly humified sphagnum moss with an organic content of >90% and a low density.

2.1.2 Reference Clays

In order to provide data which could be compared with literature results, a set of three pure reference clays was used for sorption experiments. Descriptions of clay types are given in section 1.4.1. The clays used experimentally were:-

(1) Bentonite - a 2:1 expanding clay which provides internal and external sites for adsorption. Bentonite clays can have cation exchange capacities within the range 80-150 meq/100g (Stevenson, 1982), depending upon the degree of substitution. The clay sample used was BDH Bentonite Technical.

(2) Illite - a 2:1 non-expanding clay (section 1.4.1). The cation exchange capacities of illitic clays range from 10-40 meq/100g. The sample used for experimentation was Clay Mineral Standard Fithian Illite no.35 (Ward's Natural Science Establishment, Rochester, New York).

(3) Kaolinite - a 1:1 clay consisting of alternate layers of Si-oxides and Al-hydroxides. The exchange properties of kaolinite are mainly due to unsatisfied valencies at the edge of the clay particles and the cation exchange capacity is low falling within the range 3-15 meq/100g. The experimental sample used was BDH Kaolin Light.

2.2 Sample Collection and Preparation

2.2.1 Bulk Soil Samples

The soils were collected by digging a pit of greater than 50cm depth and exposing a fresh, clean soil profile on which the A and B horizons could be clearly distinguished. A clean trowel was used to collect soil from each horizon and the samples were placed in clean plastic bags for transporting to the laboratory where they were spread out on polyethene sheeting and allowed to air-dry at room temperature. The air-dried samples were then passed through a 2mm stainless steel sieve, retaining the <2mm fraction in glass jars for experimentation.

All samples were collected and dried in October 1988.

2.2.2 Core Collection

Fenwick Moor Peat, Darleith, Dreghorn and Borders Peat samples were collected in tins of dimensions 20x10x40cm. The Inverness Peat was compacted to an extent where it was possible to cut blocks of the required size using a spade. Care was taken to prevent compaction of samples and smearing along the surfaces of the tins.

The cores were sliced horizontally, into contiguous sections of 2cm depth down the profile. The samples were then oven dried at 60°C for 24 hours after which they were passed through a sieve of 2mm mesh size, discarding stones.

The peat samples were treated differently to the

mineral soils - it was found that the most appropriate method for obtaining a fine homogeneous sample, suitable for gamma spectroscopy analysis was to blend the peat in a food processor. Large amounts of sample were taken to near dryness by placing in a drying cabinet set at 20°C for 24 hours and then could be ground in this manner and then oven dried. Samples were then placed in appropriately sized plastic containers. In order to maintain a fixed geometry for gamma spectroscopy the amount of sample used was fixed according to depth. The importance of sample geometries is explained in Section 2.4.

The use of furnacing highly organic and low density soils, in order to reduce their bulk and increase the detection efficiency obtained in gamma spectroscopic analysis is routinely employed by some workers, e.g Appleby et al. (1988). This technique was evaluated but rejected for use in the present work for the reasons outlined in section 4.1.

2.3 Characterization of Soils

Standard methods outlined below were used to determine the following properties of all 13 soil samples.

2.3.1 Gravimetric Moisture Content

10.00 g of air-dried soil was further dried for 16 hours in a weighed, dry porcelain basin at 110°C, allowed to cool in a desiccator and reweighed. (Triplicate samples were used)

$$\text{Moisture content (\%)} = 100 \times \frac{(\text{air dry wt} - \text{oven dry wt})}{\text{air dry weight}}$$

$$\text{Conversion factor (C.F)} = \frac{100 - \text{moisture content}}{100}$$

2.3.2 Loss on Ignition

Organic matter was determined gravimetrically by loss on ignition. 5.00 g of air dried soil was placed in a dried silica basin, oven dried and then placed into a muffle furnace at 550°C for 5 hours. (Triplicate samples were used)

$$\text{Organic matter (\%)} = \frac{(\text{air dry wt} \cdot \text{C.F} - \text{ashed wt}) \cdot 100}{(\text{air dry weight} \cdot \text{C.F})}$$

2.3.3 pH

10.00 g of air-dried soil was suspended in 25 ml of distilled water and shaken intermittently for 30 minutes. The pH was measured in the stirred suspension using a combination electrode. For peat

samples a ratio of 5.00 g air-dried soil to 50 ml of water was used. (Triplicate samples were used)

2.3.4 Cation Exchange Capacity (CEC)

Glass leaching columns were filled with a 2:1 mixture of air-dried soil (10.00 g) and acid-washed sand. The column was saturated with 250 ml of 1 molar potassium acetate at pH7. Excess potassium ions were removed by leaching the column with 250 ml of 90% ethanol/water. The column was then leached with 250 ml of 1 M ammonium acetate at pH7. The displaced potassium ions were collected and the concentration of potassium ions in a total volume of 250 ml was determined using a Perkin Elmer Atomic Absorption 1100B spectrophotometer in flame emission mode (Table 2.1 instrument specifications).

CEC is calculated on the premise that the number of negatively charged sites available for ion exchange is equivalent to the number of potassium ions removed from the soil.

2.3.5 Available Potassium

The most universally employed index of potassium availability is the sum of the exchangeable potassium plus the potassium in the soil solution. A wide range of extracting solutions is commonly used to extract 'plant available' potassium from

soil. In this study, 50 ml of 0.5 M acetic acid was added to 5.0 g of air dried soil (in triplicate). The suspension was shaken for 2 hours on an end-over-end shaker, filtered through Whatman No. 40 filter paper. The potassium concentration in solution was measured by flame emission spectroscopy.

2.3.6 Particle Size Distribution

Particle size analysis was carried out for the 4 soil subset of Darleith, Dreghorn, Peaty Gley and Humic Gley, and involved:

i) Oxidation of organic matter - 50 ml of 6% hydrogen peroxide and two drops of anti-foaming agent were added to 10 g of air-dried soil in a beaker which was then heated gently on a steam bath until the initial vigorous reaction ceased. Successive 50 ml portions of hydrogen peroxide were added until all the organic matter was oxidised (i.e when no further reaction took place on addition of hydrogen peroxide). The beaker was cooled and water was added to give a suspension depth of 2 cm. 10 ml of 5.7% Calgon, a deflocculating agent, was added and the suspension dispersed for 5 minutes using an ultrasonic probe. Care was taken to wash all soil adhering to the probe into the beaker.

ii) Particle Size Separation

The dispersed soil was then passed through 180 μm and 53 μm sieves into a 1000 ml graduated cylinder. The coarse and medium sand fractions were retained on the 180 μm sieve and the fine sand fraction on the 53 μm sieve. These were dried and weighed.

The finer particles of clay and silt were measured using a pipette method based on the measurement of the sedimentation rates of the particles calculated using Stoke's Law. At room temperature silt plus clay has a settling time at 20 cm depth of 64 seconds and clay has a settling time at 10 cm depth of 479 minutes. Therefore, the soil suspension in the cylinder was made up to 1000 ml and shaken thoroughly for 60 seconds to ensure that all the soil was in suspension. A clean pipette was used to collect 10 ml of the silt and clay fraction from 20 cm depth after 64 seconds. 10 ml of the clay fraction was collected at 10 cm depth after 479 minutes.

The data were then used to calculate the percentage content of sand, silt and clay for the soils.

2.4 Radionuclide Detection - Gamma Spectroscopy

2.4.1 Analysis

Specific activities of the radionuclides ^{137}Cs , ^{134}Cs and ^{210}Pb in soils were measured by Gamma spectroscopy using their characteristic emissions at 661 keV, 604 keV and 46 keV respectively.

Decay characteristics for the radionuclides are given below:

a) ^{137}Cs - Half life 30.17 years

Decay mode β^-

$E_{\beta\text{MAX}} = 1.175 \text{ MeV}$

Gamma photons: 661.7 keV (85.21% intensity)

b) ^{134}Cs - Half life 2.062 years

Decay mode β^-

$E_{\beta\text{MAX}} = 1.454 \text{ MeV}$

Gamma photons: 563.2 keV (8.38% intensity)

569.3 keV (15.4% intensity)

604.7 keV (97.6% intensity)

795.9 keV (85.4% intensity)

802.0 keV (8.7% intensity)

c) ^{210}Pb - Half life 22.3 years

Decay mode β^-

$E_{\beta\text{MAX}} = 63 \text{ keV}$

Gamma photons: 46.5 keV (4.05% intensity)

(Browne and Firestone, 1986)

Gamma measurements were used instead of beta measurements because they enabled all radionuclides of interest to be studied simultaneously. In addition, gamma spectroscopy is a non-destructive method leaving the sample unchanged for further analysis.

Gamma rays interact with matter in three ways; the Photoelectric effect, the Compton effect, and Pair production, these are described in section 1.2.2.

2.4.2 The Principles of Gamma Detection

Semiconductors are amongst the most common detector devices used in gamma spectroscopy. Semiconductors are materials with electrical properties intermediate between those of an insulator and a conductor. The electrical properties of semiconductors can be described using band theory (Adams and Dams, 1970). Electrons are considered to occupy energy bands: a lower valence band, where electrons are immobile and an upper conduction band where electrons can be mobilised and can therefore conduct.

The distance separating these bands determines the energy required to move an electron to the conduction band and hence conduct. In conductors, the upper band always contains electrons thereby enabling electron movement within the band. In insulators, the conduction

band is empty and the large difference in energy between the valence and conduction band prevents the movement of electrons into the conduction bands. In semiconductors, the conduction band is empty at absolute zero temperature but as the energy difference between the valence and conduction bands is relatively small (a few eV) electrons can be promoted into the conduction band by thermal excitation at higher temperatures. The number of electrons in the conduction band is therefore temperature dependent as expressed in the equation:

$$N_e = f(T) \cdot e^{-E_g/kT}$$

(Adams and Dams, 1970)

where

N_e = the number of electrons in the conduction band

E_g = the energy band gap

$f(T)$ = a temperature dependent function giving the number of possible positions for excited electrons

k = Boltzmann's constant

T = absolute temperature.

Therefore, semiconductors behave like insulators at low temperatures and conductors at high temperatures.

Semiconductor materials can be classified as 'intrinsic', having very high purity, or 'extrinsic', having impurities present which effect the electrical properties of the semiconductor.

Extrinsic semiconductors can be sub-divided into:
n-type - the impurity in this case is a Group V element, for example phosphorus, which adds an extra electron to the structure. The extra electron can be promoted easily to the conduction band, resulting in an electron excess.

p-type - the impurity in this case is a group III element, for example indium or gallium, which depletes the electronic structure and provides energy levels slightly above the Si or Ge valence bands. The semiconductor electrons occupy these levels, leaving positively charged electron holes which are highly mobile.

Gamma radiation requires large detector volumes due to its low ionizing power and high penetration. High purity, high resolution intrinsic Ge-detectors are now available due to improved technology. Cryogenic cooling is used to increase resolution and to decrease electronic noise.

Charge pulses are generated by the interaction of gamma rays with the detector crystal by three processes: the photoelectric effect; Compton scattering; and pair-production, (see Section 1.2.2). The charge pulses are detected by a charge-sensitive pre-amplifier which generates an electrical signal with an output voltage proportional to the input charge. The signal from the pre-amplifier is transferred via an amplifier to an analogue to digital converter (ADC)

which proportionally digitizes the input pulse amplitude. The digital signals are then stored in a computer memory as 'counts' corresponding to different gamma photon energies. The distribution of counts as a function of energy constitutes the gamma spectrum. The energy range studied in the present work was from 0-2000 keV.

Gamma spectra exhibit a number of characteristic features including:

a) discrete photopeaks produced by the photoelectric process, b) a continuum caused by Compton scattering and c) the annihilation peak at 511 keV produced by positrons from pair production combining with electrons. Net peak areas are calculated by subtraction of the continuum contribution. The continuum and net background peaks, present due to the detector, shielding and sample containers containing low activities of natural and anthropogenic radionuclides as impurities, determine the lower limit of detection of the system. Background spectra were accumulated and appropriate background subtraction from the sample spectra was performed in order to calculate the net radionuclide activities in the sample. Thompson (1988) outlined methods for shielding gamma photon detectors from background radiation. Lead is used to form the main component of the shield, but if it has not been aged for at least 100 years it will contain nuclides from the uranium and thorium series. In addition, gamma

rays from the sample being counted may interact with the lead shielding causing the production of low energy fluorescent lead X-rays. These may be removed by lining the lead shielding with a 1mm cadmium and 0.6mm copper layer.

The resultant peak activities are converted to nuclide activities by calibrating the detector efficiency with energy, using standards of known activity and emissions of known intensity.

2.4.3 Experimental Work

Two gamma spectroscopy systems were used in this work. One comprised an EG&G ORTEC Gamma-X intrinsic Ge detector (10% relative efficiency; FWHM resolution = 1.8 keV at 1333 keV) interfaced with an EG&G Ortec7032 multichannel analyser (MCA). In this case, spectra were analysed using the Ortec peak search and analysis programme GM2. The second consisted of a Canberra coaxial Ge detector. The Canberra detector was interfaced to a Series 85 MCA. Analysis was performed using the Spectran AT software package. Both the detectors were shielded by four inches of lead with a graded Cd-Cu lining.

(i) Background Spectra - these were recorded regularly throughout the experimental period in order to take these values into account when calculating results and to monitor for any contamination of the detector.

Background radiation levels for the Gamma-X detector are summarised in Table 2.1. The Canberra co-axial Ge detector used for Core Set 2. was constructed from low background materials and consequently had no net background peaks at the energies of interest as indicated in Table 2.1. In each case, background spectra were accumulated over several days in order to minimise the counting statistics uncertainty.

(ii) Calibration Standards

In order to calculate specific activities for the core samples it was essential to determine detection efficiencies for every sample matrix and for each counting geometry used. The gamma detection efficiency for a point source is inversely proportional to the square of the distance of the source from the detector crystal. It is therefore essential that sample positioning and geometry are optimised and reproducible (de Bruin and Blaauw, 1992). In addition, the density and atomic number, Z , of the sample will affect the gamma detection efficiency. Calibration standards were therefore prepared for each radionuclide studied and for every sample type, taking into account sample matrix and counting geometry considerations. Density variations and Z value were accounted for by using cellulose as an analogous matrix for the highly organic peat soils; a mineral soil taken from below 20cm depth, to ensure that it had no measurable levels of

radioactivity, to represent the mineral soil; and a mixture of this soil and cellulose to represent the Darleith sample.

In addition, the method used to prepare these standards was also examined. A 'B' horizon mineral soil sample (<2% organic matter, high density) originating from the sample area at Auchincruive was analysed repeatedly and found to have no detectable levels of ^{137}Cs , ^{134}Cs and ^{210}Pb . BDH cellulose (100% organic matter, low density) was also analysed and found to be free of ^{137}Cs , ^{134}Cs and ^{210}Pb . These two samples were used in varying proportions; 100% cellulose for peat soils, 50:50 cellulose:mineral soil for Darleith and 100% mineral soil for Dreghorn, to prepare calibration standards with density and Z value characteristics similar to the core samples.

An experiment was carried out to compare two methods of preparation of detector efficiency calibration standards for ^{137}Cs analysis. In one method the total quantity of spike used was added to the top of the cellulose matrix (5 cm deep) after which the standard was dried and mixed by shaking on an end-over-end shaker. In the second method one fifth of the spike was added to a 1 cm layer of the matrix and allowed to dry after which this process was repeated by additional 1 cm layers until the same total spike and depth of matrix was present as in the first geometry. Gamma spectra of the standards were recorded for 30 minutes,

after which the samples were shaken for 30 minutes and the spectra were recorded again. This process was repeated several times. The data obtained indicated that method 1 resulted in a standard deviation of 0.4 cps after 10 counting periods and an average count of 6.8 cps whilst method 2 resulted in a standard deviation of 0.6 cps and an average count of 7.1 cps. However if the first count period of method 2 was ignored (i.e the count taken prior to the layered calibration standard being shaken) the average count rate is 6.8 cps with an error of 0.4 cps identical to method 1. Therefore, if calibration standards undergo mechanical shaking for a period of at least 30 minutes, they will represent samples with even distributions of activity, whichever method of preparation has been used.

The calibration standards for the cores were constructed using method 1 as this minimised the number of errors which could be introduced due to manual weighing and pipetting steps. Separate geometries were used for radiocaesium and ^{210}Pb . The results for determination of detector efficiency are presented in Table 2.2a and 2.2b, with the dimensions of the containers used being provided in Table 2.3.

Table 2.1 Background gamma radiation levels recorded for the Ge detectors used from 12/88 - 10/90.

Date	^{137}Cs		^{134}Cs		^{210}Pb	
	cps $\times 10^{-4}$	error %	cps $\times 10^{-4}$	error %	cps $\times 10^{-4}$	error %
Gamma-X						
12/88	6.7	25.5	6.8	23.6	121.7	2.3
5/89	6.5	22.8	6.7	24.5	120.1	2.0
8/89	6.4	28.5	6.8	27.9	80.3	3.4
9/89	5.3	28.1	9.4	20.3	78.0	3.5
12/89	5.3	26.7	6.5	22.9	79.1	3.5
2/90	8.9	17.9	5.5	29.8	78.7	3.9
4/90	N.D		N.D		68.7	9.6
11/90	N.D		N.D		85.4	16.8
Canberra						
10/90	N.D		N.D		N.D	

N.D = not detectable

Table 2.2a Detection Efficiencies in Gamma Spectroscopy- Calibration Standards for the Gamma-X Intrinsic Ge Detector (the containers dimensions are given in Table 2.3).

	Container Depth		Matrix	Activity Bq	Detector error	
	Type	cm			Efficiency %	% of effic.
^{137}Cs	1	1	Cellulose	35	0.71	0.003
	1	4	Cellulose	35	0.49	0.003
	1	6	Cellulose	35	0.24	0.002
	2	4.5	Cellulose	35	0.48	0.004
	3	4	Cellulose	35	0.61	0.006
	2	3	50:50 mix	35	0.44	0.005
	2	7	Mineral	35	0.35	0.005
^{134}Cs	1	1	Cellulose	116	0.72	0.003
	1	6	Cellulose	116	0.33	0.003
	2	4.5	Cellulose	135	0.55	0.005
	3	4	Cellulose	107	0.71	0.007
	2	3	50:50 mix	138	0.62	0.005
	2	7	Mineral	107	0.39	0.004

Table 2.2a continued.

	Container Depth		Matrix	Activity Bq	Detector error	
	Type	cm			Efficiency %	% of effic.
^{210}Pb	1	1	Cellulose	86	0.18	0.002
	1	4	Cellulose	86	0.16	0.001
	1	6	Cellulose	86	0.09	0.001
	2	4.5	Cellulose	80	0.16	0.001
	3	4	Cellulose	72	0.18	0.002
	2	3	50:50 mix	80	0.17	0.002
	2	7	Mineral	72	0.12	0.001

Table 2.2b Detection Efficiencies in Gamma Spectroscopy.

Calibration Standards for the Canberra Intrinsic Ge Detector. (The container dimensions are given in Table 2.3)

	Container Depth		Matrix	Activity Bq	Detector error	
	Type	cm			Efficiency %	% of effic.
^{137}Cs	3	4	Cellulose	35	1.13	0.011
^{134}Cs	3	4	Cellulose	107	1.17	0.012
^{210}Pb	3	4	Cellulose	72	0.35	0.003

Table 2.3 Descriptions of Counting Geometry Containers

Container Types	Depth of Container (cm)	Sample Sets	Depth of Sample (cm)
1	6.7	Inverness Peat '89	6
		Furnace Experiment	6 & 1
2	7.0	Borders Peat	4.5
		Darleith Soil	3
		Dreghorn Soil	7
3	4.0	Fenwick Moor Peat	4
		Inverness Transect	
		Peat Cores '90	4

N.B The 'type' of container is a code used to distinguish between containers of different depth.

(iii) Low Density Samples

In order to optimize the gamma detection efficiency for samples with low bulk density, the use of furnacing to remove organic matter was explored. Initial investigations were carried out to obtain the lowest furnacing temperature which could be used in order to minimise the loss of elements due to volatilisation but still produce efficient ashing.

A bulk sample of homogenised peat was split into eight sample containers to a depth of 4 cm. The samples were gamma counted for a minimum of 24 hours to maintain a low error. After analysis, samples 1-4 were spiked with 358.26 Bq of ^{137}Cs and 12.80 Bq of ^{210}Pb . Initially, an optimum temperature was obtained by furnacing replicate samples of a bulk peat for 5 hours over the temperature range 250 - 500°C. The results indicated that, after a rapid rise in percentage mass loss, a plateau was achieved from 350°C, with a loss of approximately 90% by weight. This temperature was used in the main experiment to ascertain the losses of elements due to volatilisation during furnacing.

Samples 1-8 were then transferred to large pyrex beakers and furnaced at 350°C for 5 hours. The percentage sample loss in transfer was monitored and found to be 0.05% for each transfer step. After transfer, the samples were returned to the clean sample containers. Gamma spectra of the samples were again recorded and the activity of each sample prior to and

after furnacing was calculated using appropriate calibration standard efficiencies. This allowed for the comparison of losses due to furnacing of the two radionuclides at this temperature and also differences in behaviour between radionuclides present due to atmospheric input and those added in the laboratory.

The results of this experiment showed that for ^{137}Cs the average loss was independent of whether the ^{137}Cs was originally contained in the samples or added as 'spike'. An average of $12.7 \pm 0.4\%$ of ^{137}Cs already present in the sample (approx. 0.1 Bq g^{-1}) was lost. The spiked ^{137}Cs was lost at $17.4 \pm 3.0\%$. However, results for ^{210}Pb differed with the amount lost being dependent on its origin, with $13.4 \pm 0.1\%$ of added spike being lost, compared to $42.7 \pm 2.0\%$ of the naturally occurring lead. This was probably due to lead bound to the organic framework of the peat being lost during furnacing. The caesium ions were more likely to be bound to the small percentage of clay minerals found in the peat soil which are unaffected at these temperatures.

These results indicate that furnacing could not be used to obtain better gamma detection efficiencies without significantly affecting the accuracy of the analysis. These results differ from those of Appleby et al. (1988) who ashed peat at 450°C to improve gamma detection efficiencies. An alternative method involving grinding the peat using a food processor was therefore

used to achieve a volume reduction and associated increase in detection efficiency. This was not ideal as the fine product was still bulky and light, requiring large volumes of sample, however, it did give improved geometry and detection efficiency relative to the unground peat.

(iv) Sample Sets

Gamma spectra of the cores were recorded.

Two core sets were obtained:-

Set 1 - Fenwick Moor Peat - October 1989

Darleith soil - October 1989

Dreghorn soil - October 1989

Inverness Peat - July 1989

Borders Peat - July 1989

Set 2 - Inverness Peat - July 1990

Four cores taken from a transect running from the top of the hill site downwards to drainage stream.

The data from set 1 were used to draw comparisons between the behaviour of the radionuclides in soils of varying origin and also between similar peat soils from differing geographical locations. The results from Set 2 were used to determine the effect of topography upon caesium and lead mobility both vertically and laterally.

The mathematical treatment of the gamma

spectroscopy data was undertaken in several stages as discussed in Chapter 4.

2.5 Sorption/Desorption Methods

Experiments were carried out in order to examine the binding of metal ions to the soil. In addition, the reversibility of the isotherm was examined by measuring the desorption curve following an initial equilibration with a solution of the metal under study.

A general method will be outlined here. This method was modified for several of the experiments in order to examine the effects of changing parameters such as time, background electrolyte, metal concentration range and pH.

The use of two methods of analysis was fundamental to this experimental section. Flame emission spectroscopy (FES) for caesium (and potassium in cation exchange measurements), where the intensity of radiation emitted by an atomic species is measured after excitation of the species by the heat in a flame; and atomic absorption spectroscopy (AAS) for lead, where the amount of radiation absorbed by an atomic species is measured. The radiation source used for AAS was a lead, hollow cathode lamp. The operating conditions for the Perkin Elmer 1100B spectrophotometer used are given in Table 2.4 below.

Table 2.4 Operating conditions for the Perkin Elmer 1100B Spectrophotometer.

Element	Technique	Fuel/Oxidant	Wavelength nm	Slit Width nm
caesium	FES	acetylene/air	852.1	0.4
potassium	FES	acetylene/air	766.5	0.4
lead	AAS	acetylene/air	283.3	0.7

2.5.1 Sorption Isotherms

Six 5.00 g samples of sieved, air-dried soil were weighed into 4 oz screw cap bottles, which had been previously soaked in a 'Decon' solution, steeped in 0.01 M nitric acid and then rinsed several times with distilled water in order to prevent contamination and to minimise the sorption of metal ions onto the glass. A set of standard solutions of the metals was made using Analar quality metal salts in 0.01 M CaCl₂ as background electrolyte solution. The concentration of background electrolyte was maintained at a constant level in order to prevent competition for ion exchange sites with the metal under study and to prevent changes in ionic strength occurring.

50 ml of the standard solutions containing varying M^{n+} concentrations were added by pipette to each bottle. An example set is given below:-

<u>Weight soil (g)</u>	<u>Solution (50 ml)</u>
5.00	0 mM Cs^+ in 0.01 M $CaCl_2$
5.00	0.5 mM " " "
5.00	1.0 mM " " "
5.00	2.0 mM " " "
5.00	3.0 mM " " "
5.00	5.0 mM " " "

The bottles were shaken for a given time (as specified in the following experiments) on an end-over-end shaker and then filtered through Whatman No.40 filter paper.

The filtrate was analysed for the remaining metal ions on a Perkin Elmer 1100B AA spectrophotometer in flame emission mode, calibrated using 'Spectrosol' standards.

The data from these experiments are presented as isotherm plots of gain of metal ion by the soil versus equilibrium concentration of metal ion in solution.

$$\text{Gain} = \frac{\text{weight of initial } M^{n+} - \text{weight final } M^{n+}}{\text{weight of soil} \times \text{conversion factor}}$$

Distribution coefficients (K_D) were also calculated for several data sets using the relationship:-

$$K_d = \frac{\text{amount } M^{n+} / \text{ gram air dry soil}}{\text{amount } M^{n+} / \text{ ml of solution}}$$

These thermodynamic values can be affected by variations in temperature, variations in amounts of solid phase and the processes involved in binding the ion onto sites on the sorbent. However, the use of K_d values is helpful in assessing and predicting metal solubilities in well-defined systems.

The data were also applied to different isotherm equations in order to assess their suitability for describing the observed metal sorption.

2.5.2 Desorption Isotherms

1.00 g of soil was weighed into each of five 4 oz bottles, and to each 10 ml of the metal standard used for the highest point on the adsorption curve was added by pipette e.g 5 mM CsCl in 0.01 M CaCl₂. The bottles were shaken for a given time T_1 (specific shaking times are given in section 2.5.3) on an end-over-end shaker and then the following additions of background electrolyte were added as in the example scheme below:-

<u>Weight Soil (g)</u>	<u>Initial Addition</u>	<u>After time T_1</u>
1.00	10 mlx5 mM Cs ⁺ in CaCl ₂	0 mlx0.01 M CaCl ₂
1.00	" "	10 ml "
1.00	" "	25 ml "
1.00	" "	50 ml "
1.00	" "	100 ml "

The samples were shaken for further time 'T₂', then filtered through Whatman No. 40 filter paper. The filtrate was analysed as for the adsorption curves.

Analysis and interpretation of desorption data can be approached in several ways and these are addressed in Chapter 5. However, the majority of the desorption data in this chapter are presented in conjunction with adsorption data using a basic gain versus solution equilibrium concentration plot.

2.5.3 Method Modifications

(a) Sorption vs Soil Physical Characteristics

The basic adsorption isotherm was obtained for 13 soils using the following parameters:-

Cs⁺ concentration 0-5 mM

Background electrolyte 0.01 M CaCl₂

Sorption time 1 hour and 24 hours

The object of this experiment was to obtain a large data set to allow correlation analysis with the soils physical characteristics to be undertaken.

(b) Adsorption/Desorption Isotherms

A sub group of four soils: Darleith A, Dreghorn A, Peaty Gley 0 and Humic Gley 0, was used to obtain adsorption/desorption isotherms with the same parameters as (a) with sorption times of 1 hour, 24 hours and 1 week. In this instance the same times were

used for desorption (i.e sorption for 24 hours, desorption for 24 hours).

(c) Extended Time Sorption Experiment

For each of the four soils in the sub-group, 33 replicate 4 oz polyethylene bottles were made up containing 5.00 g of air-dried soil suspended in 50 ml of 5 mM CsCl made up in 0.01 M CaCl₂. The bottles were placed in a temperature controlled room (16-20°C). Twenty four hours prior to the assigned analysis time three randomly selected bottles of each soil were placed on an end-over-end shaker and shaken until the analysis time. At the same time the remaining bottles were shaken by hand to resuspend the soil. The bottles were prepared for analysis by filtering through no.40 filter paper and the concentration of Cs⁺ in the filtrate was determined by flame emission.

(d) Effect of Background Electrolyte

For two representative soils (Dreghorn A and Peaty Gley 0) adsorption isotherms were run, with 0.01 M KCl, 0.01 M NaCl and 0.01 M CaCl₂ as background electrolytes in order to compare the effects of changing the swamping ion upon caesium sorption and desorption.

(e) Adsorption/Desorption Isotherms for Caesium at low concentrations

Due to the low concentrations of caesium in soil

solution, experiments were carried out in order to examine laboratory findings which might more realistically be applied to the terrestrial environment. Coleman et al. (1963a) considered levels of <1 mM to be appropriate.

Experimental parameters

[CsCl] - 0 - 50 mg l⁻¹ (0-0.4 mM)

Ratio soil/liquid for sorption step - 1:25

Background electrolyte - 0.05 M NaCl

Adsorption time - 24 hours

Desorption time - 1 hour

pH - 3, 5, or 7

Soils - Darleith, Dreghorn and Peat

(f) Adsorption/Desorption Isotherms for lead at low concentrations

A comparable experiment to (e) was carried out for lead in order to examine the behaviour of a divalent metal and to compare it with the findings for caesium. Some modifications were made to the experimental parameters due to the ability of lead ions to bind to the glass walls of the bottles used, despite precautions such as pre-experiment steeping in nitric acid.

Experimental Parameters

[Pb(NO₃)₂]- 0 - 50 mg l⁻¹

Background electrolyte - 0.05 M NaCl

Adsorption time 1 hour, 24 hours pH 3 only

Desorption time 1 hour

pH - 3, 5 or 7

Soils - Darleith, Dreghorn and Peat

(g) Desorption Isotherms for Caesium and Lead

Two alternative methods for examining the desorption behaviour of these metals in greater detail were used to attempt to find a more meaningful method of presenting the data. Long sorption times were used to ensure that equilibrium had been achieved, especially for lead. Due to the length of the experiment the lead isotherms were carried out at pH 3 to prevent large losses of ions by adsorption to the glass bottle walls. Caesium experiments were carried out at the natural pH of the soil. As the degree of sorption may be dependent upon the quantity of soil present it was decided to use equivalent amounts of soil for both adsorption and desorption sets. Caesium data were collected for Darleith soil, Dreghorn soil, Peat, Bentonite, Illite and Kaolinite whereas lead isotherms were obtained only for the three soils. This was due to the high affinity of lead for the clays resulting in extremely low solution concentrations and thereby rendering analysis for lead ions by flame absorption impossible.

Part 1 Experimental Parameters

Soil: solution - 0.4 g : 10 ml

[Mⁿ⁺] - 0-50 mg l⁻¹ for adsorption curve

Background electrolyte 0.05 M NaCl

Desorption curve - 50 mg l⁻¹ Mⁿ⁺ initial addition

Dilutions - 0, 2, 5, 7, 10, 25, 50 and 100 ml of NaCl

Adsorption time - 3 days

Desorption time - 3 hours

Part 2

Three sets of five replicate bottles were made containing 0.4 g of soil and 10 ml of the appropriate standard. The following treatments were carried out as outlined below:-

	[M ⁿ⁺]	Ads.Time	Dilution(ml NaCl)	Des.Time
Set A	0	3 days	0	0
	10	"	"	"
	20	"	"	"
	30	"	"	"
	50	"	"	"
Set B	0	3 days	10	3 hrs
	10	"	10	"
	20	"	10	"
	30	"	10	"
	50	"	10	"
Set C	0	3 days	100	3 hrs
	10	"	100	3 hrs
	20	"	100	3 hrs

30	"	100	3 hrs
50	"	100	3 hrs

The soils were filtered and analysed, caesium by flame emission and lead by flame absorption.

The results of Section 2.5 are given in Chapter 5.

2.6 Organic Matter Analysis

2.6.1 The Isolation and Characterisation of Humic and Fulvic Acids.

The method selected for humic and fulvic acid extraction was modified from Stevenson (1982). Extractions were carried out on several peat samples in order to compare the extracts for any major structural and chemical differences. The samples used were:- Fenwick Moor Peat, Borders Peat and Inverness Peat. More extensive details about these peats and their sample sites can be found in section 2.1.

(1) Extraction Method:-

20g of air-dried peat was treated with 500 ml of 0.1 M HCl, mixed thoroughly and filtered. The acid-washed sample was placed into a large glass beaker, covered with 200ml of 0.5M NaOH and stirred with a magnetic stirrer bar for 12 hours. The dark coloured supernatant was decanted and filtered through glass wool. The extraction step was repeated for the residue. Concentrated HCl was added to the total supernatant to lower the pH to 1.0 and the precipitated humic acid was allowed to settle. The liquid phase (fulvic acid) was separated and evaporated to dryness in air. The humic acid was placed into 250 ml centrifuge bottles and centrifuged to remove any remaining liquid. The humic

acid was redissolved in 0.5 M NaOH, reprecipitated by adjusting the pH to 1 with HCl and then centrifuged. The centrifuged liquid was retained in each case and added to the original fulvic acid extract. This purification step was repeated a second time and then the humic acid was washed several times with distilled water to remove excess impurities. The humic acid was dried by evaporation, ground to a powder and then further dried in a vacuum oven.

Small scale extractions were carried out for most samples except Fenwick Moor Peat where 1 kg of peat was used to obtain a bulk sample for experimentation in sections 6.2 - 6.3.

(ii) The Characterisation of Humic and Fulvic Acids

The fulvic and humic extracts were characterised by the following techniques:-

(a) Infra red spectroscopy

0.7 mg of vacuum dried sample was prepared for analysis by mixing with 300 mg of KBr and pressed into a disc.

(b) Ultra violet spectroscopy - 2-4 mg of sample was dissolved in 10 ml of 0.05 M NaHCO₃. The U.V spectra were scanned and the absorbances obtained at 465 and 665 nm.

(iii) Microanalysis for carbon, hydrogen, nitrogen and oxygen.

2.6.2 Infra Red Spectroscopy Analysis of Humic Acid/Metal Interactions.

The method adopted in this section was a modified version of that of Piccolo and Stevenson (1982).

Initially, it was necessary to convert the Fenwick Moor Peat humic acid extract into its fully protonated form and this was carried out using the scheme below.

(i) The protonation of humic acid

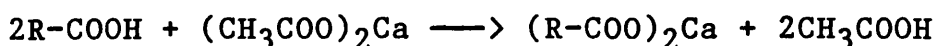
1 gram of sample was dissolved in 200 ml 0.1 M NaOH under nitrogen. The solution was immediately diluted with 300 ml of distilled water and neutralised to pH 7. The sample was dialysed extensively with distilled water to remove excess ions. The Na-humate was then protonated by passing it firstly through an anion exchange resin (Dowex 1-X8, OH⁻ form) and then through a cation exchange resin (Dowex 50-X8, H⁺ form). The final volume was then adjusted to 1 litre with distilled water.

(ii) The carboxylic acid group content of humic acid

The protonated sample was analysed for its acid content due to the presence of carboxylic groups by the Ca-acetate method (Stevenson, 1982) outlined below.

To between 50 and 100 mg of humic acid, 10 ml of 1 N (CH₃COO)₂Ca solution was added together with 40 ml of CO₂-free distilled water. A similar blank was set up

containing no humic acid. The samples were shaken for 24 hours at room temperature, then the residue was filtered and washed with CO₂-free distilled water. The filtrate and washings were combined and titrated potentiometrically with 0.1 N NaOH to pH 9.8.

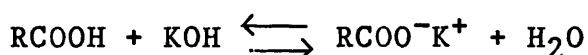


$$COOH = \frac{(V_s - V_b) \times N \times 10^3}{\text{mg of sample}}$$

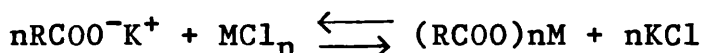
where V_s is the volume of standard base used for the sample and V_b is the volume of standard base used for the blank and N is the normality of the base.

(iii) Humic acid/metal interactions

The following procedure was carried out on replicate 10 ml aliquots of the protonated humic acid solution:- pH was adjusted to 5.0 with 0.05 M KOH; to each sample an amount of metal chloride solution was added so that the ratio of meq M⁺ : meq H⁺ fell within the range 0.1 - 1.5; the pH was readjusted to 5.0 with 0.05 M KOH; air dried and ground to a fine powder, vacuum dried and stored in a vacuum desiccator until analysed. Analysis of each sample was carried out by I.R spectroscopy using the fully protonated humic acid, the partial potassium humate salt (pH 5) and the fully converted potassium humate salt (pH 10) as references. The reactions involved in forming these standard samples can be explained by the following equations.



sample titrated to pH 5



addition of metal ion

IR spectra were obtained for a range of metal: humate complexes including: caesium; lead; magnesium; zinc; copper(II) and strontium. The metals were selected on the basis of their environmental importance both radiologically and toxicologically and also in order to give a range of Lewis acid strengths to enable the examination of functional site specificity.

2.6.3 Potentiometric Titrations of Humic Acid

In order to obtain values for the conditional stability constants for a range of radionuclides a modified potentiometric titration method was adopted. The method was devised by Stevenson (1977) in order to alleviate a problem he had experienced in his earlier research (Stevenson 1976a & b). The titration curves obtained in these studies featured horizontal displacement in the presence of metal ions due to the release of protons from an otherwise non-titratable weak acid group. The modified experimental method involved sequential additions of metal ions to solutions of humic acid at constant pH. The resultant drop in pH was due to the release of protons from participating reactive groups. Base titration was carried out under N_2 with CO_2 -free potassium hydroxide in order to return

the solution to its initial pH. The initial pH was varied by mixing, in a range of proportions, the fully protonated humic acid and the neutralised potassium humate salt, allowing the effect of pH on stability to be studied. The effect of variable ionic strength was also determined by altering the strength of the supporting electrolyte.

The humic acid extract was prepared for analysis by dissolving about 1 g of the dried HA in 500 ml of 0.01 M KOH under N₂ gas. The resulting K-humate was then neutralised to pH 7 and extensively dialysed against distilled water for 3-4 days with frequent changes of water, to remove excess salts and mineral acids. Half of the K-humate was then converted to the fully protonated humic acid by passing through ion exchange columns. Use of resins prevented the protonation of NH₂ and OH groups and the addition of excess mineral acid which accompanies methods relying on the depression of pH to less than 4 for protonation (Posner, 1964; Stevenson, 1982).

Titration curves were obtained for the humic acids as described by Stevenson (1976b). The stable metal salts of the radionuclides under study were used in all cases. Successive additions of metal ions were made at selected points along the titration curves (Stevenson 1976b, 1977) with the pH being returned to the initial starting point after each addition by

titration with CO₂-free 0.1 M KOH. All titrations were carried out at room temperature inside a N₂ glove bag to prevent contamination of solutions with CO₂.

(i) Base Titrations with Humic Acid

Values for pKa and 'n' (the average number of ligand molecules) were obtained for the humic acid solutions used by applying titration results to the Henderson-Hasselbach equation.

$$\text{pH} = \text{pKa} - n \log[(\text{HA} / \text{A}^-)] \quad (1)$$

(ii) Calculation of Stability Constants.

The method of Bjerrum (1941) as modified by Gregor et al. (1955) and further modified by van Dijk(1971) and Stevenson (1977) was adopted for the determination of stability constants. The approach is based upon the competition between metal ions and protons for reactive sites upon the ligand. The reactions outlined below are for the two step reaction path of divalent metal ions however they were modified to a form appropriate for monovalent ions as required.



Constants b1 and b2 can be expressed as :-

$$b_1 = \frac{(MA^+)(H^+)}{(HA)(M^{2+})} \quad (4) \qquad b_2 = \frac{(MA_2)(H^+)}{(HA)(MA^+)} \quad (5)$$

The overall constant B_2 is given by:-

$$B_2 = b_1 \cdot b_2 = \frac{(MA_2)(H^+)^2}{(HA)^2(M^{2+})} \quad (6)$$

The potentiometric method requires the determination of (A^-) , the concentration of free chelating species, and ' \bar{n} ', the average number of ligand molecules per metal ion. ' \bar{n} ' is Bjerrum's formation function and can be calculated from :-

$$\bar{n} = \frac{(A_t) - (HA) - (A^-)}{(M_t)} = \frac{(MA) + 2(MA_2)}{(HA)^2(M^{2+})} \quad (7)$$

where A_t and M_t are the overall concentrations of ligand and metal ion, respectively. The formation function, ' \bar{n} ', is related to the stability constant through the relationship :-

$$\sum_{n=0}^{n=N} (\bar{n} - n) B_n (HA / H^+)^n = 0 \quad (8)$$

For divalent ions this simplifies to :-

$$\frac{\bar{n}}{(n-1)(HA/H^+)} = \frac{(2-n)(HA/H^+)}{(n-1)} \cdot B_2 - b_1 \quad (9)$$

hence allowing the calculation of B_2 .

In order to calculate ' \bar{n} ' from (7) using experimental data it was necessary to use the following calculation

steps . In the absence of metal ions where K_i is the ionisation constant of the humic acid at any given pH and (KOH) is the amount of base consumed during titration :-

$$A_t = (HA) + (KOH) + (H^+) - (OH^-) \quad (10)$$

$$(A^-) = (KOH) + (H^+) - (OH^-) \quad (11)$$

$$K_i = \frac{(A^-).(H^+)}{(HA)} \quad (12)$$

The conservation equation following additions of metal is :-

$$A_t = (HA) + (A^-) + (MA^+) + 2(MA_2) \quad (13)$$

The quantity $(MA^+ + 2MA_2)$ is obtained by titration of the H^+ liberated by the addition of metal ion (pH returned to initial starting position), from which $(HA) + (A^-)$, or T, could be calculated:-

$$T = (HA) + (A^-) = A_t - (MA^+ + MA_2) \quad (14)$$

A_t refers to the total content of undissociated acidic groups (HA) at the pH at which the measurements were made . Assuming that chelation does not alter the dissociation relationship of the humic acid :-

$$(HA) = \frac{T . (H^+)}{K_i + (H^+)} \quad (15)$$

The above permits calculation of (HA/H^+) and hence ' \bar{n} '. B_2 can now be determined and subsequently K_2 (the conditional stability constant calculated using ion exchange methods) which is related to B_2 by the formula

$$b_j = K_i . k_j \quad (16)$$

2.6.4 The Effects of Humic Acid/Clay Interactions upon Caesium Sorption and Desorption.

The methods used to examine clay/humic matter interactions were modified from those of Xu et al (1989). Three clays were used as adsorbents; BDH Kaolin Light, BDH Bentonite Technical and Clay Mineral Standard Fithian Illite number 35 (Ward's Natural Science Establishment, Rochester, N.Y.). The structures and properties of these clays have been detailed in section 2.1. A 0.05 M solution of BDH Analar grade NaCl was used as the aqueous phase, and the pH adjusted to 3,5 or 7 as required with a few drops of concentrated NaOH and HCl. BDH Spectrosol quality CsCl was used for the caesium stock solution.

The experiment was designed to study the effects of the addition of humic acid on sorption and desorption by the clays.

In all cases, 0.2 g of clay was suspended in 25 ml of 0.05 M NaCl solution, the pH adjusted to 3, 5 or 7, and left for 2 days prior to the addition of humic acid or caesium. In one set, 50 mg of humic acid and 25 ml of appropriate CsCl solution were then added to give final caesium concentrations of 5,10,15 or 20mg l⁻¹. In the second set, only the humic acid was added at this stage and the system was allowed to pre-equilibrate for a further 5 days before the additions of caesium were made. When discussing the results in Section 6.3, the

first set is referred to as the 2 day treatment and the second as the 7 day treatment. In all cases, once the caesium had been added and the pH re-adjusted to the original values, the samples were shaken on an end-over-end shaker for 2.5 days at 20°C. Following that, the solution phase was separated by filtration through a Whatman No.40 filter paper and the caesium concentration in solution measured by flame emission using a Perkin-Elmer 1100B atomic absorption spectrophotometer.

In the desorption experiment, twelve replicate samples of each clay were suspended for 2 days in 0.05 M NaCl as described above, except that only pH 7 was used. To four samples, CsCl solution was added to give a range of final caesium concentrations up to 50 mg l⁻¹. This allowed measurement of an adsorption isotherm to ensure that equilibration had occurred, and that desorption was from a known starting point. An additional eight samples were prepared at 50 mg l⁻¹ to allow desorption of caesium to be measured. A set containing 50 mg humic acid and a control set with no humic acid was used as before. The range of caesium concentration was extended to 50 mg l⁻¹ to ensure that the caesium concentrations in the diluted solutions could be measured. Once these additions had been made the suspensions were shaken for 2.5 days, after which the caesium concentrations in the solutions of the sorption part of the experiment were measured. The

eight replicates of 50 mg l^{-1} were diluted over a range of dilution factors up to elevenfold, using 0.05 M NaCl at pH 7. Desorption was allowed to proceed over a period of 3 hours after which the caesium concentration in solution was measured and the percentage caesium desorbed was calculated.

The results of the experiments outlined in Section 2.6 are given in Chapter 6.

CHAPTER 3. - SAMPLE CHARACTERISTICS

This short chapter presents data describing the samples used throughout the main body of the thesis.

3.1 Soil Core Samples

The density and moisture content variations with depth for the soil cores and the transect cores are shown in Tables 3.1 and 3.2. The chemical analysis data for the soil cores for pH, organic carbon and available potassium are shown in Tables 3.3.1-3.3.5. These data sets are used in conjunction with gamma spectroscopy data in Chapter 4.

Table 3.1 Dry Density and Moisture Variations in Core Samples in Data Set 1

Depth (cm)	Inverness '89		Borders		Fenwick Moor	
	Density g cm ⁻³	Water Content g	Density g cm ⁻³	Water Content g	Density g cm ⁻³	Water Content g
Turf	0.19	214				
0-2	0.27	329	0.20	486	0.17	567
2-4	0.16	480	0.20	518	0.14	567
4-6	0.22	551	0.14	749	0.21	456
6-8	0.30	463	0.13	827	0.40	525
8-10	0.22	565	0.12	911	0.32	614
10-12	0.23	608	0.11	835	0.35	669
12-14	0.19	652	0.10	982	0.34	567
14-16	0.40	330	0.15	1039	0.31	567
16-18	0.17	660	0.10	1018	0.30	614
18-20	0.26	542	0.12	1018	0.29	567

N.B water content is expressed in terms of the mass of water removed when 100g of oven dried soil was formed from air dried soil.

Table 3.1cont

Depth (cm)	Darleith		Dreghorn	
	Density	Water	Density	Water
	g cm^{-3}	Content	g cm^{-3}	Content
		g		g
0-2	0.32	171	0.51	43
2-4	0.72	102	1.18	22
4-6	0.56	218	1.84	8
6-8	1.01	148	1.93	12
8-10	0.68	188	2.08	13
10-12	0.59	215	1.82	14
12-14	0.50	231	1.71	15
14-16	0.68	359	2.03	15
16-18	0.57	187	1.81	15
18-20	0.44	230	1.91	15

N.B water content is expressed in terms of the mass of water removed when 100g of oven dried soil was formed from air dried soil.

Table 3.2 Dry Density and Moisture Contents of the Inverness'90 Transect Peats

Depth (cm)	Core A		Core B	
	Density g cm ⁻³	Water Content g	Density g cm ⁻³	Water Content g
0-2	0.38	400	0.62	270
2-4	0.35	355	0.42	270
4-6	0.29	317	0.40	233
6-8	0.28	317	0.63	163
8-10	0.29	300	0.43	213
10-12	0.30	270	0.38	178
12-14	0.31	270	0.35	257
14-16	0.26	285	0.53	186
16-18	0.29	300	0.53	178

N.B water content is expressed in terms of the mass of water removed when 100g of oven dried soil was formed from air dried soil.

Table 3.2cont

Depth (cm)	Core C		Core D	
	Density g cm ⁻³	Water Content g	Density g cm ⁻³	Water Content g
0-2	0.38	285	0.40	317
2-4	0.41	213	0.40	317
4-6	0.50	170	0.40	285
6-8	0.41	186	0.40	245
8-10	0.42	178	0.40	233
10-12	0.42	170	0.40	233
12-14	0.44	170	0.40	233
14-16	0.44	170	0.30	257

N.B water content is expressed in terms of the mass of water removed when 100g of oven dried soil was formed from air dried soil.

Table 3.3.1 Chemical and Physical Analysis of Inverness Peat Core

Depth (cm)	pH	Organic % L.O.I.	Available potassium mg .kg ⁻¹
Turf	5.30	96.1	803.3
0-2	4.70	87.8	433.7
2-4	4.30	93.7	454.1
4-6	4.25	95.1	283.3
6-8	4.40	97.0	311.3
8-10	4.30	96.5	233.3
10-12	4.65	97.2	163.2
12-14	4.65	97.9	100.5
14-16	4.40	96.2	47.7
16-18	4.45	98.4	81.2

Table 3.3.2 Chemical and Physical Analysis of Borders Peat Core

Depth (cm)	pH	Organic % L.O.I	Available potassium mg kg ⁻¹
0-2	4.15	94.5	2833
2-4	4.10	88.0	1750
4-6	3.98	94.5	1500
6-8	3.95	94.5	1167
8-10	3.95	95.0	708
10-12	3.92	94.5	517
12-14	3.88	95.0	433
14-16	3.88	95.3	333
16-18	3.88	98.3	242
18-20	3.85	97.4	175

Table 3.3.3 Chemical and Physical Analysis of Fenwick Moor Peat Core

Depth (cm)	pH	Organic % L.O.I	Available potassium mg kg ⁻¹
0-2	3.95	94.5	694.4
2-4	3.20	96.4	748.3
4-6	3.40	90.5	744.6
6-8	3.30	93.3	628.3
8-10	3.35	93.0	500.0
10-12	3.35	93.2	242.3
12-14	3.35	91.4	78.9
14-16	3.35	93.5	33.9
16-18	3.35	89.0	20.2
18-20	3.35	84.9	15.2

Table 3.3.4 Chemical and Physical Analysis of Darleith Soil Core

Depth (cm)	pH	Organic % L.O.I	Available potassium mg kg ⁻¹
0-2	4.40	45.2	1658.3
2-4	4.00	32.7	614.0
4-6	3.85	17.7	275.0
6-8	3.75	17.7	214.1
8-10	3.80	18.0	200.3
10-12	3.90	18.4	192.2
12-14	3.95	16.0	192.0
14-16	3.90	16.1	192.0
16-18	3.90	16.4	183.5

Table 3.3.5 Chemical and Physical Analysis of Dreghorn Soil Core

Depth (cm)	pH	Organic % L.O.I	Available potassium mg kg ⁻¹
0-2	4.70	18.3	141.3
2-4	4.12	16.2	107.3
4-6	4.05	9.0	29.0
6-8	4.10	6.8	11.7
8-10	4.20	6.2	15.7
10-12	4.20	6.7	11.6
12-14	4.35	6.2	12.6
14-16	4.50	6.7	8.6
16-18	4.60	5.4	9.7
18-20	4.65	6.0	7.4

3.2 Characterisation of Soil Samples

The physical and chemical characteristics of the thirteen soil samples analysed are illustrated in Tables 3.4-3.6. These results are discussed in relation to the sorption behaviour of the soils in Chapter 5.

Table 3.4 Chemical and Physical Analysis of Soil 'A' Horizons

Soil Name	pH	Organic %	L.O.I	Cation Exchange Capacity cmol kg ⁻¹
Darleith A	4.80		32.4	51
Dunlop A	5.70		16.5	43
Peaty Gley O	4.05		70.3	101
Humic Gley O	4.20		76.0	142
Fensick Moor Peat	3.70		90.5	80
Dreghorn A	5.45		5.4	14
Bargour A	5.60		7.3	20

Table 3.5 Chemical and Physical Analysis of Soil 'B' Horizons

Soil Name	pH	Organic % L.O.I	Cation Exchange Capacity cmol Kg ⁻¹
Darleith B	6.15	8.2	30
Dunlop B	4.80	9.0	35
Peaty Gley Bg	4.50	12.2	37
Humic Gley Bg	5.15	22.5	9
Dreghorn B	6.33	2.5	9
Bargour B	6.10	3.3	12

Table 3.6 Particle Size Fractionation of a Selected Sub-set of Soils

Soil Name	Coarse Sand %	Fine Sand %	Silt and Clay %	Organic Matter %
Darleith A	25.2	8.4	34.9	32.4
Dreghorn A	59.0	15.3	14.8	5.6
Peaty Gley O	5.1	7.5	14.2	70.3
Humic Gley O	1.1	4.5	12.4	76.0

N.B Values do not add up to 100% due to losses which occur during experimentation.

3.3 Characterisation of Humic and Fulvic Acids

(a) Sample Extraction

Humic acid samples were successfully extracted from all the samples, giving a narrow range of yields of 20% for Fenwick Moor Peat, 21% for Borders Peat and 19% for Inverness Peat. The extractions of fulvic acid resulted in yields of less than 1% for all samples and the resulting product was brittle and glassy and therefore difficult to work with. Due to this, apart from initial investigations, the majority of the work in Chapter 6 was carried out upon humic acid (HA).

b) Sample Characterisation

i) Infra-red analysis was carried out for all samples. The spectra are presented in Figures 3.1 and 3.2 . All the spectra exhibited similarities, with peaks present at a number of characteristic wavelengths. It was apparent that the spectra of humic and fulvic acids differ, as expected, due to the greater degree of humification in humic acid and hence the lower relative concentration of carboxyl groups to H-C bonds, both aliphatic and aromatic. The major features of Fenwick Moor Peat humic and fulvic acids have been described in Table 3.7.1 and 3.7.2 as an illustration.

Using the classification scheme of Stevenson and

Goh (1971), the spectra fall into the categories of:-

Type I - strong bands near 3400, 2900, 1720, 1600 and 1200 cm^{-1} . The 1600 band being approximately equal to the 1720 cm^{-1} band in intensity, typical of the spectra of humic acid.
Type II - very strong adsorption around 1720 cm^{-1} and weak at 1600 cm^{-1} , typical of the fulvic acid spectra,

As all of the humic acids studied gave similar spectra, only the Fenwick Moor Peat was used in the studies described in Chapter 6.

(c) Ultra-violet analysis

Ultra-violet analysis was carried out using 2mg of each sample. The absorbances at 465 and 665nm were recorded and the E_4/E_6 were calculated. These data are presented in Table 3.8. It is thought that this ratio decreases with increasing molecular weight and condensation and is believed to serve as an index of humification (Stevenson, 1982). The values obtained for the humic acids fall in the quoted range of values found within the literature of <5.0, however the fulvic acid values lay within the range 2 - 3.5 instead of the literature range of 6.0 - 8.5. This could be due to the difficulty experienced in dissolving the fulvic acid sample for analysis, hence rendering the data invalid.

(d) Microanalysis of Humic and Fulvic Acids

Microanalysis data were collected for all samples (Table 3.9). The results illustrate the greater degree of humification of humic acids with higher carbon contents and lower oxygen contents than the fulvic acids.

Fig. 3.1 Infra-red Spectra of Peat Humic Acids

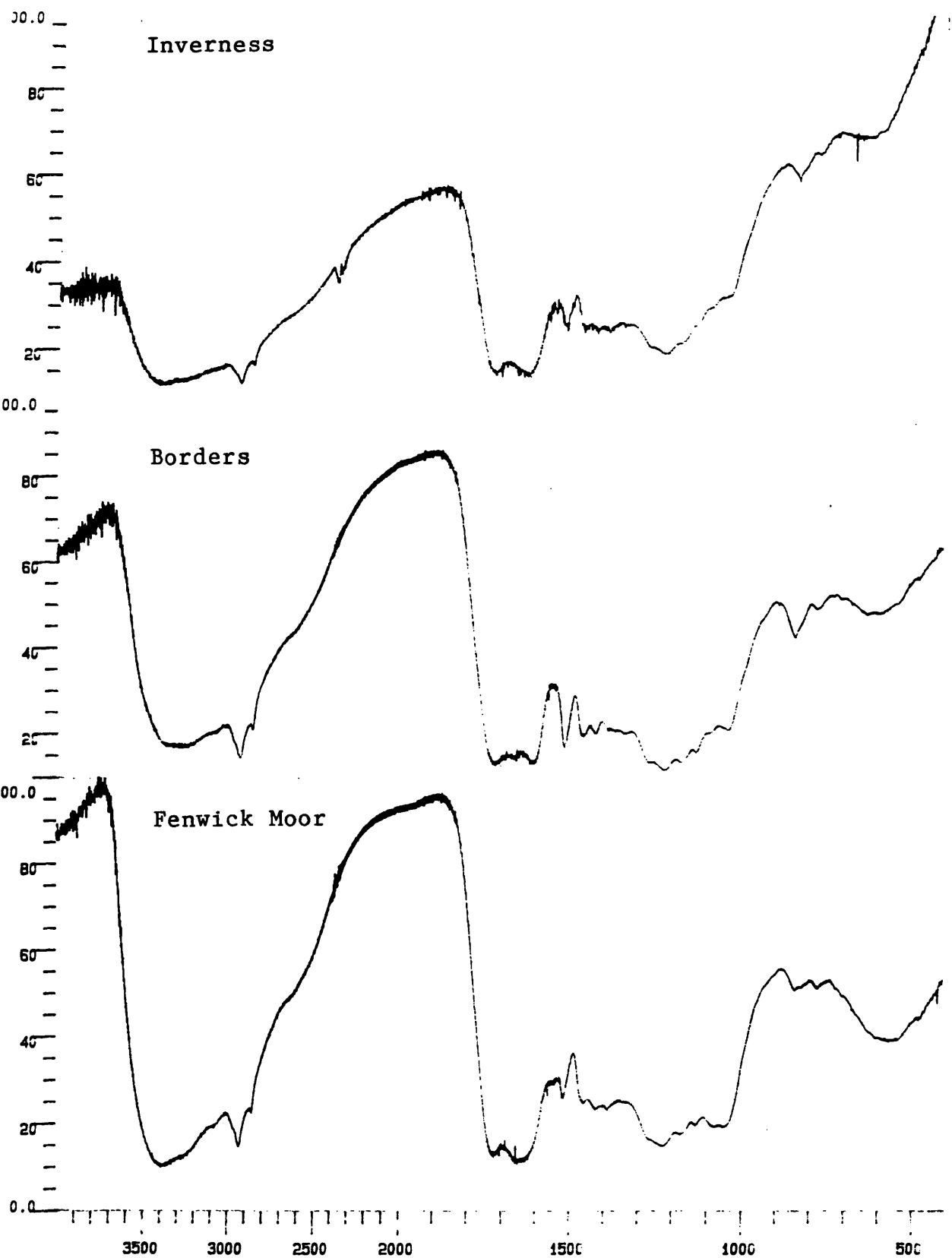


Fig. 3.2 Infra-red spectra of Peat Fulvic Acids

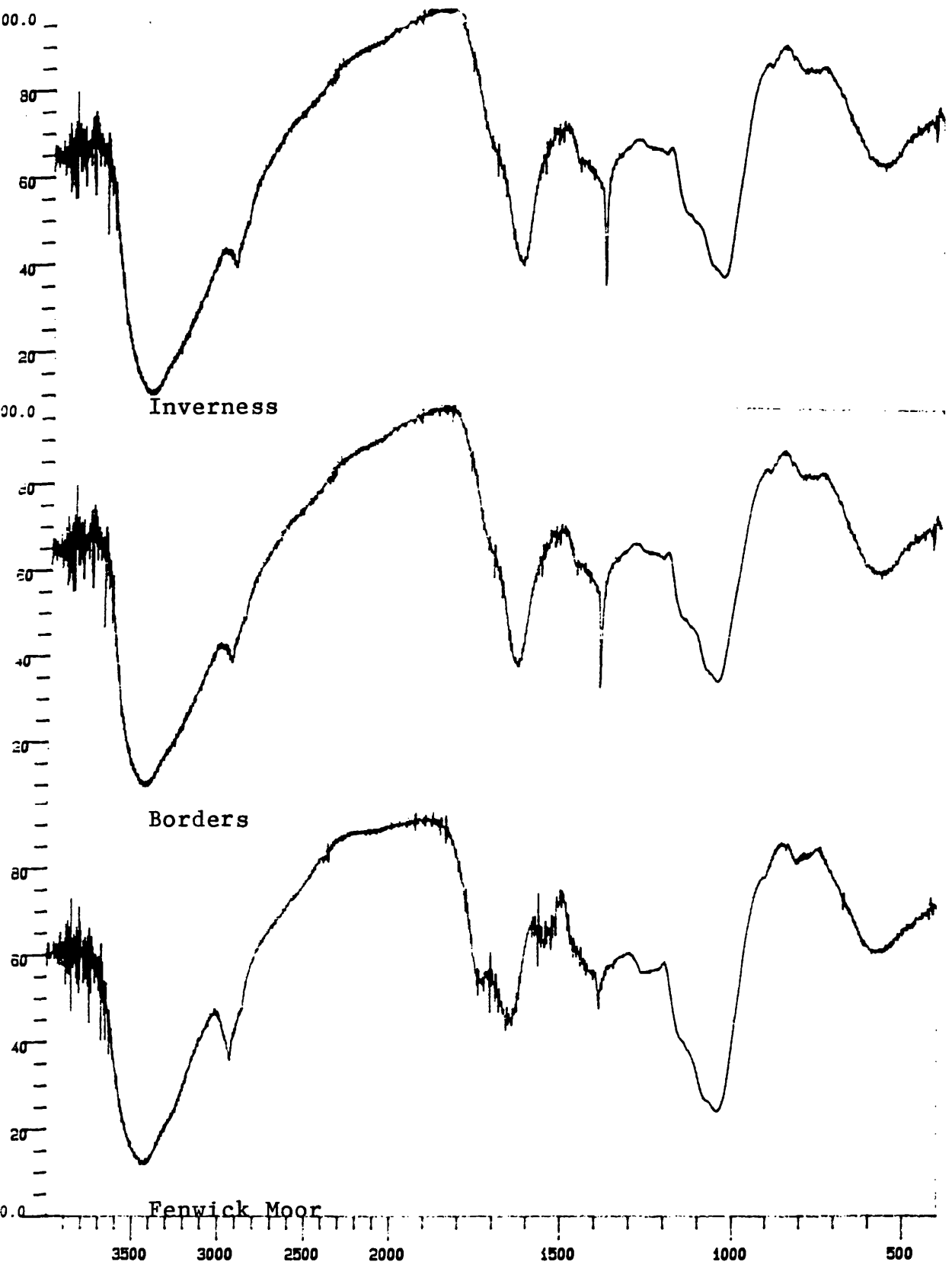


Table 3.7.1 Infra-Red Analysis of Fenwick Moor Peat Humic Acid Extract

Peak (cm^{-1})	Identification
3380	H-bonded OH groups
2930	Aliphatic C-H stretch
2855	Aliphatic C-H stretch
1736-1730	C=O stretch of COOH and ketonic C=O
1660-1600	C=O stretch of amides, quinones and H bonded conjugated ketones
1617	Aromatic C=C or H bonded C=O of conjugated ketones
1510	Aromatic C=C, amides
1385	OH deformation, C-O stretch of phenolic OH, CH deformation of CH_2 , CH_3 , COO^- antisymmetric stretch
1221	C-O stretch and OH deformation of COOH
1046	C-O stretch polysaccharides

Table 3.7.2 Infra-red Analysis of Fenwick Moor Peat Fulvic Acid Extract

Peak(cm^{-1})	Identification
3418	O-H stretch
2926	Aliphatic C-H stretch
1750-1600	C=O of amides, quinones, conjugated ketones, C=C aromatic
1460-1450	Aliphatic C-H
1400	OH deformation, C-O stretch phenolic, C-H deformation
1255	C-O stretch, OH deformation of COOH
1040	C-O stretch polysaccharides

Table 3.8 Ultra-violet Analysis of Humic and Fulvic Acids

Sample	Absorbance 465nm	Absorbance 665nm	E4/E6
<u>Fenwick Moor</u>			
Humic	0.160	0.145	4.21
Fulvic	0.144	0.059	2.44
<u>Borders</u>			
Humic	0.903	0.187	4.83
Fulvic	0.345	0.108	3.19
<u>Inverness</u>			
Humic	0.816	0.176	4.64
Fulvic	0.224	0.078	2.87

Table 3.9 Microanalysis of Humic and Fulvic Acids

Sample	% Carbon	% Hydrogen	% Nitrogen	% Oxygen
<u>Fenwick</u>				
<u>Moor</u>				
Humic	46.92	4.86	3.23	45.00
Fulvic	39.81	5.59	2.41	52.19
<u>Borders</u>				
Humic	55.69	4.91	2.95	36.45
Fulvic	29.51	3.93	1.23	65.33
<u>Inverness</u>				
Humic	54.03	4.87	2.93	38.17
Fulvic	40.24	4.17	1.61	53.98

CHAPTER 4 - RADIONUCLIDE MOBILITY IN PEAT AND SOIL

CORES

4.1 Introduction

The aim of this part of the study was to undertake analysis of peat and soil cores in order to examine the environmental behaviour of radiocaesium and ^{210}Pb within the terrestrial ecosystem.

The reasons for selecting radiocaesium and ^{210}Pb for study have been discussed fully in Chapter 1. In summary, the observed behaviour of radiocaesium, post-Chernobyl, in upland organic soils, has highlighted a high degree of mobility and availability (Livens and Loveland, 1988; Livens and Rimmer, 1988; Sugden et al., 1991). If models are to be constructed to allow predictions of environmental behaviour in the event of future Chernobyl-type accidents or for environmental impact assessment for radioactive waste disposal (McKinley and Hadderman, 1985; Hunt and Kershaw, 1990; Scott et al., 1991), it is essential that the environmental behaviour of radionuclides such as ^{137}Cs should be studied extensively and understood. The radiocaesium isotopes ^{134}Cs and ^{137}Cs , had a characteristic activity ratio in Chernobyl fallout of 0.55 (McDonald et al., 1992). This enables the mathematical calculation of the two components of

radiocaesium in soils i.e that of nuclear weapons testing fallout (mainly in the late 1950's and early 1960's and containing no ^{134}Cs) and Chernobyl fallout. ^{210}Pb has been used as a dating technique with success within aquatic sediments and this method has been applied to some soils (see section 1.2.3) in order to obtain sedimentation rates. ^{210}Pb activities were measured at all of the sites for this purpose. This enabled comparisons to be made between the radiocaesium distributions and the ^{210}Pb chronology, to investigate ^{137}Cs mobility. The calculation of total inventories for these radionuclides at each site also enabled relationships between rainfall, geographical location and deposition to be examined.

4.2 Results of the Gamma Analysis of Sample Set 1

This data set includes the following cores: Inverness '89 Peat, Borders Peat, Fenwick Moor Peat, Darleith Soil, and Dreghorn Soil. Descriptions of the sampling sites can be found in Section 2.1 and values for dry density, moisture content, pH, organic matter and available potassium content are tabulated in section 3.1. These cores were collected during the period July - October 1989.

4.2.1 ^{210}Pb :

^{210}Pb activities for the five cores in Sample set 1 are presented in Tables 4.1.1-4.1.5. In the case of the peat cores, all the ^{210}Pb present was unsupported but this was not true for the mineral soils where ^{210}Pb supported by ^{226}Ra was present. It was possible in both the Darleith and Dreghorn profiles to identify the depth below which only the supported ^{210}Pb was present and to calculate a mean value for the supported activity. This value was then subtracted from the total ^{210}Pb to estimate the excess ^{210}Pb activities.

The excess ^{210}Pb activities are presented in terms of Bq kg^{-1} and Bq m^{-2} and from the latter it is possible to calculate the total inventories of excess ^{210}Pb to the maximum sampling depth of 20cm. These values are presented in Table 4.2 together with the flux of excess ^{210}Pb calculated for each site.

Graphical representations of the data (Figs. 4.1.1-4.1.5) in terms of depth(cm) versus $\ln(\text{excess } ^{210}\text{Pb})$ enabled the calculation, where appropriate, of sedimentation rates for the peats. These results are summarised in Table 4.3. Where a mixing zone was evident, the sedimentation rate was calculated using the lower portion of the profile where an exponential decrease in unsupported ^{210}Pb with increasing depth was observed (see section 13.3). The calculations were repeated for the data plotted in terms of cumulative weight to mid-section(g cm^{-2}) versus $\ln(\text{excess } ^{210}\text{Pb})$ and these results are summarised in Table 4.4.

4.2.2 Radiocaesium

Radiocaesium activities for the five cores are presented in Tables 4.5 - 4.9 and in Graphs 4.2 - 4.6. Inventories are expressed in terms of activity per unit mass (Bq kg^{-1}) and activity per unit area (Bq m^{-2}). Total inventories were calculated for depths of 15 and 20 cm and these results are presented in Table 4.10. Total inventories for the ^{137}Cs components due to weapons testing fallout and Chernobyl fallout were decay corrected to the times of deposition, 1963 and May 1986 respectively. The total ^{137}Cs inventories were decay corrected to the dates of sampling.

The mathematical treatment of the gamma spectroscopy data was undertaken in several stages:

a) Background corrections were made to take into

account any influence from ambient radioactivity (see Section 2.4.1).

$$C(\text{counts/sec.}) = C_{\text{obs.}} - C_{\text{bkd.}}$$

where $C_{\text{obs.}}$ are the number of counts observed for the sample and $C_{\text{bkd.}}$ are the number of counts recorded by any background radiation.

b) The counting data were converted to activities using the appropriate efficiency calibrations.

$$A(\text{Bq}) = (C / \% \text{ efficiency}) \times 100$$

where A is the sample activity

$$\text{Sample Specific Activity (Bq/kg)} = \frac{A}{\text{Sample Weight(kg)}}$$

c) Due to the characteristic $^{134}\text{Cs}/^{137}\text{Cs}$ activity ratio of 0.55 in Chernobyl fallout in May 1986 (McDonald et al., 1992) and the ^{134}Cs contribution being solely of Chernobyl origin, it was possible to separate the ^{137}Cs profile into two components; Chernobyl ^{137}Cs and weapons testing fallout ^{137}Cs .

Using
$$A_t = A_0 \cdot e^{-\lambda t}$$

where:

A_0 is the activity of the radionuclide at a specified time $t=0$.

A_t is the activity of the radionuclide after time, t .

At the time of the Chernobyl accident ($t=0$) it was

known that:

$$\frac{A(^{134}\text{Cs})}{A(^{137}\text{Cs})} = 0.55$$

After a time (t) the radionuclides will have undergone decay, and the decay corrected activity ratio can be expressed as:

$$\frac{A_t(^{134}\text{Cs})}{A_t(^{137}\text{Cs})} = \frac{A_o(^{134}\text{Cs})e^{-\lambda_1 t}}{A_o(^{137}\text{Cs})e^{-\lambda_2 t}} \quad \text{at time } t=t$$

this rearranges to:

$$\frac{A_t(^{134}\text{Cs})}{A_t(^{137}\text{Cs})} = \frac{A_o(^{134}\text{Cs})e^{(\lambda_2 - \lambda_1) \cdot t}}{A_o(^{137}\text{Cs})} \quad \text{at time } t=t$$

If the activity of ^{134}Cs can be measured and as the lambda values are known:

$$^{137}\text{Cs} = 0.0230 \text{ y}^{-1}$$

$$^{134}\text{Cs} = 0.330 \text{ y}^{-1}$$

then the equation can be rearranged to:

$$A_t(^{137}\text{Cs}) = \frac{A_t(^{134}\text{Cs})e^{(0.330 - 0.0230) \cdot t}}{0.55} \text{ Bq}$$

Once the Chernobyl component has been calculated then the proportion of the total ^{137}Cs due to weapons testing can be determined by a simple subtraction step;

$$^{137}\text{Cs}(\text{pre-Chernobyl}) = ^{137}\text{Cs}(\text{total}) - ^{137}\text{Cs}(\text{Chernobyl})$$

d) Graphs of activity(Bq kg⁻¹) versus depth expressed in terms of cumulative weight per square centimetre, in order to account for fluctuations in density, were plotted for ¹³⁷Cs(Chernobyl) and ¹³⁷Cs(weapons testing). In addition, graphs of the activity ratio ¹³⁴Cs/¹³⁷Cs were also plotted in relation to depth. For each profile, the data were decay corrected to the time of sampling and one sigma error bars were plotted for the specific activities.

e) Fick's laws were applied to the caesium data in order to calculate diffusion rates for caesium through the profiles.

$$C = \frac{M \cdot e^{-x/4Dt}}{(\pi \cdot Dt)^{\frac{1}{2}}}$$

Crank (1956)

where C = concentration of the diffusing substance

M = amount of diffusing substance

D = diffusion coefficient

t = time in seconds

x = depth in centimetres

Following the development of Ben Shaban (1989).

if $(M/\pi Dt)^{\frac{1}{2}} = k_1$ at fixed t and D

and $-(1/4Dt) = k_2$

then $\ln C = k_1 - k_2 \cdot x^2$

if $z = x^2$;

$\ln C = k_1 - k_2 \cdot z$

this can now be plotted as a simple linear graph

where calculation of the gradient, $-k_2$, leads simply to D, the diffusion coefficient.

R values were also calculated for these plots to evaluate how well, statistically the data fitted the mathematical model.

Correlations were carried out to identify any relationships between the ^{137}Cs components and factors such as rainfall and excess ^{210}Pb . These results are summarised in Table 4.12.

In the following tables N.D. (not detectable) indicates that levels of radioactivity were below the instruments detection limits.

Table 4.1.1 ^{210}Pb Specific Activities in the Inverness '89 Peat Profile

Depth (cm)	Excess ^{210}Pb Bq kg^{-1}	error Bq kg^{-1}	Excess ^{210}Pb Bq m^{-2}	error Bq m^{-2}
Turf	183	13.4	695	52.6
0-2	181	13.2	977	73.9
2-4	191	10.1	611	62.9
4-6	214	5.4	942	54.2
6-8	141	9.6	846	83.0
8-10	46	3.2	202	7.6
10-12	N.D		N.D	
12-14	N.D		N.D	
14-16	N.D		N.D	
16-18	N.D		N.D	
18-20	N.D		N.D	

Table 4.1.2 ^{210}Pb Specific Activities in the Borders Peat Profile

Depth (cm)	Excess ^{210}Pb Bq kg^{-1}	error Bq kg^{-1}	Excess ^{210}Pb Bq m^{-2}	error Bq m^{-2}
0-2	130	2.9	520	15.5
2-4	163	4.6	652	22.4
4-6	163	2.8	456	12.0
6-8	143	3.3	372	11.3
8-10	138	3.8	331	11.4
10-12	116	2.1	304	8.8
12-14	89	1.6	356	9.1
14-16	62	2.2	186	7.7
16-18	42	2.1	84	2.4
18-20	69	2.4	166	6.7

Table 4.1.3 ^{210}Pb Specific Activities in the Fenwick Moor Peat Profile

Depth (cm)	Excess ^{210}Pb Bq kg^{-1}	error Bq kg^{-1}	Excess ^{210}Pb Bq m^{-2}	error Bq m^{-2}
0-2	200	4.4	680	20.2
2-4	230	5.3	644	19.6
4-6	170	6.3	714	30.0
6-8	80	5.2	640	43.5
8-10	30	0.7	192	5.7
10-12	2	0.1	14	0.7
12-14	N.D		N.D	
14-16	N.D		N.D	
16-18	N.D		N.D	
18-20	N.D		N.D	

Table 4.1.4 ^{210}Pb Specific Activities in the Darleith Soil Profile

Depth (cm)	Total ^{210}Pb Bq kg^{-1}	error Bq kg^{-1}	Excess ^{210}Pb Bq kg^{-1}	error Bq kg^{-1}	Excess ^{210}Pb Bq m^{-2}	error Bq m^{-2}
0-2	111	3.4	84	2.6	538	19.8
2-4	83	2.6	56	1.7	806	29.7
4-6	45	1.9	18	0.8	202	9.4
6-8	31	1.4	4	0.2	81	4.0
8-10	33	1.6	6	0.3	82	2.1
10-12	23	0.9	N.D		N.D	
12-14	41	1.6	14	0.1	140	6.4
14-16	23	1.0	N.D		N.D	
16-18	10	0.5	N.D		N.D	
18-20	N.D		N.D		N.D	

Table 4.1.5 ^{210}Pb Specific Activities in the Dreghorn Soil Profile

Depth (cm)	Total ^{210}Pb Bq kg^{-1}	error Bq kg^{-1}	Excess ^{210}Pb Bq kg^{-1}	error Bq kg^{-1}	Excess ^{210}Pb Bq m^{-2}	error Bq m^{-2}
0-2	34	2.2	27	1.7	275	18.4
2-4	15	0.4	8	0.2	189	6.7
4-6	10	0.3	3	0.1	110	4.2
6-8	5	0.1	N.D		N.D	
8-10	4	0.2	N.D		N.D	
10-12	10	0.4	3	0.1	109	5.3
12-14	4	0.2	N.D		N.D	
14-16	9	0.3	N.D		N.D	
16-18	5	0.2	N.D		N.D	
18-20	10	0.4	3	0.1	115	5.6

Table 4.2 Excess ^{210}Pb Inventories and Fluxes calculated for a sampling depth of 20cm.

	Inventory kBq m^{-2}	Flux $\text{Bq m}^{-2} \text{y}^{-1}$
Inverness '89	4.3	132
Borders	3.4	106
Fenwick Moor	2.9	89
Darleith	1.9	57
Dreghorn	0.8	25

Table 4.3 Sedimentation rates calculated from graphs of $\ln(\text{excess } ^{210}\text{Pb})$ vs depth(cm).

	Depth of mixed zone (cm)	Sedimentation Rate cm y^{-1}	r^2
Inverness '89	0 - 8	0.082	0.94
Borders	0 - 8	0.250	0.98
Fenwick Moor	0 - 4	0.051	0.85

Table 4.4 Sedimentation rates calculated from graphs of $\ln(\text{excess } ^{210}\text{Pb})$ vs cumulative weight to mid section (g cm^{-2}).

	Depth of mixed zone (cm)	Sedimentation Rate $\text{g cm}^{-2} \text{y}^{-1}$	r^2
Inverness '89	0 - 8	0.021	0.88
Borders	0 - 8	0.210	0.10
Fenwick Moor	0 - 4	0.017	0.88

FIG. 4.1 Lead-210 Profiles
FIG. 4.1.1 Inverness Peat

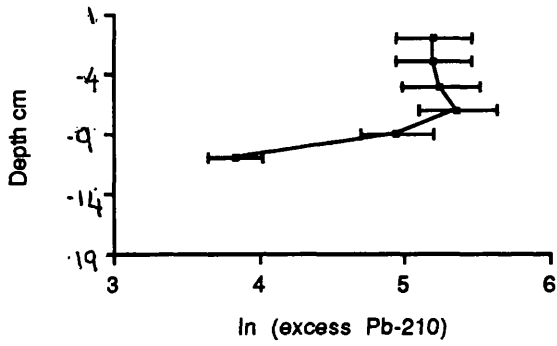


FIG. 4.1.2 Borders Peat

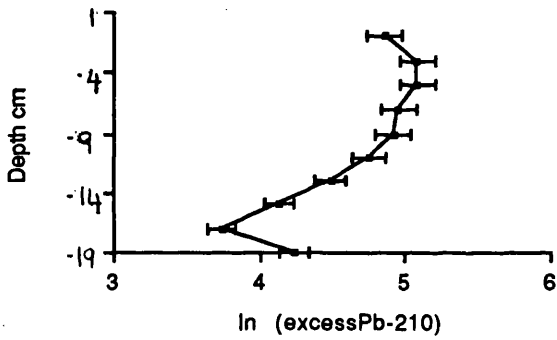


FIG. 4.1.3 Fenwick Moor Peat

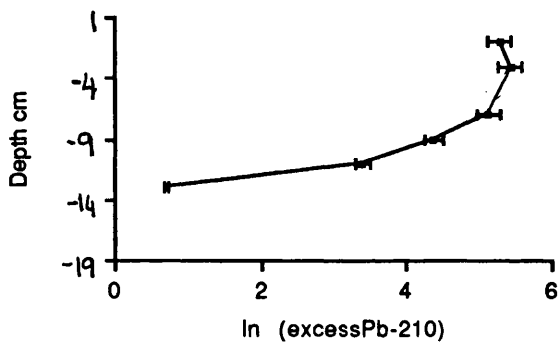


FIG. 4.1.4 Darleith

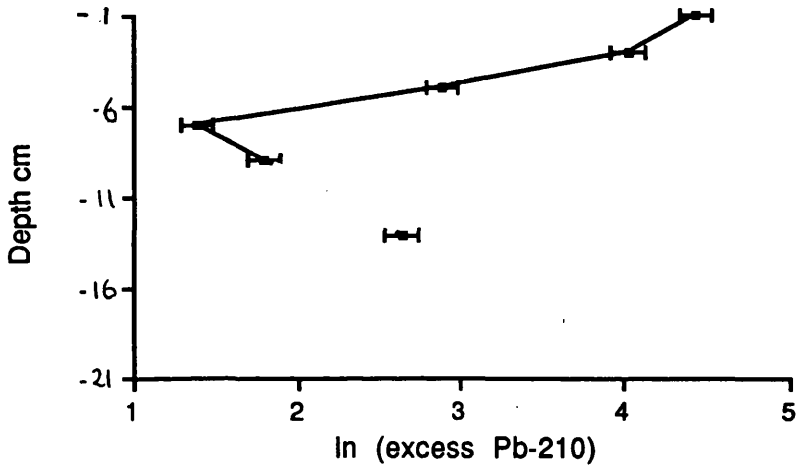


FIG. 4.1.5 Dreghorn

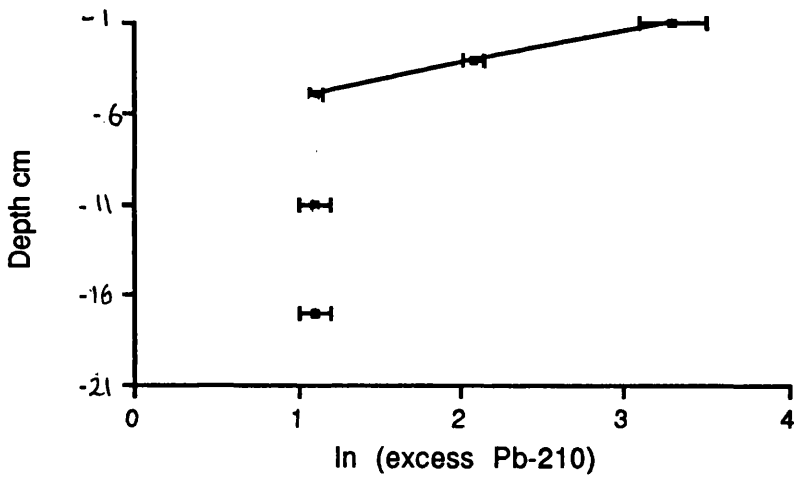


Table 4.5. Radiocaesium Activities in the Inverness '89 Peat Profile (July 1989)

Depth (cm)	^{137}Cs Total Bq kg^{-1}	error Bq kg^{-1}	^{137}Cs Total Bq m^{-2}	error Bq m^{-2}	^{134}Cs Total Bq kg^{-1}	error Bq kg^{-1}	^{134}Cs Total Bq m^{-2}	error Bq m^{-2}
Turf	1810	21.7	6920	161.9	296	8.0	1120	37.6
0-2	1770	19.5	9500	217.6	282	7.0	1523	48.8
2-4	740	10.4	2300	55.9	115	4.0	368	14.8
4-6	290	3.5	1240	29.0	42	1.3	185	6.8
6-8	190	6.5	1140	45.4	34	2.9	204	17.8
8-10	100	4.2	440	20.6	8	1.3	35	5.8
10-12	60	3.8	280	18.6	11	1.6	51	7.7
12-14	7	6.4	20	1.9	N.D		N.D	
14-16	N.D		N.D		N.D		N.D	
16-18	N.D		N.D		N.D		N.D	
18-20	N.D		N.D		N.D		N.D	

Table 4.5 cont.

Depth (cm)	$^{134}\text{Cs}/^{137}\text{Cs}$ Activity Ratio	error	^{137}Cs Chernobyl Bq kg^{-1}	error Bq kg^{-1}	^{137}Cs Chernobyl Bq m^{-2}	error Bq m^{-2}	^{137}Cs weapons testing Bq kg^{-1}	error Bq kg^{-1}	^{137}Cs weapons testing Bq m^{-2}	error Bq m^{-2}
Turf	0.16	0.004	1530	48.9	6000	282.0	280	9.0	920	43.0
0-2	0.16	0.004	1440	41.8	8000	360.0	330	9.6	1500	67.5
2-4	0.16	0.006	590	23.6	1895	83.4	150	6.0	405	11.3
4-6	0.15	0.005	220	7.7	947	4604	70	2.5	293	14.4
6-8	0.18	0.016	180	17.6	1053	105.0	10	1.0	87	8.7
8-10	0.08	0.013	40	7	105	18.8	60	10.0	335	60.0
10-12	0.18	0.026	60	10	210	37.2	N.D		N.D	
12-14			N.D		N.D		7	0.6	20	2.6
14-16			N.D		N.D		N.D		N.D	
16-18			N.D		N.D		N.D		N.D	
18-20			N.D		N.D		N.D		N.D	

Table 4.6 Radiocaesium Activities in the Borders Peat Profile (July 1989)

Depth (cm)	137Cs Total Bq kg ⁻¹	error Bq kg ⁻¹	137Cs Total Bq m ⁻²	error Bq m ⁻²	134Cs Total Bq kg ⁻¹	error Bq kg ⁻¹	134Cs Total Bq m ⁻²	error Bq m ⁻²
0-2	128	1.9	410	10.3	19	0.7	76	3.3
2-4	159	2.7	820	21.3	12	0.9	48	3.5
4-6	94	1.5	490	12.7	8	0.5	22	1.3
6-8	56	1.3	200	6.0	3	0.3	8	0.9
8-10	40	1.4	130	5.2	N.D		N.D	
10-12	40	1.0	120	4.0	N.D		N.D	
12-14	31	1.6	100	5.4	N.D		N.D	
14-16	29	1.6	100	5.8	N.D		N.D	
16-18	19	1.9	50	5.0	N.D		N.D	
18-20	22	1.2	50	3.0	N.D		N.D	

Table 4.6 cont.

Depth (cm)	$^{134}\text{Cs}/$ ^{137}Cs Activity Ratio	error	^{137}Cs Chernobyl Bq kg^{-1}	error Bq kg^{-1}	^{137}Cs Chernobyl Bq m^{-2}	error Bq m^{-2}	^{137}Cs weapons testing Bq kg^{-1}	error Bq kg^{-1}	^{137}Cs weapons testing Bq m^{-2}	error Bq m^{-2}
0-2	0.15	0.006	101	4.4	319	15.0	27	1.2	90	40.1
2-4	0.08	0.006	64	4.8	319	24.2	95	7.1	501	37.8
4-6	0.09	0.005	43	2.6	160	10.3	51	3.1	330	20.6
6-8	0.05	0.006	16	1.9	53	6.1	40	4.7	147	17.3
8-10			N.D		N.D		40	1.4	130	5.2
10-12			N.D		N.D		40	1.0	120	4.0
12-14			N.D		N.D		31	1.6	100	5.4
14-16			N.D		N.D		29	1.6	100	5.8
16-18			N.D		N.D		19	1.9	50	5.0
18-20			N.D		N.D		22	1.2	50	3.0

Table 4.7 Radiocaesium Activities in the Fenwick Moor Peat Profile (October 1989)

Depth (cm)	^{137}Cs Total Bq kg^{-1}	error Bq kg^{-1}	^{137}Cs Total Bq m^{-2}	error Bq m^{-2}	^{134}Cs Total Bq kg^{-1}	error Bq kg^{-1}	^{134}Cs Total Bq m^{-2}	error Bq m^{-2}
0-2	680	8.0	2244	52.0	90	2.0	306	9.3
2-4	790	9.0	2212	52.2	100	2.0	280	8.5
4-6	450	8.1	1890	51.1	50	1.9	210	8.1
6-8	210	6.2	1649	58.3	20	1.8	160	13.5
8-10	290	2.9	1813	42.0	40	1.0	256	7.8
10-12	40	0.7	276	8.0	3	0.1	21	0.9
12-14	30	0.5	198	4.9	2	0.1	14	0.5
14-16	20	0.4	121	2.8	2	0.1	12	0.5
16-18	20	0.8	116	5.2	N.D		N.D	
18-20	10	0.5	58	3.0	N.D		N.D	

Table 4.7 cont.

Depth (cm)	$^{134}\text{Cs}/$ ^{137}Cs Activity Ratio	error	^{137}Cs Chernobyl Bq kg^{-1}	error Bq kg^{-1}	^{137}Cs Chernobyl Bq m^{-2}	error Bq m^{-2}	^{137}Cs weapons testing Bq kg^{-1}	error Bq kg^{-1}	^{137}Cs weapons testing Bq m^{-2}	error Bq m^{-2}
0-2	0.14	0.003	480	13.9	1632	57.0	200	5.8	680	24.1
2-4	0.13	0.003	530	15.4	1484	52.4	260	7.5	728	26.3
4-6	0.11	0.004	270	10.3	1134	49.2	180	6.8	756	32.0
6-8	0.10	0.009	110	10.1	880	82.8	100	9.2	769	71.8
8-10	0.14	0.004	210	6.1	1344	47.3	80	2.3	512	15.6
10-12	0.08	0.003	16	0.7	112	5.2	24	1.1	469	17.0
12-14	0.07	0.003	11	0.4	75	3.0	19	7.4	164	8.2
14-16	0.07	0.003	11	0.5	68	3.1	9	0.4	46	2.1
16-18	N.D		N.D		N.D		20	0.8	48	1.9
18-20	N.D		N.D		N.D		10	0.5	54	3.1

Table 4.8 Radiocaesium Activities in the Darleith Soil Profile (October 1989)

Depth (cm)	^{137}Cs Total Bq kg^{-1}	error Bq kg^{-1}	^{137}Cs Total Bq m^{-2}	error Bq m^{-2}	^{134}Cs Total Bq kg^{-1}	error Bq kg^{-1}	^{134}Cs Total Bq m^{-2}	error Bq m^{-2}
0-2	990	7.9	6600	142.0	103	1.8	659	17.1
2-4	848	5.9	12800	271.0	102	1.0	1469	32.3
4-6	245	2.5	2800	63.2	17	0.6	190	8.2
6-8	115	1.6	2400	58.1	3	0.4	61	8.2
8-10	116	1.6	1600	38.7	3	0.4	41	8.1
10-12	116	1.6	1400	34.4	3	0.4	35	3.9
12-14	22	0.3	200	5.2	N.D		N.D	
14-16	63	1.3	900	25.0	10	1.4	136	18.7
16-18	46	1.2	600	20.1	15	2.5	171	28.0
18-20	26	0.8	200	7.2	N.D		N.D	

Table 4.8 cont.

Depth (cm)	$^{134}\text{Cs}/$ ^{137}Cs Activity Ratio	error	^{137}Cs Chernobyl Bq kg^{-1}	error Bq kg^{-1}	^{137}Cs Chernobyl Bq m^{-2}	error Bq m^{-2}	^{137}Cs weapons testing Bq kg^{-1}	error Bq kg^{-1}	^{137}Cs weapons testing Bq m^{-2}	error Bq m^{-2}
0-2	0.10	0.002	548	11.5	3507	102.2	442	9.3	3093	90.0
2-4	0.12	0.001	543	7.6	7819	190.8	305	4.3	4981	121.2
4-6	0.07	0.002	90	3.5	1008	44.2	155	6.0	1792	78.1
6-8	0.03	0.003	16	2.0	323	41.5	99	12.6	2077	266.1
8-10	0.03	0.003	16	2.0	218	28.3	100	12.7	1382	177.4
10-12	0.03	0.003	16	2.0	189	23.6	100	12.7	1211	155.2
12-14			N.D		N.D		22	0.3	200	4.8
14-16	0.02	0.003	5	0.7	50	7.3	58	8.3	850	124.1
16-18	0.03	0.005	8	1.3	11	1.9	38	6.4	589	100.0
18-20			N.D		N.D		26	0.8	200	7.2

Table 4.9 Radiocaesium Activities in the Dreghorn Soil Profile (Cooper 1989)

Depth (cm)	137Cs Total Bq kg ⁻¹	error Bq kg ⁻¹	137Cs Total Bq m ⁻²	error Bq m ⁻²	134Cs Total Bq kg ⁻¹	error Bq kg ⁻¹	134Cs Total Bq m ⁻²	error Bq m ⁻²
0-2	358	3.9	3652	83.3	59	1.7	602	21.2
2-4	140	1.0	3304	70.0	22	0.6	519	13.0
4-6	29	0.4	1067	26.0	3	0.2	110	6.8
6-8	8	0.1	309	8.1	N.D		N.D	
8-10	6	0.1	250	7.4	N.D		N.D	
10-12	23	0.5	837	23.7	N.D		N.D	
12-14	7	0.2	239	7.5	N.D		N.D	
14-16	27	0.4	1096	27.4	N.D		N.D	
16-18	7	0.2	253	7.7	N.D		N.D	
18-20	24	0.5	917	25.9	N.D		N.D	

Table 4.9 cont.

Depth (cm)	$^{134}\text{Cs}/^{137}\text{Cs}$ Activity Ratio	error	^{137}Cs Chernobyl Bq kg^{-1}	error Bq kg^{-1}	^{137}Cs Chernobyl Bq m^{-2}	error Bq m^{-2}	^{137}Cs weapons testing Bq kg^{-1}	error Bq kg^{-1}	^{137}Cs weapons testing Bq m^{-2}	error Bq m^{-2}
0-2	0.17	0.005	314	10.4	3203	123.6	44	1.5	449	17.3
2-4	0.16	0.003	117	2.1	2761	74.3	23	0.4	543	14.6
4-6	0.10	0.006	16	1.0	589	37.8	13	0.8	478	30.7
6-8			N.D		N.D		8	0.1	309	8.1
8-10			N.D		N.D		6	0.1	250	7.4
10-12			N.D		N.D		23	0.5	837	23.7
12-14			N.D		N.D		7	0.2	239	7.5
14-16			N.D		N.D		27	0.4	1096	27.4
16-18			N.D		N.D		7	0.1	253	7.7
18-20			N.D		N.D		24	0.5	917	25.9

FIG. 4.2 Inverness Peat
 FIG. 4.2.1 Total Cs-137 Activity

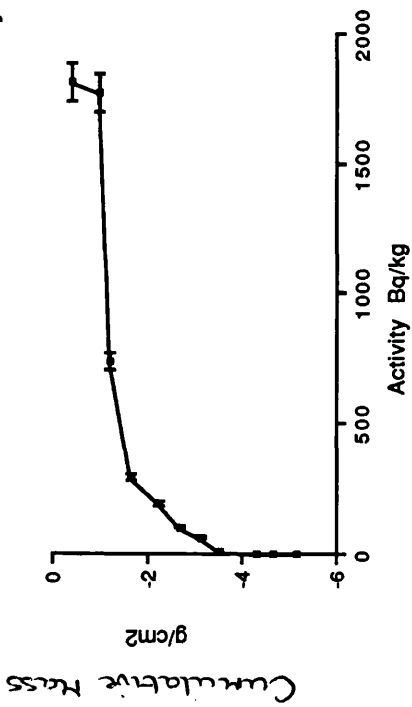


FIG. 4.2.2 Cs-134 Activity

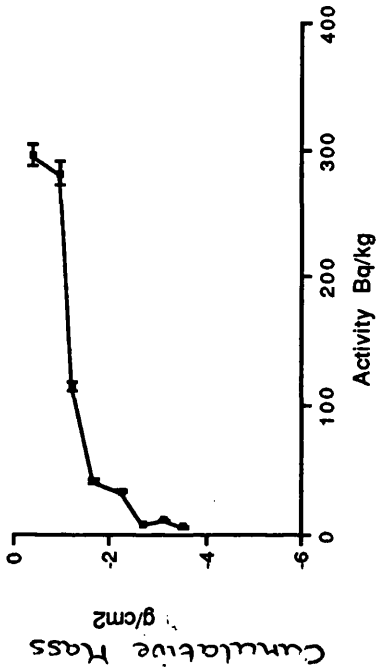


FIG. 4.2.3 Activity Ratio Cs-134/Cs-137

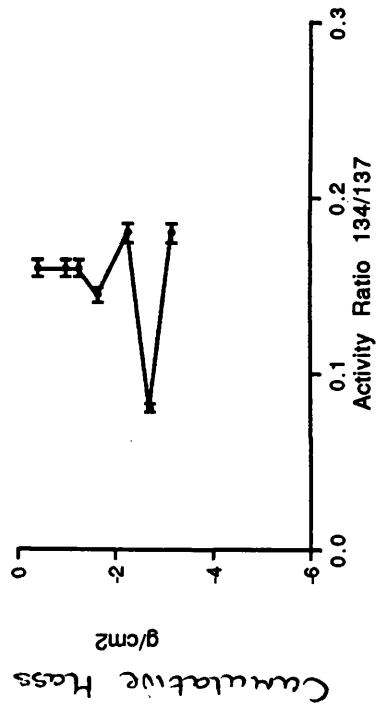


FIG. 4.2.4 Cs-137 Components

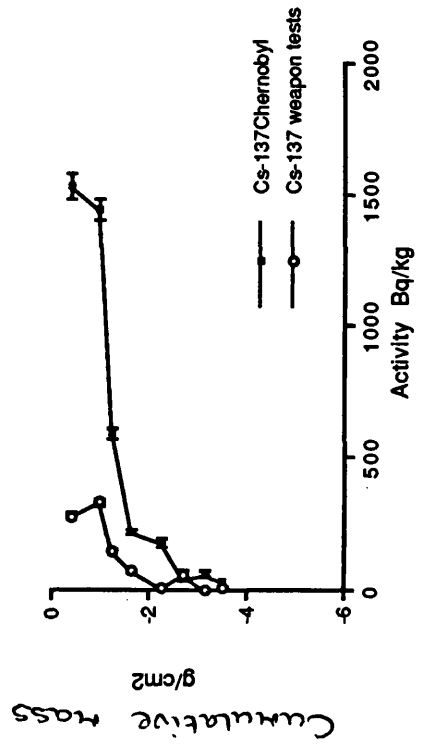


FIG. 4.3 Borders Peat
 FIG. 4.3.1 Total Cs-137 Activity

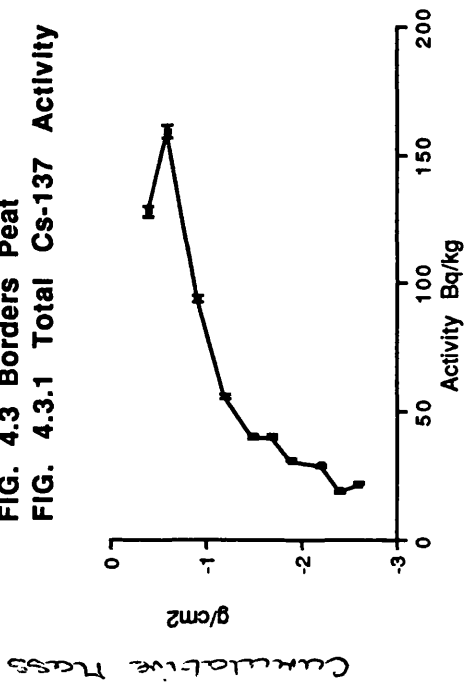


FIG. 4.3.2 Cs-134 Activity

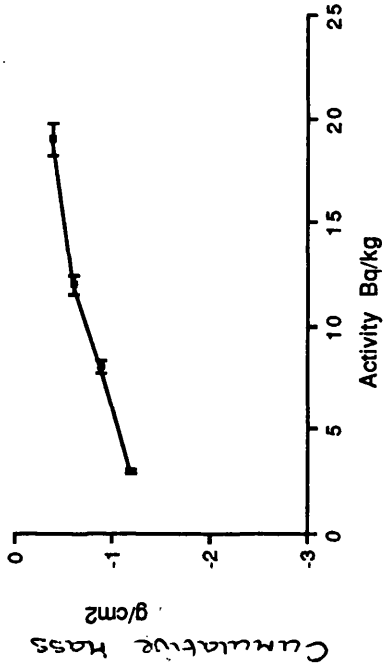


FIG. 4.3.3 Activity Ratio Cs-134/Cs-137

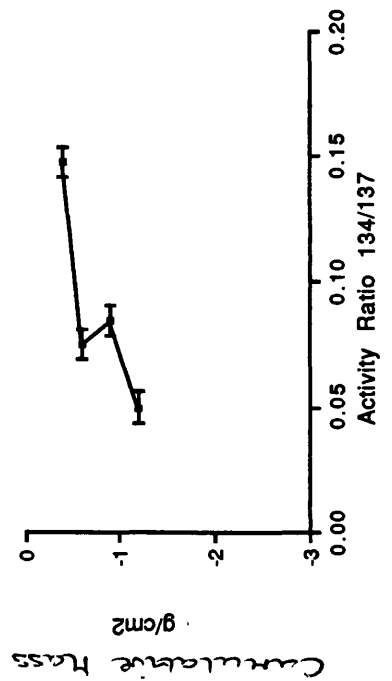


FIG. 4.3.4 Cs-137 Components

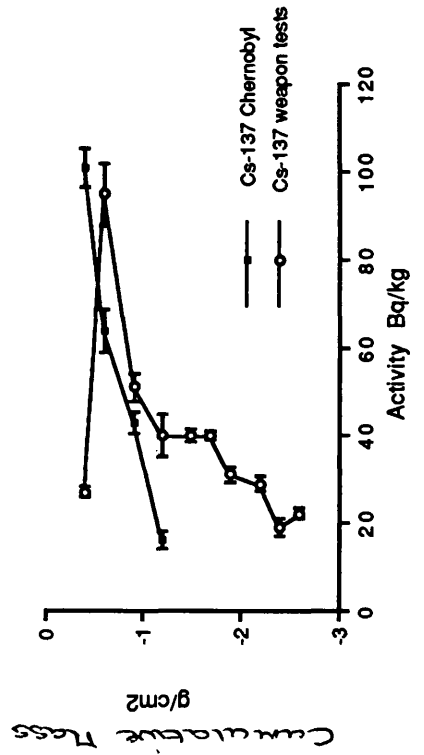


FIG. 4.4 Fenwick Moor Peat
 FIG. 4.4.1 Total Cs-137 Activity

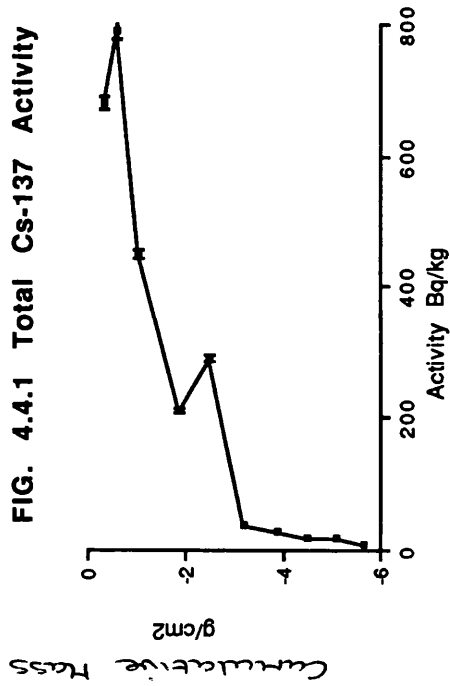


FIG. 4.4.2 Cs-134 Activity

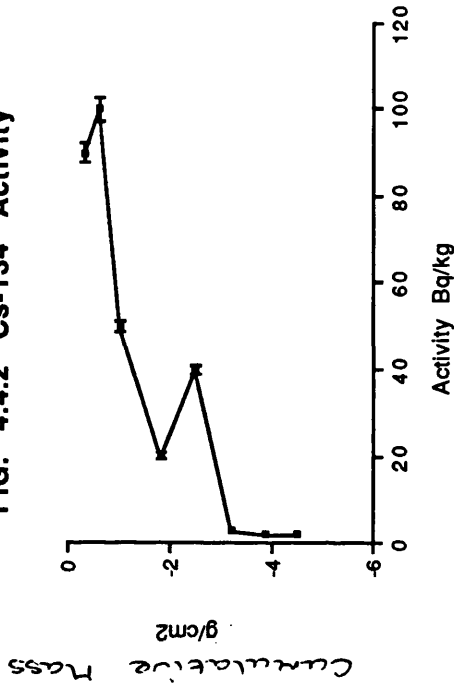


FIG. 4.4.3 Activity Ratio Cs-134/Cs-137

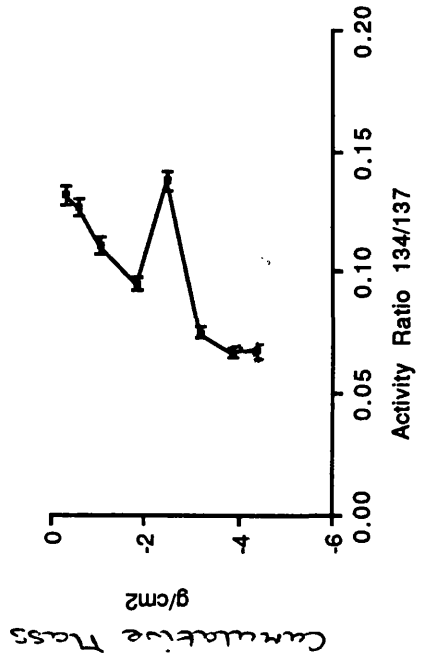


FIG. 4.4.4 Cs-137 Components

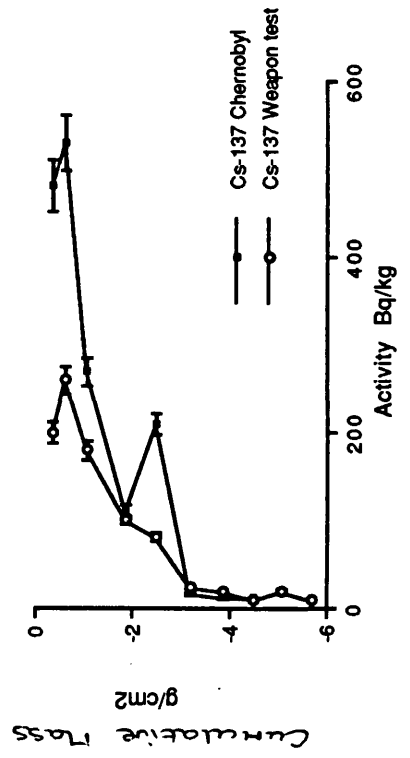


FIG. 4.5.2 Cs-134 Activity

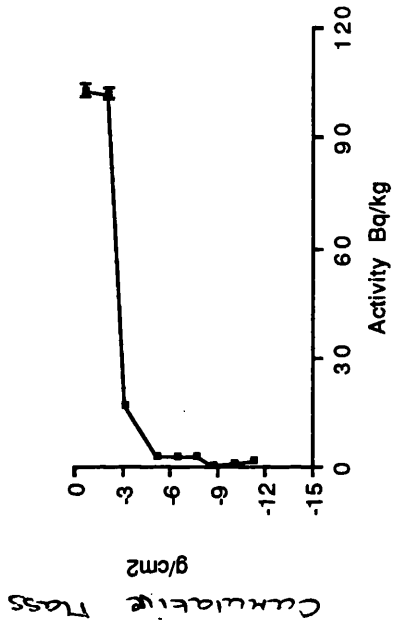


FIG. 4.5 Darleith Soil
FIG. 4.5.1 Total Cs-137 Activity

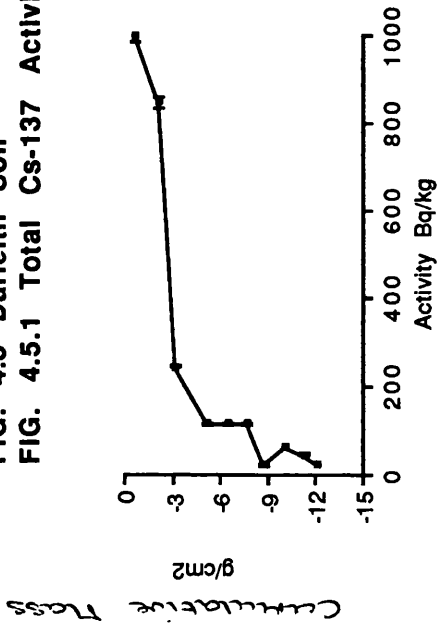


FIG. 4.5.4 Cs-137 Components

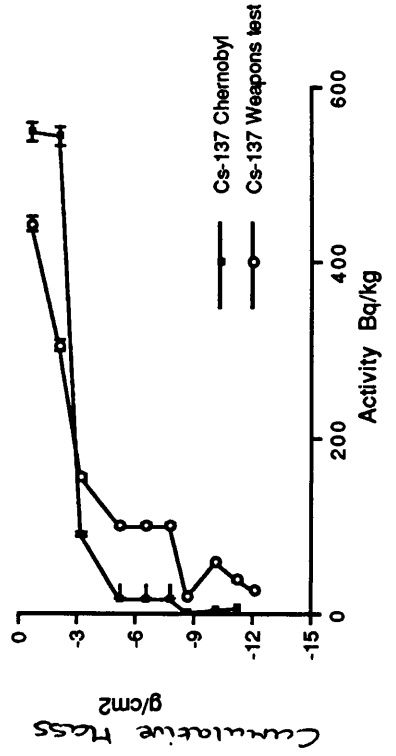


FIG. 4.5.3 Activity Ratio Cs-134/Cs-137

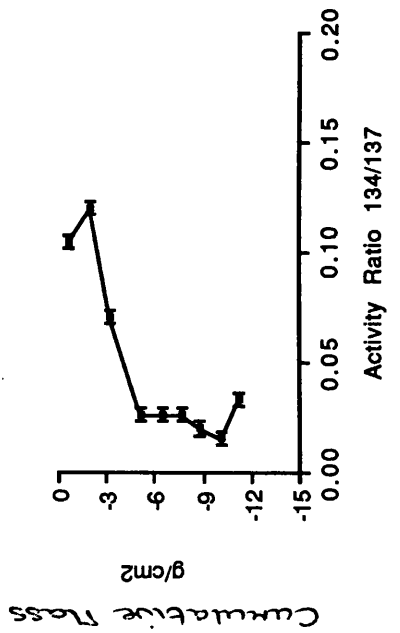


FIG. 4.6 Dreghorn Soil
 FIG. 4.6.1 Total Cs-137 Activity

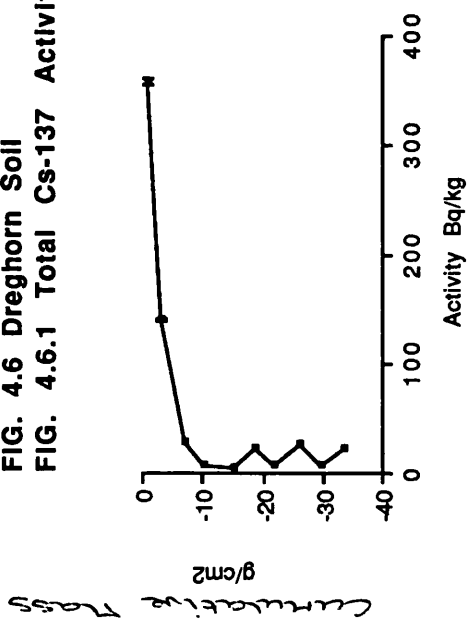


FIG. 4.6.2 Cs-134 Activity

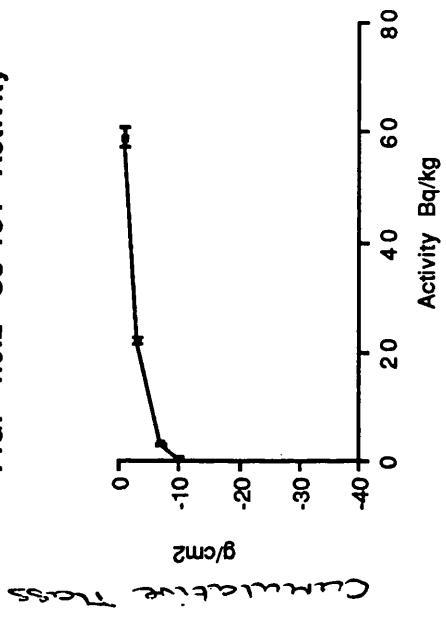


FIG. 4.6.3 Activity Ratio Cs-134/Cs-137

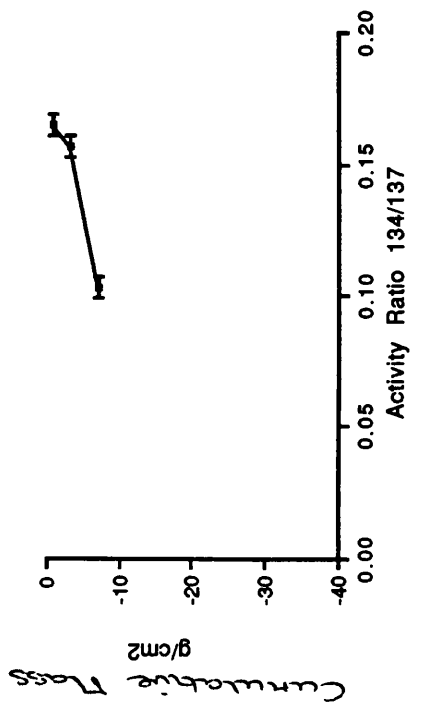


FIG. 4.6.4 Cs-137 Components

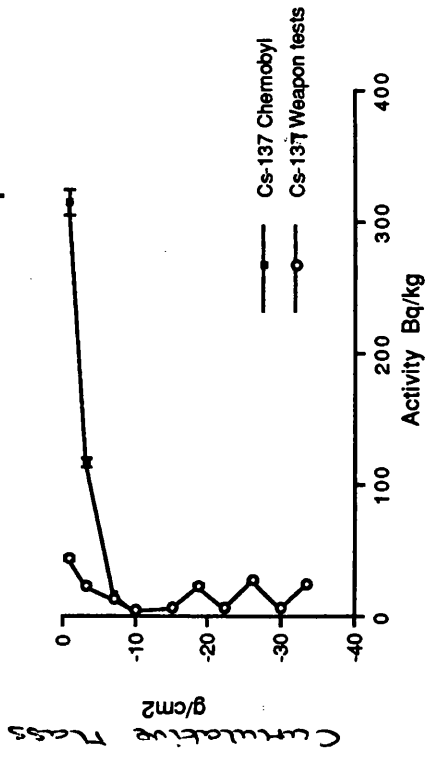


Table 4.10.1 ^{137}Cs Inventories for Sample Set 1.-
calculated for samples to 15cm depth.

	^{137}Cs	^{137}Cs	^{137}Cs	
	Total	Chernobyl	Weapons Testing	
			in 1989	in 1963
	kBq m^{-2}	kBq m^{-2}	kBq m^{-2}	kBq m^{-2}
Inverness '89	21.8	19.5	3.5	6.4
Borders	2.3	0.9	1.5	2.7
Fenwick Moor	10.3	7.2	4.1	7.4
Darleith	28.3	14.0	15.1	27.4
Dreghorn	10.2	7.0	3.6	6.6

N.B Weapons testing data were decay corrected from the sample date in 1989 to 1963 and Chernobyl data to May 1986.

Table 4.10.2 ^{137}Cs Inventories for Sample Set 1.-
calculated for the total sampling depth of 20cm.

	^{137}Cs	^{137}Cs	^{137}Cs	
	Total	Chernobyl	Weapons Testing	
			in 1989	in 1963
	kBq m^{-2}	kBq m^{-2}	kBq m^{-2}	kBq m^{-2}
Inverness '89	21.8	19.5	3.6	6.5
Borders	2.5	0.9	1.6	2.9
Fenwick Moor	10.6	7.2	4.2	7.6
Darleith	29.5	14.0	16.4	29.8
Dreghorn	11.9	7.0	5.4	9.8

N.B Weapons testing data were decay corrected from the sample date in 1989 to 1963 and Chernobyl data to May 1986.

Table 4.11 Average annual rainfall data for the sample sites

Sample	Rainfall mm yr ⁻¹
Inverness	953
Borders	889
Fenwick Moor	1400
Darleith	1400
Dreghorn	940

Reference Source: Ordnance Survey Average Annual Rainfall Map of the United Kingdom, 1929.

Table 4.12.1 Correlation coefficients for linear regression of total inventories with average annual rainfall for Sample Set 1.

	$^{137}\text{Cs(T)}$	$^{137}\text{Cs(WT)}$	^{210}Pb
rainfall	0.004	0.42	0.04

Table 4.12.2 Total inventory correlations for Sample Set 1.

	^{210}Pb
$^{137}\text{Cs(WT)}$	0.22

N.B $^{137}\text{Cs(WT)}$ = weapons testing component

$^{137}\text{Cs(T)}$ = total ^{137}Cs

4.3 Discussion of the Analyses of Sample Set 1

4.3.1 ^{210}Pb

The results for flux and total inventory indicate that the Inverness site in the North East of Scotland had the highest level of excess ^{210}Pb (Table 4.2). Excess ^{210}Pb inventories will be governed by deposition rate and by any post-depositional mobility (Urban et al, 1990). The rate of deposition of ^{210}Pb will be affected by variations in annual rainfall, the frequency of rainfall and the mist and cloud cover of the area (Urban, 1990). High lying areas such as the Inverness site may have a cover of low lying mist for long periods of the year and this may affect the relationship between ^{210}Pb deposition and average annual rainfall. The relationship between deposition and average annual rainfall at each site was investigated using the data in Table 4.11. This resulted in an r^2 value of 0.04 i.e. showing no significant relationship.

Local differences in inventories of 50-300% have been found between adjacent hummocks and hollows (Aaby and Jacobsen, 1979; Oldfield et al., 1979; El-Daoushy, 1988). Urban et al. (1990) concluded that ^{210}Pb is mobile in oxygen depleted saturated peats and can be transported out of peatlands by the lateral flow of water. Darleith soil and Fenwick Moor peat should have similar excess ^{210}Pb flux values as both samples were

taken from the site at South Drumbooy hill. However, values of 57 and 89 Bq m⁻² y⁻¹ respectively were recorded. The sampling point for the Fenwick Moor peat was at the lower edge of the area of peat, which, under wet conditions becomes waterlogged due to runoff from the higher lying areas of peat. Under these conditions it is possible that ²¹⁰Pb levels in the peat have been enhanced by the movement from higher areas of ²¹⁰Pb complexed onto dissolved organic matter present in the soil water (Heinrichs and Mayer, 1977). This would explain the higher flux of ²¹⁰Pb in the Fenwick Moor peat compared to the Darleith soil. The difference in altitude between the two sites was very small resulting in only small variations in the frequency of mist or rain cover at the sites.

Depth profiles of ²¹⁰Pb in peat often appear anomalous with subsurface maxima in the zone of water table fluctuations indicating the physical transport of ²¹⁰Pb (Pakarinen and Tolonen, 1977). However, concentration profiles can be affected by processes such as rates of primary production, decomposition and vegetational change which are unrelated to any ²¹⁰Pb mobility and which give rise to mixing zones. The ²¹⁰Pb profiles for the three peats analysed in this study exhibit mixed zones of 0-8 cm depth with near constant ²¹⁰Pb concentrations, followed by a region at greater depth in which ²¹⁰Pb concentrations undergo an apparent exponential decrease which could be attributed either

to growth of the peats and decay of the ^{210}Pb in unmixed layers or to a reduction in the degree of mixing with increasing depth. For these three peat cores, density measurements were variable but there were no changes over the sampling depth which appeared to be significant enough to affect the intensity of mixing due to biological activity (Table 3.1). Excess ^{210}Pb could be measured to a depth of 20 cm in the Borders profile but only to 10 cm in the Inverness'89 core and 12 cm in the Fenwick Moor core. The calculated sedimentation rates, (Tables 4.3 and 4.4), indicate an apparent rate of peat formation of:

	Borders	> Inverness	> Fenwick
$\text{g cm}^{-2} \text{ y}^{-1}$	0.21	0.021	0.017

These compare favourably with literature values of 0.1-0.15 $\text{g cm}^{-2} \text{ y}^{-1}$ for an ombrotrophic mire from Lough Fea, Northern Ireland and values ranging from 0.005 - 0.1 $\text{g cm}^{-2} \text{ y}^{-1}$ for cores sampled from an area of ombrotrophic peat at Bolton Fell 15 km northwest of Carlisle (Oldfield et al. (1979). Sugden et al. (1991) measured sedimentation rates of 0.031 $\text{g cm}^{-2} \text{ y}^{-1}$ for a peat core from North Uist in the Outer Hebrides and 0.0098 $\text{g cm}^{-2} \text{ y}^{-1}$ for a core from Flanders Moss in Stirlingshire, Central Scotland.

In the Darleith soil, which has a greater proportion of mineral material than the peat soils, excess ^{210}Pb appears to be held in the upper 4 cm with a small degree of penetration to the lower layers.

However, in the even more mineral Dreghorn soil excess ^{210}Pb appears to be more firmly bound to the upper 4 cm of the soil preventing its penetration of the soil layers.

In summary, the three peats have excess ^{210}Pb profiles comprising an upper mixing zone and a lower zone of exponential decrease in concentration. The excess ^{210}Pb flux values varied over the range 89-132 $\text{Bq m}^{-2} \text{ y}^{-1}$ and this could not be attributed to variations in average annual rainfall. Potential lateral mobility of ^{210}Pb is apparent at the South Drumbooy site and this finding agrees with the conclusion of Urban (1990). If this lateral movement does occur it would invalidate the use of ^{210}Pb dating at the site.

4.3.2 Radiocaesium

Total inventories for ^{137}Cs of Chernobyl origin and weapons testing fallout can be compared with literature values of 2 - 14 kBq m^{-2} for weapons testing fallout and 5 - 38 kBq m^{-2} for Chernobyl fallout (Peirson et al., 1982; McAulay and Moran, 1992; MacNeil et al., 1992; McDonald et al., 1992a). Using the contour map produced by Peirson et al. (1982), cumulative depositions of weapons testing fallout up to 1977 for the four sites in sample set 1. were predicted to be: Inverness '89, 3 kBq m^{-2} (6.5 kBq m^{-2}); Borders, 3-4 kBq

m^{-2} (2.9 kBq m^{-2}); Fenwick Moor and Darleith, 3 kBq m^{-2} (7.6 and 29.8 kBq m^{-2}); and Dregghorn, < 1.7 kBq m^{-2} (9.8 kBq m^{-2}). Measured values for the sites were in most cases significantly higher than predicted, these are shown above in parenthesis (Table 4.10.2). The particularly high value for Darleith may be due to the clay minerals in this soil acting as a "sink" for ^{137}Cs leaching out of the peat soils surrounding it. Table 4.8 illustrates the high levels of radiocaesium present in the upper 4 cm of the Darleith profile, these may reflect the lateral movement of radiocaesium from adjacent areas such as Fenwick Moor peat. In addition, Fenwick Moor peat probably receives an input of ^{137}Cs which is leaching from higher lying peats. The decay corrected Chernobyl $^{134}\text{Cs}/^{137}\text{Cs}$ ratio was 0.19 at the time of sampling. The recorded ratios for Darleith soil fall in the range 0.02-0.12, and for Fenwick Moor peat in the range 0.07-0.14. These low ratios indicate that there has been an input of ^{137}Cs of origin other than the deposition of Chernobyl fallout to the profiles i.e. there is proportionally more weapons testing ^{137}Cs present, it is possible that this input is due to post-depositional migration of radiocaesium from higher lying areas. In order to confirm this argument it would be necessary to take samples from a transect down the gradient of the hillside, this was carried out at the Inverness site, where only peat soils were present, and the results are discussed in section 4.4. No

correlation was found between total inventories and average annual rainfalls for the sites.

Chernobyl ^{137}Cs inventories fell within the range 0.9-19.5 kBq m^{-2} at the time of deposition (Borders, 0.9; Dreghorn, 7.0; Fenwick Moor, 7.2; Darleith 14.0; Inverness, 19.5 kBq m^{-2}). These values fall within the range of values recorded by other researchers (see Section 1.5.2.2). In general, the magnitude of these inventories probably reflects the local rainfall pattern over the deposition period. However, the difference in values between Darleith soil and Fenwick Moor peat may reflect the post-depositional mobility of radiocaesium.

The profiles for Sample Set 1 show that most of the radiocaesium present is contained in the upper few centimetres of the cores (see Tables 4.5 - 4.9). In general, more than 40% of the total ^{137}Cs inventory was present in the upper 4 cm of the cores with values of 86% for Inverness'89 and 67% for Darleith. The most recently deposited Chernobyl contribution was present in the top 4 cm of the profiles at percentage levels of total Chernobyl ^{137}Cs inventory of: 47% for Fenwick Moor; 75% for Borders; 85% for Darleith and 90% for both Inverness'89 and Dreghorn. These values compare well with literature reports where the majority of Chernobyl ^{137}Cs is found in the top few centimetres of forest soil profiles (Bunzl et al., 1992; Kirchner and Baumgartner, 1992). MacNeil et al. (1992) measured 77 -

96% of Chernobyl ^{137}Cs in the 0 - 5 cm section of profiles at eleven sites in Ireland in April 1987, sampling soils with a range of properties. By October 1988 this had been reduced to 63 - 95%. The older weapons testing fallout would be expected to have migrated to greater depths and in agreement with this, the percentages held in the upper 4 cm were: 18% for Dreghorn; 33% for Fenwick Moor; 39% for Borders; 49% for Darleith and 79% for Inverness'89. MacNeil et al., (1992) measured >70% of ^{137}Cs of weapons testing origin at eleven permanent pasture sites of varying soil type in Ireland to be held in the upper 15 cm of the profiles, these correspond to values of: 68% for Dreghorn; 90% for Borders; 93% for Darleith; 97% for Fenwick Moor and 100% for Inverness'89.

It is apparent that although ^{137}Cs has moved downwards in the peats and soils studied in the time since deposition this movement is slow. The most substantial movement of radiocaesium, at certain sites, that occurs post-deposition appears to be by rapid lateral displacement due to surface water movement, e.g. between Fenwick Moor peat and Darleith. Therefore, for ^{137}Cs of weapons testing origin surface concentrations have been reduced slightly by downward mobility but to a greater degree by lateral movement where applicable and the radioactive decay of ^{137}Cs over the post-deposition time period of 26 years. It is possible that the caesium held in the upper layers of the peat soils

is available for recycling into plant material and hence through grazing can enter into the animal food chain. It is more probable that for the mineral soils ^{137}Cs binds to clay surfaces and that subsequent desorption is less likely (Coleman et al., 1963a and b).

A turf sample was included in the Inverness'89 profile. This sample was made up predominantly of herbage together with the matted top layer of the true peat. Significant radiocaesium activities were recorded in this layer, indicating that radiocaesium may be being taken up by plants. Assuming that the majority of the radiocaesium was held in plant material, soil to plant concentration ratios could be calculated using the formula:

$$\text{CR} = \frac{\text{Activity concentration in plant (Bqkg}^{-1} \text{ dry)}}{\text{Activity concentration in soil (0-5cm)(Bqkg}^{-1})}$$

CR - concentration ratio

(MacNeil et al., 1992)

Values for this parameter at the Inverness site were calculated to be: ^{137}Cs (total), CR = 0.7; ^{137}Cs (weapons testing), CR = 0.5; and ^{137}Cs (Chernobyl), CR = 0.7. These compare with literature values of 0.03 - 0.49 for brown earth soils (MacNeil et al., 1992).

The profiles also illustrate that small amounts of radiocaesium have penetrated to depths of at least 20 cm for Borders, Fenwick Moor, Darleith and Dreghorn.

When compared with the ^{210}Pb profiles, the mobilisation of radiocaesium in the peat cores appears to be due to mixing in the upper few centimetres of the profiles, possibly due to biological mixing and peat growth, followed by slower downward movement to lower depths. It is therefore necessary to construct a diffusion model to enable the prediction of radiocaesium mobility with time, this is attempted in Section 4.5.

The behaviour of radiocaesium in the Inverness'89 peat does not appear to fit this explanation as the weapons testing component has penetrated to only 14 cm. In order to investigate this further, correlations were performed on the excess ^{210}Pb and ^{137}Cs (weapons testing) inventories. The results are presented in Table 4.12. No relationship was found between ^{210}Pb deposition and ^{137}Cs (weapons testing).

As the Inverness sample site was hilly it would be possible for radiocaesium to experience downslope movement by surface runoff i.e. advective movement. At the Fenwick Moor site downslope leaching may again be of importance resulting in the redistribution of radiocaesium. This may explain why neither Inverness'89 or Fenwick Moor inventories measured several years after deposition correlate with rainfall. The influence of topography upon radiocaesium mobility is discussed further in Section 4.4.

4.4 Gamma Analysis of Sample Set 2 - Inverness'90 Peat Transect

4.4.1 Results

In order to further investigate the influence of topography upon the mobility of radiocaesium in peat soils, four cores were sampled down a hillside transect at the Inverness site in July 1990. A diagrammatic representation of the transect is given in Fig. 4.7. Core A at the top of the transect was probably truly ombrotrophic with no input of radiocaesium to it other than via aerial deposition. This was not true for the three remaining cores as they will have received inputs of trace elements due to the downslope movement of water. This section aims to examine the extent to which water flow affects the mobility of radiocaesium in peats.

^{210}Pb profiles were measured for each core and these are presented in Tables 4.13.1-4.13.4 and Figs. 4.8.1-4.8.4. Total inventories, ^{210}Pb fluxes and sedimentation rates were calculated for the sampling depth of 18 cm for Cores A and B and 16 cm for Cores C and D (the base of the peat layer was reached at 16 cm at the lower end of the transect), these are presented in Table 4.14.

The radiocaesium data for the cores are presented in Tables 4.15-4.18 and Figs. 4.9-4.13. Total inventories, decay corrected to the times of

deposition, for the sampling depths are presented in Table 4.19.

FIG: 4.1 Inverness'90 Transect Sampling Plan

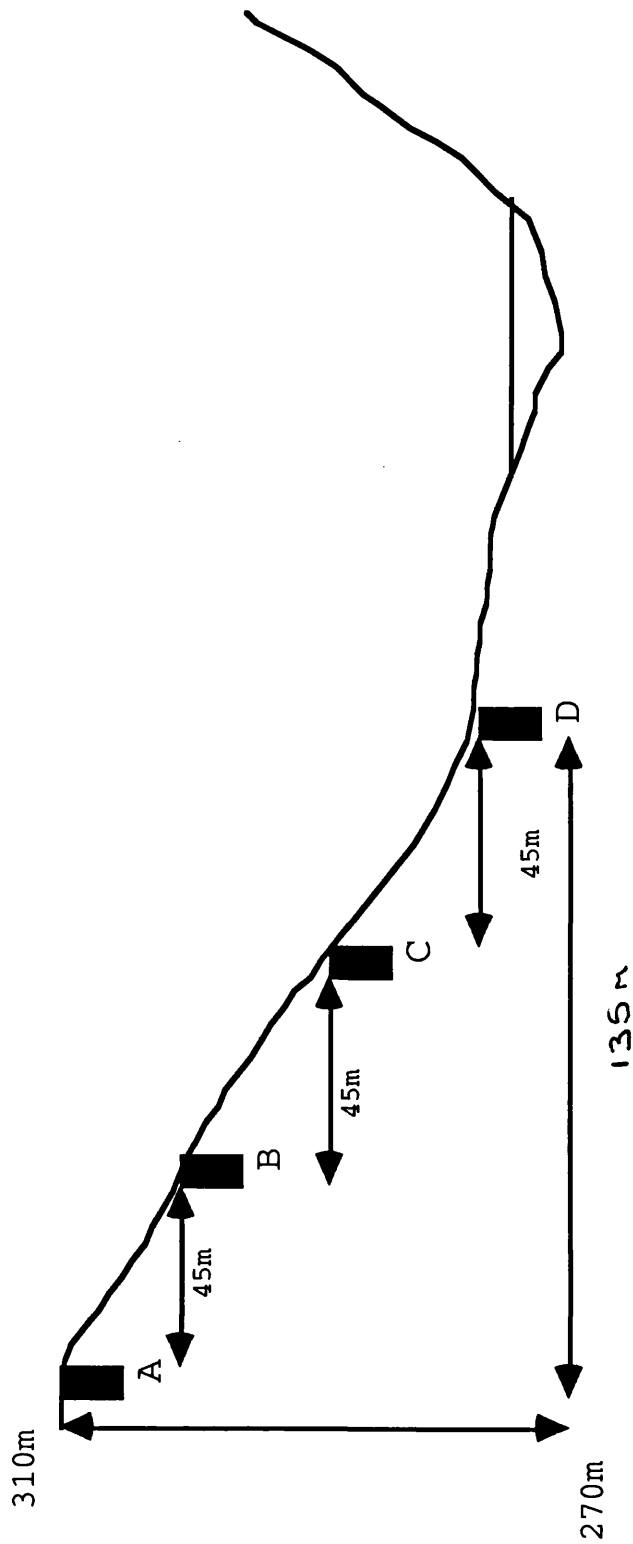


Table 4.13.1 ^{210}Pb Specific Activities in the Inverness'90 Peat Transect Core A

Depth (cm)	Excess ^{210}Pb Bq kg^{-1}	error Bq kg^{-1}	Excess ^{210}Pb Bq m^{-2}	error Bq m^{-2}
0-2	673	23.6	5115	20.6
2-4	71	5.9	497	42.4
4-6	40	3.8	232	22.3
6-8	24	2.9	134	16.4
8-10	10	1.4	58	8.3
10-12	N.D		N.D	
12-14	N.D		N.D	
14-16	N.D		N.D	
16-18	N.D		N.D	

Table 4.13.2 ^{210}Pb Specific Activities in the Inverness'90 Peat Transect Core B

Depth (cm)	Excess ^{210}Pb Bq kg^{-1}	error Bq kg^{-1}	Excess ^{210}Pb Bq m^{-2}	error Bq m^{-2}
0-2	158	7.3	1959	98.3
2-4	57	2.8	479	25.4
4-6	19	1.8	152	14.8
6-8	5	0.8	63	9.7
8-10	4	0.7	34	5.9
10-12	N.D		N.D	
12-14	N.D		N.D	
14-16	N.D		N.D	
16-18	N.D		N.D	

Table 4.13.3 ^{210}Pb Specific Activities in the Inverness'90 Peat Transect Core C

Depth (cm)	Excess ^{210}Pb Bq kg^{-1}	error Bq kg^{-1}	Excess ^{210}Pb Bq m^{-2}	error Bq m^{-2}
0-2	117	10.6	889	82.8
2-4	76	4.2	623	36.5
4-6	33	2.1	330	22.1
6-8	29	2.7	238	22.9
8-10	26	3.2	218	27.0
10-12	17	2.2	143	18.7
12-14	10	1.9	88	16.4
14-16	17	2.2	150	19.4

Table 4.13.4 ^{210}Pb Specific Activities in the Inverness'90 Peat Transect Core D

Depth (cm)	Excess ^{210}Pb Bq kg^{-1}	error Bq kg^{-1}	Excess ^{210}Pb Bq m^{-2}	error Bq m^{-2}
0-2	136	14.1	1088	115.2
2-4	96	5.7	768	47.8
4-6	86	5.3	688	44.8
6-8	40	2.1	320	17.8
8-10	26	3.2	208	26.1
10-12	23	3.3	184	26.4
12-14	27	3.4	216	27.8
14-16	16	3.8	128	30.4

Table 4.14.1 ^{210}Pb Inventories and Flux values for the Inverness'90 Transect Cores

	Inventory kBq m^{-2}	Flux $\text{Bq m}^{-2} \text{ y}^{-1}$
Core A	6.0	187
Core B	2.7	83
Core C	2.7	83
Core D	3.6	112

Table 4.14.2 Sedimentation Rates calculated from ^{210}Pb data for the Inverness'90 Transect Cores.

	Sedimentation Rate cm y^{-1}	r^2
Core A	0.065	0.90
Core B	0.065	0.96
Core C	0.190	0.86
Core D	0.210	0.91

N.B no mixing zones were observed for the four cores.

FIG. 4.8 Lead-210 Profiles
FIG. 4.8.1 Core A

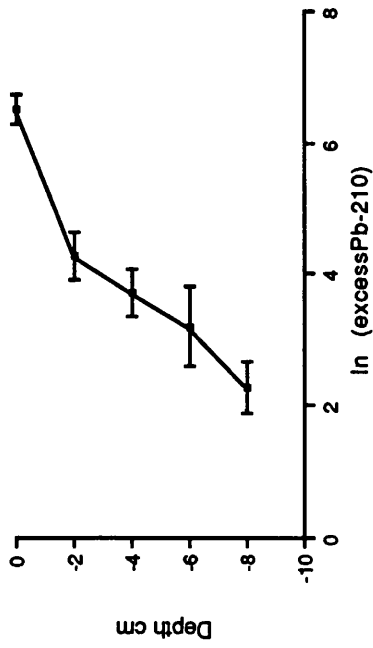


FIG. 4.8.2 Core B

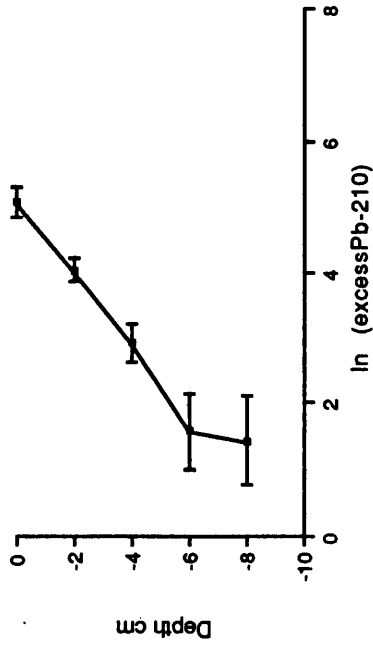


FIG. 4.8.3 Core C

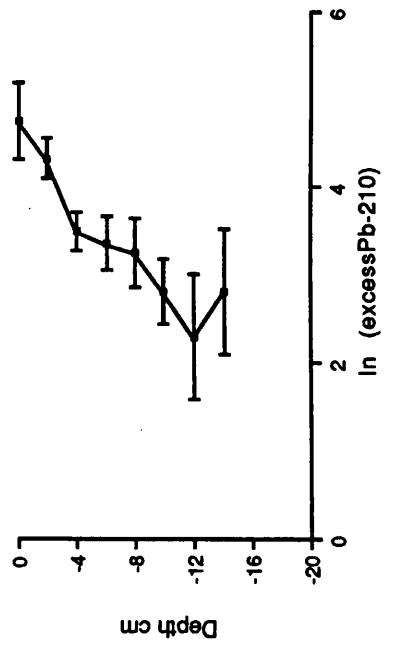


FIG. 4.8.4 Core D

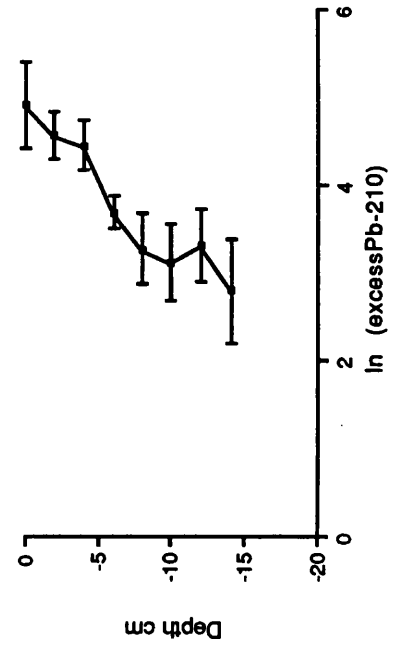


Table 4.15 Radiocaesium Activities in the Inverness '90 Transect Peat Core A

Depth (cm)	^{137}Cs Total Bq kg^{-1}	error Bq kg^{-1}	^{137}Cs Total Bq m^{-2}	error Bq m^{-2}	^{134}Cs Total Bq kg^{-1}	error Bq kg^{-1}	^{134}Cs Total Bq m^{-2}	error Bq m^{-2}
0-2	134	0.9	1018	21.6	19	0.5	144	4.6
2-4	108	2.0	756	20.7	8	0.5	56	3.7
4-6	65	1.3	377	10.8	N.D		N.D	
6-8	49	1.4	274	9.7	N.D		N.D	
8-10	33	0.4	191	4.9	N.D		N.D	
10-12	18	0.5	108	3.7	N.D		N.D	
12-14	12	0.3	74	2.4	N.D		N.D	
14-16	11	0.3	57	1.9	N.D		N.D	
16-18	9	0.3	52	1.8	N.D		N.D	

Table 4.15 Cont.

Depth (cm)	$^{134}\text{Cs}/^{137}\text{Cs}$ Activity Ratio	error	^{137}Cs Chernobyl Bq kg^{-1}	error Bq kg^{-1}	^{137}Cs Chernobyl Bq m^{-2}	error Bq m^{-2}	^{137}Cs weapons testing Bq kg^{-1}	error Bq kg^{-1}	^{137}Cs weapons testing Bq m^{-2}	error Bq m^{-2}
0-2	0.14	0.004	124	3.1	942	30.0	10	0.3	76	2.5
2-4	0.07	0.005	51	3.0	357	23.3	57	3.7	399	27.2
4-6			N.D		N.D		65	1.3	377	10.8
6-8			N.D		N.D		49	1.4	274	9.7
8-10			N.D		N.D		33	0.4	191	4.9
10-12			N.D		N.D		18	0.5	108	3.7
12-14			N.D		N.D		12	0.3	74	2.4
14-16			N.D		N.D		11	0.3	57	1.9
16-18			N.D		N.D		9	0.3	52	1.8

Table 4.16 Radiocaesium Activities in the Inverness '90 Transect Peat Core B

Depth (cm)	^{137}Cs Total Bq kg^{-1}	error Bq kg^{-1}	^{137}Cs Total Bq m^{-2}	error Bq m^{-2}	^{134}Cs Total Bq kg^{-1}	error Bq kg^{-1}	^{134}Cs Total Bq m^{-2}	error Bq m^{-2}
0-2	1013	7.2	12561	26.6	143	3.3	1773	54.0
2-4	134	1.3	1126	24.7	15	0.8	126	7.1
4-6	38	0.6	304	7.8	4	0.3	32	2.4
6-8	20	0.2	252	57.5	2	0.1	25	1.6
8-10	14	0.2	120	2.8	1	0.1	9	0.6
10-12	12	0.2	91	2.3	N.D		N.D	
12-14	14	0.2	98	2.4	N.D		N.D	
14-16	9	0.1	95	2.3	N.D		N.D	
16-18	8	0.1	95	2.3	N.D		N.D	

Table 4.16 Cont.

Depth (cm)	$^{134}\text{Cs}/^{137}\text{Cs}$ Activity Ratio	error	^{137}Cs Chernobyl Bq kg^{-1}	error Bq kg^{-1}	^{137}Cs Chernobyl Bq m^{-2}	error Bq m^{-2}	^{137}Cs weapons testing Bq kg^{-1}	error Bq kg^{-1}	^{137}Cs weapons testing Bq m^{-2}	error Bq m^{-2}
0-2	0.14	0.003	937	21.6	11619	35401	76	1.8	942	66.5
2-4	0.11	0.006	99	5.2	832	47.1	35	1.9	294	16.9
4-6	0.12	0.009	29	2.0	232	17.1	9	0.7	72	5.4
6-8	0.09	0.006	12	0.7	151	9.8	8	0.5	101	6.6
8-10	0.07	0.005	6	0.4	52	3.5	8	0.5	68	4.6
10-12			N.D		N.D		12	0.2	91	2.3
12-14			N.D		N.D		14	0.2	98	2.4
14-16			N.D		N.D		9	0.1	95	2.3
16-18			N.D		N.D		8	0.1	95	2.3

Table 4.17 Radiocaesium Activities in the Inverness '90 Transect Peat Core C

Depth (cm)	^{137}Cs Total Bq kg^{-1}	error Bq kg^{-1}	^{137}Cs Total Bq m^{-2}	error Bq m^{-2}	^{134}Cs Total Bq kg^{-1}	error Bq kg^{-1}	^{134}Cs Total Bq m^{-2}	error Bq m^{-2}
0-2	697	6.3	5297	116.2	100	4.7	760	38.8
2-4	246	2.5	2017	45.1	26	1.2	213	10.5
4-6	77	0.9	770	18.0	7	0.6	70	5.8
6-8	46	0.7	337	9.7	5	0.4	41	3.5
8-10	34	0.3	286	6.4	2	0.1	17	0.9
10-12	22	0.3	185	4.4	2	0.1	17	1.0
12-14	37	0.4	326	7.6	2	0.1	18	1.0
14-16	51	1.0	449	12.7	6	0.5	53	4.5

Table 4.17 Cont.

Depth (cm)	$^{134}\text{Cs}/$ ^{137}Cs Activity Ratio	error	^{137}Cs Chernoby1 Bq kg^{-1}	error Bq kg^{-1}	^{137}Cs Chernoby1 Bq m^{-2}	error Bq m^{-2}	^{137}Cs weapons testing Bq kg^{-1}	error Bq kg^{-1}	^{137}Cs weapons testing Bq m^{-2}	error Bq m^{-2}
0-2	0.10	0.005	655	30.8	4978	254.3	42	2.0	19	16.6
2-4	0.11	0.005	156	7.0	1279	63.0	90	4.1	738	37.0
4-6	0.11	0.009	56	4.5	560	46.2	20	1.6	210	17.5
6-8	0.11	0.009	33	2.7	271	23.1	13	1.1	106	9.3
8-10	0.07	0.003	14	6.7	118	6.1	19	0.9	168	8.9
10-12	0.08	0.005	12	0.7	101	5.9	10	0.6	84	5.1
12-14	0.06	0.003	15	0.8	132	7.2	22	1.1	194	10.8
14-16	0.11	0.009	6	0.5	53	4.5	15	1.3	396	34.2

Table 4.18 Radiocaesium Activities in the Inverness '90 Transect Peat Core D

Depth (cm)	^{137}Cs Total Bq kg^{-1}	error Bq kg^{-1}	^{137}Cs Total Bq m^{-2}	error Bq m^{-2}	^{134}Cs Total Bq kg^{-1}	error Bq kg^{-1}	^{134}Cs Total Bq m^{-2}	error Bq m^{-2}
0-2	626	9.0	5008	122.3	79	2.3	632	39.4
2-4	395	3.6	3160	69.3	47	2.0	392	18.6
4-6	301	3.0	2408	53.8	29	1.6	232	13.8
6-8	191	1.3	1528	32.4	22	0.9	176	8.2
8-10	120	1.7	960	23.4	14	1.1	112	8.7
10-12	101	0.9	808	17.7	11	0.5	88	4.3
12-14	84	1.1	672	16.0	9	0.6	72	5.3
14-16	83	1.0	498	11.6	7	0.5	42	3.2

Table 4.18 Cont.

Depth (cm)	$^{134}\text{Cs}/$ ^{137}Cs Activity Ratio	error	^{137}Cs Chernobyl Bq, kg^{-1}	error Bq, kg^{-1}	^{137}Cs Chernobyl Bq, m^{-2}	error Bq, m^{-2}	^{137}Cs weapons testing Bq, kg^{-1}	error Bq, kg^{-1}	^{137}Cs weapons testing Bq, m^{-2}	error Bq, m^{-2}
0-2	0.13	0.008	514	30.3	4112	256.2	112	6.8	896	57.5
2-4	0.12	0.005	307	13.2	2456	116.5	88	3.9	704	34.0
4-6	0.10	0.006	190	10.6	1520	90.4	111	6.3	888	53.6
6-8	0.12	0.005	144	6.0	1152	53.6	47	2.0	376	17.8
8-10	0.12	0.009	90	6.8	720	55.9	30	2.3	240	18.9
10-12	0.11	0.005	73	3.3	584	28.8	28	1.3	224	11.2
12-14	0.11	0.008	60	4.3	480	35.9	24	1.7	192	10.7
14-16	0.09	0.007	45	3.2	360	27.2	37	2.7	138	10.4

FIG. 4.9.1 Cs-137 Activity Transect Core A

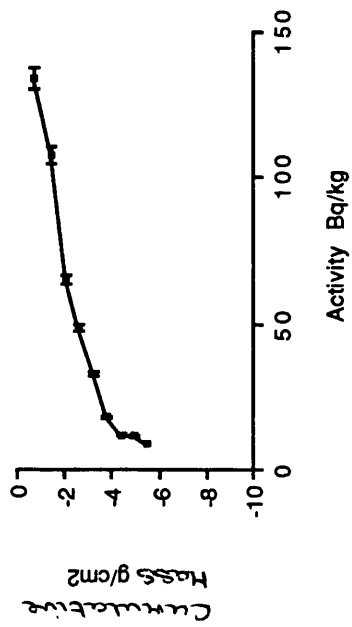


FIG. 4.9.2 Cs-137 Activity Transect Core B

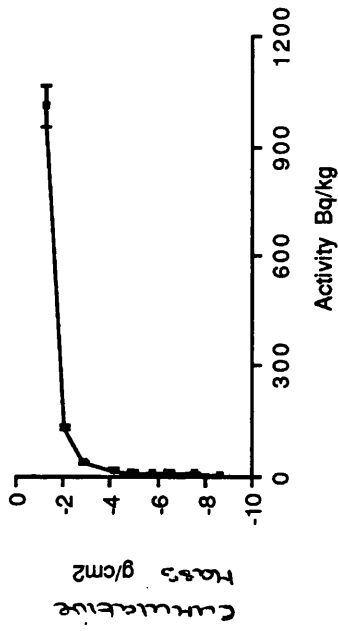


FIG. 4.9.3 Cs-137 Activity Transect Core C

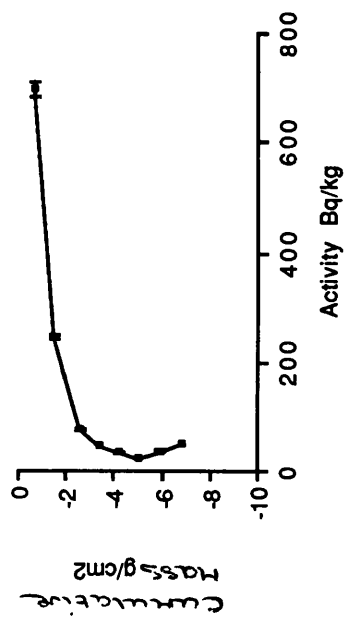


FIG. 4.9.4 Cs-137 Activity Transect Core D

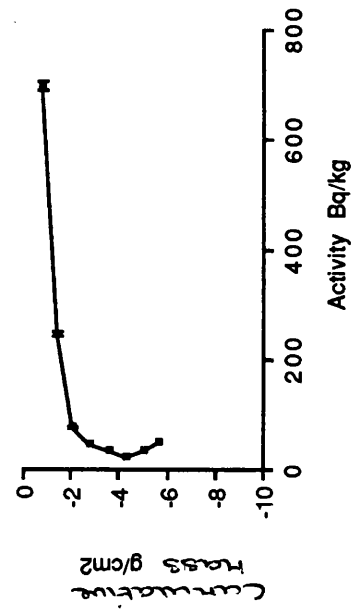


FIG. 4.10.1 Cs-134 Activity Transect Core A

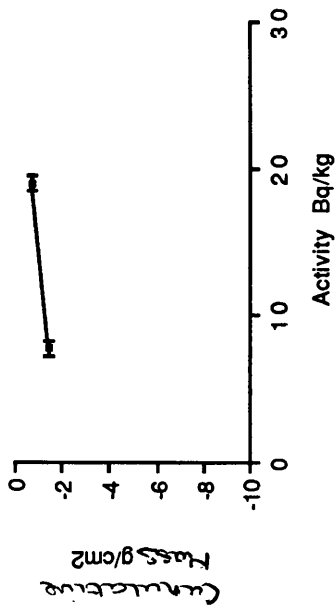


FIG. 4.10.2 Cs-134 Activity Transect Core B

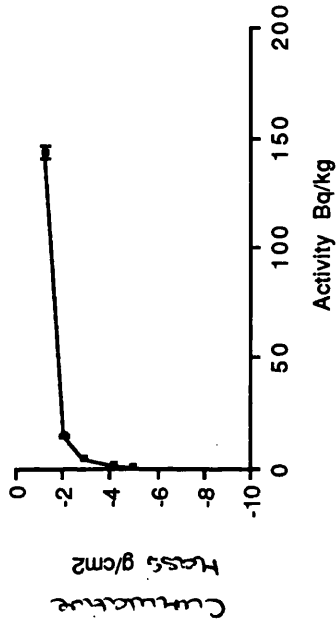


FIG. 4.10.3 Cs-134 Activity Transect Core C

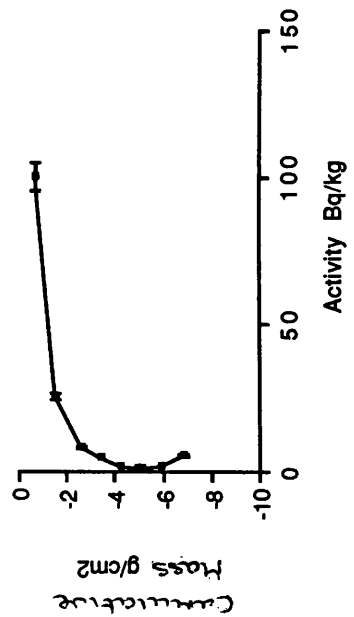


FIG. 4.10.4 Cs-134 Activity Transect Core D

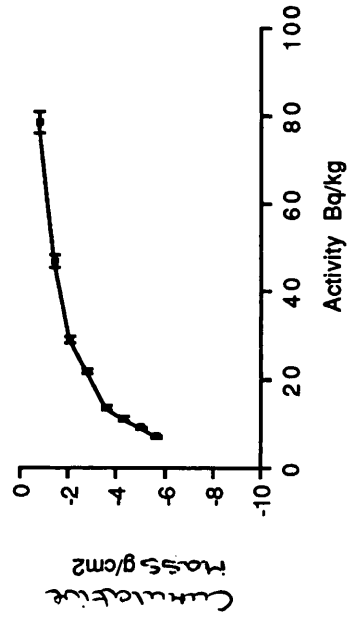


FIG. 4.11 Cs-134/Cs-137 Activity Ratios

FIG. 4.11.1 Core A

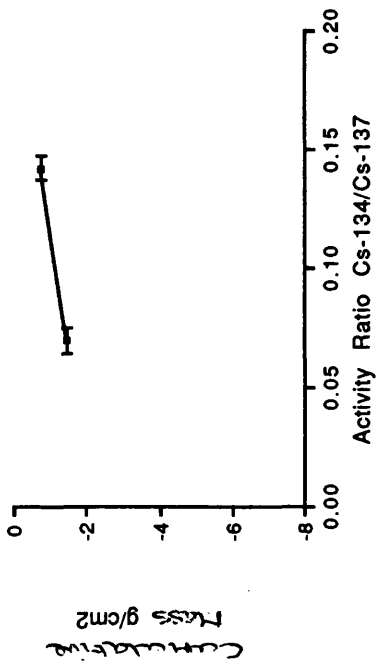


FIG. 4.11.2 Core B

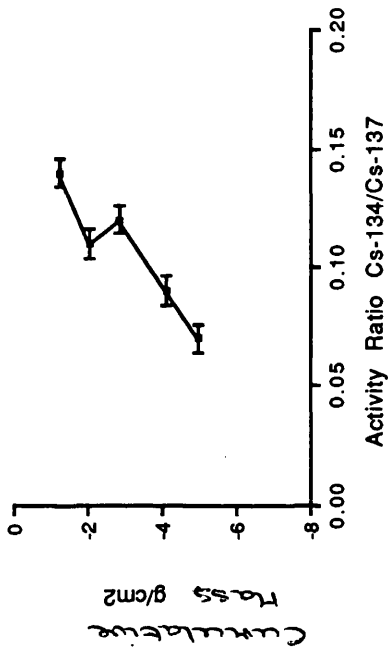


FIG. 4.11.3 Core C

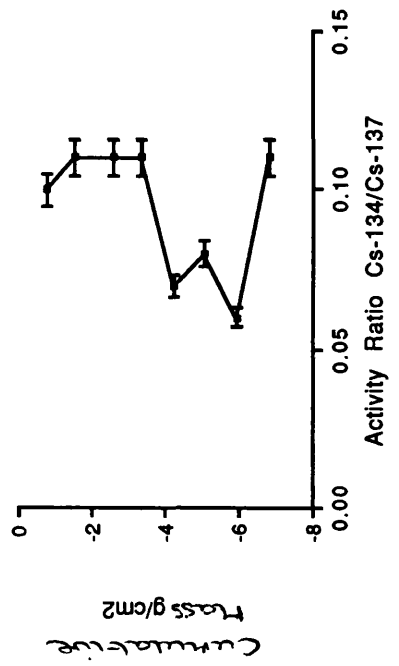


FIG. 4.11.4 Core D

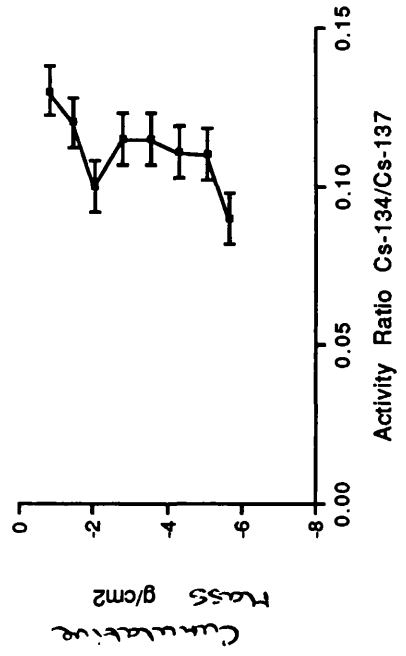


FIG. 4.12 Chernobyl Cs-137 Activity
 FIG. 4.12.1 Core A

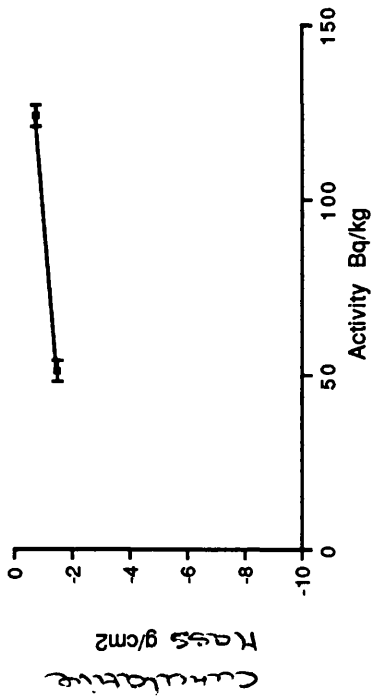


FIG. 4.12.2 Core B

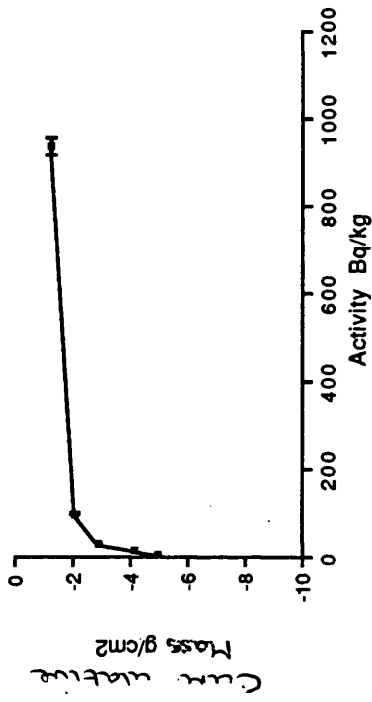


FIG. 4.12.3 Core C

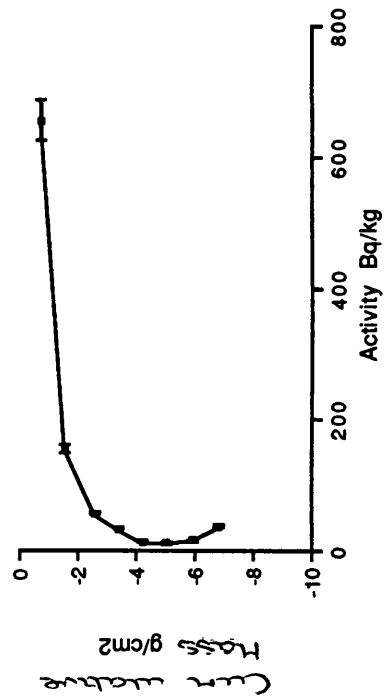


FIG. 4.12.4 Core D

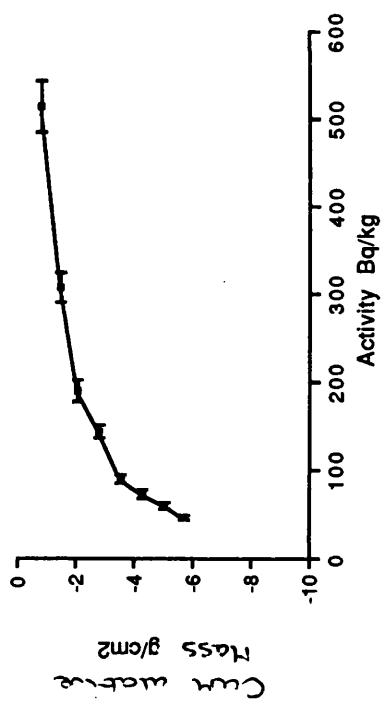


FIG. 4.13 Weapons Testing Cs-137 Activity
 FIG. 4.13.1 Core A

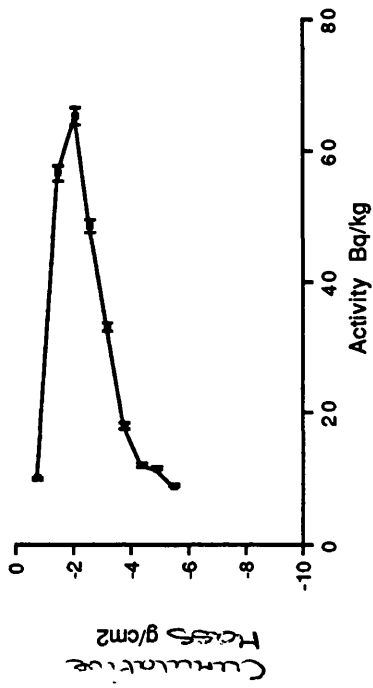


FIG. 4.13.2 Core B

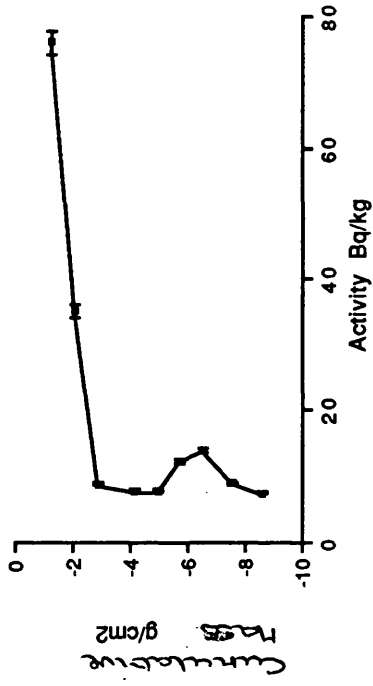


FIG. 4.13.3 Core C

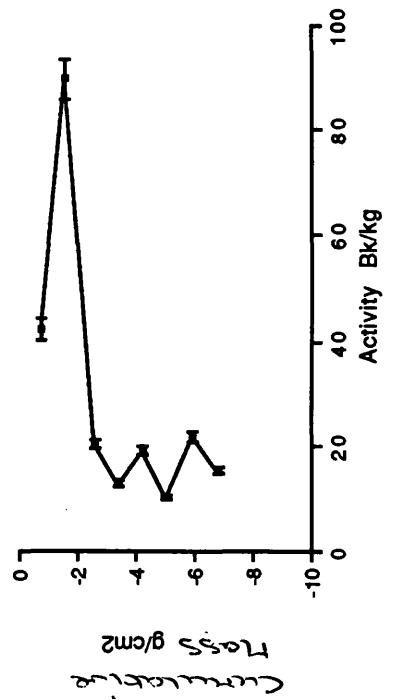


FIG. 4.13.4 Core D

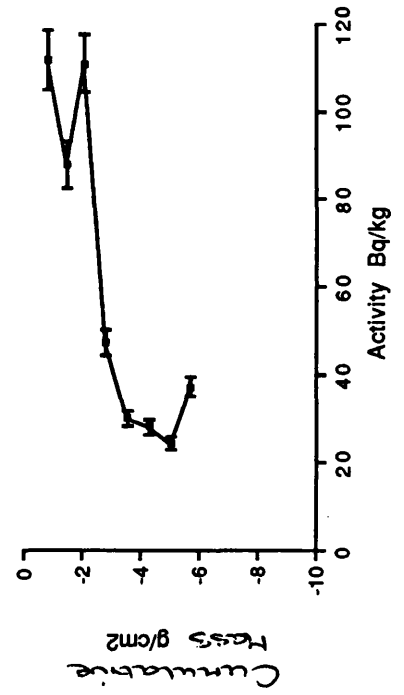


Table 4.19 Radiocaesium Total Inventories for the Inverness'90 Transect Cores.

	^{137}Cs	^{137}Cs	^{137}Cs	
	Total	Chernobyl	Weapons testing	
	kBq m ⁻²	kBq m ⁻²	1990	1963
			kBq m ⁻²	
Core A	2.9	1.4	1.6	3.0
Core B	14.7	14.1	1.8	3.3
Core C	9.7	8.2	1.9	3.6
Core D	15.0	12.5	3.7	6.8

4.4.2 Discussion

^{210}Pb

From the ^{210}Pb data it appears that the input of ^{210}Pb to Core A was unusually high ($187 \text{ Bq m}^{-2} \text{ y}^{-1}$). A flux of similar magnitude ($132 \text{ Bq m}^{-2} \text{ y}^{-1}$) was recorded for the Inverness'89 core sampled at approximately the same site a year earlier, confirming that the elevated levels were not due to experimental error. As discussed earlier (section 4.3.1) ^{210}Pb deposition may be controlled by the frequency of rainfall and mist or cloud cover. In addition, post-depositional mobilisation of ^{210}Pb may occur, resulting in local anomalies in flux measurements (Oldfield et al., 1979).

No mixing zones were evident for the cores and sedimentation rates were therefore calculated using the complete profiles. From the ^{210}Pb sedimentation rates, an apparent order of peat accumulation for the transect was:

	Core A	= Core B	< Core C	< Core D
cm y^{-1}	0.065	0.065	0.190	0.210

These compare favourably with the literature value measured by Sugden et al. (1991) of 0.059 cm y^{-1} for a peat core from Easter Deans, Midlothian, east Scotland.

Radiocaesium

The radiocaesium profiles for Core A show maximum concentration levels of ^{137}Cs in the upper 4 cm. ^{137}Cs of weapons testing origin has penetrated to 18 cm depth whereas the Chernobyl component has reached only 4 cm in the 4 years between deposition and sampling. It is apparent from the relatively low inventory values, (see Table 4.19 e.g. the ^{137}Cs (Chernobyl) inventories are: 1.4 kBq m⁻², Core A; 14.1 kBq m⁻², Core B; 8.2, Core C; and 12.5 kBq m⁻², Core D), that some ^{137}Cs (Chernobyl) has been lost from the upper layers due to a mechanism other than downward diffusion. The differences in inventory values cannot be due to differences in deposition with altitude as between Core A and Core B the change was only approximately 10 m. Also McGee et al. (1992) found in peat soils that Chernobyl deposition decreased with decreasing altitude with no evidence of downslope accumulation, while at this site an increase was observed. This would suggest that a redistribution of radiocaesium post deposition had occurred at the Inverness site, not only vertically but also laterally i.e. advective movement.

The surface layer of Core B had a much higher concentration of ^{137}Cs (Chernobyl) with 11.6 kBq m⁻² in the top 2 cm compared with 0.9 kBq m⁻² at Core A. Probably, this is due to surface runoff of ^{137}Cs as rainwater moves down the hillside. At Core B, ^{137}Cs (Chernobyl) has penetrated to 10 cm depth

indicating that the vertical migration of ^{137}Cs is significant to the overall mobility of ^{137}Cs . At Core C, ^{137}Cs (Chernobyl) again was present in much higher levels in the 0-2 cm layer, 5.0 kBq m^{-2} , compared to Core A. However, at this point in the transect, downward movement has become a more significant mechanism for ^{137}Cs mobility resulting in the penetration of ^{137}Cs (Chernobyl) to depths of 16 cm at relatively high concentration levels (53 Bq m^{-2}). At Core D the levels of ^{137}Cs (Chernobyl) were relatively high down to depths of 8cm (176 Bq m^{-2}) with significant levels being found at 16cm (42 Bq m^{-2}). Core D therefore acts as a sink for ^{137}Cs being transported in the surface water, but does not undergo surface runoff itself due to its topographical position at the base of the slope. In addition ^{137}Cs deposited at Core D either via aerial deposition or surface water movement can subsequently diffuse to lower depths.

In Cores C and D, it was possible to see sub-surface maxima at 2-4 cm in the weapons testing ^{137}Cs profiles. This may be due to surface runoff depleting the concentrations of ^{137}Cs in the upper layer but the gradual accumulation of peat over 27 years since deposition is the most probable cause, (with an accumulation rate of around 0.2 cm y^{-1} , and a 27 year time interval the weapons testing fallout should be at approximately 5 cm depth).

In summary, it is apparent that local topography

has a significant effect upon the mobility of radiocaesium in peat soils. Radiocaesium deposited on hillside peats apparently undergoes lateral transport through surface water run-off resulting in radiocaesium enriched surface layers of peat lower down the hillside and depleted layers at the upper end of the hillside. The degree to which this advective movement governs the mobility of radiocaesium will be determined at least in part by the slope of the hill and the average annual rainfall.

4.5 Radiocaesium Mobility - a proposed model.

In the previous section it became apparent that substantial advective movement has taken place in several of the cores studied. Due to this radiocaesium mobility cannot be treated as diffusion. However, the decrease in ^{137}Cs concentration with depth could be modelled using a diffusion type equation to derive an empirical parameter to characterise the rate of downwards movement at individual sites. Coefficients were calculated for the ^{137}Cs components, where possible, using Fick's Law based on a situation where the ^{137}Cs is assumed to be added to a uniform plane surface at a given time and then undergoes diffusion into the layer (Crank, 1956). For the weapons testing fallout, a single input in 1963 was assumed. The mixing zones present in some peat cores precluded the calculation of a coefficient due to the continuous transfer of radiocaesium at the interface between mixing and diffusion zones. It is probable that the calculated values for Core D reflect most closely a situation where downwards movement only was responsible for the mobility of radiocaesium in peat soils. However, the calculated coefficients must be considered to be 'effective' coefficients only due to the influence of other mobilising and demobilising mechanisms such as lateral advection and sorption onto soil particles.

The results are presented in Table 4.20. The

values obtained approximate to $10^{-11} \text{ m}^2 \text{ s}^{-1}$ for ^{137}Cs from Chernobyl deposition in peat and mineral soils. These compare with literature values for the diffusion coefficients of silts and clays of $10^{-12} - 3.3 \times 10^{-11} \text{ m}^2 \text{ s}^{-1}$ (Aston and Stanners, 1979; Christiansen and Torstenfelt, 1988; Higgs et al., 1988). A broader spread of values was obtained for ^{137}Cs of weapons testing origin. Generally coefficients for the older ^{137}Cs were smaller than for ^{137}Cs (Chernobyl), this may be due to the gradual fixation of ^{137}Cs taking place with time resulting in a reduction in radiocaesium mobility. This may be the reason why a coefficient could not be calculated for ^{137}Cs (weapons testing) in the Dreghorn profile with the distribution pattern being a result of variable degrees of fixation taking place down the profile. The coefficient of $3 \times 10^{-12} \text{ m}^2 \text{ s}^{-1}$ for ^{137}Cs (Chernobyl) in the Inverness'90 Core B is an order of magnitude lower than the coefficients for the ^{137}Cs (Chernobyl) components of Cores C and D. This is possibly due to Core B having a higher mineral content than the other cores.

Table 4.20 Coefficients characterising the downwards movement of Radiocaesium.

	^{137}Cs	r^2	^{137}Cs	r^2
	Chernobyl		Weapon	
	m^2s^{-1}		Testing	
	m^2s^{-1}		m^2s^{-1}	
Inverness '89	N.A		N.A	
Borders	N.A		N.A	
Fenwick Moor	N.A		N.A	
Darleith	N.A		7×10^{-12}	0.25
Dreghorn	2×10^{-12}	0.98	N.A	
Inverness '90				
Core A	N.A		5×10^{-12}	0.55
Core B	3×10^{-12}	0.70	8×10^{-12}	0.20
Core C	1×10^{-11}	0.69	N.A	
Core D	2×10^{-11}	0.83	3×10^{-12}	0.84

N.B N.A indicates that the coefficients were not available due either to the presence of mixing zones in the cores, insufficient data points (<3), or extremely low r^2 values.

A box model can be used to attempt to predict the mobility of radiocaesium in the peat profiles and hence enable the calculation of the amount present in the surface layers after a specified time period. A diagram of the model is shown in Diag.4.2. For the Inverness'90 Transect there was no apparent mixing zone but the influence of downslope accumulation of radiocaesium complicates the model considerably, preventing the application of a linear model to predict future radiocaesium movement. For Inverness'89 a mixing zone further complicates the situation, thus preventing much speculation of future radiocaesium behaviour at this site.

Calculations and predications will therefore be made using Borders and Fenwick Moor peats. Both have a mixing zone below which diffusion occurs. It was not possible to calculate coefficients for the cores due to the continual input of radiocaesium into them from the mixing zone. However, it was possible to calculate the changes in activity levels that would take place in the mixing zones. Assuming an exponential decrease in concentration in the mixing zone with time:

$$C = C_0 \cdot e^{-kt}$$

where C_0 is the concentration of the radionuclide at deposition i.e 100%

C is the concentration after time t

k is a constant.

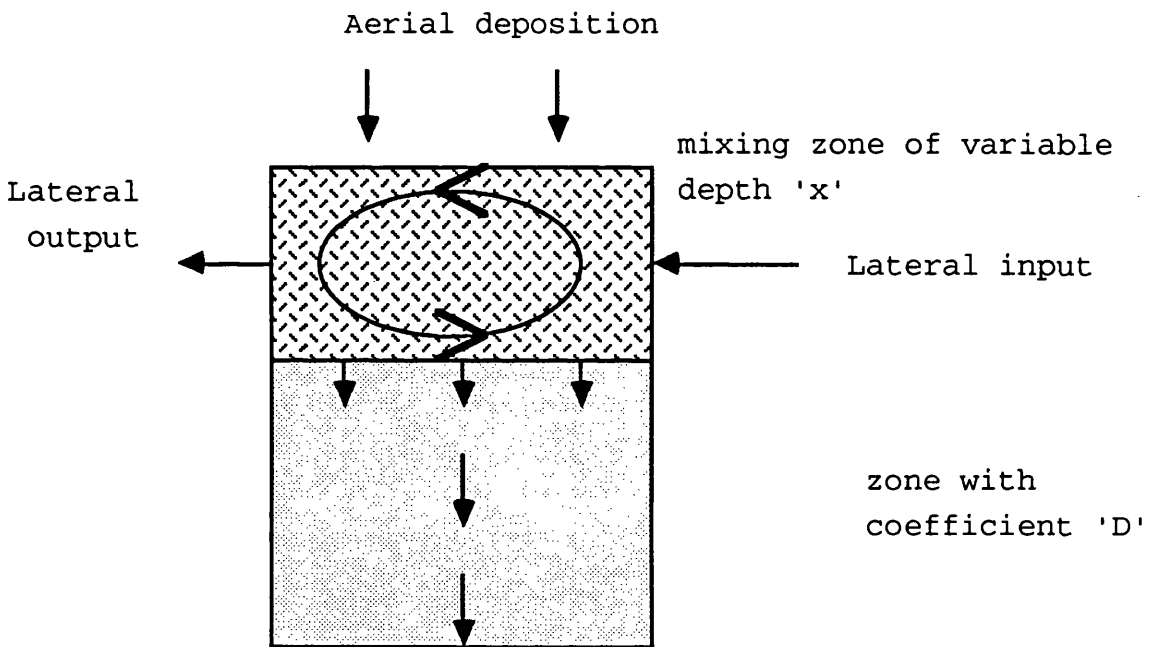
For Borders peat, 94% of ^{137}Cs (Chernobyl) and 57% of ^{137}Cs (weapons testing) were present in the mixing zone (0-6 cm) at the time of sampling.

For Fenwick Moor peat, 63% of ^{137}Cs (Chernobyl) and 51% of ^{137}Cs (weapons testing) were present in the mixing zone (0-5 cm) at the time of sampling.

Using these data 'k' values can be calculated, as shown in Table 4.21.1. Using these values, predications can be made of the time that it will take for the mixing zone concentrations of radiocaesium to fall to a certain percentage of the original concentration deposited. Some time values (years) are presented in Table 4.21.2. By presenting the mixing zone model graphically, it is possible to calculate concentrations for any time post-deposition (Fig. 4.14). It is apparent that for the Borders peat removal of radiocaesium from the mixing layer is controlled primarily by the decay of the radionuclide i.e for the concentration of ^{137}Cs to be reduced to 50% of its original concentration takes 36 years for ^{137}Cs of weapons testing origin and 33 years for Chernobyl ^{137}Cs , these values compare well with the half-life of 30.17 years for ^{137}Cs . The half-life time for weapons testing ^{137}Cs of 28 years in the Fenwick Moor peat again compares well with the isotope half-life. However, the Chernobyl ^{137}Cs has a much shorter half-life possibly due to the lateral movement of radiocaesium re-mobilised in water run-off. If this is

the situation then for this peat the model would not be valid.

^{210}Pb sedimentation rates can be used to calculate the maximum depth to which ^{137}Cs could have penetrated to below the mixing zone without the assistance of diffusion. These would be, assuming at least 1 year is spent in the mixing zone: for Borders, 0.5 cm for ^{137}Cs (Chernobyl) and 6.3 cm for ^{137}Cs (weapons testing); and for Fenwick Moor, 0.1 cm for ^{137}Cs (Chernobyl) and 1.3 cm for ^{137}Cs (weapons testing). It is obvious therefore that diffusion has enhanced the mobility of the radiocaesium such that it has been able to penetrate to greater depths in the peat samples.



DIAG. 4. | Radiocaesium Mobility Model

Table 4.21.1 Mixing Zone Constants

	'k' ^{137}Cs Chernobyl y^{-1}	'k' ^{137}Cs Weapons testing y^{-1}
Borders	0.019	0.021
Fenwick Moor	0.142	0.025

Table 4.21.2 Projected times in years for mixing zone concentrations of ^{137}Cs to be reduced, expressed as a percentage of original deposition concentration.

	90%	75%	50%	25%	10%
	of original concentration of ^{137}Cs				
Borders					
$^{137}\text{Cs}(\text{Ch})$	5	15	36	73	121
$^{137}\text{Cs}(\text{WT})$	5	14	33	66	110
Fenwick Moor					
$^{137}\text{Cs}(\text{Ch})$	1	2	5	10	16
$^{137}\text{Cs}(\text{WT})$	4	12	28	55	92

FIG. 4.14 Predicted Removal of Radiocaesium from the Mixing Zones of Peat Soils

FIG. 4.14.1 Borders Peat

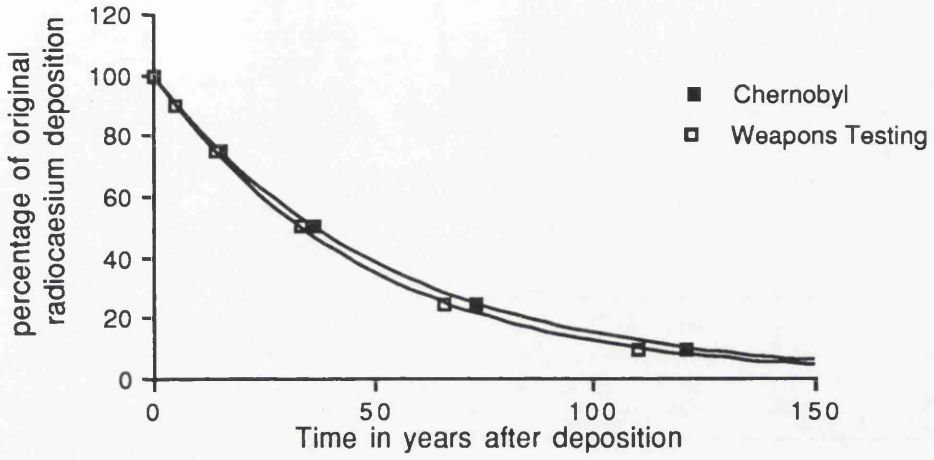
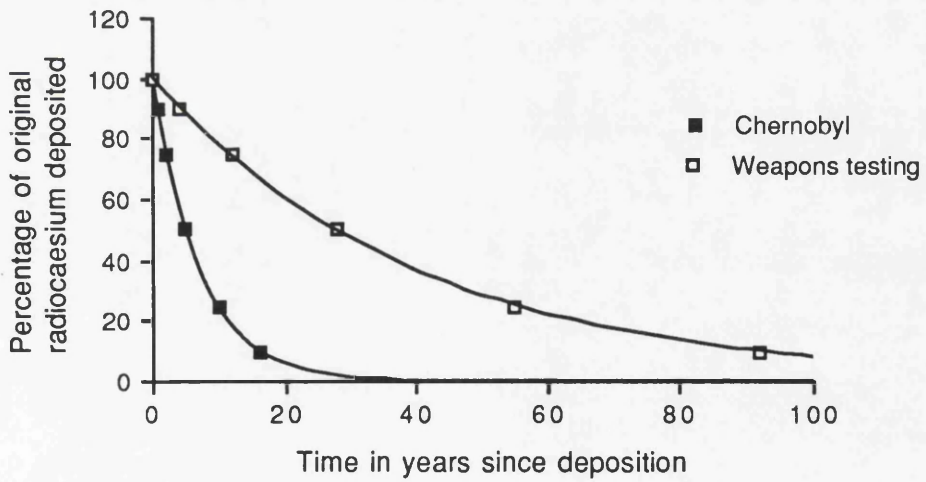


FIG. 4.14.2 Fenwick Moor Peat



4.6 Summary

Several important points regarding the mobility of radiocaesium in organic soils have been revealed in this section of work:

- a) Radiocaesium data cannot be used to derive a chronology for peat profiles due to its mobility.
- b) Local variations in topography can result in downslope mobilisation of radiocaesium resulting in downslope accumulation.
- c) For peat soils with a mixing zone underlain by an area of downwards movement, an exponential model can be used to predict the reduction in radiocaesium concentration in the mixed zone with time.

In order to gain more information about the interactions which take place when caesium and lead bind to the soils examined in this chapter laboratory experiments were carried out (see Chapter 5). These looked at the sorption of stable caesium and lead by a group of soils ranging from those with a high mineral content (Dreghorn) to a high organic content (Fenwick Moor peat). It was hoped that by examining the behaviour of caesium under controlled conditions it might be possible to determine the extent to which caesium binds to soils, the factors which control this behaviour and in particular to ascertain the importance of the organic fraction of soils in the control of caesium uptake.

The qualitative evaluation of the soils adsorption

and desorption trends could possibly lead to the use of Isotherm equations to describe the observed behaviour. These may then provide data of use in environmental modelling packages.

It was hoped that the combination of field and laboratory results would assist in the interpretation of environmental observations.

CHAPTER 5 - LABORATORY EXPERIMENTS EXAMINING THE
SORPTION OF CAESIUM AND LEAD BY SOILS AND CLAYS.

5.1 Introduction

The aims of this study were to elucidate the uptake and degree of retention of both caesium and lead by soil using laboratory methods. Much work has previously been undertaken examining the behaviour of caesium in clay systems leading to the conclusion that the metal ions are sorbed onto ion exchange sites on the clay surface and caesium specific sites at the clay edges. This sorption is thought to be irreversible in the main (Coleman et al., 1963; see Section 1.5.1). The sorption of lead by soils has also been the subject of many studies due to its high toxicity and conclusions have been drawn that lead ions bind strongly and irreversibly with clay surfaces and organic matter by metal bridge formation and are also associated with oxides present in the soil (Evans, 1989; see Section 1.3).

The work described here examined a range of soils of varying physico-chemical properties in order to correlate these with the apparent sorption behaviour of caesium, and studied the adsorption and desorption of caesium and lead by a representative set of clay minerals. The study concentrated more on caesium due to current environmental concern following the Chernobyl

reactor explosion. Experiments were designed to examine the effects, if any, that changing the external parameters such as time and background solution had upon sorption.

The experimental work can be divided into three main sections:

- i) The analysis of a range of soils for their physico-chemical properties and their sorption capacities for caesium over the concentration range 0-5 millimolar (mM). Therefore providing a large data set for correlation analysis to examine the influence of parameters such as pH, cation exchange capacity and organic matter content on the sorption of caesium.
- ii) The further analysis of a subset of four soils to determine the effects of time and background electrolyte on sorption and desorption behaviour and equilibrium of caesium ions, the applicability of data to the Langmuir equation was investigated in this section,
- iii) The analysis of caesium and lead sorption behaviour of soils and clays at solution concentrations in the range 0-50 mg l⁻¹, with particular emphasis upon developing methods for measuring desorption.

5.2 Sorption Experiments

5.2.1 Caesium adsorption isotherms

Caesium adsorption isotherms were measured for thirteen soils. Primarily the isotherm data were expressed as simple isotherms in order to draw comparisons between soil types and also the length of adsorption time (Figs 5.1.1-5.1.13). Characteristic values of pH, organic matter content and cation exchange capacity (CEC) for these soils are tabulated in Chapter 3, Tables 3.4-3.6.

In all cases, the isotherms exhibited steep initial gradients at equilibrium concentrations of <0.5 mM. This is due to the adsorption of caesium onto high energy caesium specific sites. At equilibrium concentrations >0.5 mM the gradient lessened and for certain soils (Dreghorn A and B; and Bargour A and Bg), a plateau was reached. This can be attributed to the gradual filling of low energy ion exchange sites. For the remaining soils the saturation of these sites had not occurred with the concentration range and contact times used. These phenomena can be illustrated quantitatively using K_d values calculated for lower (0.5 mM) and higher (3.0 mM) equilibrium concentrations (Table 5.1). These values will be discussed in section 5.2.2.

For most of the soils (Dunlop A and Bg; Peaty Gley Bg; Humic Gley Bg; Dreghorn A and B; Bargour A and Bg; and Peat), the effect of increased adsorption time


resulted in only a slight increase in adsorption after 24 hours. However, for the remaining soils (Darleith A; Peaty Gley 0; and Humic Gley 0), a more marked increase in the amount of caesium adsorbed at higher equilibrium solution concentrations was seen after 24 hours contact time. These soils have relatively high organic matter, clay contents and CEC values (Tables 3.4 -3.6). This indicates that contact times of >24 hours were required for adsorption to achieve equilibrium with these soils.

The apparent order of adsorption for caesium for the 13 soils studied after 24 hours was:-

Humic Gley Bg > Dunlop A > Peaty Gley 0 > Darleith A >
Dunlop Bg > Humic Gley 0 > Darleith B > Peaty Gley Bg >
Bargour A > Peat > Bargour Bg > Dreghorn A > Dreghorn B

In all cases, apart from Humic Gley Bg, the B horizon of a soil type adsorbed less caesium than the corresponding A horizon. This is as expected, due to the lower CEC. values and organic matter contents of the B horizons compared to A horizons.

Figure 5.1 Caesium Adsorption Isotherms for:-

1 Hour 

24 Hours 

Figure 5.1.1 Darleith A

Figure 5.1.2 Darleith B

Figure 5.1.3 Dunlop A

Figure 5.1.4 Dunlop Bg

Figure 5.1.5 Peaty Gley Oh

Figure 5.1.6 Peaty Gley Bg

Figure 5.1.7 Humic Gley Top

Figure 5.1.8 Humic Gley Bg

Figure 5.1.9 Dreghorn A

Figure 5.1.10 Dreghorn B

Figure 5.1.11 Bargour A

Figure 5.1.12 Bargour Bg

Figure 5.1.13 Peat

FIG. 5.1.1 DARLEITH A

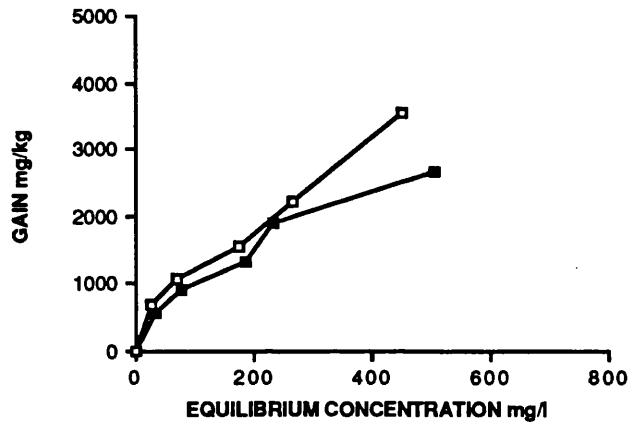


FIG. 5.1.2 DARLEITH B

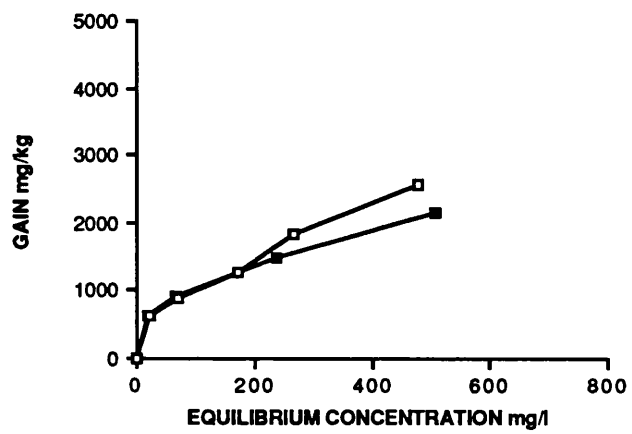


FIG. 5.1.3 DUNLOP A

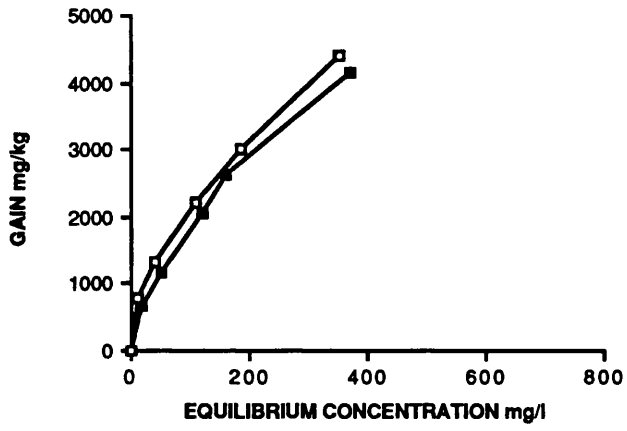


FIG. 5.1.4 DUNLOP B

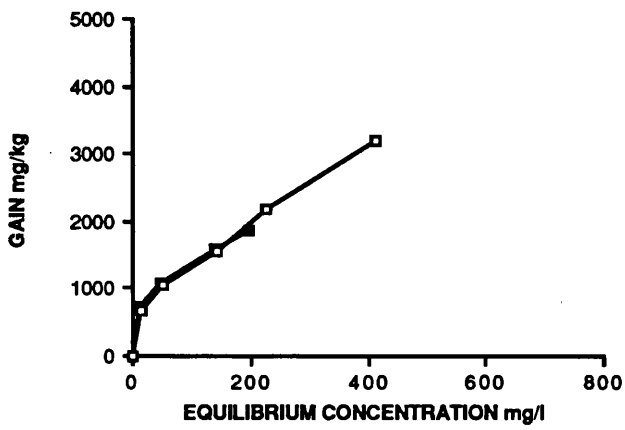


FIG. 5.1.5 PEATY GLEY O

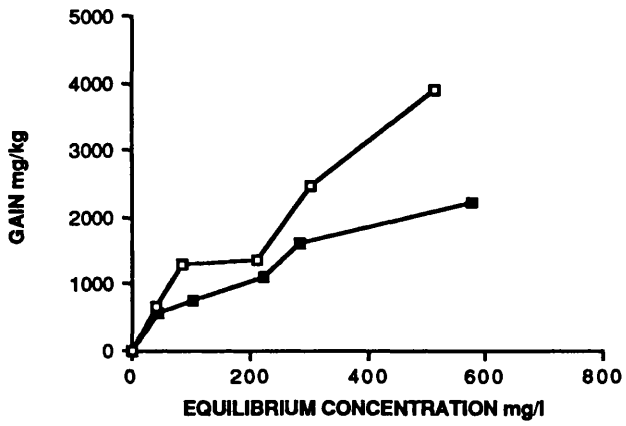


FIG. 5.1.6 PEATY GLEY Bg

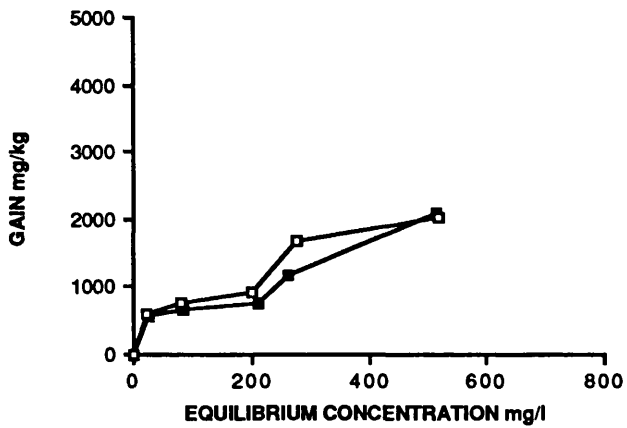


FIG. 5.1.7 HUMIC GLEY O

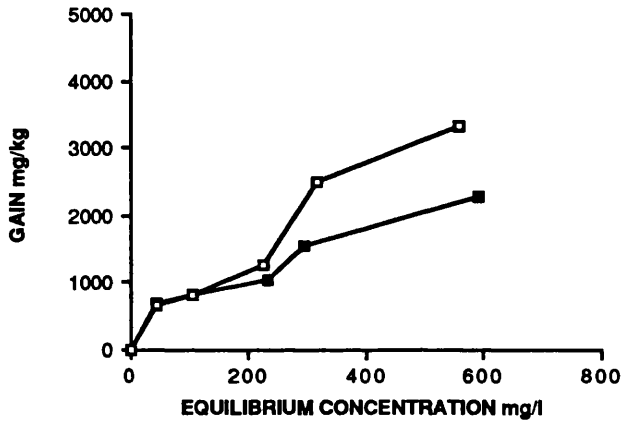


FIG. 5.1.8 HUMIC GLEY B

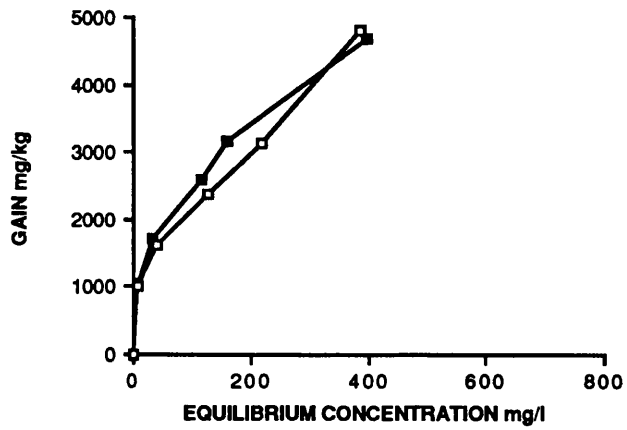


FIG. 5.1.9 DREGHORN A

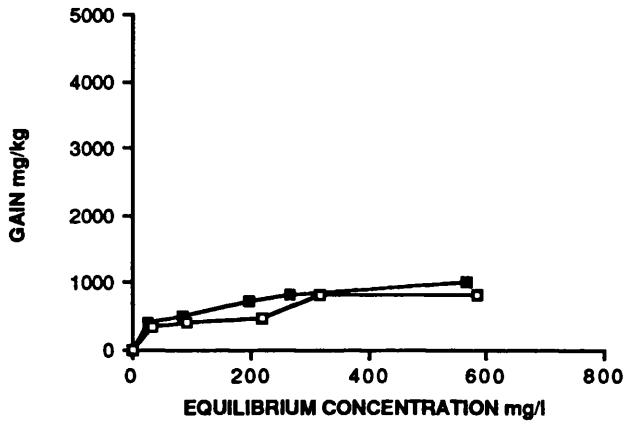


FIG. 5.1.10 DREGHORN B

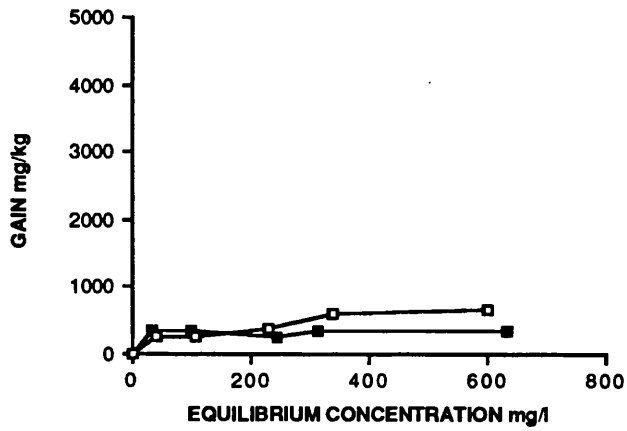


FIG. 5.1.11 BARGOUR A

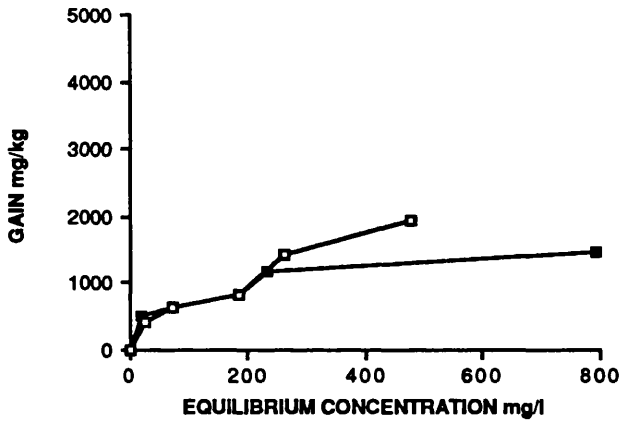


FIG. 5.1.12 BARGOUR B

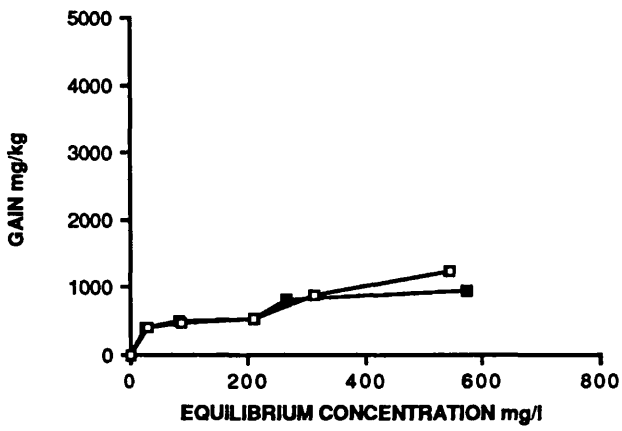
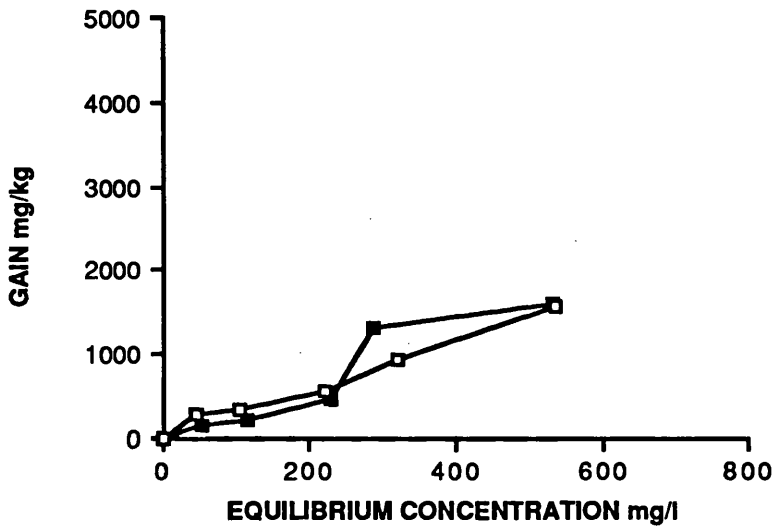


FIG. 5.1.13 PEAT



5.2.2 K_d Calculations

K_d values were calculated for the isotherms in order to obtain quantitative descriptions for the adsorption behaviour of the soils. K_d is the distribution coefficient where:

$$K_d = \frac{\text{amount } M^{n+}/\text{gram of air dry soil}}{\text{amount } M^{n+}/\text{ml of solution}}$$

K_d values were calculated for all the soils at solution equilibrium concentrations of 0.5 mM and 3 mM in order to express the differences between the lower and upper regions of the isotherms (Table 5.1). The following conclusions can be drawn from the data :-

1) For all the soils except Peat at the 1 hour shaking time, the statement:

$$K_d (0.5 \text{ mM}) > K_d (3.0 \text{ mM})$$

was true. This can be explained by the sorption of caesium onto specific sites in this concentration range. Peat soil does not exhibit this behaviour over the shorter time and this may be due to its high organic matter content (>90%) and subsequently low clay content providing few specific sites. This would suggest that it is the mineral phase of the soil that is responsible for this specific adsorption.

2) In general K_d values at 0.5 mM were similar at 1 and 24 hours shaking times confirming that equilibrium was reached rapidly (<24 hours) within this concentration range. Sawhney's (1966) research into the kinetics of

caesium sorption showed that the uptake of caesium by some clay minerals is rapid.

3) For the majority of soils K_d values at 3mM were greater for the 24 hour shaking times than for the 1 hour shaking time due to equilibrium not having been achieved at 1 hour within this concentration range.

4) In general the statement:

$$K_d \text{ (A horizon)} > K_d \text{ (B horizon)} \text{ at } 3.0 \text{ mM}$$

was true for both shaking times, at 0.5 mM there was no discernable trend. This suggests that changes in sorption behaviour for longer shaking times may be governed by soil organic matter as this varies considerably between horizons, whereas sorption over shorter shaking times is similar between the two horizons due to the less variable mineral content. For Humic Gley the reverse trend is seen and this may be due to the presence of minerals with a high sorption capacity for caesium in the B horizon, this would also agree with the much higher K_d values at 0.5 mM for this horizon.

McKinley and Hadderman (1984) published K_d value of 2000 l kg^{-1} for bentonite clay at concentrations of 10^{-7} M , however, they emphasised that K_d is concentration dependent and that for every order of magnitude increase in concentration the K_d value should be halved. Therefore a value of 125 l kg^{-1} can be calculated for the concentrations used here of 10^{-3} M . The experimental values compare reasonably well as much

lower values would be expected for soils in comparison to pure clays.

Table 5.1 K_d Values for caesium sorption calculated for two equilibrium solution concentrations (0.5 mM and 3 mM) and for two shaking times (1 hour and 24 hours).

Soil Name	1 Hour		24 Hours	
	0.5 mM 1 kg ⁻¹	3 mM 1 kg ⁻¹	0.5 mM 1 kg ⁻¹	3mM 1 kg ⁻¹
Darleith A	10.0	5.9	10.0	7.6
Darleith B	13.0	4.5	13.0	5.4
Dunlop A	20.0	N.A	25.0	N.A
Dunlop Bg	17.6	N.A	15.3	7.8
Peaty Gley O	9.4	4.5	15.3	7.6
Peaty Gley Bg	9.4	3.9	10.6	4.4
Humic Gley O	10.6	4.5	10.6	6.9
Humic Gley Bg	30.6	11.8	27.1	N.A
Dreghorn A	7.1	2.2	5.9	2.0
Dreghorn B	4.7	0.8	3.5	1.6
Bargour A	8.2	3.1	8.2	4.3
Bargour Bg	7.1	2.2	7.1	2.5
Peat	2.4	3.5	4.7	2.9

N.A - not available

5.2.3 The application of the Langmuir equation

Langmuir maxima were calculated for the isotherm curves using the equation:-

$$c/x = c/x_m + 1/kx_m$$

where x = amount absorbed at equilibrium concentration c

x_m = maximum sorbate capable of being adsorbed - the Langmuir maxima and k is a constant relating to bonding (see Section 1.4.6.1).

The values are presented in Table 5.2., graphs illustrating the isotherm data are presented in Appendix 1. The probability values 'p' were used to determine if there was a significant effect of the x axis upon the y and whether the line obtained from the Langmuir equation was linear, ($p < 0.02$ was taken as an appropriate indication of a significant effect of x on y). A survey of literature was carried out to find comparative data for x_m values but none were found.

Using $p < 0.02$ the majority of isotherms appeared to be described accurately by the Langmuir isotherm.

For two soils, Peaty Gley O and Humic Gley O, (and Darleith A to a lesser extent), the data did not fit the isotherms. Both of these soils have a high organic matter content; loss on ignition of 70.3% and 76.0% respectively (Table 3.4). The contribution of organic matter to the sorption of caesium may become significant at these levels in comparison to the ion-exchange reactions of caesium with the mineral phase. Due to the involvement of two mechanisms for sorption, the Langmuir isotherm cannot adequately describe the sorption of caesium by these soils. A third soil, peat, failed to fit the isotherm at both shaking times. The peat sample had an organic matter content of 90.5%.

It is probable that sorption of caesium takes place mainly by uptake onto the organic fraction, and that the mechanism by which this occurs cannot be described by the Langmuir isotherm.

However, Langmuir isotherms can be used to describe accurately the uptake of caesium by less organic soils over this concentration range.

TABLE 5.2 Langmuir Maxima for caesium sorption calculated for two shaking times (1 hour and 24 hours).

Soil Name	Langmuir Maxima		p<	R ²	Langmuir Maxima		p<	R ²
	1 hour	cmol kg ⁻¹			24 hours	cmol kg ⁻¹		
Darleigh A	2.9	0.010	0.010	91	3.7	0.450	0.450	79
Darleigh B	1.6	0.020	0.020	97	2.4	0.020	0.020	87
Dunlop A	5.5	0.010	0.010	91	4.2	0.010	0.010	92
Dunlop B	1.6	0.010	0.010	98	2.9	0.020	0.020	88
Peaty Gley O	2.5	0.030	0.030	84	4.7	0.180	0.180	50
Peaty Gley Bg	2.0	0.150	0.150	56	1.9	0.060	0.060	74
Humic Gley O	2.3	0.450	0.450	79	5.1	0.210	0.210	46
Humic Gley B	4.0	0.006	0.006	94	4.1	0.020	0.020	87
Dreghorn A	0.9	0.001	0.001	98	0.7	0.160	0.160	89
Dreghorn B	0.3	0.002	0.002	97	0.7	0.020	0.020	87
Bargour A	1.3	0.001	0.001	98	2.1	0.060	0.060	75
Bargour B	0.8	0.010	0.010	92	1.1	0.050	0.050	76
Peat	-3.3	0.570	0.570	12	2.8	0.280	0.280	37

For corresponding isotherms see Appendix 1.

N.B.:

- p values refer to the probability level of the F statistic and indicate the significance level of regression effect;

- R² is the coefficient of determination.

5.2.4 Correlation Analysis

Correlations were carried out using a linear fit for Langmuir maxima at 1 hour and 24 hours shaking time, and for K_d values taken from the 24 hour isotherms at 0.5 mM and 3.0 mM equilibrium solution concentrations, in order to calculate the relationship between the measured soil physical parameters of pH, CEC and organic matter, and caesium sorption (Fig. 5.2-5.5). Data points for Darleith A, Peaty Gley 0 and Humic Gley 0 are identified with the labels d,p and h respectively.

The data have been summarised in terms of the r^2 value for each line in Table 5.3. In order for a correlation equation to be significant at the 95% confidence level r^2 must be greater than 0.33.

The only significant correlations were between the Langmuir maxima values for 24 hours and pH, organic carbon and CEC (Table 5.3). When comparing the shapes of the soil distributions for these data (Fig. 5.2.4-5.2.6) with the distributions at 1 hour (Fig. 5.2.1-5.2.3) it is apparent that the anomalous points at 1 hour, those with $\text{pH} < 4.5$, $\text{CEC} > 50 \text{ cmol kg}^{-1}$ and organic carbon content $> 25 \%$, have been redistributed to the upper end of the graph. This effect must be due to these soils (Darleith A, Peaty Gley 0 and Humic Gley 0) requiring longer to attain equilibrium due to their greater capacity for caesium uptake. This behaviour is discussed further below.

There was no significant relationship between the K_d value at 0.5 mM or 3.0 mM equilibrium solution concentrations and the pH, CEC or organic matter content of the soils (Table 5.3). The K_d values at the two equilibrium concentrations were correlated and related by the equation:-

$$K_d(3.0 \text{ mM}) = 0.45 K_d(0.5 \text{ mM}) + 0.511$$

with a r^2 value of 0.86, which is significant at greater than 99%. This implies that although caesium uptake occurs at different rates within the two concentration regions there are some similarities in behaviour.

The correlation analysis was carried out for a second time after removing the data for Darleith A, Peaty Gley 0 and Humic Gley 0 (Table 5.4). The results show a good correlation between the Langmuir maxima, at both equilibrium times, and the K_d , at 0.5 mM only, with both organic carbon and CEC. K_d values at 3.0 mM were more poorly correlated than K_d values at 0.5 mM. Therefore, the use of a single value, either Langmuir maximum or one K_d value, to model the sorption behaviour of these soils would be inappropriate. This is too simple an approach, disregarding the effects of concentration dependency. However, sorption over the concentration range 0-0.5 mM, is dependent on the soil's CEC and organic matter content in these soils.

The sorption behaviour of the soils; Darleith A,

FIG. 5.2.1 LANGMUIR MAXIMA versus pH

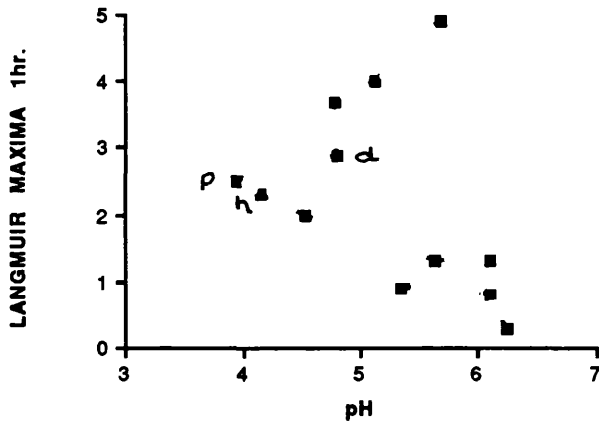


FIG. 5.2.2 LANGMUIR MAXIMA versus C.E.C

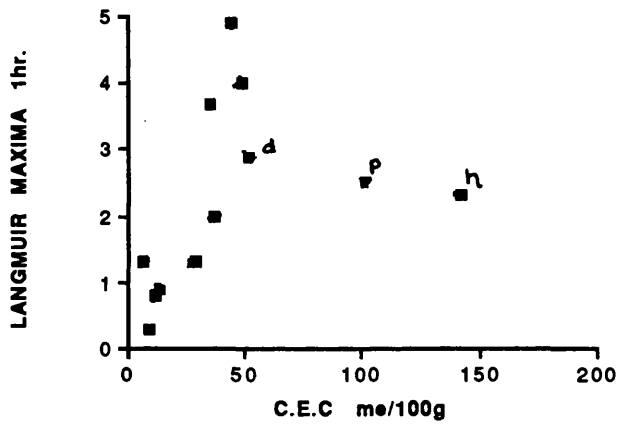


FIG. 5.2.3 LANGMUIR MAXIMA versus ORGANIC CARBON

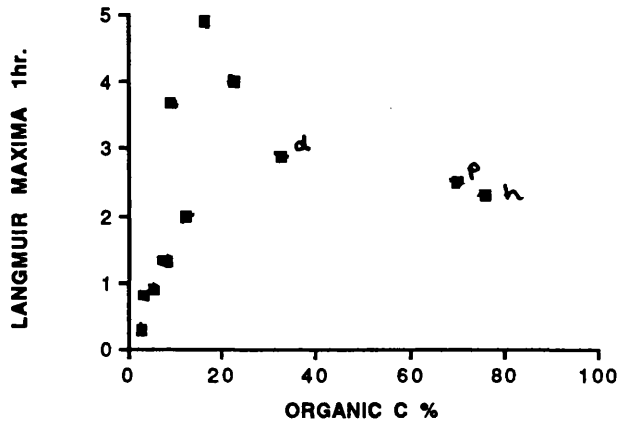


FIG. 5.2.4 LANGMUIR MAXIMA (24 hrs.) versus pH

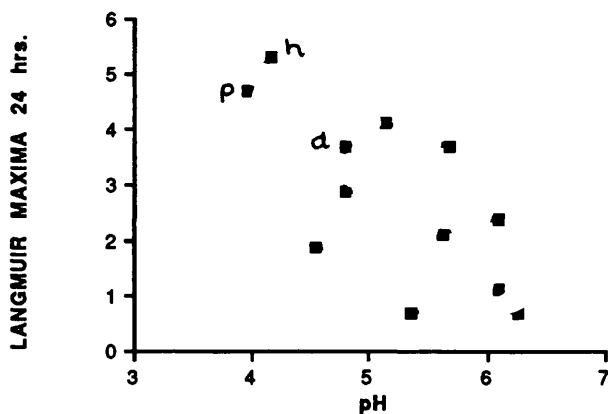


FIG. 5.2.5 LANGMUIR MAXIMA (24 hrs.) versus C.E.C

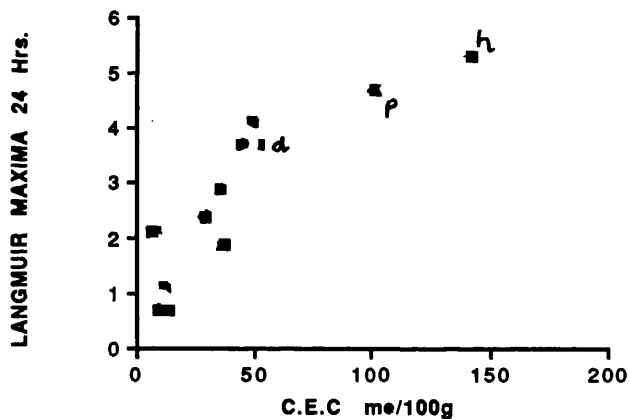


FIG. 5.2.6 LANGMUIR MAXIMA (24 hrs.) versus ORGANIC CARBON

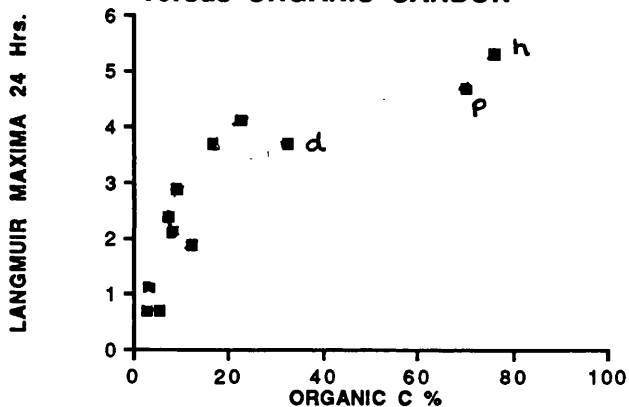


FIG. 5.3.1 K_d VALUES AT 0.5mM (24hrs) versus pH

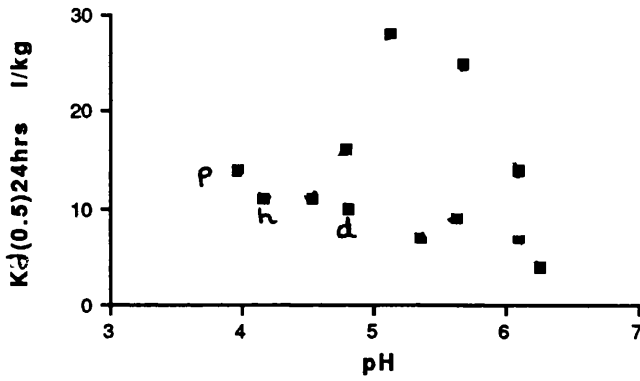


FIG. 5.3.2 K_d VALUES AT 0.5mM (24hrs) versus C.E.C

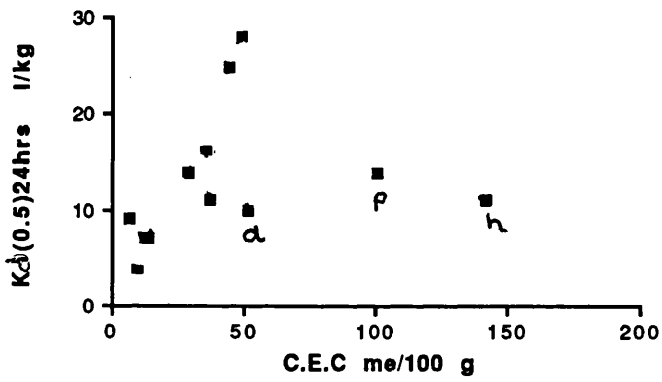


FIG. 5.3.3 K_d VALUES AT 0.5mM (24hrs) versus ORGANIC CARBON

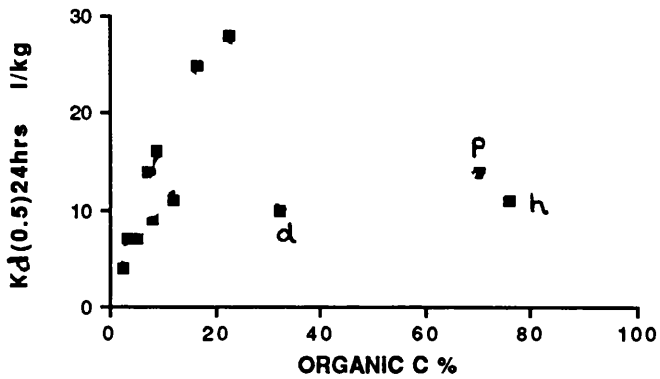


FIG. 5.4.1 K_d VALUES AT 3mM (24hrs) versus pH

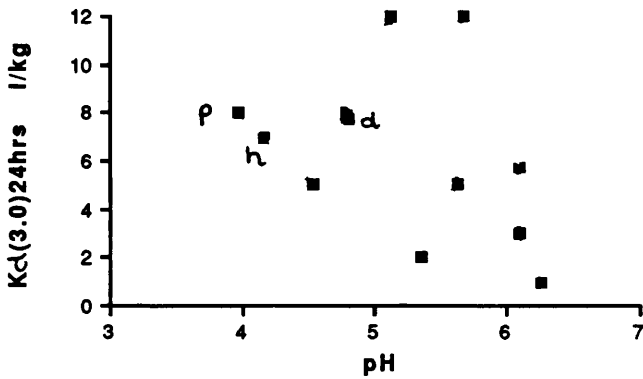


FIG. 5.4.2 K_d VALUES AT 3mM (24hrs) versus C.E.C

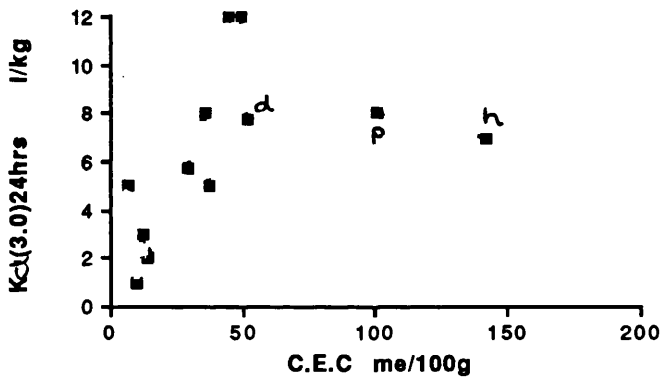


FIG. 5.4.3 K_d VALUES AT 3mM (24 hrs) versus ORGANIC CARBON

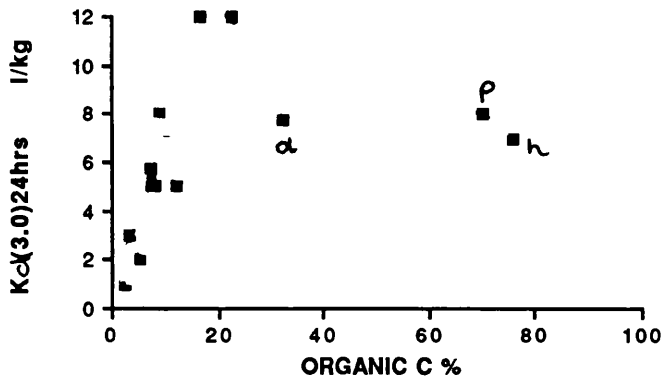


FIG.5.5 Kd VALUES AT 0.5 mM VERSUS VALUES AT 3.0 mM

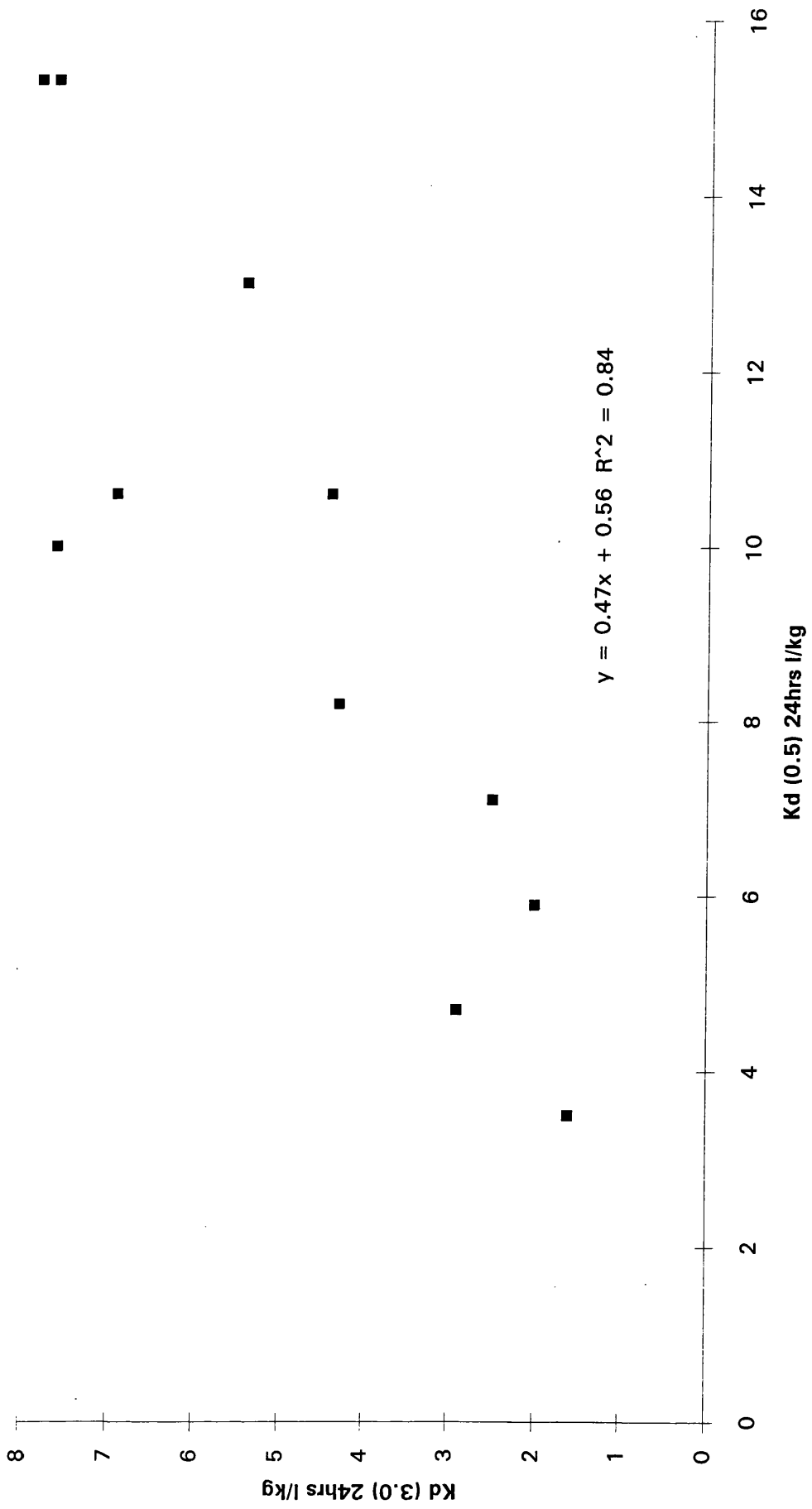


Table 5.3 Correlation Data - Linear Correlations between Langmuir maxima and K_d values and the pH, cation exchange capacity and organic matter content of the soils.

$r^2 > 0.33$ at 95% confidence level

	pH	CEC	O.M
Langmuir Maxima 1 Hr.	0.15	0.13	0.07
Langmuir Maxima 24 Hrs.	0.48	0.75	0.71
K _d (0.5mM)	0.03	0.05	0.02
K _d (3.0mM)	0.14	0.19	0.14

Table 5.4 Correlation Data - Linear Correlations

Calculated with the data for Darleith A, Peaty Gley 0 and Humic Gley 0 removed.

$r^2 > 0.44$ at 95% confidence level

	pH	CEC	O.M
Langmuir Maxima 1 Hr.	0.22	0.75	0.70
Langmuir Maxima 24 Hrs.	0.12	0.72	0.80
K _d (0.5mM)	0.10	0.80	0.86
K _d (3.0mM)	0.27	0.52	0.47

5.3 Caesium Adsorption / Desorption Isotherms

Isotherms were measured for the sub-group of soils, Darleith A, Peaty Gley 0, Humic Gley 0 and Dreghorn A, which were thought to be representative of all the soils. In order to examine the effect of time upon adsorption, and the subsequent desorption the shaking time of the experiments was varied from 1 hour to 1 week. The results of these experiments are presented in Figures 5.6-5.9. Langmuir maxima were calculated for the adsorption curves and this data is presented in Table 5.5.

Due to the large dilutions in the desorption experimental method at the lower end of the curves and the extremely small volume of filtrate obtained at the upper end of the curves (< 5 ml for the gley soils) the experimental errors involved in obtaining the data were high. The interpretation of the data is therefore undertaken with this in mind.

The effect of time upon the adsorption of caesium by Darleith seems to be significant only up to 24 hours, after this time a steady value of around 2.5 cmol kg^{-1} was obtained for the maximum gain, this compares with an average Langmuir maximum of 3.4 cmol kg^{-1} . The desorption of caesium from Darleith appears to follow the adsorption curve, resulting in complete release of the metal ions back to solution upon dilution with CaCl_2 . This was not expected due to the high clay content of Darleith and contradicts the

findings of Erten et al. (1988a and b) whose sorption experiments illustrated that caesium sorption processes for soils were only partially reversible. However the data reinforces the findings at the sample site where sheep grazing on this land have continued to have a high radiocaesium burden and agrees with the findings of Coughtry and Thorne (1983) and Livens and Loveland (1988).

The Peaty Gley isotherms were more variable. After 1 hour a maximum gain of approximately 1 cmol kg^{-1} was attained, the corresponding desorption curve lay below the adsorption curve. This implied that the caesium was partitioned between the solution and soil phases such that less caesium was held by the soil than at equivalent equilibrium concentration points on the adsorption curve. This would imply that caesium was released from the soil over and above that added during the adsorption step. Alternatively the difference may be due to analytical errors. After 24 hours the maximum gain for adsorption had increased to 3 cmol kg^{-1} reinforcing the idea that a longer shaking time is required for some soils to come to equilibrium, the gain can be compared with a Langmuir maximum of 4.7 cmol kg^{-1} at 24 hours. Again the desorption curve was displaced from the adsorption curve although here it was above the adsorption curve. A similar pattern was seen at 1 week. These curves separate from the corresponding adsorption curves at the highest

concentration points and this may be due to continued adsorption occurring in the sample which remained undiluted during the desorption period. This feature would obviously be emphasised more at longer desorption times. For samples which achieve equilibrium more quickly this feature of the method would not be a problem.

The curves for Humic Gley showed similar features to Peaty Gley, with higher gains being achieved after 24 hours shaking. The displacement of the desorption points makes it almost impossible to draw any firm conclusions about the desorption of caesium from the Humic Gley. Repeat runs of the experiments produced similar adsorption isotherms, but the desorption curves were not reproducible. This behaviour emphasised the need to develop a different method for measuring the desorption of caesium from soils (see section 5.7).

Dreghorn's isotherms were more easily assessed. The desorption curves partly followed the adsorption curves; explainable by the complete release of any sorbed caesium back to solution. Time appeared to have little significance upon the observed behaviour.

The application of the Langmuir equation to data for the Darleith and Dreghorn soils seemed appropriate, with the values obtained increasing slightly with the adsorption time. The experimental maximum gain values were in agreement with the theoretical maxima. However due to the more complex

adsorption behaviour of the Peaty Gley and Humic Gley soils, the Langmuir equation could not be used.

None of the data sets gave any indication of the ability of the soils to fix caesium, which has been so widely reported in the literature (Coleman et al, 1963). Although the observed behaviour was unexpected from a theoretical viewpoint, it supports the observed environmental behaviour of Chernobyl derived caesium in organic soils (Livens and Loveland, 1988).

Figure 5.6-5.9

Adsorption / desorption isotherms of :-

5.6 Darleith A

at equilibrium times of 5.6.1 1 hour

5.6.2 24 hours

5.6.3 1 week

adsorption isotherm ■ , desorption isotherm □

5.7 Peaty Gley 0

at equilibrium times of 5.7.1 1 hour

5.7.2 24 hours

5.7.3 1 week

adsorption isotherm ■ , desorption isotherm □

5.8 Humic Gley 0

at equilibrium times of 5.8.1 1 hour

5.8.2 24 hours

5.8.3 1 week

adsorption isotherm ■ , desorption isotherm □

5.9 Dreghorn A

at equilibrium times of 5.9.1 1 hour

5.9.2 24 hours

5.9.3 1 week

adsorption isotherm ■ , desorption isotherm □

FIG. 5.6.1 DARLEITH A 1 HOUR

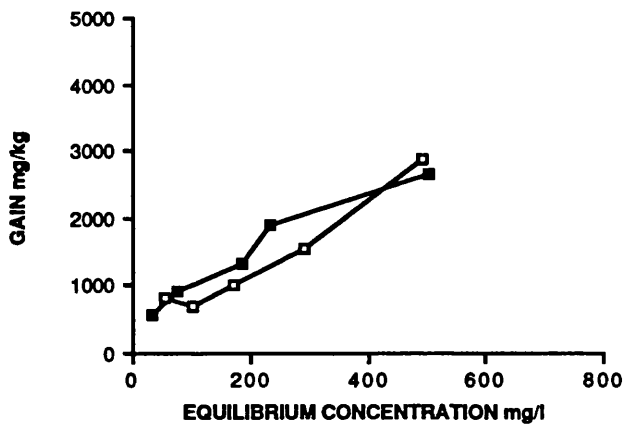


FIG. 5.6.2 DARLEITH A 24 HOURS

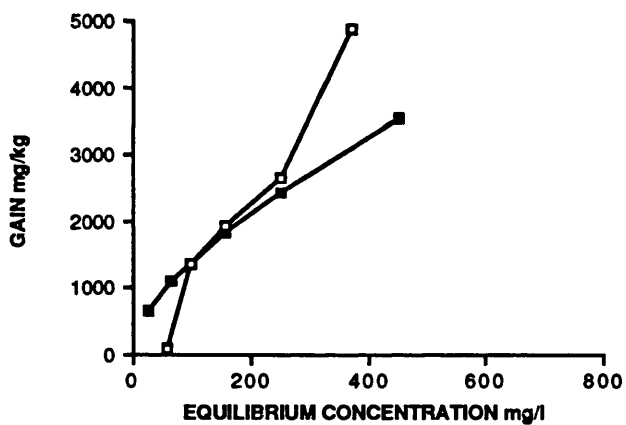


FIG. 5.6.3 DARLEITH A 1 WEEK

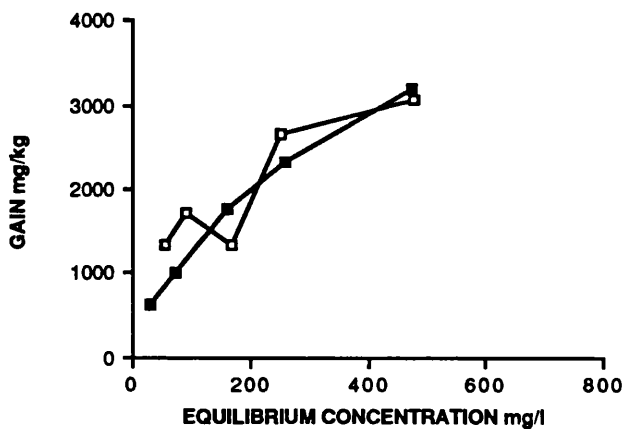


FIG.5.7.1 PEATY GLEY Oh 1 HOUR

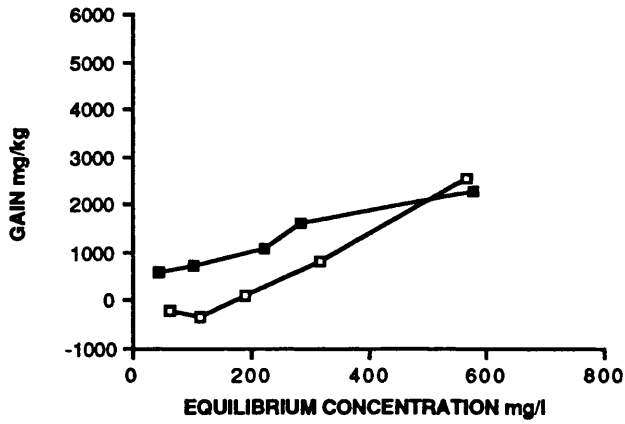


FIG. 5.7.2 PEATY GLEY Oh 24 HOURS

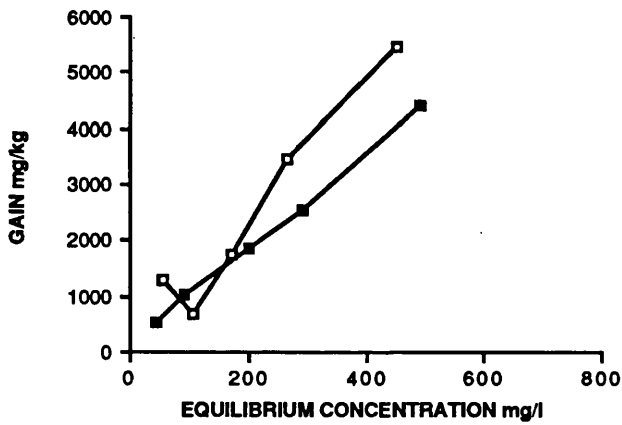


FIG. 5.7.3 PEATY GLEY Oh 1 WEEK

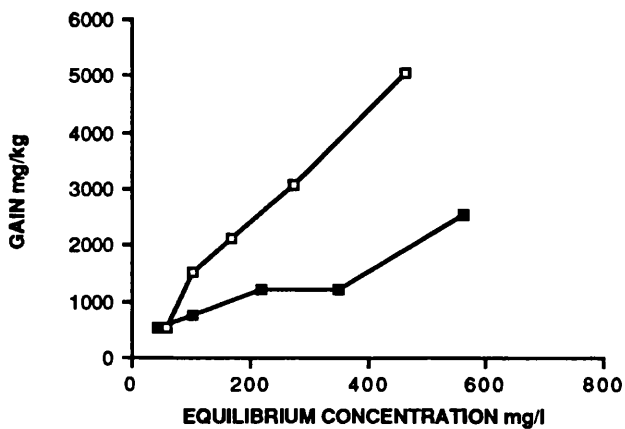


FIG. 5.8.1 HUMIC GLEY TOP 1 HOUR

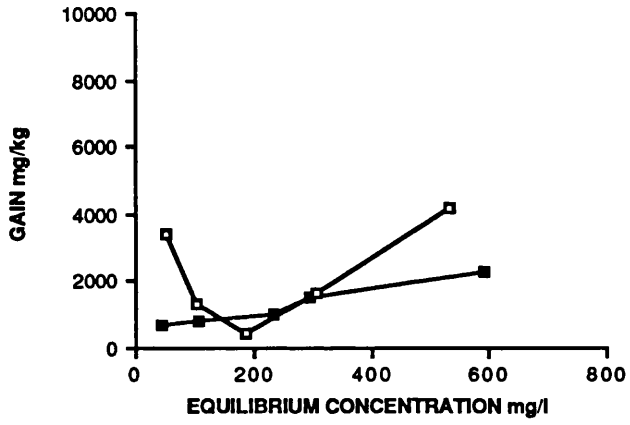


FIG. 5.8.2 HUMIC GLEY TOP 24 HOURS

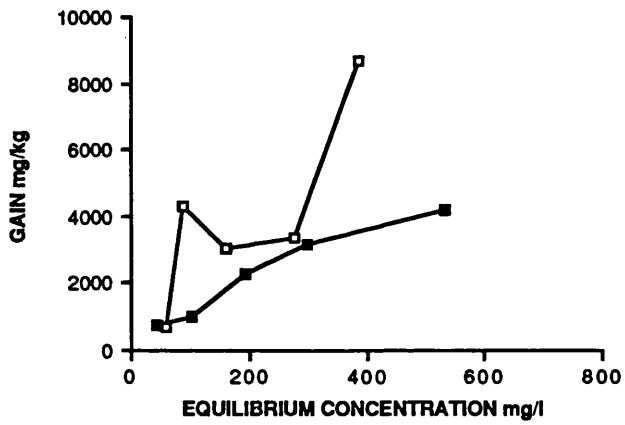


FIG. 5.8.3 HUMIC GLEY TOP 1 WEEK

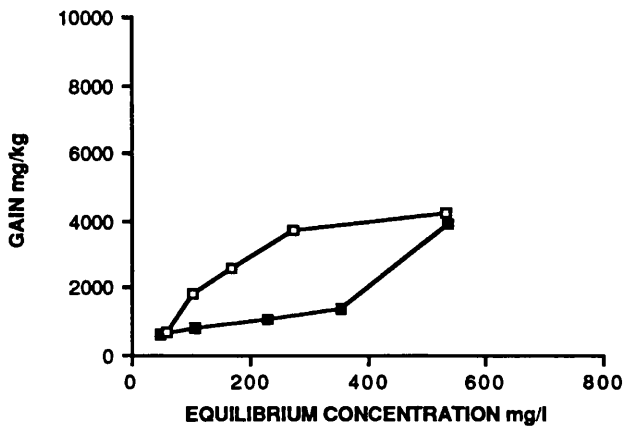


FIG. 5.9.1 DREGHORN 1 HOUR

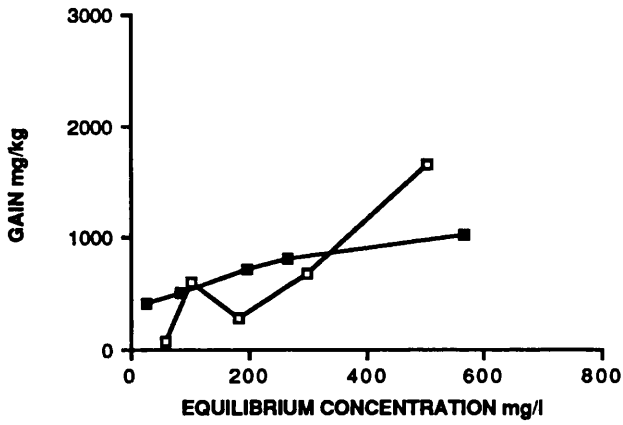


FIG. 5.9.2 DREGHORN 24 HOURS

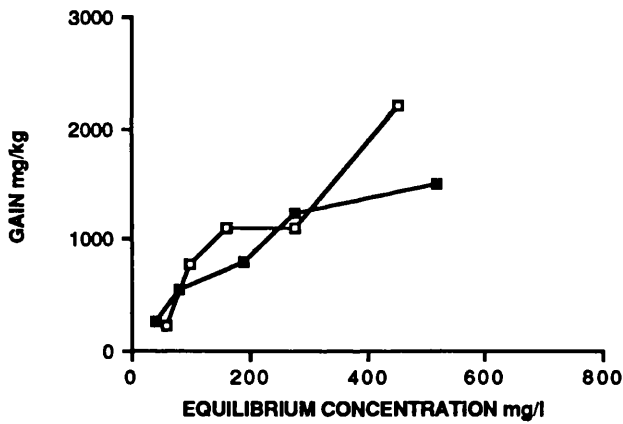


FIG. 5.9.3 DREGHORN 1 WEEK

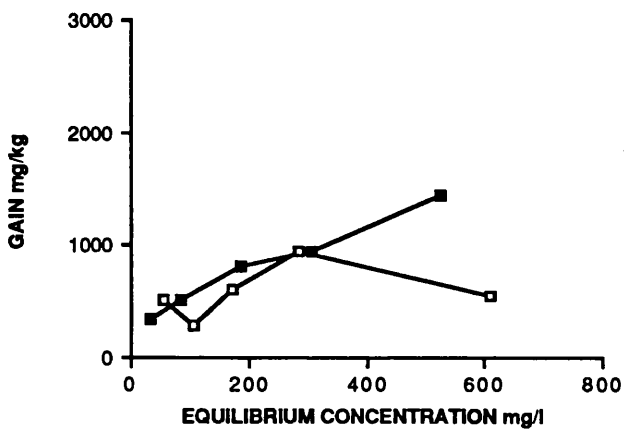


Table 5.5 Langmuir Maxima for Caesium Adsorption
Isotherms

Soil Name	Adsorption Time	Langmuir Maximum cmol kg^{-1}	r^2
Darleith	1 hour	2.90	0.90
	24 hours	3.86	0.92
	1 week	3.43	0.97
Peaty	1 hour	2.45	0.84
Gley	24 hours	4.70	0.48
	1 week	2.62	0.54
Humic	1 hour	2.33	0.76
Gley	24 hours	5.28	0.42
	1 week	4.95	0.17
Dreghorn	1 hour	0.87	0.97
	24 hours	0.72	0.91
	1 week	1.42	0.92

For corresponding isotherms see Appendix 1.

5.4 Long Term Adsorption Experiment

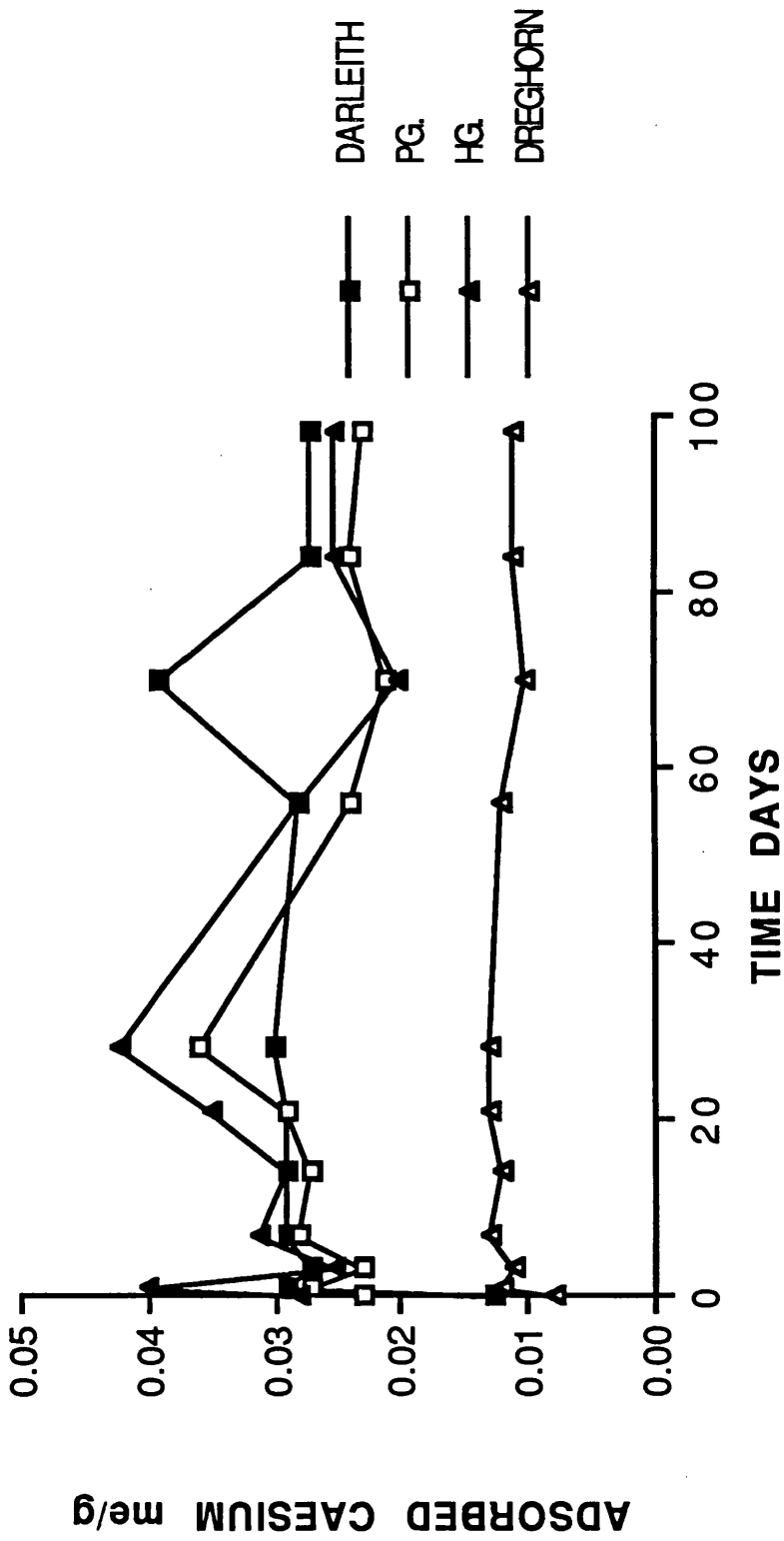
In order to investigate further the effect of time upon caesium adsorption, measurements were made for the four soils (Darleith A, Dreghorn A, Peaty Gley 0 and Humic Gley 0) over 98 days (14 weeks). Each data point was obtained using three replicate samples of 5.0 g of soil in 50 ml of 5 mM CsCl in 0.01 M CaCl₂. The data, illustrated as a graph (Fig. 5.10), were expressed in terms of the amount adsorbed per gram of soil (mmoles gram⁻¹).

Darleith exhibited an initial steep rise over the first day reaching an average value of 0.030 mmol g⁻¹ with a standard deviation of 0.0036 mmol g⁻¹. This could also be expressed as 5.8% of the soil's CEC. Adsorption by the Peaty Gley followed a less consistent trend, with a large increase at 28 days to 0.036 mmol g⁻¹. The average adsorption was 0.026 mmol g⁻¹ with a standard deviation of 0.009 mmol g⁻¹, this was 2.6% of the soil's total CEC. A similar trend was observed in Humic Gley mimicking the Peaty Gley peak at 28 days. This was possibly due to a fluctuation in the temperature of the room. When examined carefully both Darleith and Dreghorn also have small increases at this point. The average uptake of Humic Gley was 0.30 mmol g⁻¹ with a standard deviation of 0.0071 mmol g⁻¹ and this was 2.1% of the total CEC. The adsorption trend for Dreghorn was more consistent with an average value

of 0.012 mmol g⁻¹ with a standard deviation of 0.001 mmol g⁻¹ and this was 8.6% of the soil's CEC.

Although the sorption of caesium by the four soils was in line with their relative CEC values, when this was expressed as a percentage of CEC a reverse trend was observed. This may reflect the organic matter content of the soils. It is possible that a greater proportion of the sites on clay surfaces were available for caesium uptake in low organic content soils than for those soils where the organic content is high enough for the clay and organic matter to interact (see Chapter 6). (In Fig. 5.10 PG. is an abbreviation of Peaty Gley and HG. of Humic Gley.)

FIG. 5.10 LONG TERM CAESIUM ADSORPTION



5.5 Effect of Background Electrolyte

Adsorption / desorption isotherms were run with three different background electrolytes in order to determine the effect that changing the swamping ion had upon these processes. The electrolytes used were KCl (0.01 M), NaCl (0.01 M) and CaCl₂ (0.01 M). The results of the experiment are presented in Figs. 5.11-5.12 and illustrate the effects observed for the two soils Peaty Gley and Dreghorn. For Dreghorn it was apparent that adsorption times of 24 hours were insufficient for equilibrium to be achieved when the background electrolyte was monovalent (Na⁺ and K⁺) as the desorption curve had been displaced above the adsorption curve indicating that adsorption continued during the desorption shaking period. This does not take place with CaCl₂. Similar, but more variable, desorption patterns were observed for Peaty Gley in NaCl and KCl. It would seem that swamping the soil with a monovalent ion provides a greater number of sites for caesium adsorption and also as the desorption curves failed to rejoin the adsorption curves at lower concentrations provides sites for caesium fixation. This could be due to the presence of potassium and sodium ions causing the clay lattices to collapse trapping caesium ions or conversely that caesium ions cannot compete for sorption sites with calcium due to its greater charge and thus are desorbed as a result of preferential ion exchange. The adsorption curves showed

similar trends for both soils in the different electrolytes.

For both soils the adsorption of caesium in the different electrolytes followed the trend:-

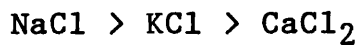


FIG. 5.11.1 DREGHORN / KCl

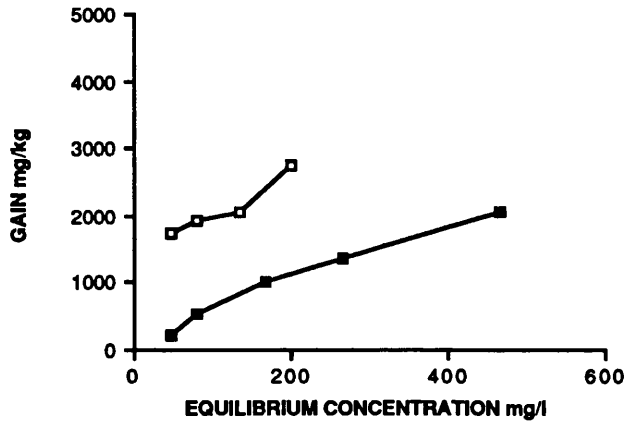


FIG. 5.11.2 DREGHORN / NaCl

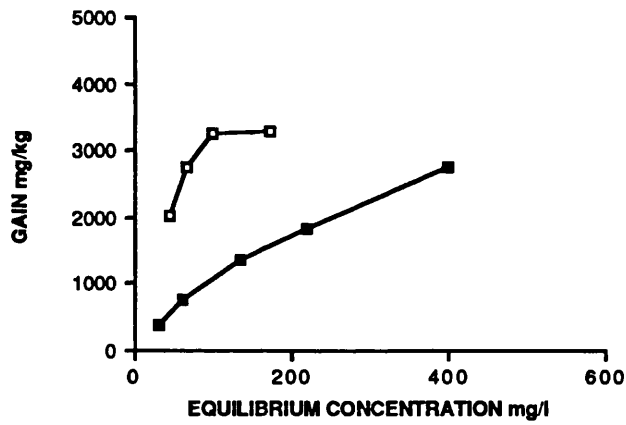


FIG. 5.11.3 DREGHORN CaCl2

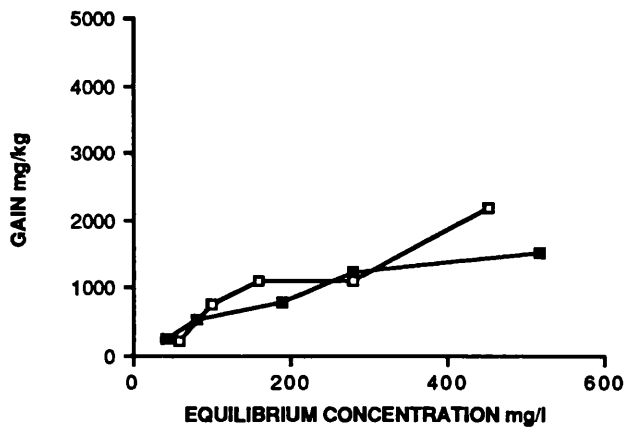


FIG. 5.12.1 PEATY GLEY / KCl

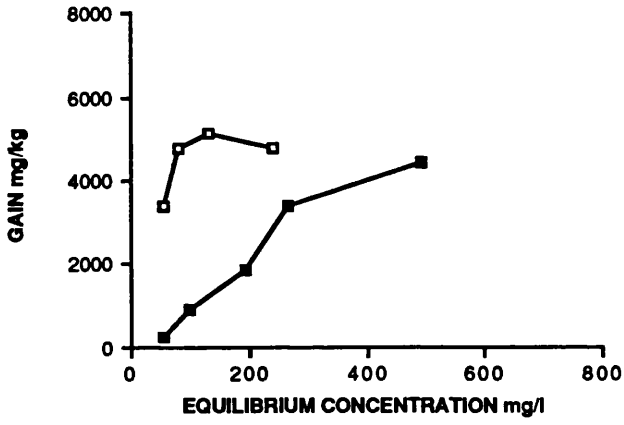


FIG. 5.12.2 PEATY GLEY / NaCl

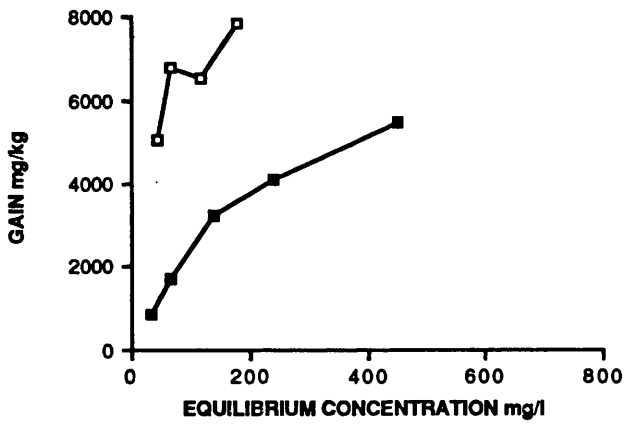
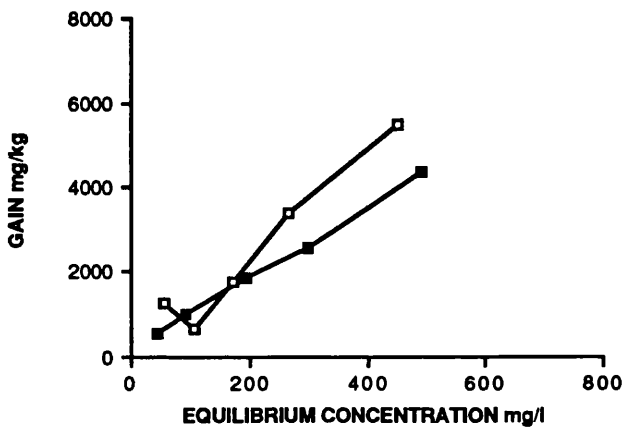


FIG. 5.12.3 PEATY GLEY / CaCl2



5.6 Adsorption / Desorption Isotherms at Low Solution Concentrations

5.6.1 Caesium

In order to extend the laboratory studies to solution concentrations which might more realistically reflect the total caesium (stable and radioactive) content of soils, experiments were carried out for three soils using caesium concentrations of 0 - 50 mg l⁻¹. The background electrolyte used was KCl as this reflects the higher potassium ion concentrations compared to caesium found in the soils used; Darleith A, Dreghorn A and a peat soil. Equilibration times of 24 hours followed by a short desorption time of 1 hour were used to minimise problems with continued adsorption during the desorption period. The natural pH values of the soils were all acidic but ranged between 3 - 6 therefore it was decided to fix the experimental pH values at 3,5 and 7 in order to examine the variation of sorption behaviour with pH. The results are illustrated in Figs. 5.13-5.15.

Figures 5.13-5.15 Low Level caesium adsorption /
desorption isotherms Darleith, Dreghorn and Peat

.1 pH 7

.2 pH 5

.3 pH 3

Adsorption ■ Desorption □

Figure 5.16 The effect of increasing the degree of
dilution upon the percentage of caesium held after
desorption at:-

pH 7 ■

pH 5 □

pH 3 ▲

for:-

.1 Darleith

.2 Dreghorn

.3 Peat

FIG. 5.13.1 DARLEITH pH 7

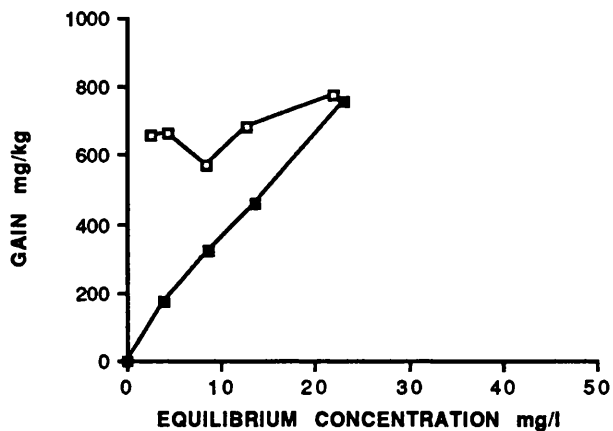


FIG. 5.13.2 DARLEITH pH 5

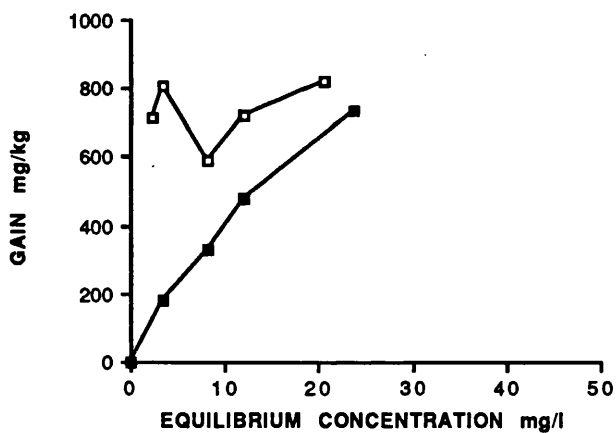


FIG. 5.13.3 DARLEITH pH 3

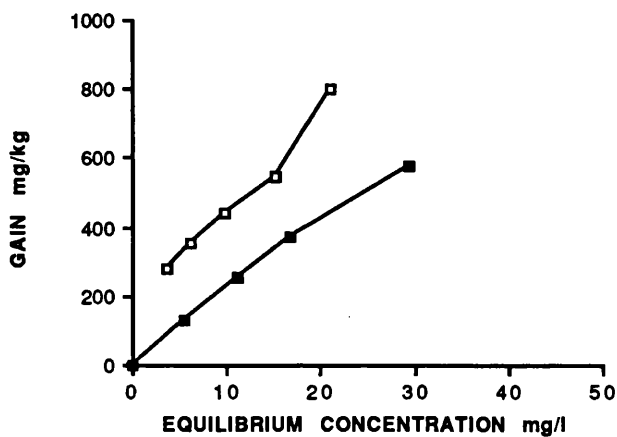


FIG. 5.14.1 DREGHORN pH 7

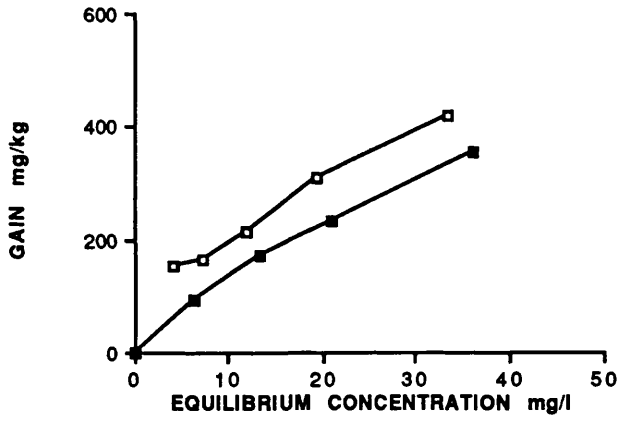


FIG. 5.14.2 DREGHORN pH5

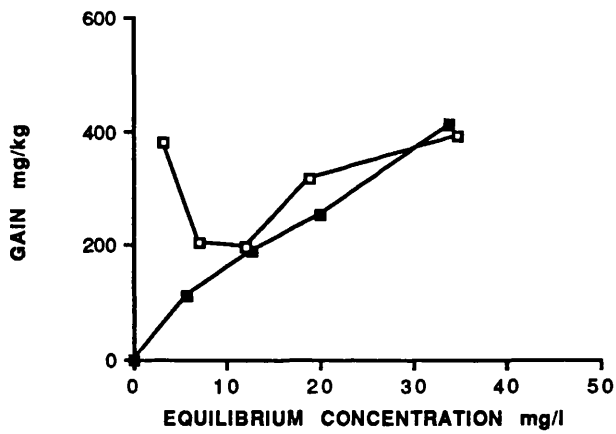


FIG. 5.14.3 DREGHORN pH3

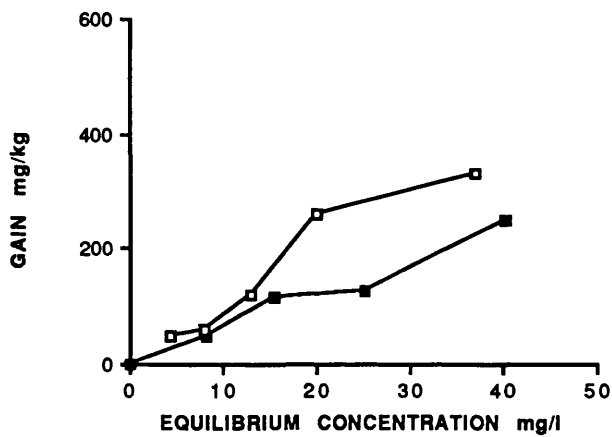


FIG. 5.15.1 PEAT pH 7

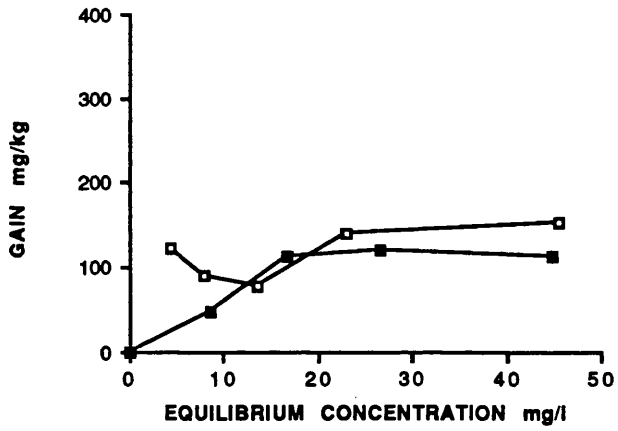


FIG. 5.15.2 PEAT pH 5

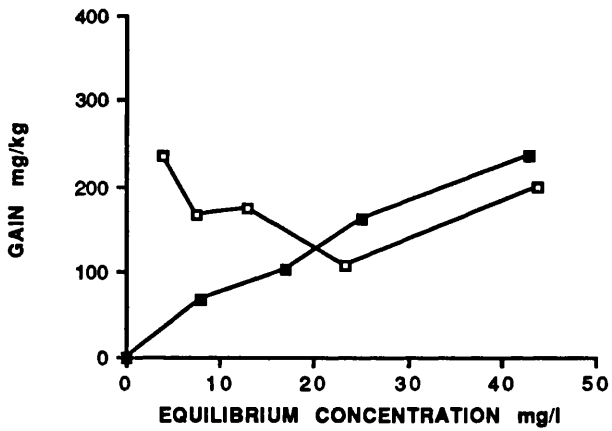


FIG. 5.15.3 PEAT pH 3

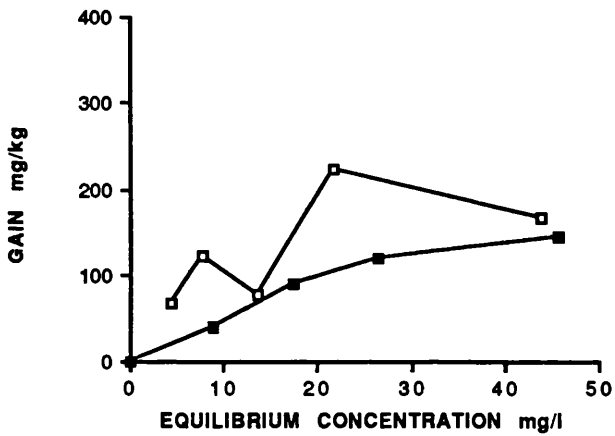


FIG. 5.16.1 DARLEITH

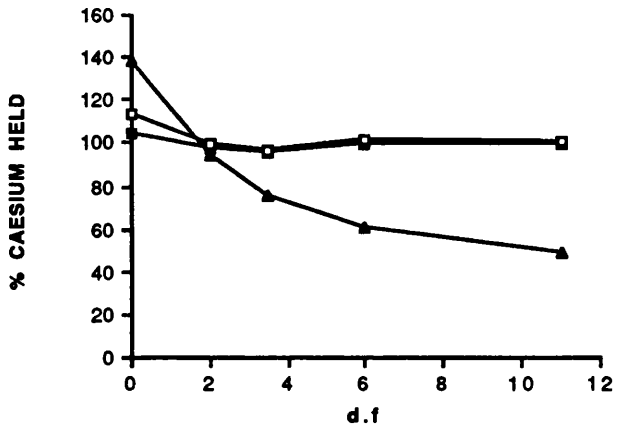


FIG. 5.16.2 DREGHORN

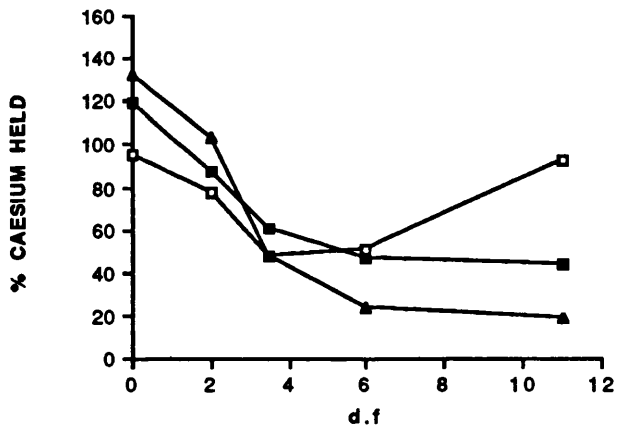
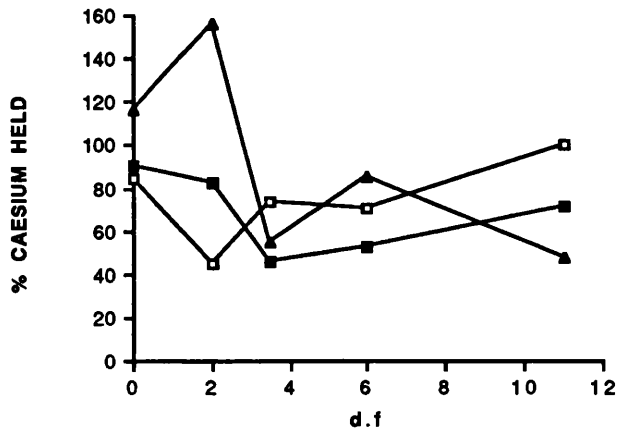


FIG. 5.16.3 PEAT



The desorption curves are summarised in Fig. 5.16 as the percentage of caesium held by the soil after dilution.

The effect of varying the pH of the reaction appeared to result in a maximum uptake of caesium at pH 5. This was true for the three soils and at both ends of the concentration range. The only exception was the upper end of the Darleith curves where adsorption at pH 7 was comparable to adsorption at pH 5. For all the soils the degree of adsorption was lowest at pH 3, due to the pH dependent ion exchange sites being protonated and the inability of caesium to compete successfully with protons for these sites.

The overall affinity of the soils for caesium adsorption followed the order Darleith > Dreghorn > Peat. This was true at both upper and lower ends of the concentration range and at all pH values.

The caesium desorption isotherms were very irregular with many peaks and troughs however it was possible to draw some comparisons between results and trends at different pH values.

In general all three soils exhibited an ease of desorption which followed the order:-

$$\text{pH } 3 > \text{pH } 7 > \text{pH } 5$$

However for Peat and Dreghorn at maximum dilution (x11) the overall desorption was negligible at pH 5. Desorption at pH 3 was almost complete with much smaller amounts of caesium remaining fixed than at pH 7

and 5. Comparing the three soils, Darleith fixed > 600 mg kg⁻¹ caesium at pH 5 and 7 although most was desorbed at pH 3. Dreghorn fixed > 200 mg kg⁻¹ at pH 5 and Peat fixed < 200 mg kg⁻¹ at pH 5. An overall order of fixation can therefore be stated as:-

Darleith $>$ Dreghorn $>$ Peat

5.6.2 Lead

The adsorption / desorption method for lead had to be modified slightly - for pH 5 and 7 the adsorption time was reduced to one hour in order to prevent adsorption of lead on the walls of the glass bottle. This adsorption was monitored during adsorption and desorption steps using control bottles containing no soil. The lead concentrations in these bottles were then measured and used in calculations instead of the actual lead concentration added initially. At pH values of 3 this adsorption was much smaller due to the protonation of adsorption sites on the glass therefore isotherms were measured for adsorption times of both 1 hour and 24 hours.

The results are shown in Figs 5.17-5.19. By examining the adsorption curves it was possible to determine an order of overall affinity for lead adsorption by the different soils. This was :-

Peat $>$ Darleith $>$ Dreghorn

This result was true at all pH values and reflects the

ability of lead to bind to organic matter present in the soil. The effect of pH on adsorption was that as pH fell the adsorption of lead decreased due to the increased competition of protons for sorption sites. Changing the contact time at pH 3 from 1 hour to 24 hours caused a much greater increase in the amount of lead adsorbed. This indicates that lead adsorption required longer to equilibrate than 1 hour.

The lead desorption curves reflected the need for longer contact times to achieve equilibration, because of this the desorption curve was displaced to the left of the last adsorption point. This was still a problem at 24 hour adsorption times despite greater amounts of lead having been adsorbed, implying greater contact times than 24 hours would be required to achieve equilibrium.

Conclusions that could be drawn from the observed trends were that:

a) For all sites maximum desorption occurred at pH 3 with an adsorption contact time of 1 hour. Adsorption times of 24 hours resulted in the subsequent desorption becoming much harder (Fig. 5.20).

b) For Darleith and Dreghorn the apparent desorption trend was:

pH 3 (1hr) > pH 3 (24hrs) > pH 7 > pH 5

c) For Peat the trend was:

pH 3 (1hr) > pH 5 > pH 3 (24hrs) > pH 7

It was apparent therefore that lead sorbs most strongly to mineral soils at pH 7. In comparison with caesium isotherms the most obvious difference was the large number of lead ions which remain fixed by the soil at all conditions.

Figures 5.17-5.19 Low Level lead adsorption/ desorption isotherms for Darleith, Dreghorn & Peat

- .1 pH 7
- .2 pH 5
- .3 pH 3 1 hour
- .4 pH 3 24 hours

Adsorption ■ Desorption □

Figure 5.20 The effect of increasing the degree of dilution upon the percentage of lead held after desorption at:-

- pH 7 ■
- pH 5 □
- pH 3 (1 hour) ●
- pH 3 (24 hours) ○

for:-

- .1 Darleith
- .2 Dreghorn
- .3 Peat

FIG. 5.17.2 DARLEITH pH5

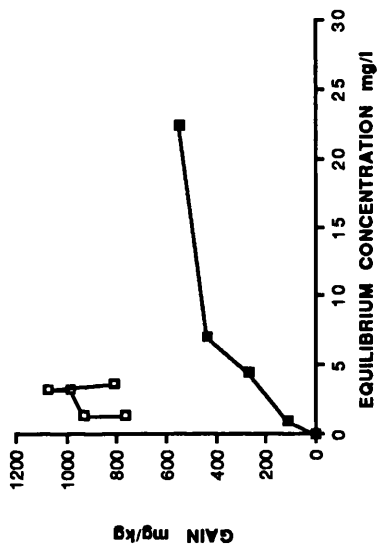


FIG. 5.17.4 DARLEITH pH3 (24 HOURS)

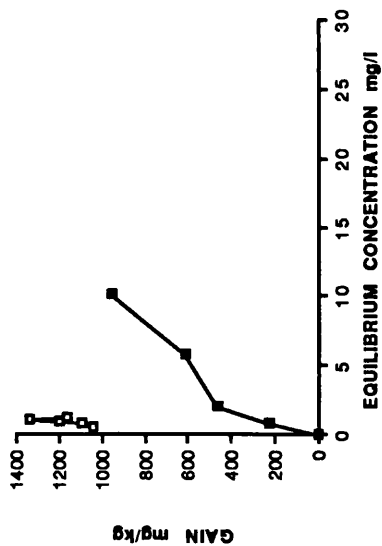


FIG. 5.17.1 DARLEITH pH 7

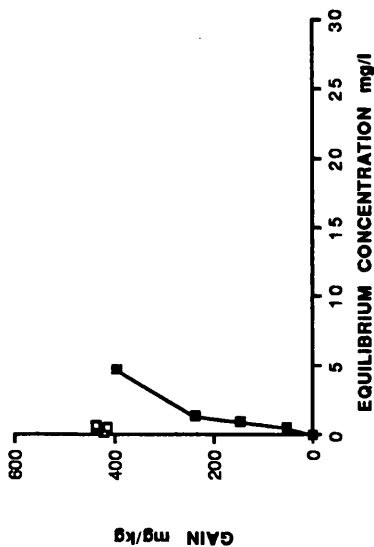


FIG. 5.17.3 DARLEITH pH3 (1 HOUR)

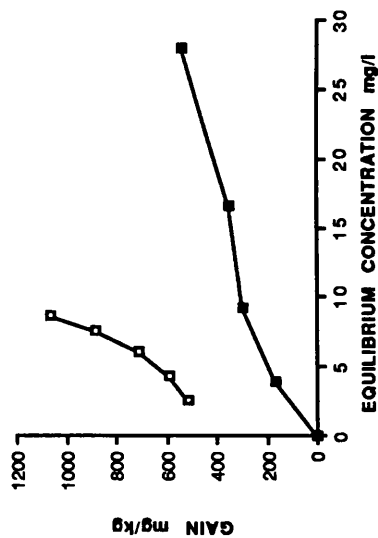


FIG. 5.18.2 DREGHORN pH5

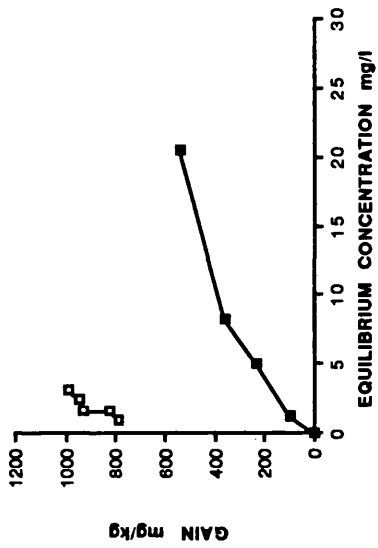


FIG. 5.18.4 DREGHORN pH3 (24 HOURS)

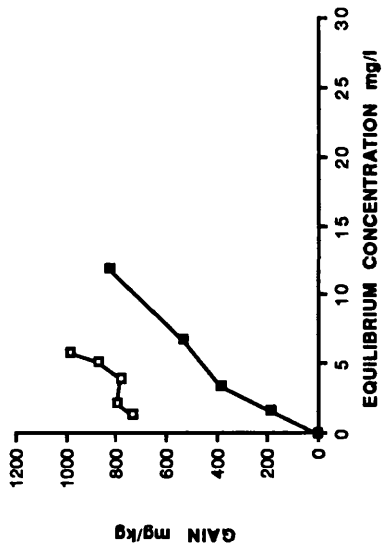


FIG. 5.18.1 DREGHORN pH7

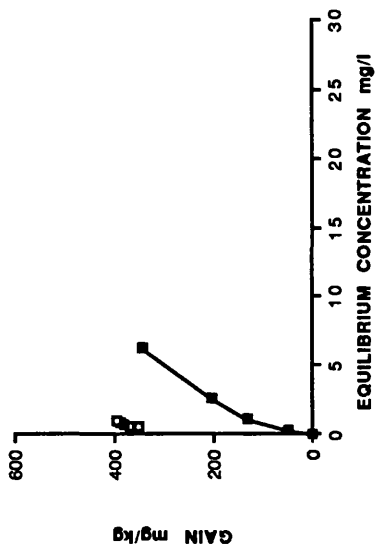


FIG. 5.18.3 DREGHORN pH3 (1 HOUR)

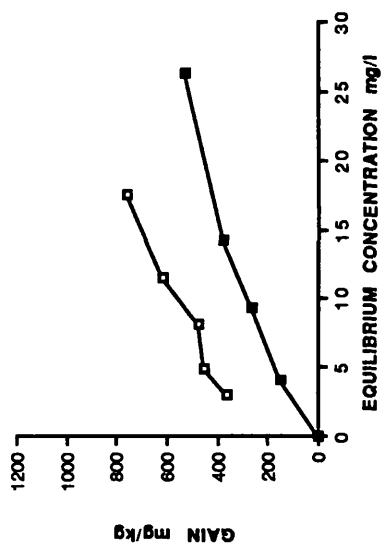


FIG. 5.19.2 PEAT pH5

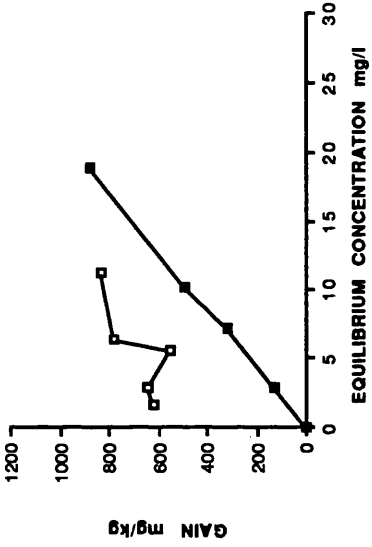


FIG. 5.19.4 PEAT pH3 (24 HOURS)

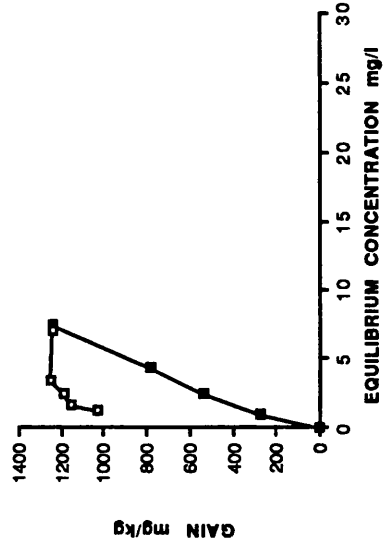


FIG. 5.19.1 PEAT pH7

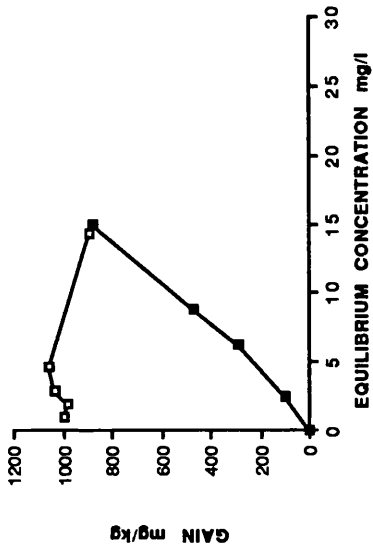


FIG. 5.19.3 PEAT pH3 (1 HOUR)

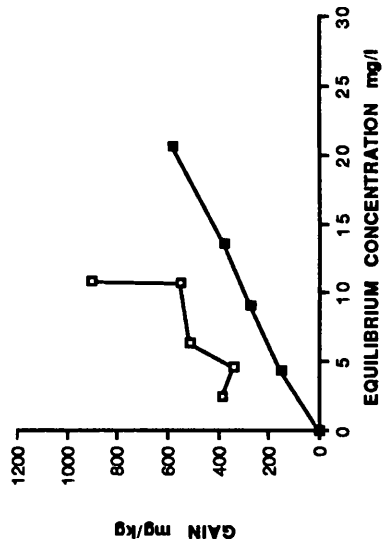


FIG. 5.20.1 DARLEITH

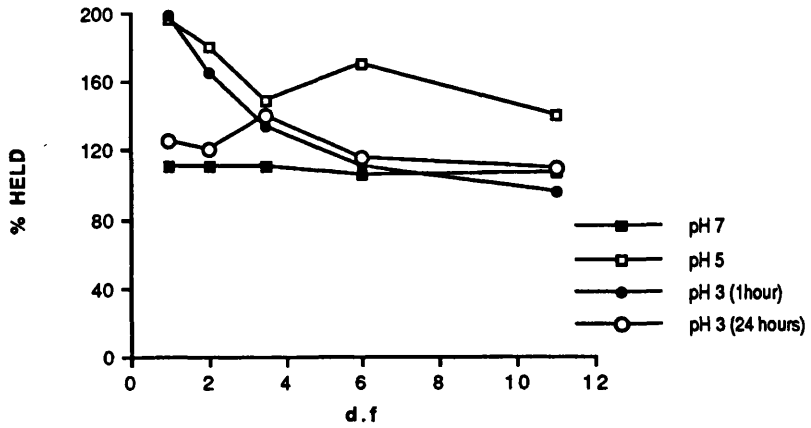


FIG. 5.20.2 DREGHORN

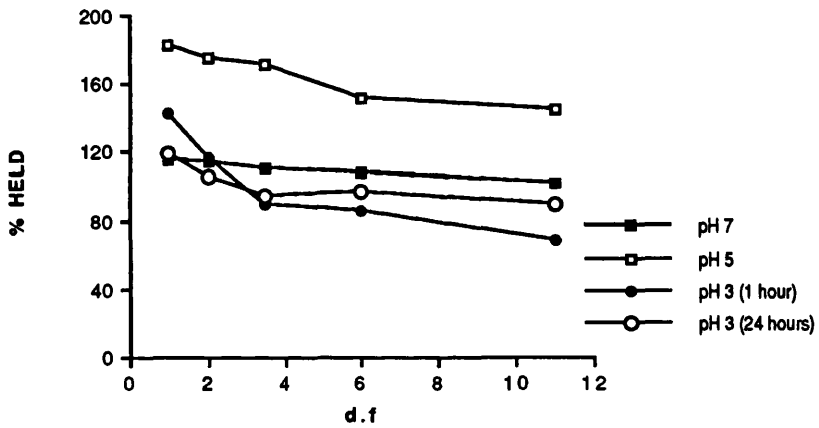
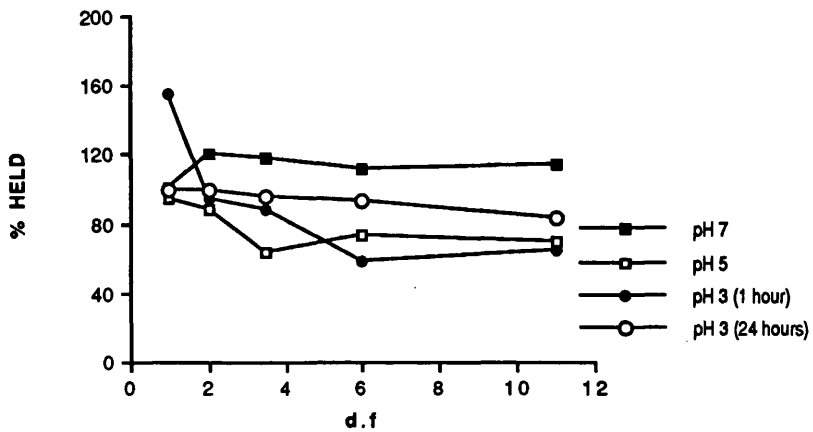


FIG. 5.20.3 PEAT



5.7 The Development of a Method to Measure Desorption of Added Metal from Soil

Due to the difficulties experienced in assessing the desorption behaviour of caesium, it was decided to attempt a modified approach to measuring desorption. Initially caesium adsorption/desorption isotherms were obtained for three clays and three soils. The method had several small modifications:-

- the soil to solution ratio was constant for both the adsorption and desorption steps until the dilution step in order to prevent effects due to sorption dependency upon the amount of solid phase.

- a greater number of dilution points was included to provide a more complete isotherm

- an adsorption time of 3 days was used to ensure that equilibrium had been achieved.

- the clay samples were included to provide a sample set of known composition.

The results of this experiment are presented in the form of a plot of gain of metal by the soil or clay solution versus equilibrium concentration. Three lines are included on this graph which enable the checking of the validity of the data points collected for the desorption curve. This was felt to be an important feature in the analysis due to the random nature of some desorption data. The lines were :-

(1) a plot of the initial caesium concentration divided by the dilution factor (D.F). This line illustrates the line obtained for complete desorption i.e Gain = 0

(2) a plot of the gain of the highest adsorption point versus the equilibrium concentrations obtained by diluting this point if no desorption occurs i.e complete caesium retention at maximum gain.

(3) the third line consists of the actual desorption points measured experimentally.

As no caesium can enter or leave the system during the desorption step, if corresponding points on lines 1 and 2 are connected by line A the equivalent point on line 3 should intersect this line and the ratio with which it splits this line indicates the degree of desorption which has taken place. Any outlying points can therefore be assumed to be experimentally incorrect due to contamination of glassware or operator errors.

The lines joining the three data points for each dilution can be described by the equation:-

$$y = \frac{10 [50 - nx]}{a}$$

Where $y = \text{Gain (mgkg}^{-1}\text{)}$

$n = \text{Dilution Factor}$

$a = \text{Weight of Soil (g)}$

x = Equilibrium concentration (mg l^{-1})

The desorption data were also plotted as the percentage held on the soil after dilution. These graphs enable comparisons to be made more easily between one isotherm and another, a definite advantage over the standard isotherm plot. The results of this experiment are presented in Figs. 5.21-5.26.

From the graphs it was possible to identify a few points at the upper ends of the Darleith soil and Bentonite clay desorption isotherms where adsorption had continued after the dilution step, indicating the need for still longer contact times to achieve equilibrium. Generally the accuracy of the experiment appeared to be satisfactory with data points falling on or within the range of experimental error of their respective 'Line A'. Conclusions that could be drawn from the trends observed were that:-

- an apparent order of adsorption of caesium was;

Bentonite > Illite > Darleith > Kaolinite >
Dreghorn > Peat

- an apparent order of retention was;

Illite (74%) > Darleith (70%) > Bentonite (66%) >
Peat (65%) > Dreghorn (50%) > Kaolinite (40%)

At the point of maximum dilution there appeared to be a high degree of caesium retention for all the solid phases.

Similar experiments were carried out for lead with some obvious restrictions:-

- the pH of the suspension was adjusted to pH 3 to prevent sorption of lead upon the glass container walls becoming a problem during the contact time of 24 hours for adsorption and 24 hours for desorption, any loss to the glass was accounted for by running blank samples.

- isotherms were obtained for the three soils only due to the inability to measure the low levels of lead remaining in solution by atomic absorption after interaction with the clays.

- soil weights of 0.1g were used as greater amounts of soil removed such a high proportion of the added lead from the solution that analysis proved difficult.

The data was presented in Figs. 5.27-5.29. The use of the adsorption/desorption isotherm provided the following information:-

Equilibrium had not been achieved within the adsorption time allowed and therefore continued after dilution resulting in points lying above the uppermost adsorption point. As these points lay upon the

extrapolated 'line A' relevant to them this proves the continuation of adsorption rather than experimental error.

A few points were displaced from their relevant 'line A' and this could be attributed to experimental errors.

Graphs of the amount of lead held after dilution provided information about the degree of retention of lead by the soils, approximately 40% for Darleith, 33% for Peat and 30% of initially adsorbed lead for Dreghorn was fixed. An apparent order of adsorption and ease of retention for lead under these experimental conditions was:-

Darleith > Peat > Dreghorn

This differs from the previous findings for these soils (5.6.2) where the order was:-

Peat > Darleith > Dreghorn




and was probably due to the differences in the experimental conditions such as pH and contact time and also the soil : solution ratio.

Comparisons can be drawn between the sorption behaviour of lead and caesium. The retention of the two metal ions by the three soils follows the same order.

The soils adsorb approximately four times more lead than caesium. However, the soils retain roughly fifty percent less of the initially adsorbed metal ion for lead than caesium. This may be due to the mechanism for fixation requiring longer for lead than for caesium.

Figures 5.21-5.26 Caesium Desorption isotherms

.1 assesment of experimental error




- zero desorption 
- complete desorption 
- experimental desorption results 

.2 the effect of increasing the degree of dilution upon the percentage of caesium desorbed.

for:- Darleith, Dreghorn, Peat, Bentonite, Illite and Kaolinite

Figures 5.27-5.29 Lead Desorption isotherms

.1 assesment of experimental error

- zero desorption 
- complete desorption 
- experimental desorption results 

.2 the effect of increasing the degree of dilution upon the percentage of lead desorbed.

for:- Darleith, Dreghorn and Peat.

FIG. 5.21.1 DARLEITH

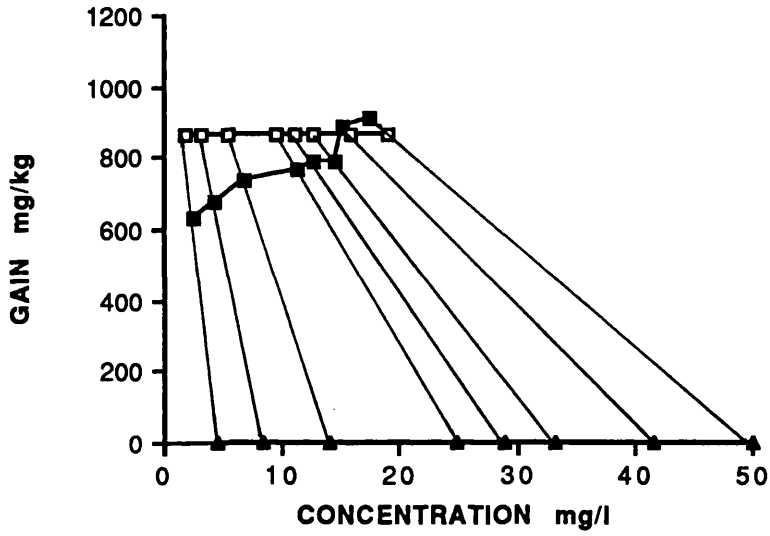


FIG. 5.21.2 DARLEITH

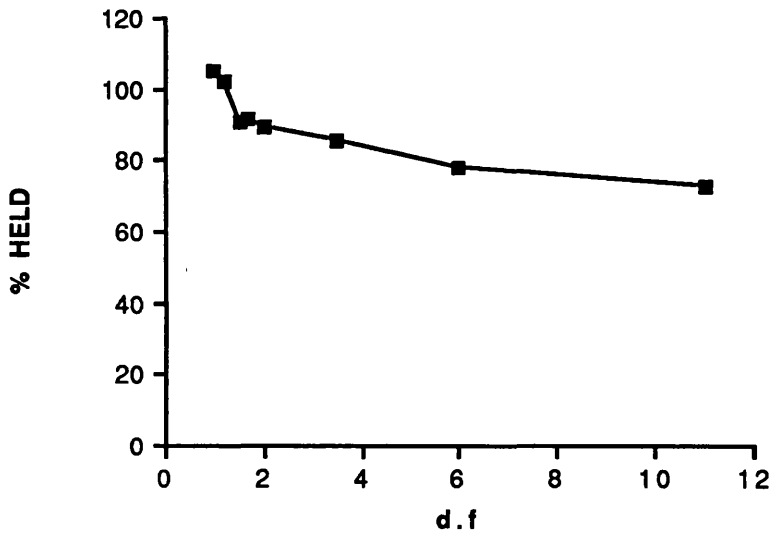


FIG. 5.22.1 DREGHORN

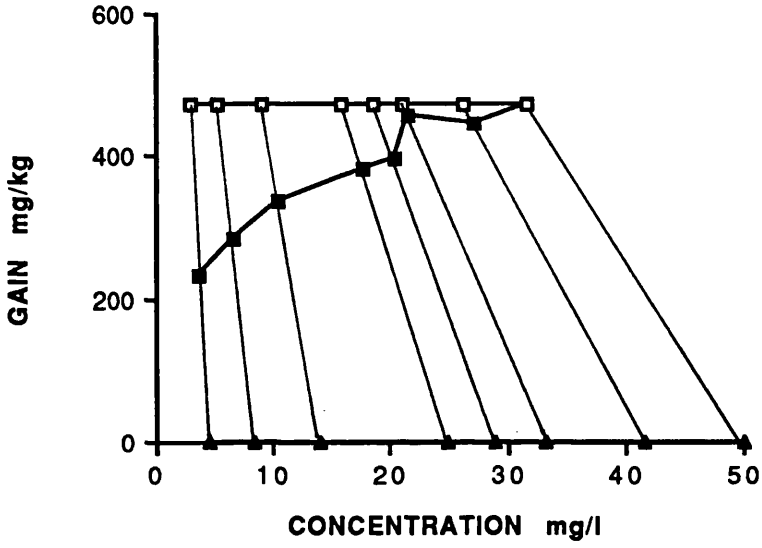


FIG. 5.22.2 DREGHORN

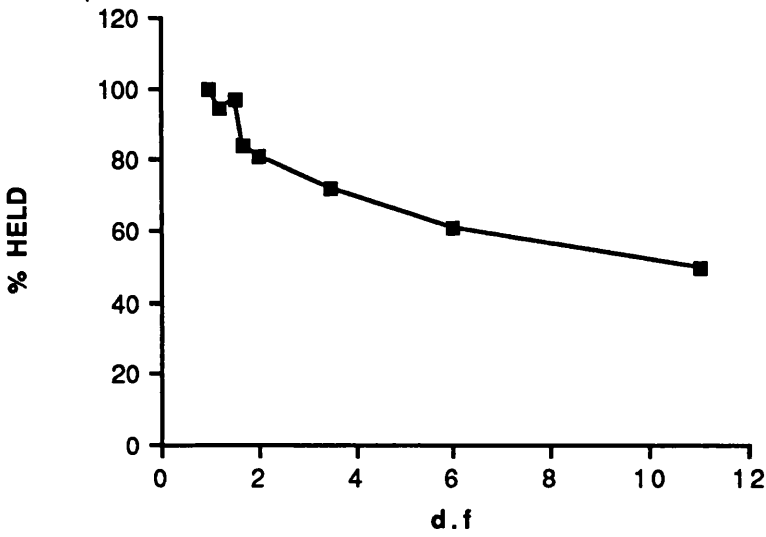


FIG. 5.23.1 PEAT

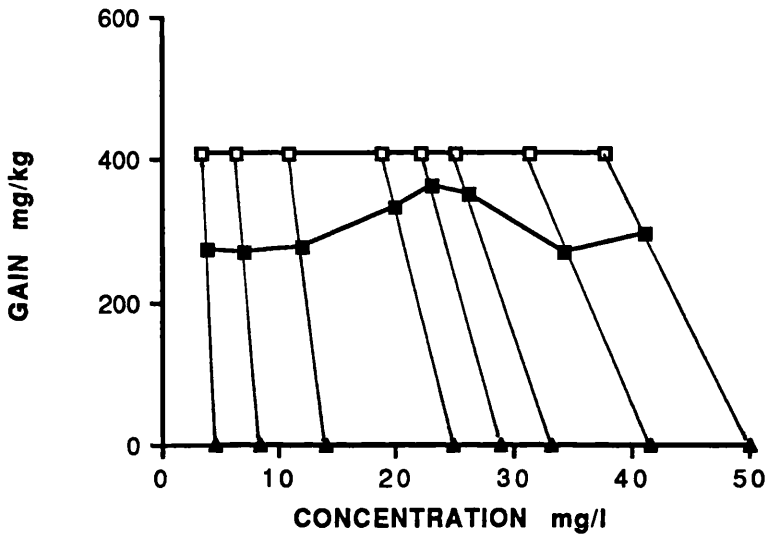


FIG. 5.23.2 PEAT

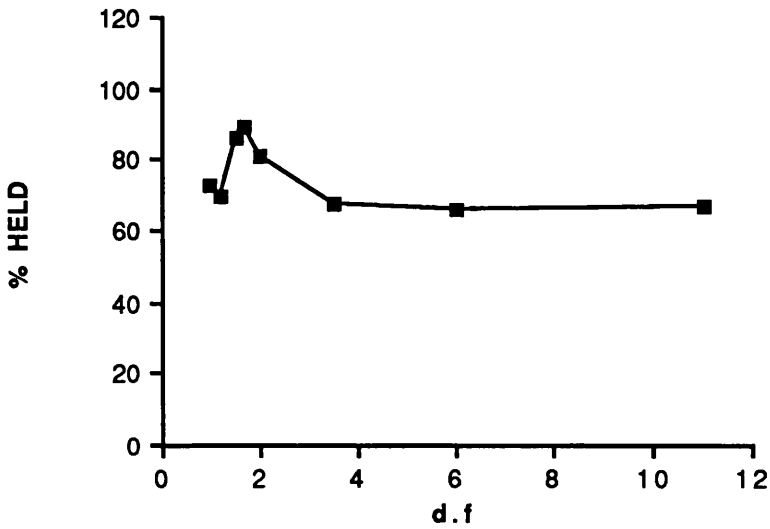


FIG. 5.24.1 BENTONITE

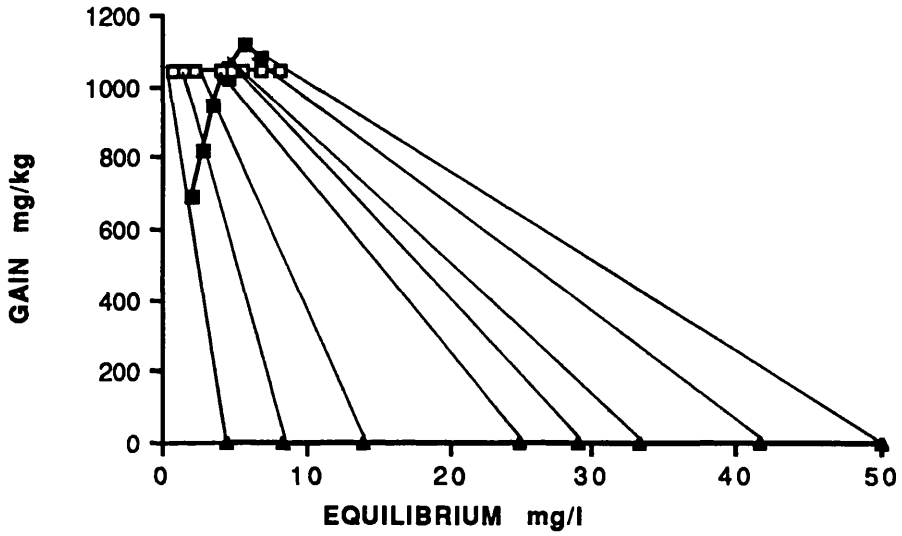


FIG. 5.24.2 BENTONITE

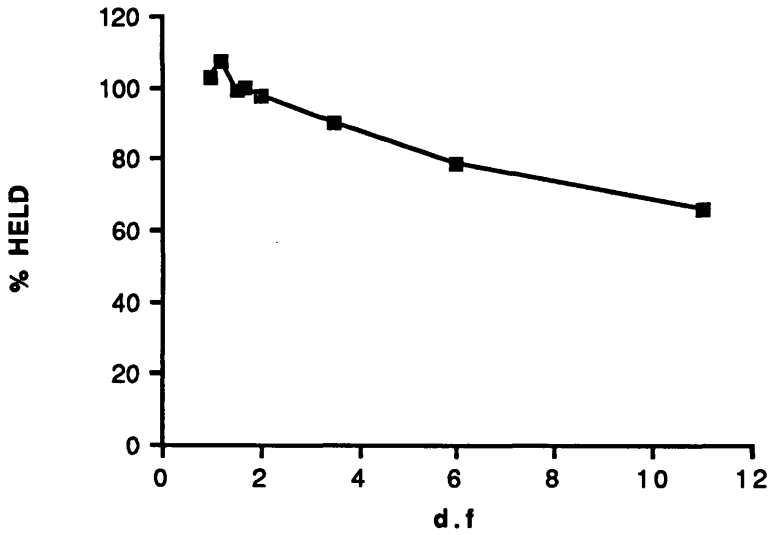


FIG. 5.25.1 ILLITE

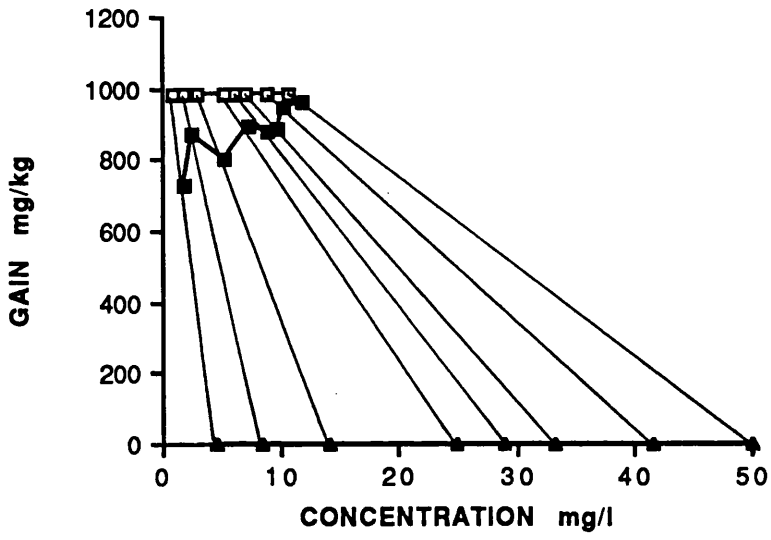


FIG. 5.25.2 ILLITE

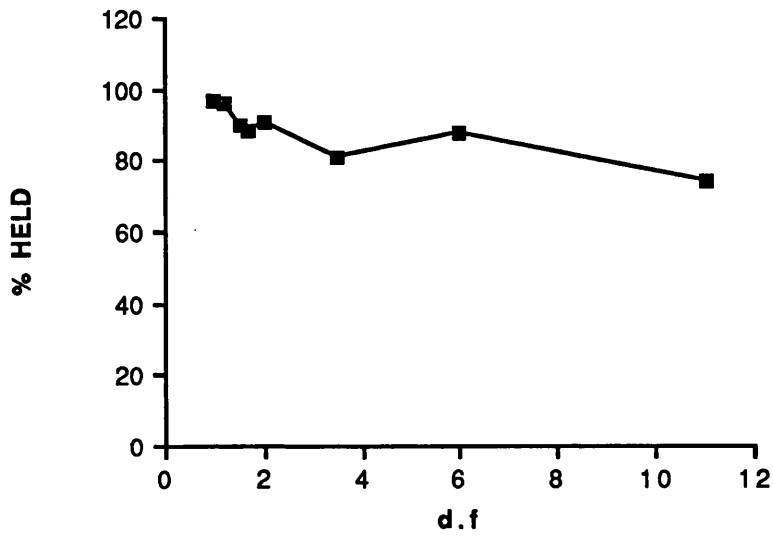


FIG. 5.26.1 KAOLINITE

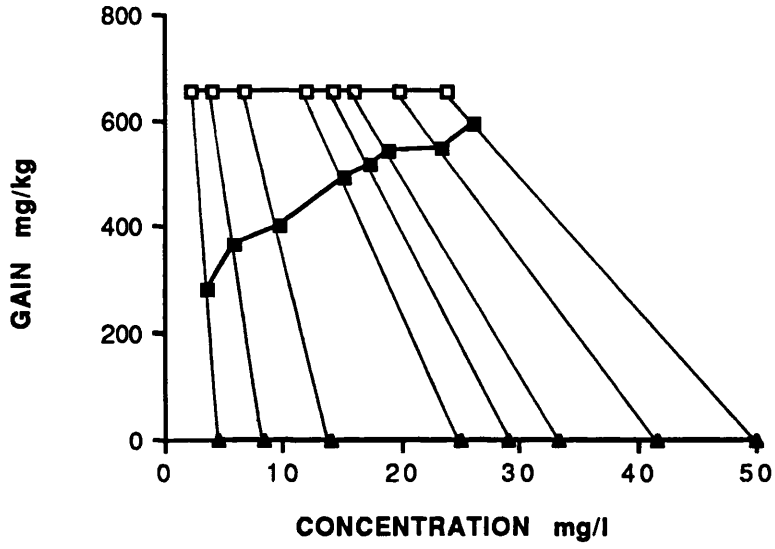


FIG. 5.26.2 KAOLINITE

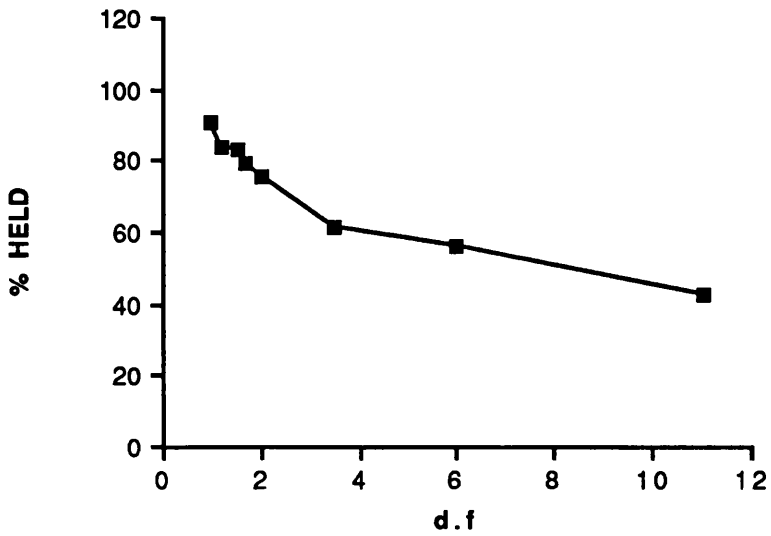


FIG. 5.27.1 DARLEITH

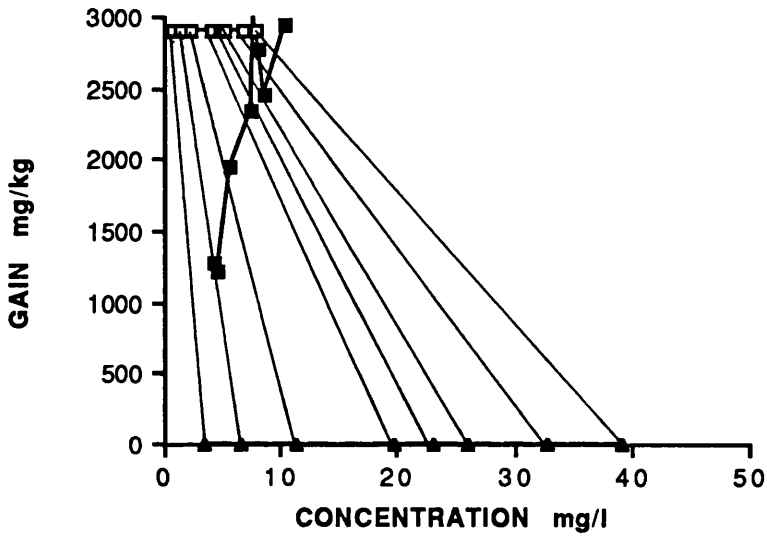


FIG. 5.27.2 DARLEITH

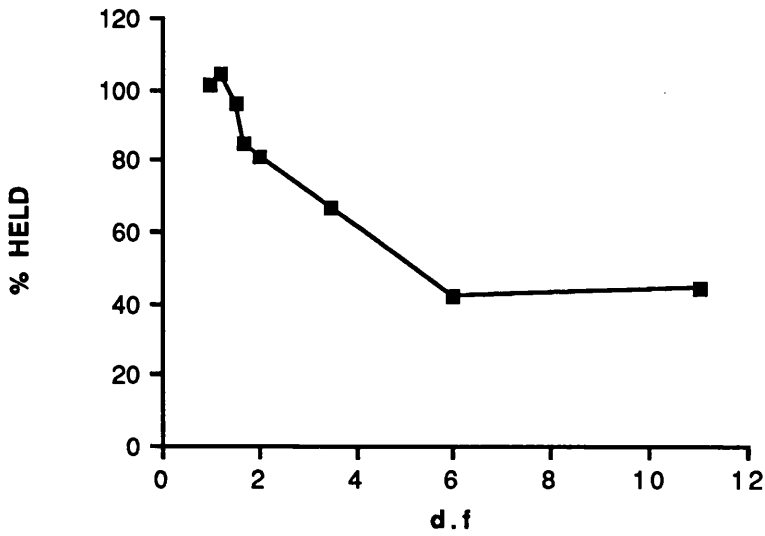


FIG. 5.28.1 DREGHORN

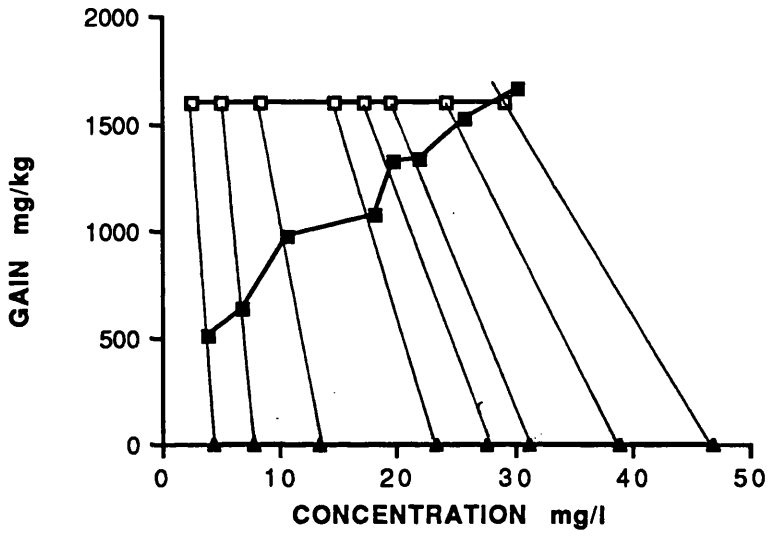


FIG. 5.28.2 DREGHORN

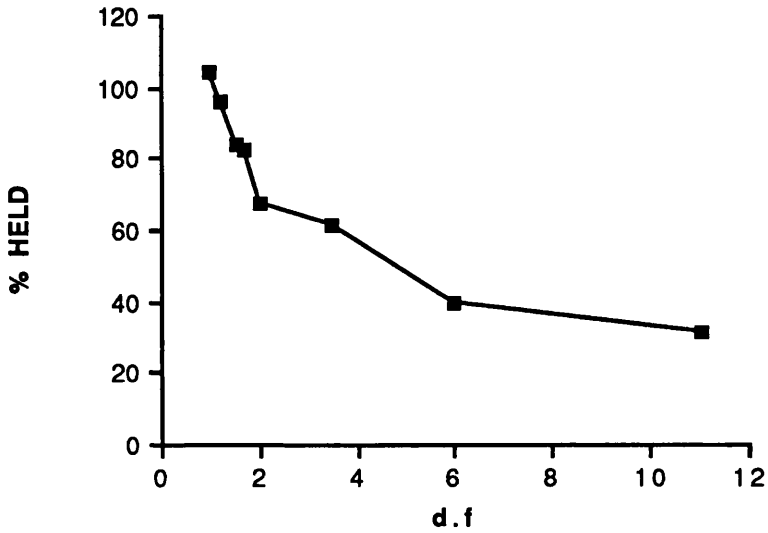


FIG. 5.29.1 PEAT

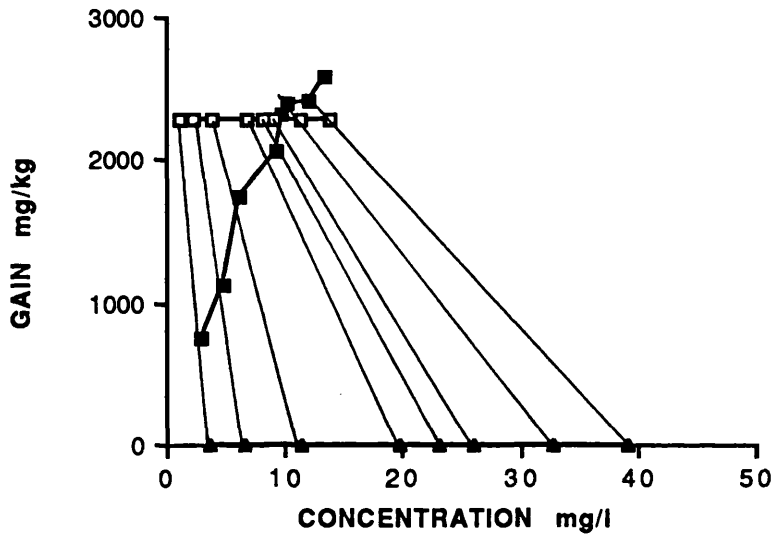
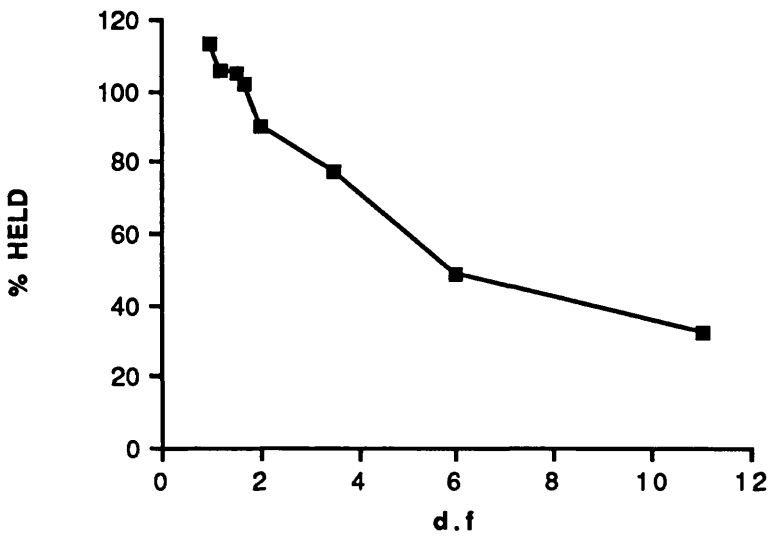


FIG. 5.29.2 PEAT



5.8 Summary

Some general statements can be made from the results obtained in this chapter:-

a) Caesium sorption at equilibrium concentrations less than 0.5 mM appears to be governed by adsorption onto specific sites on the mineral fraction of soils. Equilibrium is achieved rapidly. At higher concentrations a slower equilibrium is achieved possibly governed by the soil organic matter. Langmuir isotherms accurately describe the uptake of caesium by soils of organic matter content <70% over the concentration range studied. Desorption experiments carried out showed that at pH 5 desorption is incomplete, but at pH 3 almost complete desorption occurs.

b) Lead sorption over the concentration range 0-50 mg l⁻¹ illustrated that the ions bind strongly to soil organic matter. The desorption of lead proved to be difficult with a much lesser degree of retention of lead ions occurring compared to caesium.

c) The experimental results highlighted areas of anomalous behaviour towards caesium sorption in soils of high organic matter content, low pH and high cation exchange capacity.

The laboratory experiments discussed in this chapter have provided data for the sorption of caesium

and lead by whole soils. In order to understand more fully the anomalous behaviour which occurs in soils of high organic matter content, experiments looking at the organic fraction in isolation are required. In addition, modelling packages such as GEOCHEM (Sposito and Mattigod, 1979) treat complex organic ligands such as humic acid as simple organic acids with functional groups, whose formation constants for interaction with metal are known e.g acetic acid, salicylic acid (Wild, 1988). By examining the behaviour of humic acid with caesium and other relevant metals it may be possible to provide more useful constants to use in environmental modelling packages.

It may be possible that the anomalous behaviour observed in soils of high organic content may be due to interactions which occur between the organic and mineral phases of the soil. This idea will be investigated further in chapter 6 where the influence of humic acid/ clay interactions upon caesium sorption will be discussed.

CHAPTER 6 - SOIL ORGANIC MATTER AND ITS INFLUENCE ON SOIL METAL INTERACTIONS.

6.1 Introduction

The interaction of heavy metals with natural organic materials is poorly understood despite the potential importance of such processes in the transport and retardation of metals (Choppin, 1988; Smith et al, 1990; Scott et al, 1991). Moreover, specific modifications of existing models are often required to permit their use in modelling the interactions of radionuclides in particular with organics (Falck, 1989). Particular attention has recently been focussed upon this problem by the high degree of mobility and availability of Chernobyl radiocaesium deposited on organic soils (Livens and Loveland, 1988; Livens and Rimmer, 1988; Sugden et al., 1991) which clearly demonstrated that an improved understanding of caesium geochemistry was required for modelling its behaviour in such environments.

The structure of humic acids has been the subject of many studies dating from the eighteenth century, (see review chapter 1.3) for the purposes of this chapter the definitions accepted were:-

-humic substances - a series of relatively high molecular weight, brown to black coloured substances formed by secondary synthesis reactions. The term is used as a generic name to

describe the coloured material or its fractions obtained on the basis of solubility characteristics.

-humic acid - the dark coloured organic material which can be extracted from soil by various alkaline reagents and which is insoluble in dilute acid.

-fulvic acid - the coloured material which remains in solution after removal of humic acid by acidification, (quoted from Stevenson, 1982).

In general humic and fulvic acids are large molecular weight heterogeneous molecules which behave like weak acid polyelectrolytes due to the high concentration of acid carboxylate sites. These sites and other functional groups thus enable the binding of metals to the organic matter and also the interaction of organic matter with other soil constituents such as clay minerals.

The objectives of this study were:-

- to use Fourier Transform Infra-Red spectroscopy to follow the changes which occurred as metal ions bind to a protonated sample of humic acid and to determine the roles of functional group specificity in these reactions.
- to carry out potentiometric titrations for several metal ions in order to obtain quantitative data to allow for the calculation of conditional stability constants for the metal - humic

interactions.

- to carry out experiments to examine the effect of humic metal additions on the sorption and desorption of caesium by clay minerals.

6.2 Infra red analysis of Metal-Humate Binding

Controversy exists as to whether humic-metal linkages are ionic or covalent, a factor of major importance since the nature of the bonding clearly affects the stability of the complex. Using Fourier Transform Infra-Red Spectroscopy, it was possible to obtain spectra illustrating the sequence of transformations which occurred as the metal became bound. This provided information allowing the determination of the contribution of groups other than carboxyls. The spectra for the fully protonated humic acid, the partial potassium salt at pH 5 and the complete potassium salt at pH 10 are shown in Fig 6.1.1. This represents a system changing from one in which the carboxyl groups are fully protonated (-COOH) to one where the carboxylate ions are fully dissociated and holding potassium ions ($\text{-COO}^-\text{K}^+$), with the partial potassium salt at pH 5 being an intermediate stage. The major changes to the spectra during the formation of this simple salt by ionic carboxylate linkages were the loss of the shoulder at 1720 cm^{-1} , due to complete ionization of carboxyl groups, and corresponding increases in the peaks at 1610 cm^{-1} and 1400 cm^{-1} due to the formation of carboxylate ions.

An experiment was carried out to calculate the total acidity of the protonated solution due to -COOH .

This was calculated to be 2.75 mmol g⁻¹ with a standard deviation of 0.12 mmol g⁻¹. This value was used to determine the concentrations of the metal solutions used.

Example - for a solution containing 0.5g of humic acid in 500ml there are 0.0275 mmoles H⁺ in 10ml. Therefore the range of metal required was:-

$$\begin{aligned} \text{mmoles of charge } M^{n+} &= [0.1 \rightarrow 0.5] \times \text{mmoles } H^+ \\ &= 0.0028 \rightarrow 0.04 \end{aligned}$$

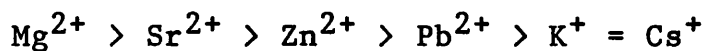
- for caesium, a stock solution of 0.00496 mmol ml⁻¹ was made and the incremental additions were in 1 ml aliquots.

When the humic acid was treated with caesium chloride the spectra (Fig. 6.1.2) were analogous to the potassium humate indicating the formation of simple metal humate salts by ionization of acid carboxyl groups.

Investigations of the divalent complexes showed more significant spectral changes. The spectra of all four metal humates showed similar changes with incremental additions of the metal salts, (Figs 6.1.2-6.1.7). The main spectral changes were: the peak at 3400 cm⁻¹ broadened and increased due to the formation of co-ordination covalent linkages; the shoulder at 1720 cm⁻¹ disappeared as carboxyl groups became ionized; the peaks at 1610 cm⁻¹ and 1400 cm⁻¹ became more defined due to an increased carboxylate ion content. When compared with the weaker corresponding peaks in

the potassium complex at pH 10, however, it is apparent that the increase cannot be accounted for wholly by the conversion of -COOH to -COO^- . An explanation for this is the reaction of other functional groups with the metals to form conjugated ketonic structures. These structures absorb at around 1600 cm^{-1} , which explains the greater band increase at 1600 cm^{-1} than at 1400 cm^{-1} .

From the experimental results, it can be concluded that monovalent metals reacted to form simple metal humate salts, binding with acid carboxyl groups. Divalent metals can utilize more fully the range of functional groups available on the humic acid, resulting in the formation of conjugated ketonic structures. The presence of these structures prevented the determination of whether linkages were ionic or covalent by masking absorbances. An apparent order of reaction of the metal ions with humic acid was:



Hard divalent metal ions, such as Mg^{2+} , appear to react more fully than soft metals, such as Pb^{2+} , which is in agreement with their preference for binding to oxygen.

FIGURE 6.1

6.1.1 Infra-red spectra of a) fully protonated humic acid, b) partial potassium salt pH 5, c) complete potassium salt pH 10

6.1.2 Infra-red spectra of the formation of caesium salt by incremental additions of CsCl a-c

6.1.3 Infra-red spectra of a) reference potassium salt, protonated, b-d) formation of lead salt by incremental addition of lead ions.

6.1.4 Infra-red of a-c) gradual conversion to magnesium humate complex.

6.1.5 Infra-red spectra of a-d) gradual conversion to strontium humate complex.

6.1.6 Infra-red spectra of a-c) gradual conversion to zinc humate complex.

6.1.7 Infra-red spectra of a-d) gradual conversion to copper (II) humate complex.

FIG. 6.1.1

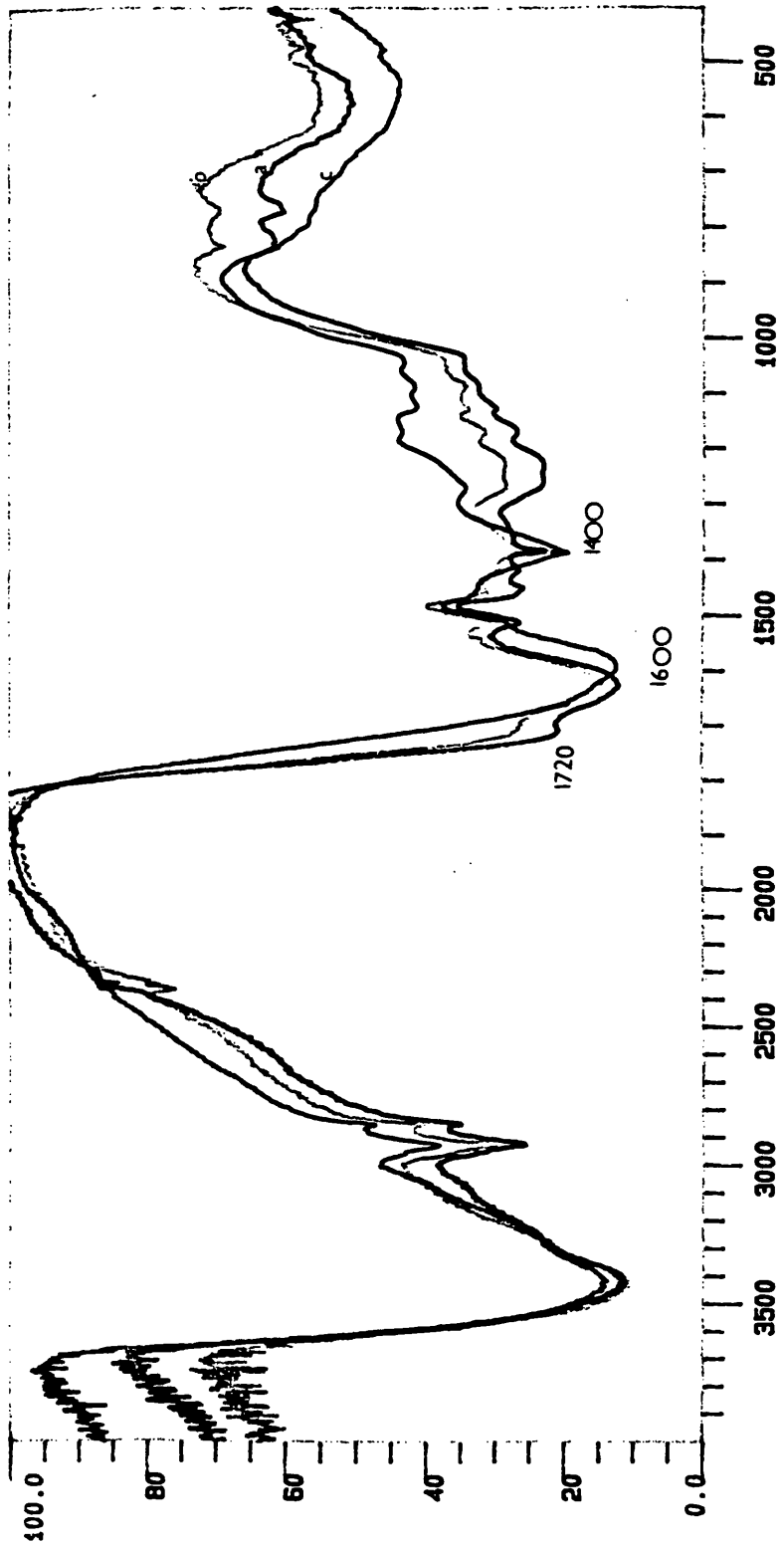


FIG. 6.1.2

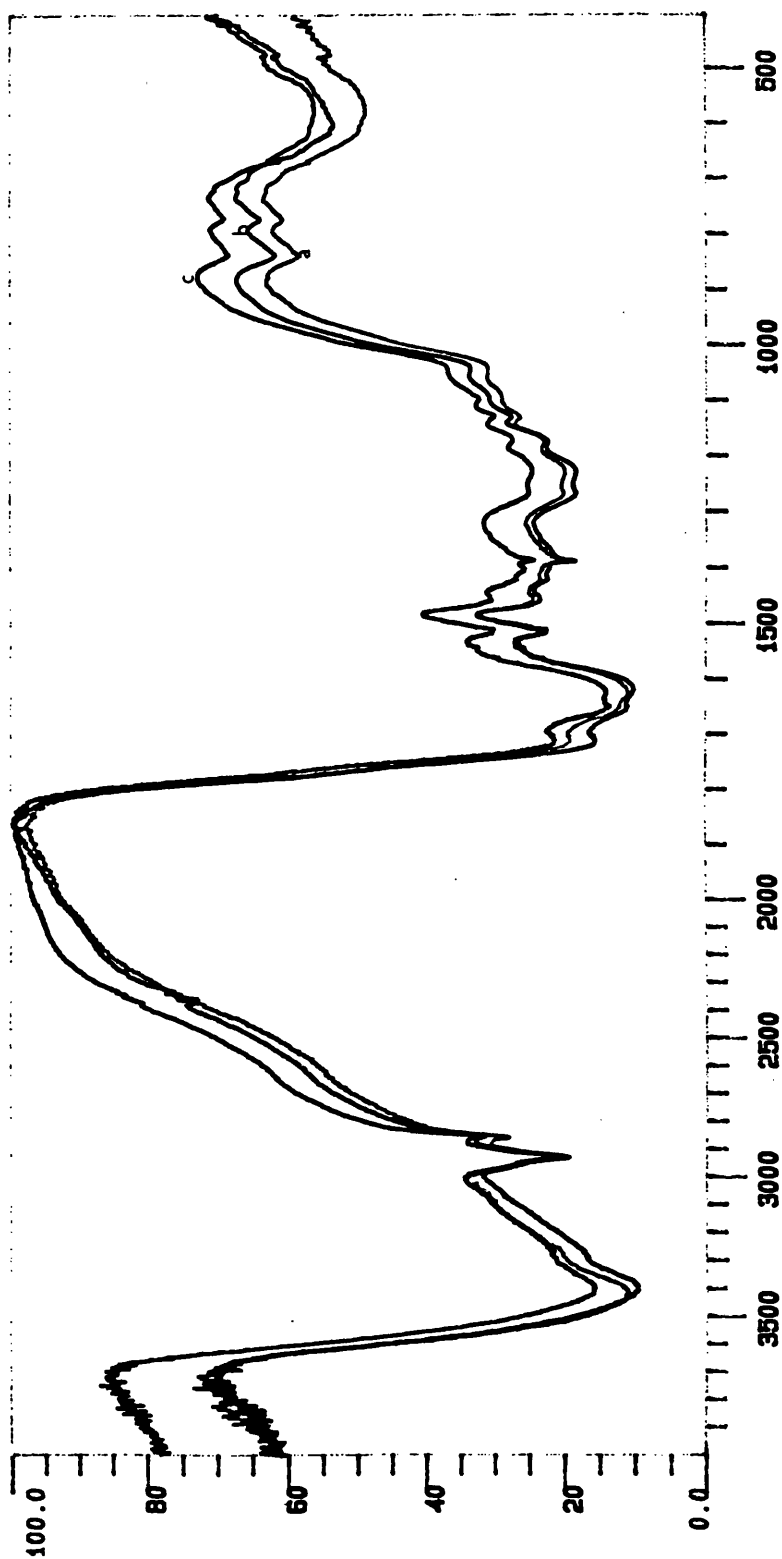


FIG. 6.1.3

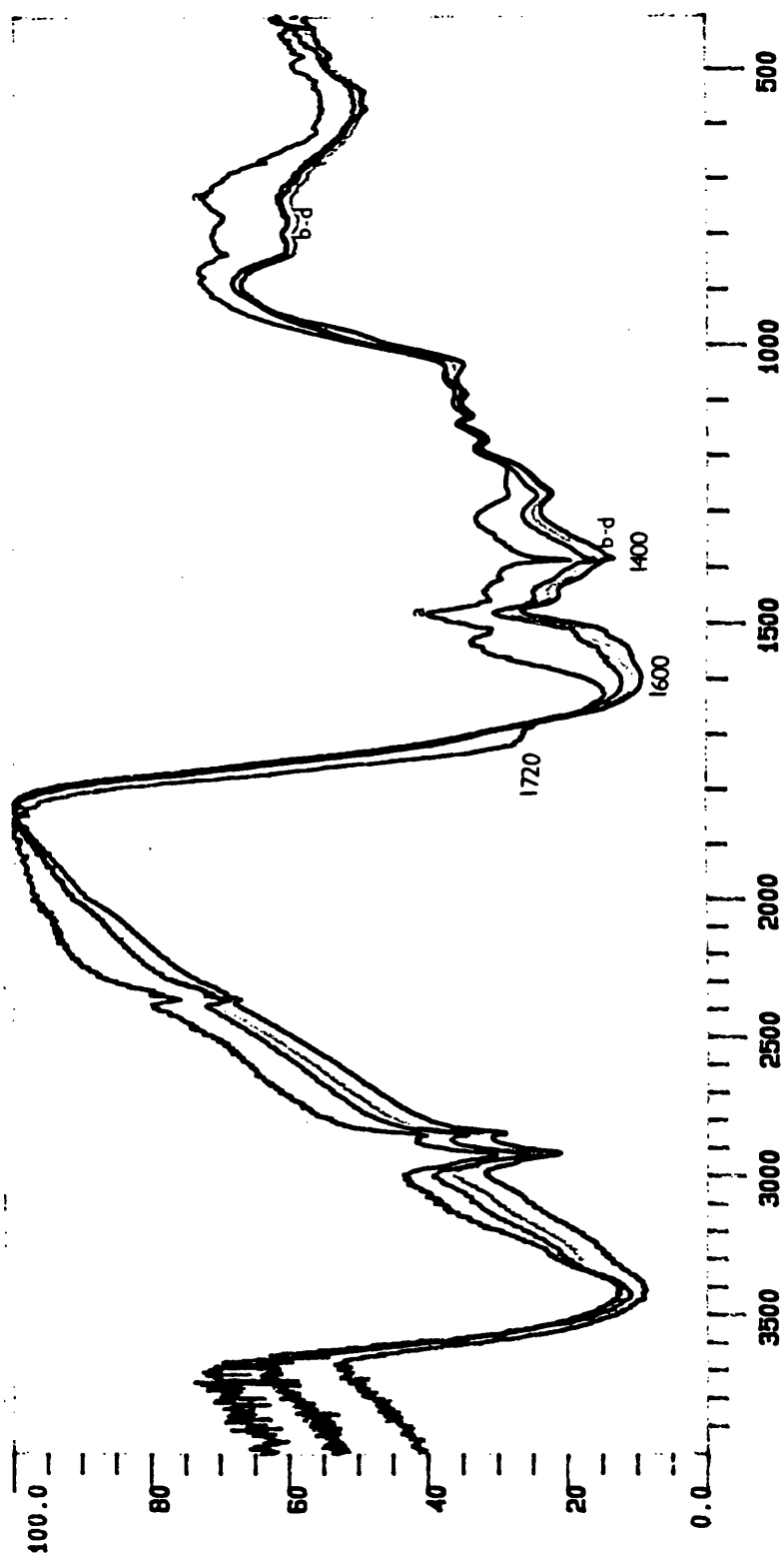


FIG. 6.1.4

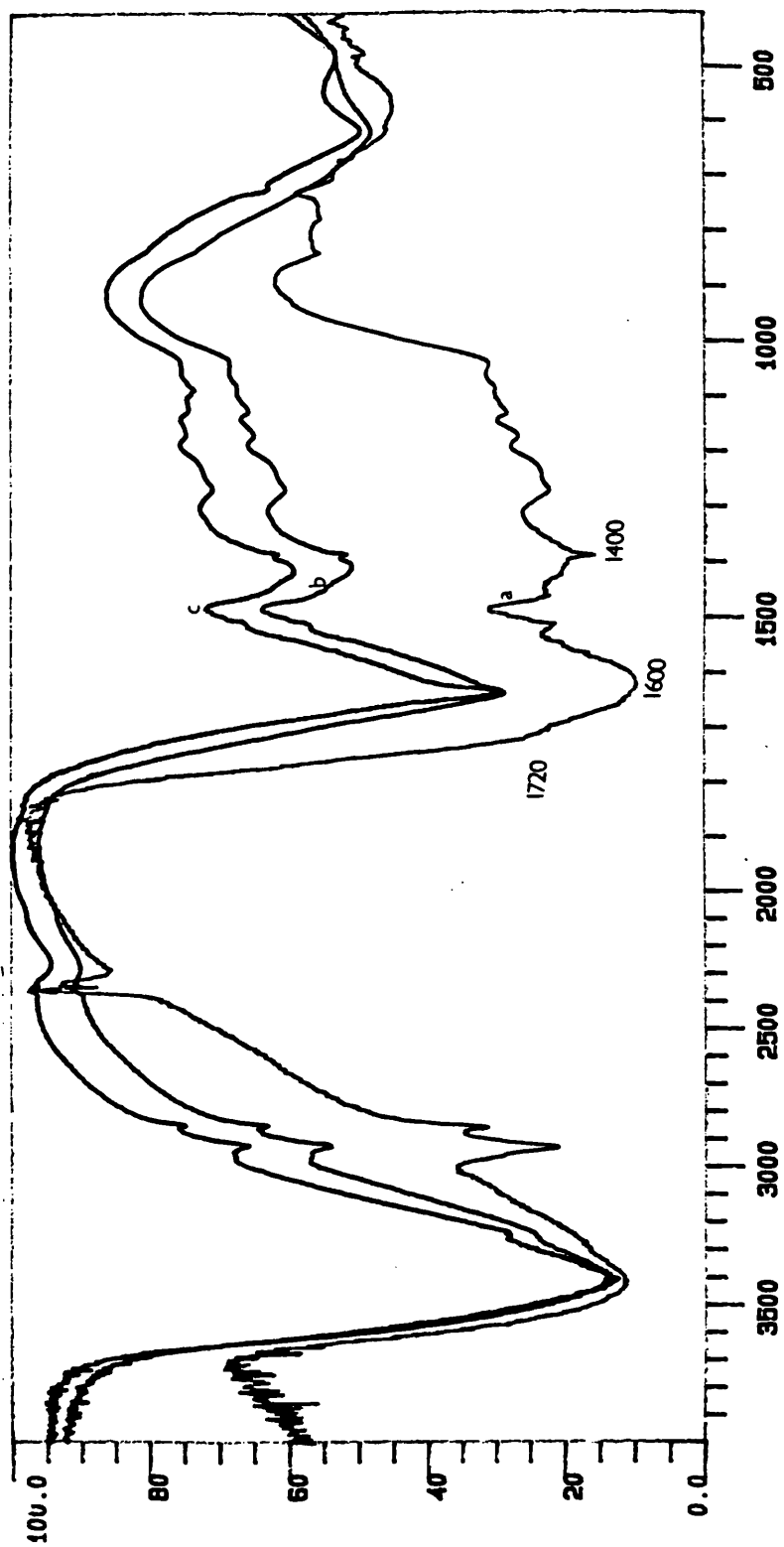


FIG. 6.1.5

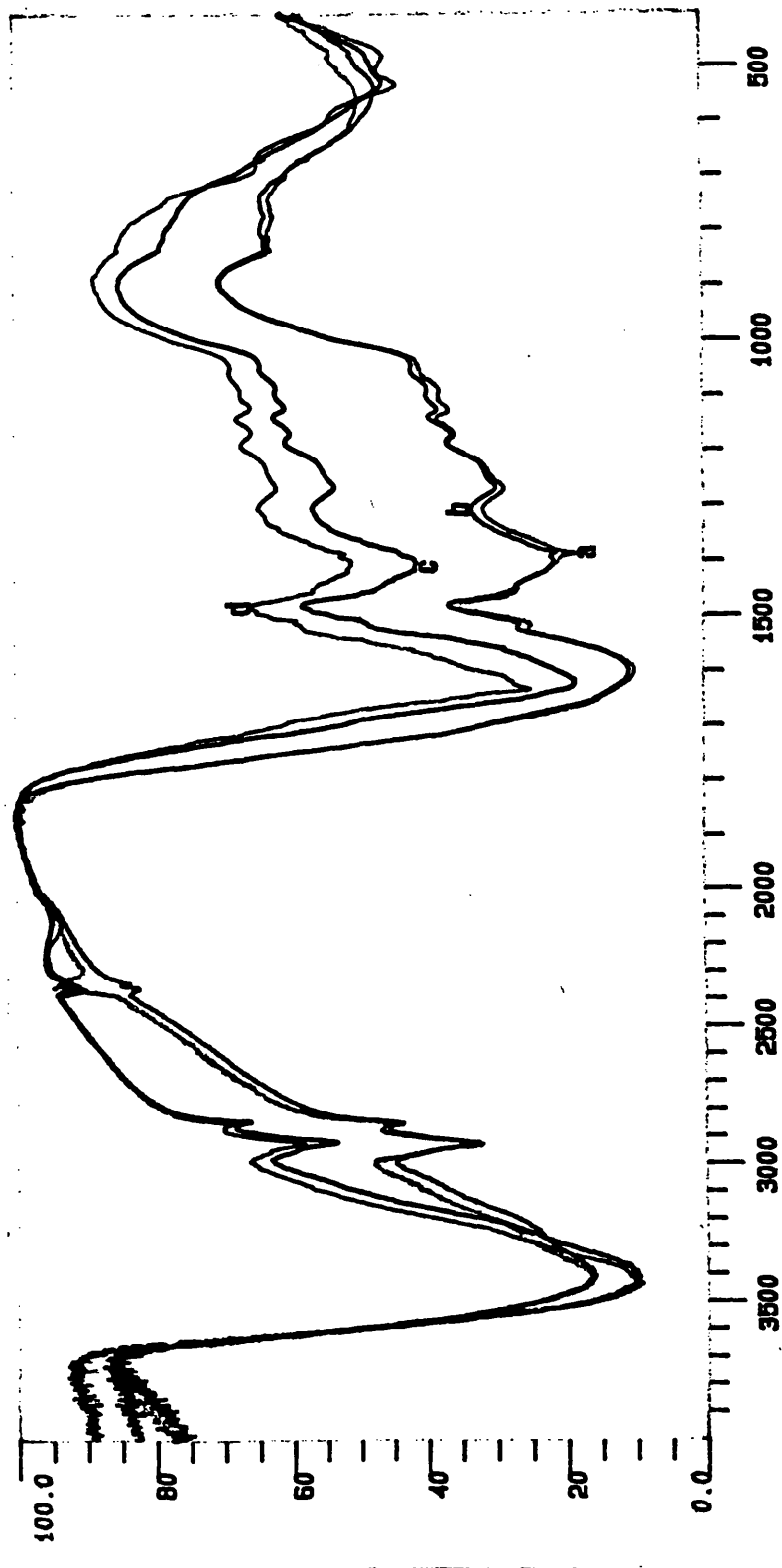


FIG. 6.1.6

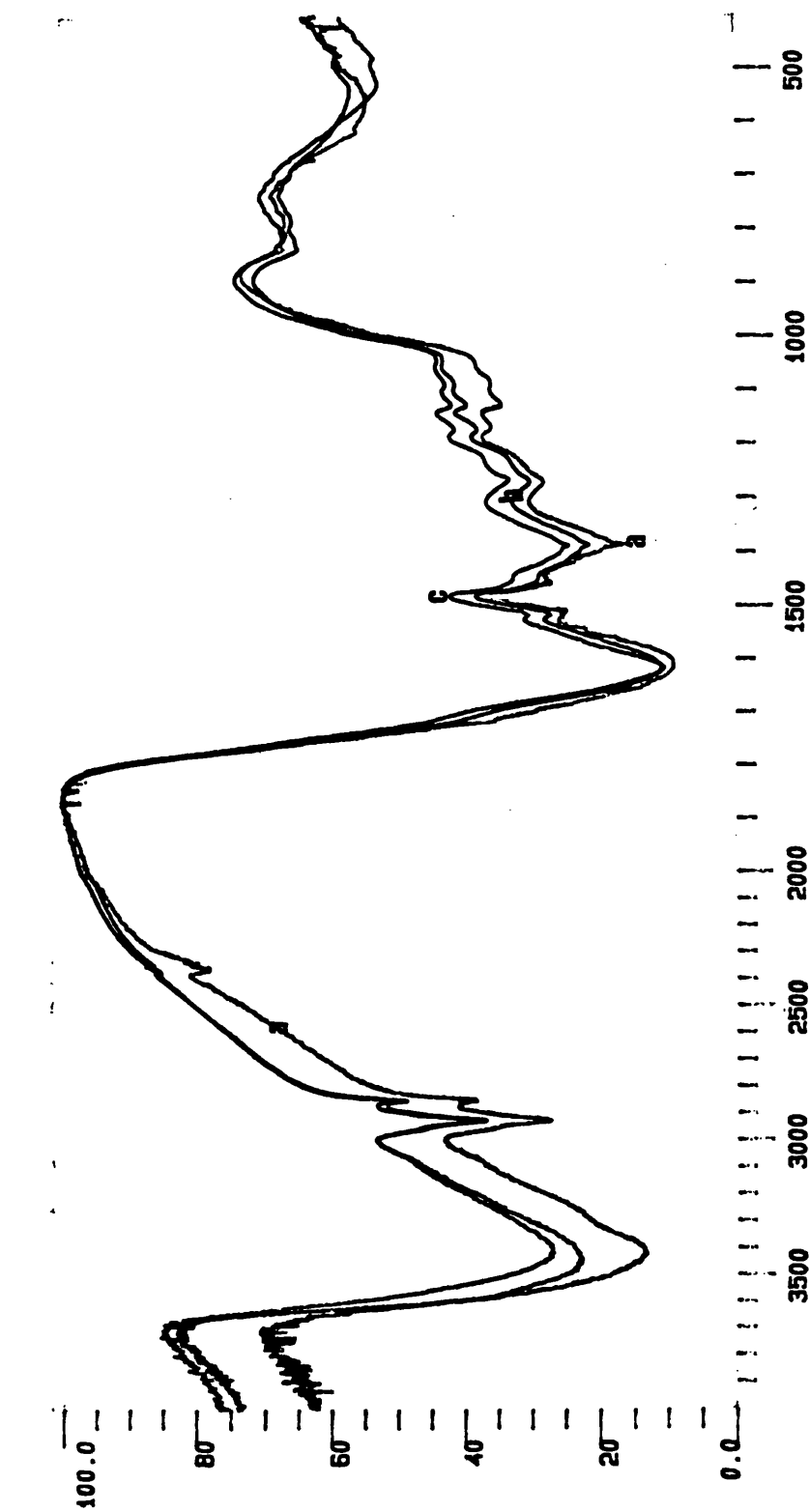
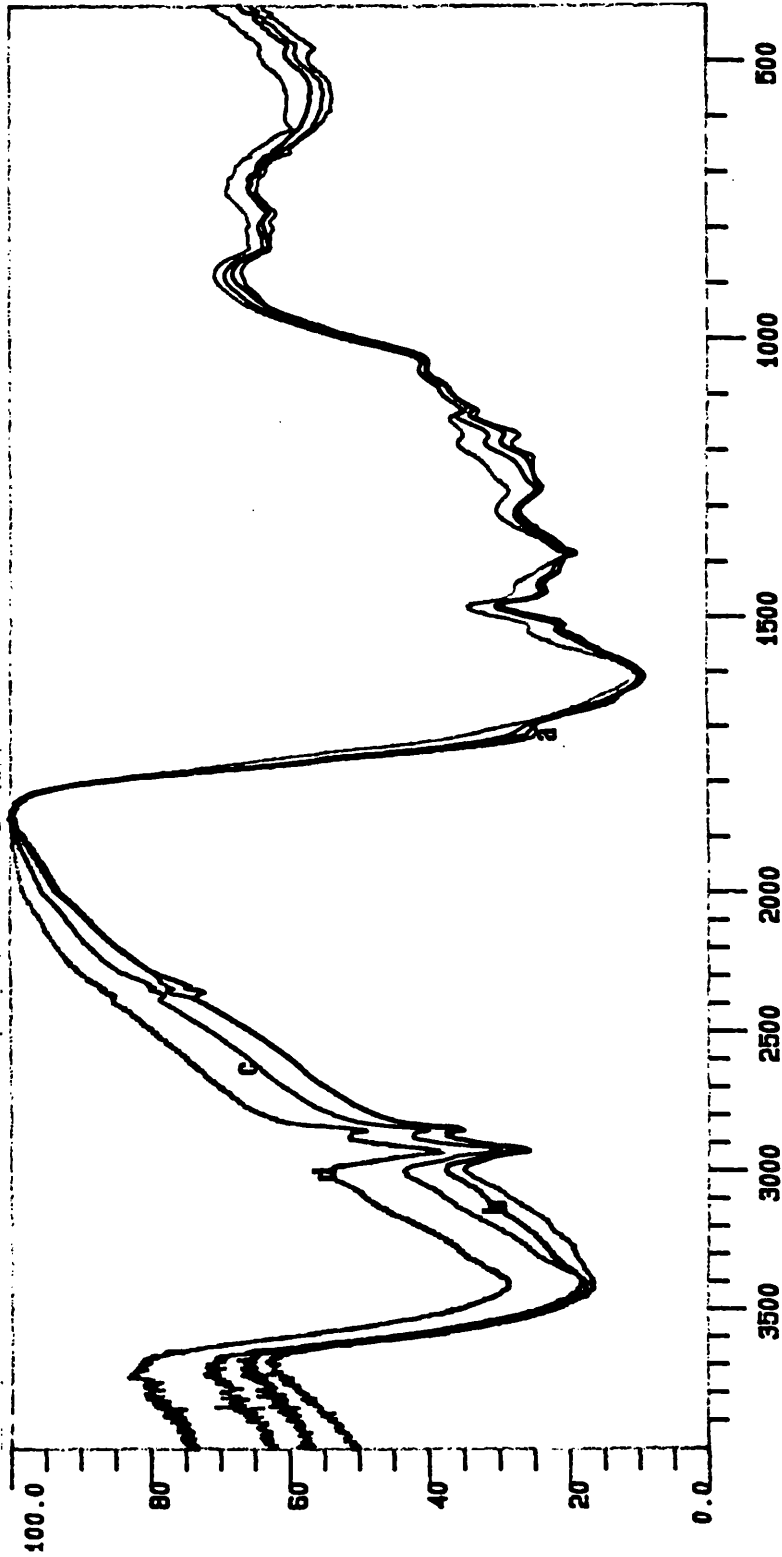


FIG. 6.1.7



6.3 Potentiometric Titrations of Humic Acid

6.3.1 Titration curves of humic acids

The humic acid samples of differing ionic strength exhibited titration curves typical of weak acid polyelectrolytes, (Fig. 6.2), indicating a high buffering capacity over a wide pH range. The Henderson - Hasselbach equation for $I=0.001$ was calculated ;

$$\text{pH} = 5.5 - 1.82 \log \left[\frac{[\text{HA}]}{[\text{A}^-]} \right]$$

giving a pKa value of 5.5 in agreement with those quoted by Stevenson, 1976b. The titration data allowed calculation of the ionization constant at any pH. The point where base consumption was at its maximum was used to calculate A_t , an estimate of the number of carboxyl groups on the humic acid .

6.3.2 Potentiometric titrations in the presence of metal ions.

Results obtained by the sequential addition of caesium, lead ,strontium and cobalt ions to humic acid ($I=0.001$) at variable pH are shown in Figs 6.3.1-6.3.4. The humic acid sample used for Sr and Co (Batch 2) was less concentrated than that used for Cs and Pb (Batch 1) and therefore had a lower content of acidic groups in the solution volume used for the titrations. For all four metal ions each subsequent addition depressed the pH to a lesser extent and required less base to

return the pH to its initial value by neutralising the protons released.

Cs⁺ - the humic acid used had an A_t value of 0.115 mmoles of charge equivalent to its acidic group content. As can be seen from the graph (Fig. 6.3.1) at no pH had all the acidic groups reacted with Cs⁺ due to the competition of protons for these sites however this competition was decreased as the pH increased.

Pb²⁺ - the same strength humic acid sample was used as for caesium (Fig. 6.3.2). It was impossible to measure any depressions of pH at values below pH 5 implying that H⁺ successfully protonates all available sites. Above pH 5 additions of Pb²⁺ do cause pH depressions requiring base additions approaching the acidic group content due to almost complete reaction of these sites with Pb²⁺. It is possible that some of the protons released at these pH values were due to the formation of insoluble oxide hydrates at pH>6. Evidence supporting this was the visible formation of precipitates at higher metal additions at pH 6. Another possible source of excess protons was the release of protons from the hydration water of metal ions held in 1:1 complexes which would agree with the findings of van Dijk (1971) and Stevenson (1976a&b, 1977).

Sr²⁺ and Co²⁺ - these metal ions gave almost identical results with a humic acid sample of $A_t=0.045$ mmoles of charge (Fig. 6.3.3-6.3.4), with Co²⁺ requiring slightly more base than Sr²⁺ to neutralise the protons liberated. At no pH value did the numbers of protons released exceed the available acidic group content indicating that 2:1 complexes were formed. If 1:1 complexes had formed the numbers of protons released would be expected to exceed the available acidic group content due to the release of protons from the hydration water of these 1:1 complexes.

In Figs 6.4.1-6.4.3 the data are presented as plots of the quantity of base consumed vs the quantity of metal ion added. In Fig. 6.4.1 Cs⁺ results are shown for pH 5 and 6 and $I=0.001$. The undissociated acidic group content (HA) was calculated at both pH values; pH 5 HA=0.079 mmoles, pH 6 HA=0.055 mmoles, with the curves obtained falling well below these values. In Fig 6.4.2 Pb²⁺ results are presented for $I=0.001$ and $I=0.01$ at pH 5 and 6. For $I=0.01$; pH 5 HA=0.075 mmoles, pH 6 HA=0.040 mmoles. Smooth curves were obtained up to metal additions of 0.01mmoles with the curves tailing off after an initial steep rise. The curve for pH 6, $I=0.001$ is superimposed upon the curve for $I=.01$, pH 6. For metal additions greater than 0.01mmoles an inflexion point in the slope occurred, this could be due to a greater release of protons due to the

formation of insoluble oxide hydrates enhancing the dissociation of hydration water from the metal ion in 1:1 complexes. This agrees with the findings of Stevenson (1976b,1977). In Fig. 6.4.3 results for strontium and cobalt are presented for $I=0.001$ with the curve obtained for Co^{2+} , $\text{pH}=5$ overlying that at $\text{pH}=4$. For this humic acid sample the undissociated acid content was; $\text{pH}=4$ $\text{HA}=0.042$ mmoles, $\text{pH}=5$ $\text{HA}=0.029$ mmoles, neither of which values are approached by either metal. The curves rose steeply and then tailed off giving no evidence to support the formation of 1:1 complexes as discussed above.

Stability constants were calculated using data where no evidence of precipitation occurred thus avoiding errors due to the presence of excess protons. Titrations were carried out in triplicate in order to determine the reproducibility of the method which was found to be excellent (standard deviation $<1\%$). A literature survey was carried out of available stability constants for lead, (Table 6.1), the most widely researched of the four metal ions to determine the closeness of the results obtained to the range reported by other researchers. The values obtained for this study fell within the reported range giving confidence in the experimental setup.

The calculated results are summarised in Table 6.2. Strontium and cobalt showed little variation with pH with Log K values falling within the range 7.0-7.6

agreeing with the research of Stevenson (1977) which showed little pH dependence. Log K for lead however decreased significantly with pH, although only two data points were available, which disagrees with the literature review of Stevenson and Ardakani (1972) of data obtained by the ion exchange method for determining stability constants. Cs^+ also showed an inverse relationship with pH, with Log K decreasing with increasing pH.

Monovalent ions formed significantly weaker 1:1 complexes with humic acid groups but were not insignificant enough to be ignored in calculations of metal speciation. The pH dependence observed may be of importance when modelling the availability of radiocaesium in the natural environment as it will determine its solubility.

The divalent metal ions formed complexes of similar stability with humic acid with titration data strongly indicating the formation of 2:1 complexes with $-\text{COOH}$ groups and possibly phenolic $-\text{OH}$ groups. Evidence suggests that Pb^{2+} can form 1:1 complexes at high pH values and at higher metal concentrations resulting in the formation of lead oxide hydrate precipitates.

In conclusion at pH 5 the apparent order of stability was;

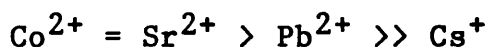


Table 6.1 Lead Stability Constants - Literature Review

LIGAND REF.	METHOD	IONIC ST.	pH	LOG K
F.A 1	I.E	-	3.5	2.7
F.A 1	I.E	-	5.0	4.0
H.A 2	B.T	0.2	4.0	6.6
soil H.A 2	B.T	0.1	4.0	7.2
soil H.A 2	B.T	0.01	4.0	8.7
soil H.A 3	M.B.T	0.1	5.0	7.03
soil H.A 3	M.B.T	0.01	5.0	7.65
soil H.A 3	M.B.T	0.1	5.0	7.00
peat H.A 3	M.B.T	0.01	5.0	8.11
peat H.A 4	M.B.T	0.01	6.2	6.35
peat H.A 4	M.B.T	0.001	6.3	3.82
peat H.A 4	M.B.T	0.001	5.2	6.53

REFERENCES: 1. Schnitzer and Hansen, 1970
 2. Stevenson F.J, 1976b
 3. Stevenson F.J, 1977
 4. Own work.

I.E = ion exchange, B.T = base titration, M.B.T = modified base titration, H.A = humic acid, F.A = fulvic acid.

Table 6.2 Conditional Stability Constants of Fenwick
Moor Peat Humic Acid

METAL	IONIC STRENGTH	pH	LOG K
Cs	0.001	4.0	3.14
	0.001	5.3	1.43
	0.001	6.4	0.72
	0.01	6.2	0.58
Pb	0.001	5.2	6.53
	0.001	6.3	3.82
	0.01	6.2	6.35
Sr	0.001	3.9	7.46
	0.001	4.3	7.08
	0.001	5.1	7.02
Co	0.001	3.9	7.57
	0.001	4.3	7.25
	0.001	5.1	7.03

FIGURE 6.2 Base titration curves for humic acid at ionic strength (I = 0.001, 0.01)

FIGURE 6.3 - Consumption of base by sequential additions of M^{n+} to humic acid (I = 0.001) at variable pH values. The pH was returned to the initial starting point after each addition.

6.3.1 Cs^+

6.3.2 Pb^{2+}

6.3.3 Sr^{2+}

6.3.4 Co^{2+}

FIGURE 6.4 - Base consumption vs amount of M^{n+} added to humic acid at variable pH values and ionic strengths.

6.4.1 Cs^+ pH 5, 6 I = 0.001

6.4.2 Pb^{2+} pH 5, 6 I = 0.001, pH 5,6
I = 0.01

6.4.3 Sr^{2+} and Co^{2+} pH 5, 6 I = 0.001.

**FIG. 6.2 Base Titrations of Humic Acid
Solutions of Differing Ionic Strength**

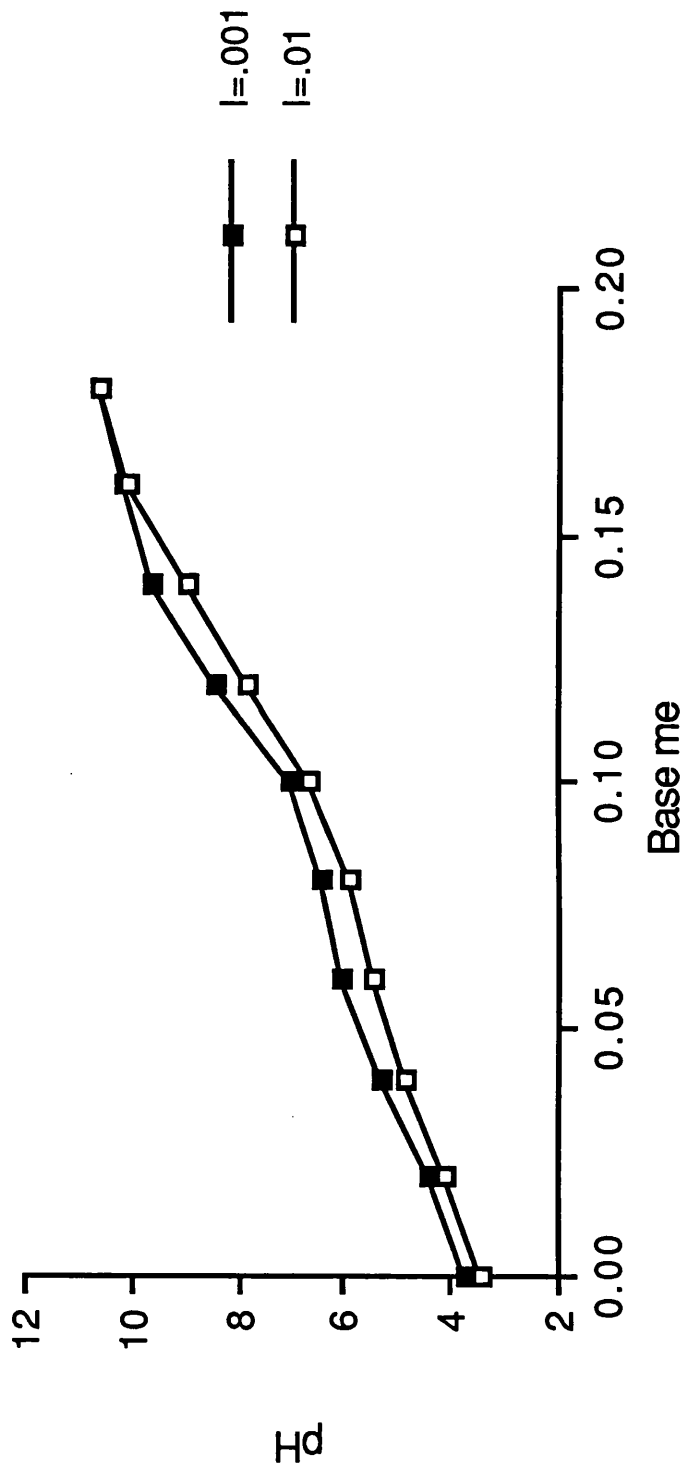


FIG. 6.3.1 Caesium

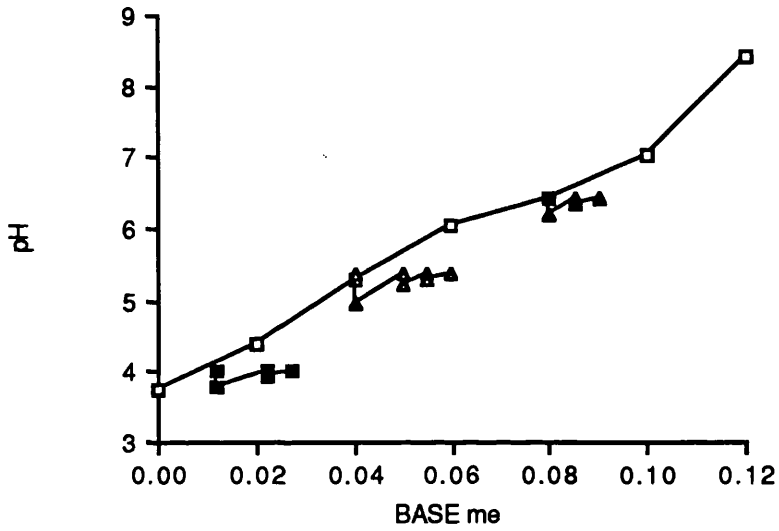


FIG. 6.3.2 Lead

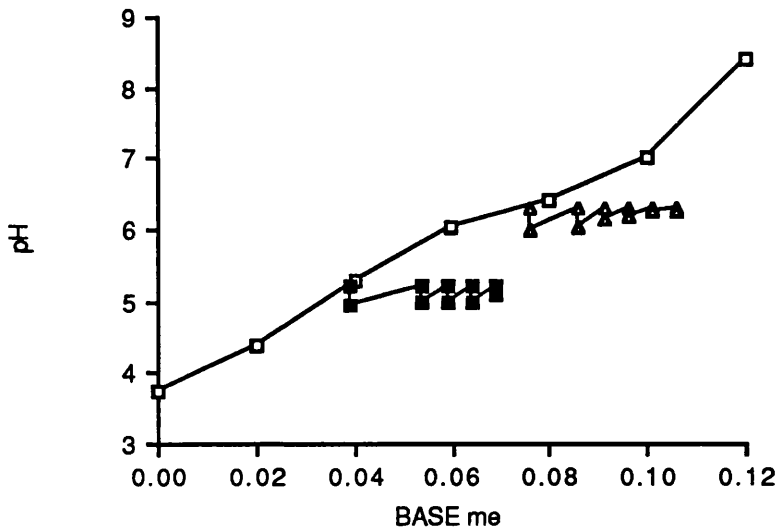


FIG. 6.3.3 Strontium

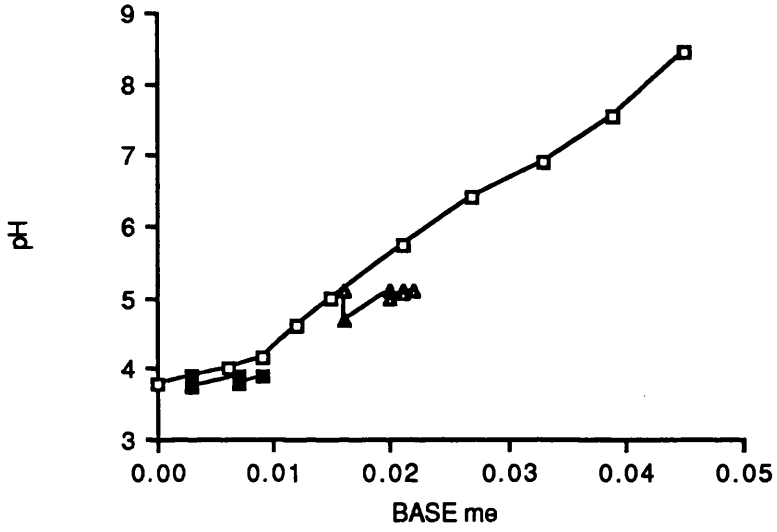


FIG. 6.3.4 Cobalt

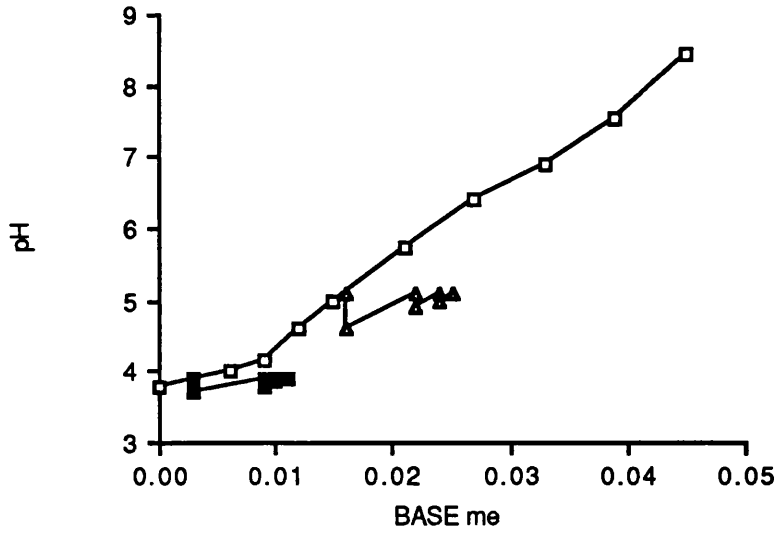


FIG. 6.4.1 Caesium

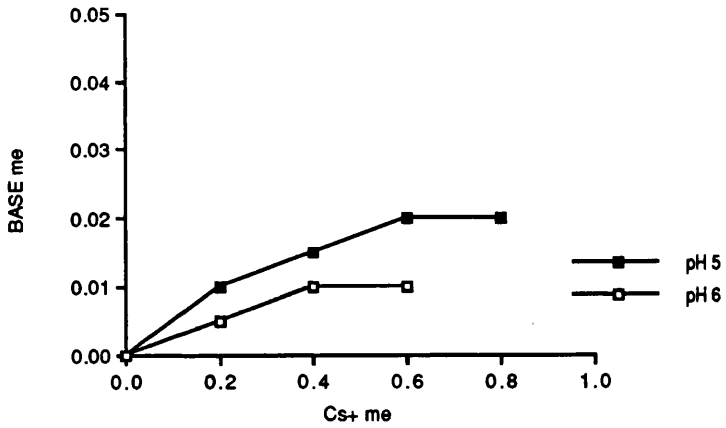


FIG. 6.4.2 Lead

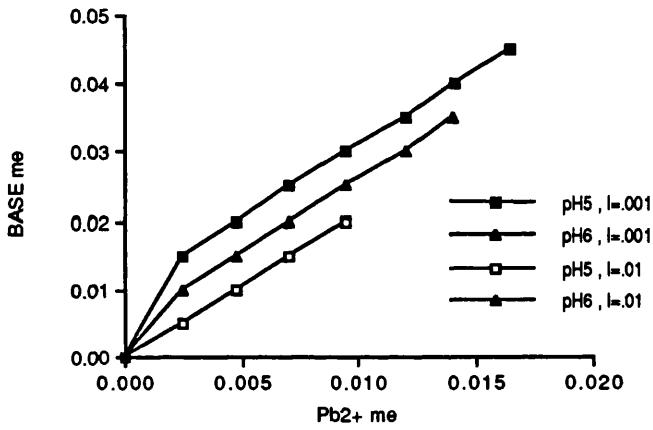
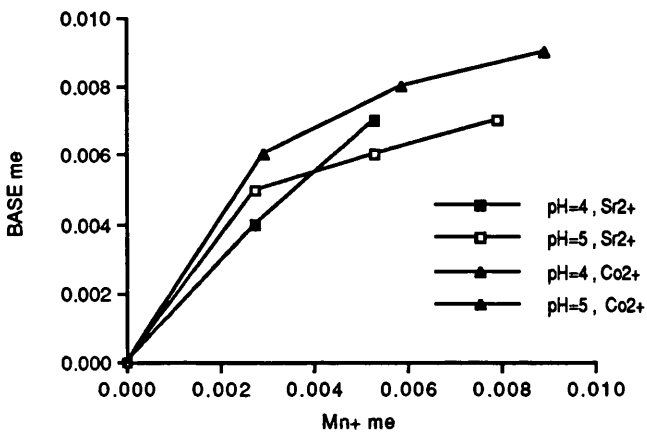


FIG. 6.4.3 Strontium and Cobalt



6.4 Caesium sorption/desorption by clay/humic acid mixtures.

6.4.1 Caesium sorption by clays

Isotherms describing the sorption of caesium by bentonite at pH 3, 5 and 7, and at both equilibrium times, are illustrated in Figure 6.5. In general, equilibration of the bentonite with 0.05 M NaCl for 7 days resulted in less caesium being sorbed than equilibration for 2 days. Two processes may explain this observation. Sodium ions could be preferentially held at some sites and not be exchangeable with caesium ions. The sodium ions may also block some exchange sites, preventing access of the smaller caesium ions. At pH3 the number of cation exchange sites will be fewer due to many pH dependant sites being below their point of zero charge. The percentage of caesium sorbed decreased slightly with increasing concentration (Table 6.3) indicating decreasing availability of exchange sites at higher caesium concentrations, in agreement with the hypothesis of Gaudette et al, (1966).

Unlike bentonite, the caesium sorption onto illite and kaolinite was unaffected by pH variations in the range 3-7. with the data being shown in Figures 6.6 and 6.7. Increasing the soaking time in NaCl solution to 7 days resulted in an increase in the amount of caesium sorbed by illite at solution Cs concentrations greater than 10 mg l⁻¹. This may be due to sodium ions

stabilising wedge sites and allowing access for the caesium ions to diffuse into interlamellar sites. In contrast, the longer soaking time in NaCl solution depressed the amount of Cs sorbed by kaolinite, similar to the above observation for bentonite. Both illite and kaolinite exhibited decreasing percentage sorption as a function of increasing caesium concentration (Table 6.3) in agreement with the above observation for bentonite. Consistent with the fact it has only surface sites, kaolinite exhibited the lowest level of caesium sorption. The convergence of all the isotherms at the point of lowest concentration suggests that there are some caesium specific sites on the clays which are filled first. Overall, the above results demonstrate that for both 2 and 7 days soaking in NaCl solution, the order of sorption of caesium by the clays was; bentonite > illite > kaolinite.

6.4.2 Caesium sorption by clay/humic acid mixtures

In this experiment comparisons are being made between the simultaneous addition of humic acid and caesium chloride, and a 5 day pre-equilibration of the humic acid with the clay prior to addition of caesium chloride. In both cases the clay had been soaked in NaCl for 2 days prior to treatment. Isotherms for the sorption of caesium in mixed clay/humic acid systems are shown in Figs 6.5-6.7. The effect of humic acid can be seen by comparing each pair of symbols (open and

closed) for each time.

The sorption of caesium onto bentonite was depressed at all three pH values for the simultaneous addition of humic acid and caesium. However, sorption was depressed at pH 7 only when the clay and humic acid were pre-equilibrated (Fig. 6.5). For illite and kaolinite the addition of humic acid resulted in a decrease in caesium sorption at all pH values and at both times. However, for kaolinite the amount of caesium sorbed was low and the differences between treatments small (Figs 6.6-6.7).

Humic acids bonded to clay surfaces potentially block exchange sites which could sorb caesium. The effect of this was seen particularly with illite, where access to stabilized wedge sites would also be impeded. In addition to this blocking effect, humic acid also decreased caesium sorption because the sites on the humic polymer were low energy exchange sites with no specificity for caesium. These two factors combined to make the clay/humic acid system one in which caesium sorption was not favoured.

6.4.3 Desorption of Caesium from clay/humic acid mixtures

The results of the desorption experiment are summarised in Figure 6.8 as the percentage of added caesium held on the clay surfaces at dilution factors ranging from x1 (no dilution) to x11 (10cm³ diluted to 110cm³).

The addition of humic acid enhanced desorption from bentonite and to a lesser extent from kaolinite. However, no increase in desorption from illite was observed. In addition the caesium held by bentonite was removed more easily in the presence of humic acid. In highly organic soils this would make caesium more mobile. The opposite effect was observed for illite with the caesium becoming immobilised. For kaolinite the effect is less clear. It held much less caesium than the other clays and that was easily removed; some was lost with no dilution.

6.4.4 Distribution Coefficients(K_d)

For all three clays the percentage of caesium sorbed decreased or changed little with increasing caesium concentration in solution (Table 6.3). This observation clearly illustrates that the use of a single K_d value is inadequate to describe sorption over this concentration range. For this reason K_d values were calculated for each isotherm at different caesium concentrations to represent the whole isotherm (Table 6.4). These values agree with those of McKinley and Hadderman (1984). They quoted a value of 2000 kg^{-1} for bentonite at concentrations of caesium below 10^{-7}M , but cautioned that the value should be halved for each order of magnitude of concentration higher than this. Calculating for a concentration of 10^{-4}M (the concentration range used in this study), a value of 250

1kg^{-1} is obtained. This compares well with values of approximately 200 kg^{-1} obtained in this study.

The addition of humic acid to the clays results in lower K_d values being obtained for sorption (Table 6.4). K_d values for desorption were consistently greater than for sorption, in the absence of humic acid, with the difference being more pronounced at lower caesium concentrations. This indicates that the sorption of caesium was not totally reversible under these experimental conditions, with the lack of reversibility being most pronounced for illite. In almost all cases, humic acid additions caused the desorption K_d values to decrease. Thus for both the sorption and desorption process the presence of humic acid resulted in lower K_d values than in its absence.

TABLE 6.3 Percentage Caesium Sorbed at pH 5

CLAY	Initial Conc. [Cs+] mg l ⁻¹	% Sorbed at 2 day Equilibration	% Sorbed at 7 day Equilibration
Bentonite	5	46	40
	10	44	36
	15	40	34
	20	37	30
Illite	5	36	30
	10	29	25
	15	23	26
	20	22	26
Kaolinite	5	16	10
	10	13	7
	15	11	8
	20	11	7

TABLE 6.4 Kd values at pH7 for caesium adsorption and desorption at given solution concentrations of Cs at equilibrium, with and without humic acid (HA) addition.

Solution Concentrations at Equilibrium mg l ⁻¹	Kd Value (l kg ⁻¹)			
	Adsorption		Desorption	
	+HA	-HA	+HA	-HA
Bentonite				
2	105	224	300	334
4	98	200	212	263
8	113	130	125	-
Illite				
2	110	140	300	360
4	88	130	163	200
8	63	103	91	106
12	54	-	64	-
16	50	-	-	-
Kaolinite				
2	15	38	75	100
4	17	38	50	70
8	14	31	34	49
16	13	31	19	31
30	16	-	13	-

FIGURE 6.5 - Bentonite/Humic Acid sorption isotherms;
.1 = pH 3, .2 = pH 5, .3 = pH 7
Humic acid, 7 days equilibration = ■
No humic acid, 7 days equilibration = □
Humic acid, 2 days equilibration = ▲
No humic acid, 2 days equilibration = △

FIGURE 6.6 - Illite/Humic Acid sorption isotherms;
.1 = pH 3, .2 = pH 5, .3 = pH 7
Humic acid, 7 days equilibration = ■
No humic acid, 7 days equilibration = □
Humic acid, 2 days equilibration = ▲
No humic acid, 2 days equilibration = △

FIGURE 6.7 - Kaolinite/Humic Acid sorption isotherms;
.1 = pH 3, .2 = pH 5, .3 = pH 7
Humic acid, 7 days equilibration = ■
No humic acid, 7 days equilibration = □
Humic acid, 2 days equilibration = ▲
No humic acid, 2 days equilibration = △

FIGURE 6.8 - Effect of dilution factor on the
percentage Cs desorbed.

a = bentonite

b = illite

c = kaolinite

clay = ■

clay + HA = □

FIG. 6.5.1 Bentonite pH 3

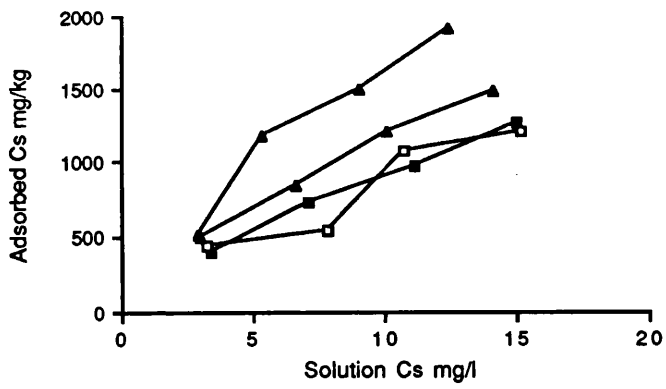


FIG. 6.5.2 Bentonite pH 5

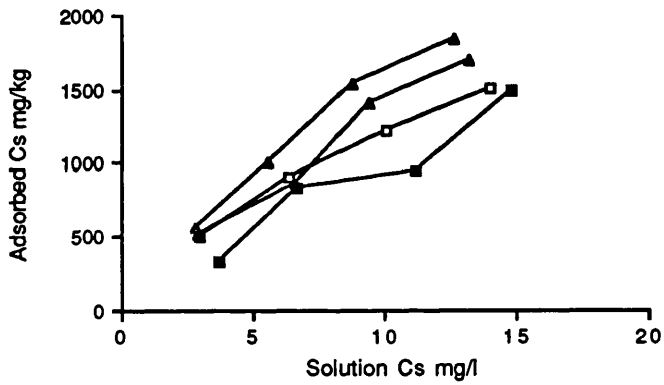


FIG. 6.5.3 Bentonite pH 7

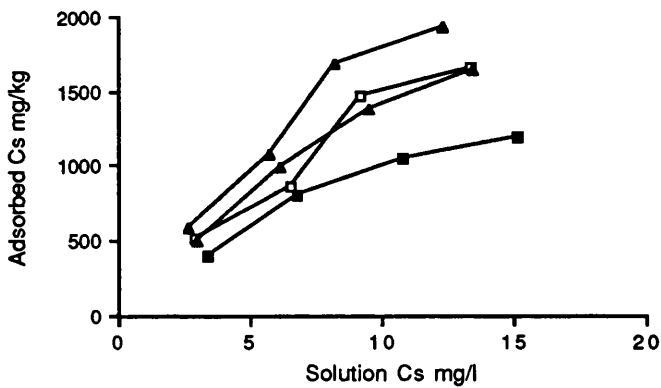


FIG. 6.6.1 Illite pH 3

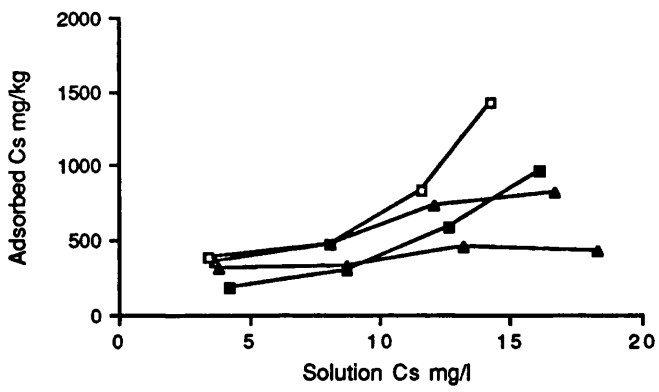


FIG. 6.6.2 Illite pH 5

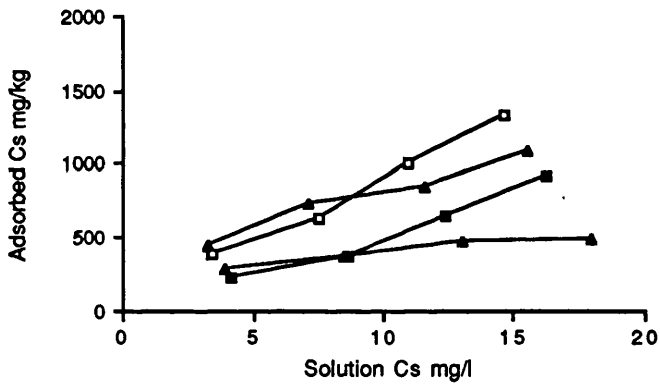


FIG. 6.6.3 Illite pH 7

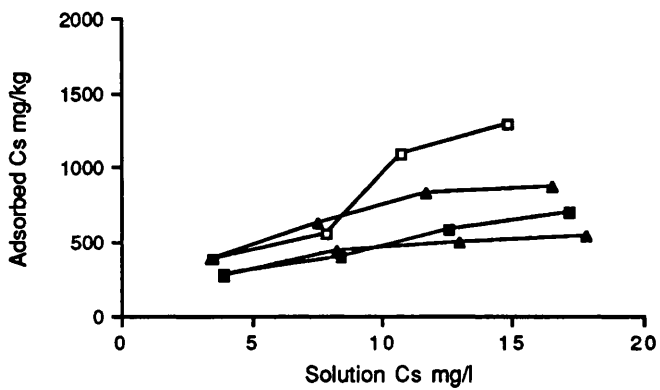


FIG. 6.7.1 Kaolinite pH 3

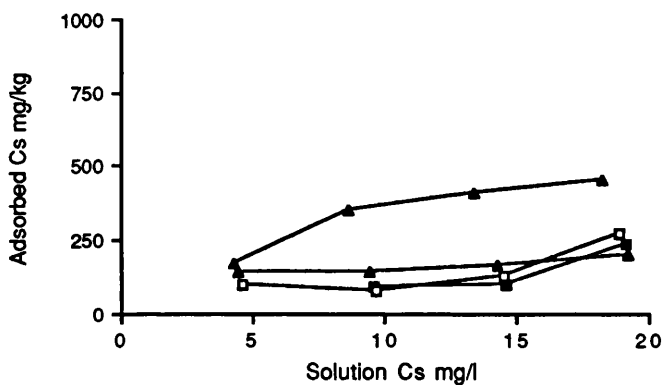


FIG. 6.7.2 Kaolinite pH 5

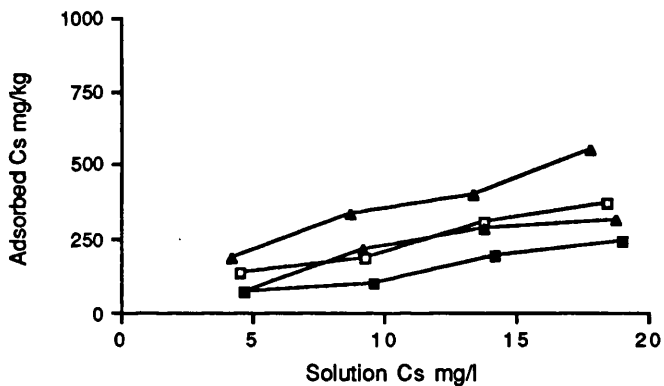


FIG. 6.7.3 Kaolinite pH 7

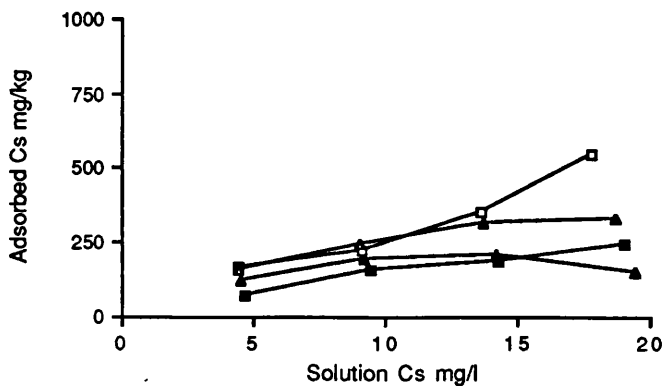


FIG. 6.3.1 Bentonite

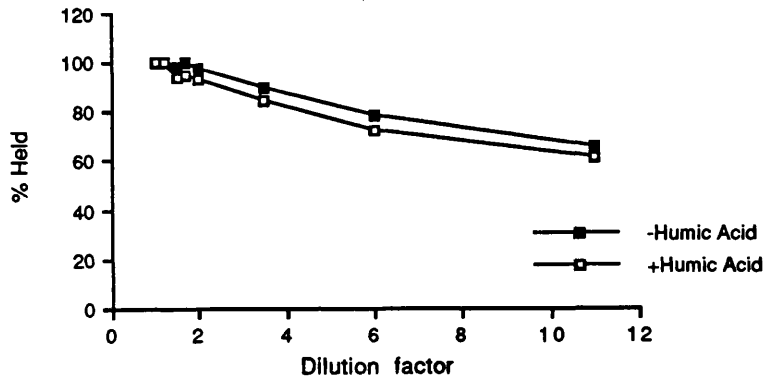


FIG. 6.3.2 Illite

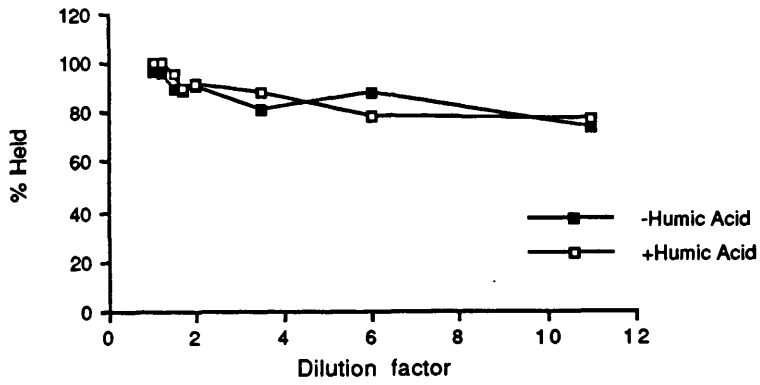
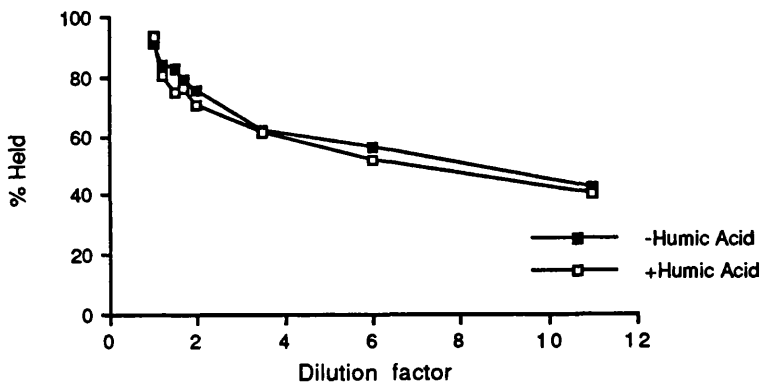


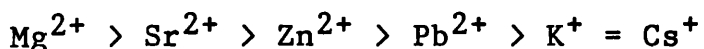
FIG. 6.3.3 Kaolinite



6.5 Summary

The main findings of this chapter are:

a) A qualitative examination of the binding of metals with humic acid showed an apparent order of reaction of:



with monovalent ions forming simple metal humate salts and divalent ions using more of the available functional groups to form conjugated ketonic structures.

b) A quantitative approach to metal ion/humic acid binding resulted in an apparent order of stability at pH 5 of:



Log K 7.03 7.02 6.53 1.43

The log K values for Pb^{2+} and Cs^+ are inversely related to pH but those for Co^{2+} and Sr^{2+} are directly related to pH.

c) Addition of humic acid to the clays used depressed the sorption of caesium, with illite showing the greatest effect. For both sorption and desorption, the presence of humic acid resulted in lower K_d values than in its absence.

CHAPTER 7 - CONCLUSIONS

7.1 Conclusions

This research examined the behaviour of radionuclides, in particular radiocaesium, in organic rich soils (see Section 1.6).

Measurements taken from environmental samples of soils and peats enabled the following statements to be made concerning the behaviour of radiocaesium and ^{210}Pb (see Chapter 4). Radiocaesium deposited on acid peat soils appears to be mobilised by the lateral flow of surface water. This movement is governed by local variations in topography. There was no convincing evidence that diffusion occurs within the cores but small amounts of radiocaesium do penetrate to depths of up to 20cm. The downward movement of radiocaesium could be attributed in some cases to the growth of the peat core, for example. In Chapter 4 a simple exponential model was constructed in an attempt to predict the reduction in radiocaesium concentrations with time in the mixed zone of a peat soil where a mixed zone is underlain by a zone of downwards movement. Estimates for two peats were calculated predicting that the time for 50% of Chernobyl radiocaesium to be removed from the mixed zone would be 36 years for Borders peat (mixed zone = 6cm deep) and 5 years for Fenwick Moor peat (mixed zone = 5cm deep). The shorter residence time for

Fenwick Moor peat may be due to the lateral movement of radiocaesium affecting the calculation.

These findings imply that due to its mobility radiocaesium data cannot be used to derive a chronology for peat profiles. In addition some evidence of ^{210}Pb re-mobilisation was found questioning the use of ^{210}Pb data in the calculation of sedimentation rates.

Chapter 5 utilised laboratory methods to study the adsorption and desorption behaviour of caesium. The experiments found that caesium uptake appears to take place by two mechanisms: rapid sorption onto caesium specific sites on the soil's mineral phase, at low equilibrium concentrations; and at higher concentrations a slower sorption occurs possibly due to the uptake of caesium by soil organic matter. The uptake of caesium by soils containing <70% organic matter can be described using the Langmuir equation. The desorption of caesium from soils was affected by the pH of the soil solution with almost complete desorption occurring at pH 3.

These findings concur with environmental measurements where radiocaesium sorbed onto acid, organic soils can be remobilised and hence made available for plant uptake. Further evidence supporting this remobilisation was found in Chapter 6 where humic acid was found to influence the sorption/desorption of caesium by clays. Humic acid

blocked access to high energy binding sites on the clays for caesium ions, while itself presenting only low energy sites from which caesium can be easily displaced. In addition to this, humic acid resulted in more of the adsorbed caesium being readily desorbed from bentonite and kaolinite. Overall therefore, the presence of humic acid can be seen to have caused caesium to be more mobile.

7.2 Recommendations for Further Work

This study has identified several areas where further work could be undertaken.

1. A continuing study of radiocaesium and ^{210}Pb mobility, over several years, examining both lateral and downwards movement in peat. Detailed measurements of slope, changes in altitude and a record of rainfall and surface water run-off would enable the data to be used in the construction of a model describing the advective movement of radiocaesium.
2. The continuation and development of laboratory work initiated in Chapter 6 measuring stability constants for radionuclide/humic acid mixtures and studying other organic components in soil. These values may then be used in models of radionuclide migration.
3. The extension of the study examining the influence of the clay/humic acid interactions on the subsequent

binding of metal to the solid phase to ions other than caesium.

APPENDIX 1

This appendix contains graphs representing Langmuir plots relating to the data given in Table 5.2, Chapter 5. Best fit lines were calculated in order to obtain values for Langmuir maxima and these values are expressed in terms of cmol kg^{-1} in Table 5.2 and mg kg^{-1} in Appendix Table 1.

APPENDIX TABLE 1 Langmuir Maxima for caesium sorption calculated for two shaking times (1 hour and 24 hours).

Soil Name	Langmuir Maxima		p<	R ²	Langmuir Maxima		p<	R ²
	1 hour	mg kg ⁻¹			24 hours	mg kg ⁻¹		
Darleith A	3817	0.010	91	4739	0.450	79		
Darleith B	2146	0.020	97	3155	0.020	87		
Dunlop A	7299	0.010	91	5556	0.010	92		
Dunlop B	2049	0.010	98	3876	0.020	88		
Peaty Gley O	3257	0.030	84	6289	0.180	50		
Peaty Gley Bg	2604	0.150	56	2639	0.060	74		
Humic Gley O	3077	0.450	79	6711	0.210	46		
Humic Gley B	5263	0.006	94	5376	0.020	87		
Dreghorn A	1160	0.001	98	921	0.160	89		
Dreghorn B	335	0.002	97	909	0.020	87		
Bargour A	1623	0.001	98	2725	0.060	75		
Bargour B	1072	0.01	92	1513	0.050	76		
Peat	-4444	0.57	12	3663	0.280	37		

N.B.:

- p values refer to the probability level of the F statistic and indicate the significance level of regression effect;

-R² is the coefficient of determination.

FIG 1.1 Darleith A

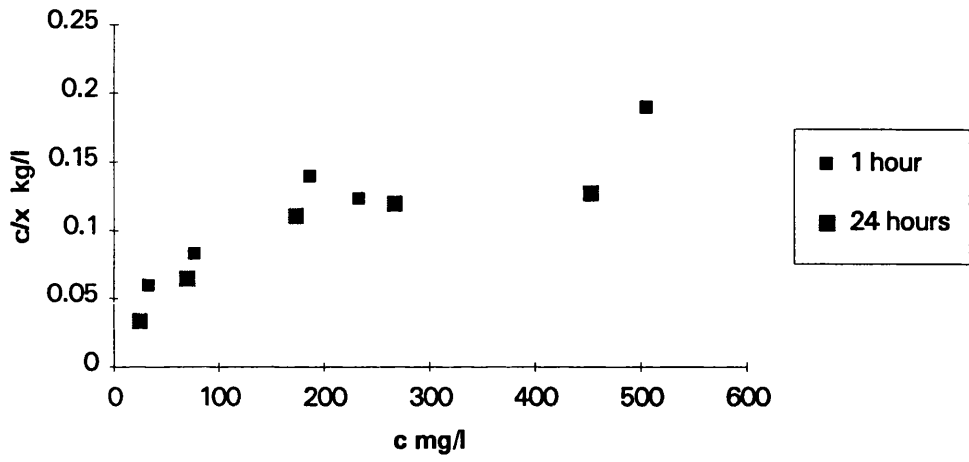


FIG 1.2 Darleith B

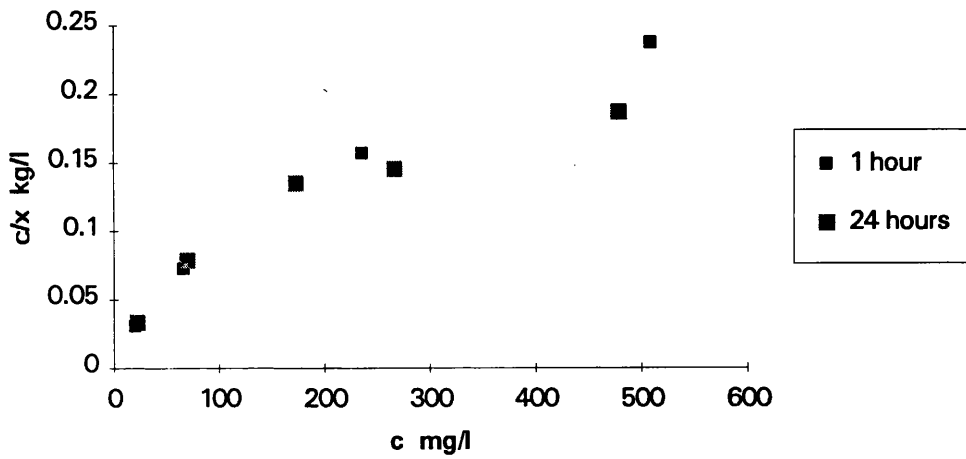


FIG 2.1 Dunlop A

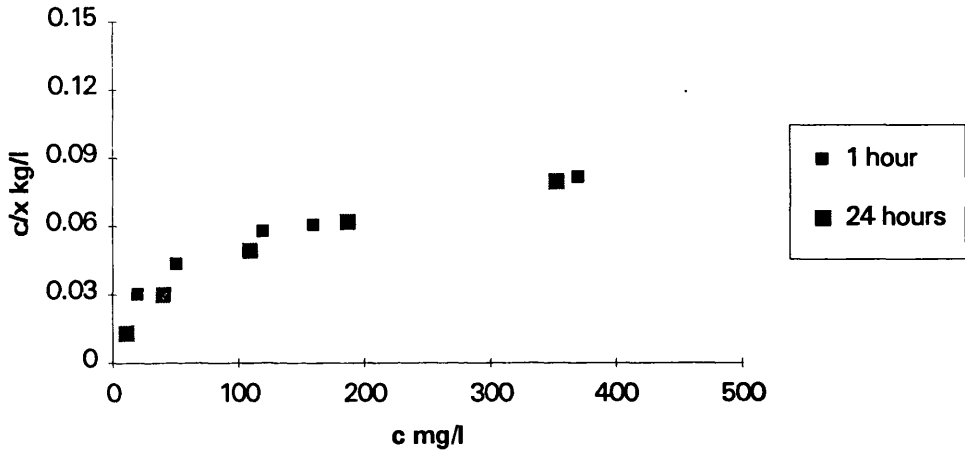


FIG 2.2 Dunlop B

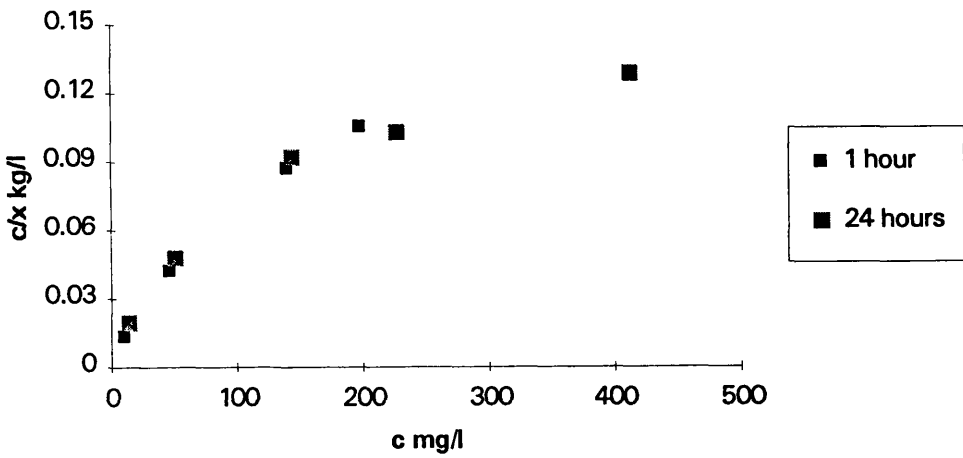


FIG 3.1 Peaty Gley O

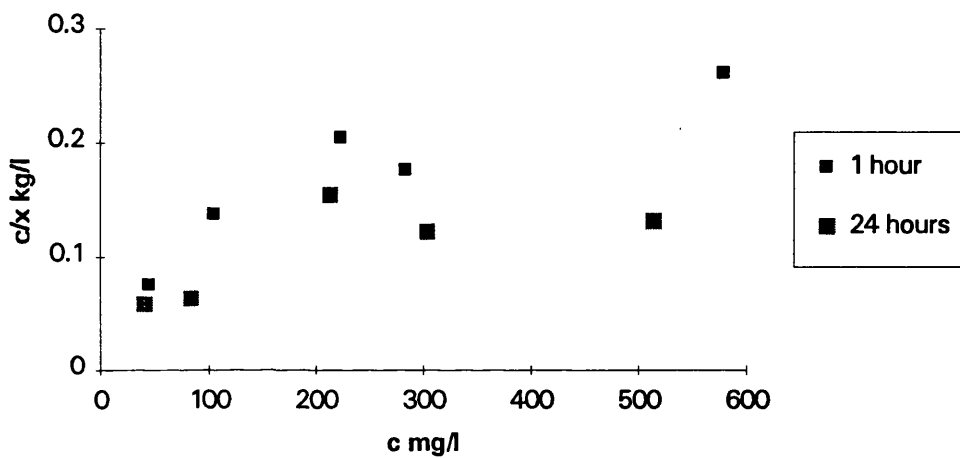


FIG 3.2 Peaty Gley Bg

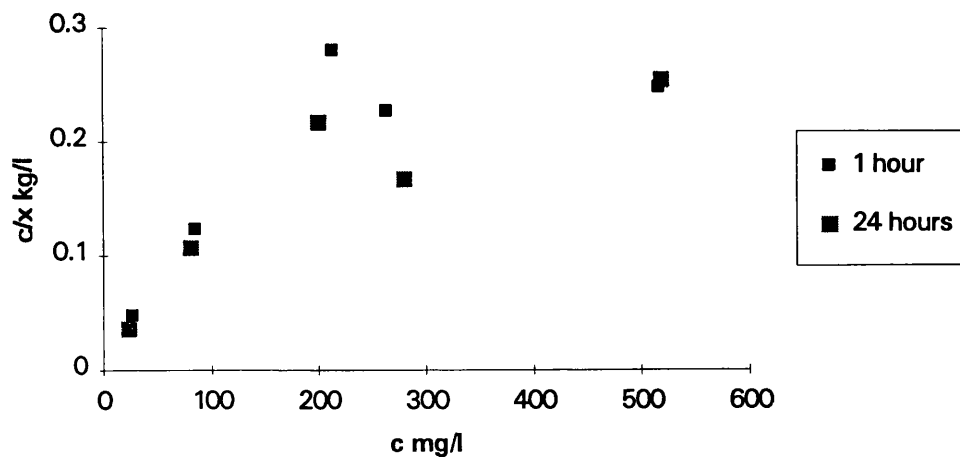


FIG 4.1 Humic Gley Top

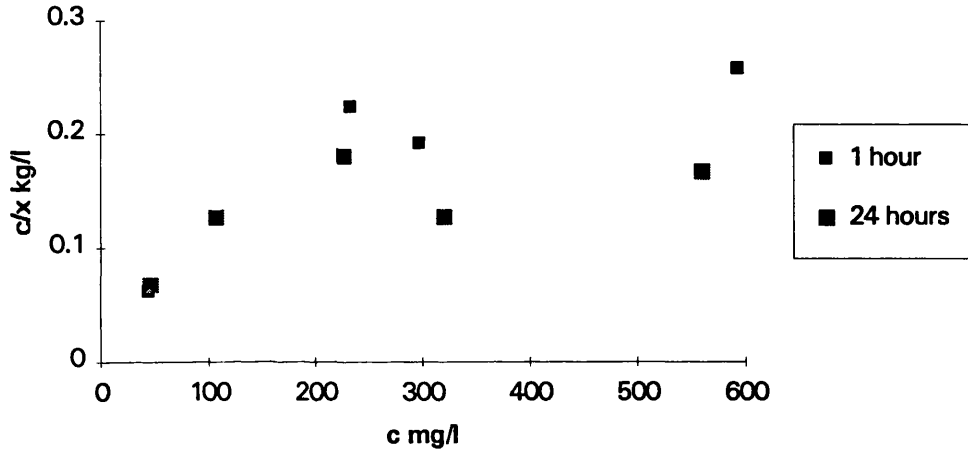


FIG 4.2 Humic Gley B

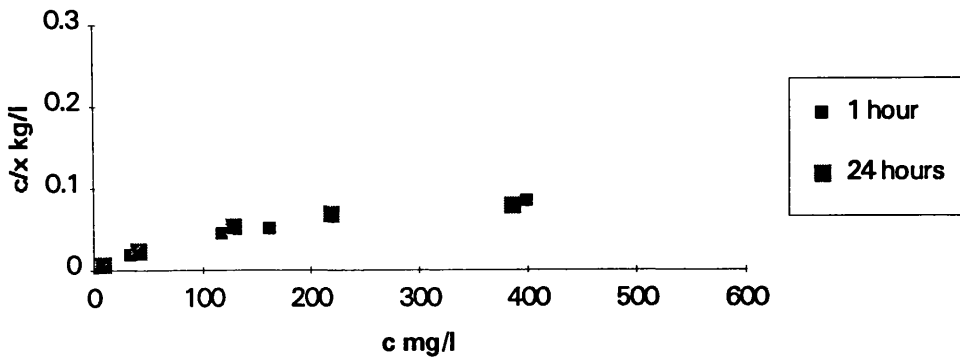


FIG 5.1 Dreghorn A

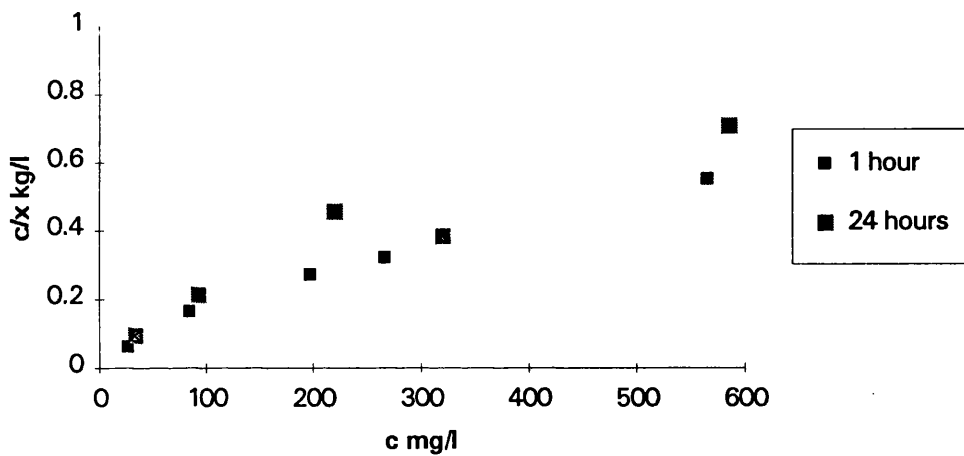


FIG 5.2 Dreghorn B

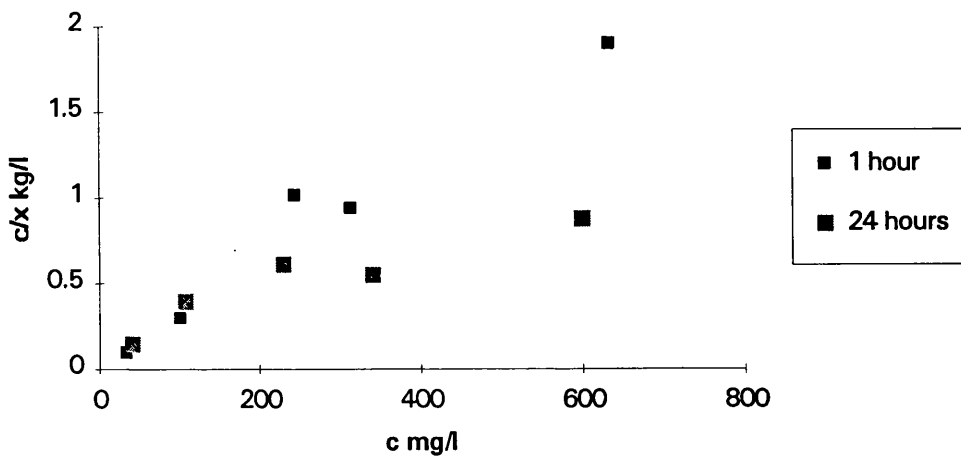


FIG 6.1 Bargour A

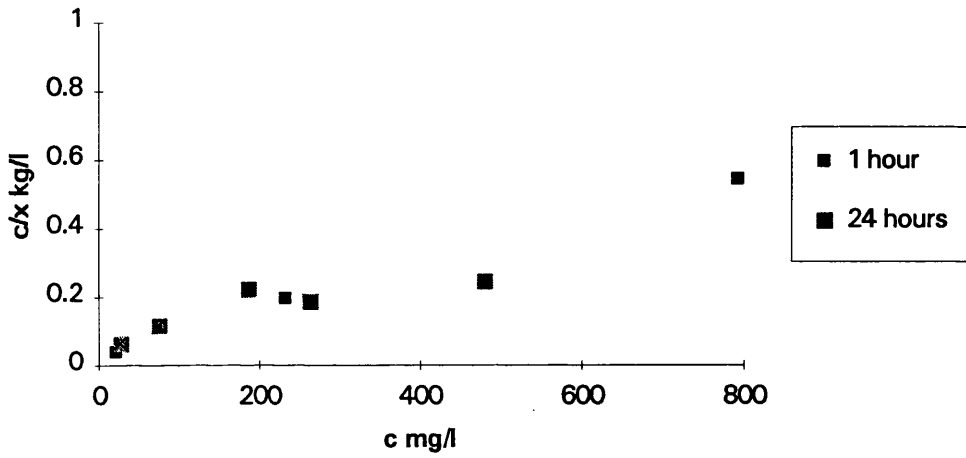


FIG 6.2 Bargour B

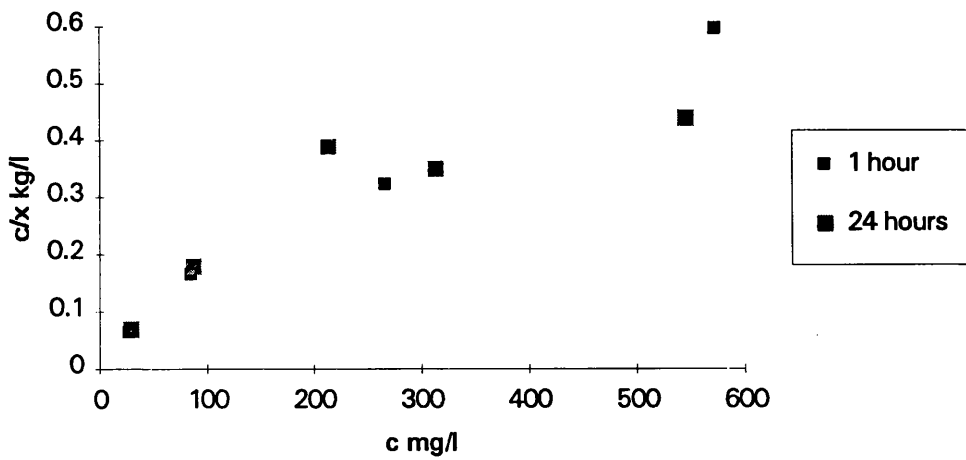
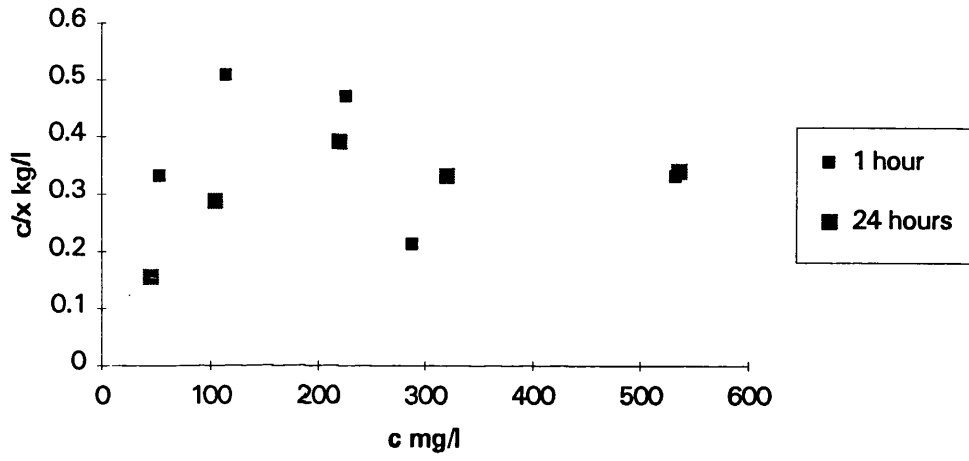


FIG 7 Peat



REFERENCES

Aaby, B. and Jacobsen, J. (1979). 'Changes in biotic conditions and metal deposition in the last millenium as reflected in ombrotrophic peat in Draved Mose, Denmark.' *Damn. Geol. Unders. (Arbog 1978)*, 5-43.

Appleby, P.G., Nolan, P.J., Oldfield, F., Richardson, N. and Higgett, S.R. (1988). '²¹⁰Pb dating of lake sediments and ombrotrophic peats by gamma assay.' *Science of the Total Environment*, 69, 157-177.

Adams, F and Dams, R. (1970). 'Applied Gamma-Ray spectrometry.' Pergamon Press, Oxford.

Andolina, J. and Guillitte, O. (1990). 'Radiocaesium availability and retention sites in forest humus.' In 'Transfer of Radionuclides in the Natural and Semi-Natural Environment.'pp 135-142 Eds. G. Desmet, P. Nassimbeni and M. Belli. Elsevier Applied Science, London.

Aston, S.R. and Stanners, D.A. (1979). 'The determination of estuarine sedimentation rates by ¹³⁴Cs/¹³⁷Cs and other artificial radionuclide profiles.' *Estuarine Coastal Marine Science*, 9, 529-541.

Beckwith, R.S. (1959). 'Titration curves of soil organic matter.' *Nature*, 184, 745-746.

Ben Shaban, Y.A. (1989). 'Radionuclide movement and geochemistry in intertidal sediments in South-West Scotland.' PhD Thesis University of Glasgow.

Bertell, R. (1985). 'No Immediate Danger - prognosis for a radioactive earth.' Womens Press, London.

Bjerrum, J. (1941). 'Metal Amine Formation in Aqueous Solutions.' P. Haase & Son, Copenhagen

BNFL (1982). Annual report for 1981 on radioactive discharges and monitoring of the environment. British Nuclear Fuels Limited. Health and Safety Directorate. Risley.

BNFL (1983). Annual report for 1982 on radioactive discharges and monitoring of the environment. British Nuclear Fuels Limited. Health and Safety Directorate. Risley.

BNFL (1985). Annual report for 1984 on radioactive discharges and monitoring of the environment. British Nuclear Fuels Limited. Health and Safety Directorate. Risley.

BNFL (1986). Annual report for 1985 on radioactive discharges and monitoring of the environment. British Nuclear Fuels Limited. Health and Safety Directorate. Risley.

BNFL (1987). Annual report for 1986 on radioactive discharges and monitoring of the environment. British Nuclear Fuels Limited. Health and Safety Directorate. Risley.

BNFL (1988). Annual report for 1987 on radioactive discharges and monitoring of the environment. British Nuclear Fuels Limited. Health and Safety Directorate. Risley.

BNFL (1989). Annual report for 1988 on radioactive discharges and monitoring of the environment. British Nuclear Fuels Limited. Health and Safety Directorate. Risley.

Bohn, H., McNeal, B. and O'Connor, G. (1985). 'Soil Chemistry.' 2nd edn. Wiley Interscience, New York

Browne, E. and Firestone, R.B. (1986). 'Table of Radioactive Isotopes.' John Wiley and Sons, New York.

Bunzl, K., Kracke, W. and Schimmack, W. (1992). 'Vertical migration of plutonium-239 and -240,

americium-241 and caesium-137 fallout in a forest soil under spruce.' *Analyst*, 117(3), 469-474.

Cambray, R.S. (1982). 'Annual discharges of certain long lived radionuclides to the sea and to the atmosphere from the Sellafield works, Cumbria 1975-1981.' UKAEA report AERE-M-3269, HMSO London.

Cambray, R.S., Cawse, P.A., Garland, J.A., Gibson, J.A.B., Johnson, P., Lewis, G.N.J., Newton, D., Salmon, L. and Wade, B.O. (1987). 'Observations on radioactivity from the Chernobyl accident.' *Nuclear Energy*, 26, 77-101

Cawse, P.A. (1980). 'Studies of environmental radioactivity in Cumbria, Part 4. Caesium-137 and plutonium in soils of Cumbria and the Isle of Man.' AERE Harwell Report R-9016. HMSO, London.

Cawse, P.A. (1983). 'The accumulation of caesium-137 and plutonium-239+240 in soils of Great Britain, and transfer to vegetation.' In 'Ecological aspects of radionuclide release' - special publications series of the British Ecological Society, Number 3. 47-62 Ed. P.J. Coughtry.

Cawse, P.A. and Horrill, A.D. (1986). 'A survey of caesium-137 and plutonium in British soils in 1977'. AERE report 10155, UKAE Authority, Harwell.

Choppin, G.R. (1988). 'Humics and radionuclide migration.' *Radiochimica Acta*, 44/45, 23-28.

Christiansen, B. and Torstenfelt, B. (1988). 'Diffusion of Nickel, Strontium, Iodine, Caesium and ammonium in loosely compacted bentonite at high pH.' *Radiochimica Acta*, 44/45, 219-230.

Clark, S.B. and Choppin, G.R. (1990). 'Kinetics of rare earth metal binding to aquatic humic metals.' In 'Chemical Modelling of Aqueous Systems II.' 519-525, American Chemical Society, New York.

Cline, J.F. and Rickard, W.H. (1971). 'Radioactive strontium and caesium in cultivated and abandoned field plots.' In 'Radionuclides in Ecosystems.' Proceedings of third national Symposium on Radioecology. Vol. 1, 209-212 Ed. D.J. Nelson.

Clymo, R.S. (1983). 'Peat.' In 'Mires: swamp, bog, fen and moor.' 159-225 Ed. A.J.P. Gore, Elsevier Publishing Company, New York.

Coleman, N.T., Craig, D. and Lewis, R.J. (1963a). 'Ion exchange reactions of cesium.' Soil Science Society of America Proceedings, 27, 287-289.

Coleman, N.T., Lewis, R.J. and Craig, D. (1963b). 'Sorption of cesium by soils and its displacement by salt solutions.' Soil Science Society of America Proceedings, 27, 290-294.

Cotton, F.A. and Wilkinson, G. (1972). 'Advanced Inorganic Chemistry.' 3rd edition, Wiley Interscience, New York.

Coughtry, P.J. and Thorne, M.C. (1983). 'Radionuclide Distribution and Transport in Terrestrial and Aquatic Ecosystems.' Vol. 1 'Caesium' p321-424, Balkema, Rotterdam, The Netherlands.

Cremers, A., Elsen, A., De Preter, P. and Maes, A. (1988). 'Quantitative analysis of radiocaesium retention in soils.' Nature, 335, 247-249.

Cremers, A., Elsen, A., Valcke, E., Wauters, J. and Gauders, S.L. (1990). 'The sensitivity of upland soils to radiocaesium contamination.' In 'Transfer of Radionuclides in the Natural and Semi-Natural Environment.' 238-248 Eds. G. Desmet, P. Nassimbeni and M. Belli, Elsevier Applied Science, London.

Dahlman R.C. (1975). 'Radiocaesium cycling in vegetation and soil.' In 'Mineral Cycling in South Eastern Ecosystems' U.S. ERDA CONF-740513, pp462-481 Eds. F.G. Howell, J.B. Gentry and M.H. Smith.

de Bruin, M. and Blaauw, M. (1992). 'Sources of error in analytical gamma-ray spectroscopy.' *Analyst*, 117³, 431-434.

D'Souza, T.J. (1980). 'Effects of clay mineral type and organic matter on the uptake of caesium.' Centre d'Etude Nucleaire, Report BLG. 538.CEEN.M01, Belgium

Dumontet, S., Levesque, M. and Mather, S.P. (1990). 'Limited downward migration of pollutant metals (Cu, Zn, Ni and Pb) in acidic virgin peat soils near a smelter.' *Water, Air and Soil Pollution*, 49, 329-342

El-Daoushy, F. (1988). 'A summary on the lead-210 cycle in nature and related applications in Scandinavia.' *Environment International*, 14, 305-319.

Erten, N.N., Aksoyoglu, S. and Gokturk, H. (1988a). 'Sorption/desorption of caesium on clay and soil fractions from various regions of Turkey.' *Science of the Total Environment*, 69, 269-296.

Erten, N.N., Aksoyoglu, S., Hatipoglu, S. and Gokturk, H. (1988b). 'Sorption of caesium and strontium on montmorillonite and kaolinite.' *Radiochimica Acta*, 44/45, 147-151.

Esteban, B.L. and Choppin, G.R. (1978). 'Interaction of humic and fulvic acids with Eu(III) and Am(III).' *Journal of Inorganic and Nuclear Chemistry*, 40, 655-658.

Evans, L.T. and Russell, E.W. (1959). 'The adsorption of humic and fulvic acids by clays.' *Journal of Soil Science*, 10(1), 119-132.

Evans, L.J. (1989). 'Chemistry of metal retention by soils.' *Environmental Science and Technology*, 23, 1049-1056.

Fahad, A.A., Ali, A.W. and Shihab, R.M. (1989). 'Mobilisation and fractionation of ^{137}Cs in calcareous soils.' *Journal of Radioanalytical and Nuclear Chemistry, Articles*, 130(1), 195-201.

Falck, W.W. (1989). 'Two Modified Versions of the Speciation Code PHREEQE for Modelling Macromolecule-Proton/Cation Interaction.' BGS Technical Report WE/89/57. British Geological Survey, Keyworth.

Filipovic-Vincecovic, N., Brecevic, Lj. and Kralj. D (1989). 'Interactions in clay/electrolyte systems.' Journal of Radioanalytical and Nuclear Chemistry, Articles, 130(1), 155-167.

Friedlander, G., Kennedy, J.W., Macias, E.S. and Miller, J.M. (1981). 'Nuclear and Radiochemistry.' 3rd edition, Wiley Interscience, New York.

Frissel, M.J., Stoutjesdijk, J.F., Koolwijk, A.C. and Koster, H.W. (1987). 'The Cs-137 contamination of soils in the Netherlands and its consequences for the contamination of crop products.' Netherlands Journal of Agricultural Science, 39, 339-346.

Frissel, M.J., Noordijk, H. and van Bergeijk, K.E. (1990). 'The impact of extreme environmental conditions, as occurring in natural ecosystems, on the soil to plant transfer of radionuclides.' In 'Transfer of Radionuclides in the Natural and Semi-Natural Environment.' 39-47 Eds. G. Desmet, P. Nassimbeni and M. Belli, Elsevier Applied Science, London.

Fry, F.A. and Summerling, T.J (1984). 'Measurements of caesium-137 in residents of Seascale and its environs.' NRPB report R172, National Radiological Protection Board, Didcot.

Gale, H.J., Humphreys, D.L.O. and Fisher, E.M.R. (1964). 'Weathering of ^{137}Cs in soils.' *Nature*, 201, 257-261.

Garten, C.R.J. and Paine, D. (1977). 'A multivariate analysis of factors affecting radiocaesium uptake by Sagittaria latifolia in coastal plain environments.' *Journal of Environmental Quality*, 6, 78-82.

Gaudette, H.E., Grim, R.E. and Metzger, C.F. (1966). 'Illite: a model based on the sorption behaviour of cesium.' *The American Mineralogist*, 51, 1649-1656.

Geyh, M.A. and Schleicher, H. (1990). 'Absolute Age Determination - physical and chemical dating methods and their application.' Springer-Verlag, Berlin, London.

Goldberg, E.D. and Koide, M. (1963). 'Rates of sediment accumulation in the Indian Ocean.' in 'Earth Science and Meteoritics.' pp 90, Eds. Geiss, J. and Goldberg, E.D., Amsterdam, Holland.

Grant, R., Brown, C.J. and Birse, E.L. (1962). 'Map sheet 14, Ayr. Soil Survey of Scotland.' The Macaulay Institute for Soil Research. Aberdeen.

Greenland, D.J. (1971). 'Interactions between humic and fulvic acids and clays.' *Soil Science*, 111, 34-41.

Gregor, H.P., Luttinger, L.B. and Loebel, E.M. (1955). 'Metal polyelectrolyte complexes. I. The polyacrylic acid-copper complex.' *Journal of Physical Chemistry* 59, 34-39.

Heal, O.W. and Horrill, A.D. (1983). 'Terrestrial ecosystems: an ecological context for radionuclide research.' In 'Ecological aspects of radionuclide release' - special publications series of the British Ecological Society, Number 3. 31-46 Ed. P.J. Coughtry.

Heinrichs, H. and Mayer, R. (1977). 'Distribution and cycling of major and trace elements in two central European forest eco-systems.' *Journal of Environmental Quality*, 6, 402-407.

Higgo, J.J.W., Cole, T.G. and Rees, L.V.C. (1988). 'Diffusion of radionuclides through deep sea sediments.' *Radiochimica Acta*, 44/45, 231-238.

Horrill, A.D., Kennedy, V.H. and Harwood, T.R. (1990). 'The concentrations of Chernobyl derived radionuclides in species characteristic of natural and semi-natural ecosystems.' In 'Transfer of Radionuclides in the Natural and Semi-Natural Environment.' 27-39 Eds. G. Desmet, P. Nassimbeni and M. Belli, Elsevier Applied Science, London.

Hunt, G.J. and Kershaw, P.J. (1990). 'Remobilisation of artificial radionuclides from the sediment of the Irish Sea.' *Journal of Radiological Protection*, 10, 147-151.

Jahnke, D.J. and Radke, C.J. (1987). 'Electrolyte diffusion in compacted montmorillonite engineered barriers.' In 'Coupled Processes Associated with Nuclear Waste Repositories.' 287-297, Ed. Chin-Fu Tsang, Academic Press, New York.

Jensen, D.J. and Radke, C.J. (1988). 'Caesium and strontium diffusion through sodium montmorillonite at elevated temperature.' *Journal of Soil Science*, 39, 53-64.

Jensen, B.S. and Jensen, H. (1988). 'Complex formation of radionuclides with organic ligands commonly found in groundwater.' *Radiochimica Acta*, 44/45, 45-49.

Jones, D.G., Miller, J.M. and Roberts, P.D. (1984). 'The distribution of ^{137}Cs in surface intertidal sediments from the Solway Firth.' *Marine Pollution Bulletin*, 15, 187-194.

Joseph, A.B., Gustafson, P.F., Russell, I.R., Schuert, E.A., Volchok, H.L and Tamplin, A. (1971).

'Sources of radioactivity and their characteristics.'
In 'Radioactivity in the marine environment.'
National Academy of Science, 6-41 Washington D.C.

Khanna, S.S. and Stevenson, F.J. (1962). 'Metallo-organic complexes in soil: I.' Soil Science, 93, 298-305.

Kinniburgh, D.G. and Jackson, M.L. (1981). 'Adsorption of Inorganics at Solid-Liquid Interfaces.' 91-160, Eds. M.A. Anderson, A.J. Rubin, Ann Arbor Science, Ann Arbor, MI.

Kirchner, G. and Baumgartner, D. (1992). 'Migration rates of radionuclides deposited after the Chernobyl accident in various north German soils.' The Analyst, 117(3), 475-479.

Klobe, W.D. and Gast, R.G. (1967). 'Reactions affecting cation exchange kinetics in vermiculite.' Soil Science Society of America Proceedings, 31, 744-749.

Klobe, W.D. and Gast, R.G. (1970). 'Conditions affecting caesium fixation and sodium entrapment in hydrobiotite and vermiculite.' Soil Science Society of America Proceedings, 34, 746-750.

Krishnamoorthy, C. and Overstreet, R. (1950). 'An experimental evaluation of ion-exchange relationships.' *Soil Science*, 69, 41-53.

Kubiens, W. (1953). 'Soils of Europe.' Murby, London/Madrid.

Linsley, G.S., Crick, M.J., Simmonds, J.R. and Haywood, S.M. (1986). 'Derived emergency reference levels for the introduction of counter measures in the early to intermediate phases of emergencies involving the release of radioactive materials to atmosphere.' NRPB-DL10, National Radiological Protection Board, Didcot.

Livens, F.R. and Loveland, P.J. (1988). 'The influence of soil properties on the environmental mobility of caesium in Cumbria.' *Soil Use and Management*, 4(3), 69-75.

Livens, F.R. and Rimmer, D.L. (1988). 'Physico-chemical controls on artificial radionuclides in soil.' *Soil Use and Management*, 4(3), 63 - 69.

MacKenzie, A.B. and Scott, R.D. (1984). 'Some aspects of coastal marine disposal of low-level liquid radioactive waste.' *The Nuclear Engineer*, 25, 110-122.

MacKenzie, A.B., Scott, R.D. and Williams, T.M. (1987). 'Mechanisms for northwards dispersal of Sellafield waste.' *Nature*, 329, 42-45.

MacNeil, G., Duffy, J.T., Cunningham, J.D., Coulter, B., Diamond, S., McAulay, I.R. and Moran, D. (1992). 'Transfer characteristics of radiocaesium from soils to permanent pasture.' *Analyst*, 117(3), 521-524.

Maes, A., De Brabandere, J. and Cremers, A. (1988). 'A modified Schubert method for the measurement of the stability of europium humic acid complexes in alkaline conditions.' *Radiochimica Acta*, 44/45, 51-57.

Maguire, S., Pulford, I.D., Cook, G.T. and MacKenzie, A.B. (1991). 'The use of infra-red spectroscopy to elucidate the role of functional groups in the bonding of metals to humic acids.' in *Heavy Metals in the Environment*, Edinburgh, 177-180, Ed. J.G Farmer.

Maguire, S., Pulford, I.D., Cook, G.T. and MacKenzie, A.B. (1992). 'Caesium sorption-desorption in clay-humic acid systems.' *Journal of Soil Science*, 43, 689-696.

Mantoura, R.F.C., Dickson, A. and Riley, J.P. (1978). 'The complexation of metals with humic materials in

natural waters.' Estuarine and Coastal Marine Science, 6, 387-408.

McAuley, I.R. and Moran, D. (1992). 'Relationships between deposition of Chernobyl originating caesium and ruthenium radionuclides and rainfall in Ireland.' The Analyst, 117(3), 455-459.

McDonald, P., Cook, G.T., Baxter, M.S. and Thompson, J.T. (1992a). 'The terrestrial distribution of artificial radioactivity in south-west Scotland.' The Science of the Total Environment, 111, 59-82.

McDonald, P., Allan, R.L., MacKenzie, A.B., Cook, G.T. and Pulford, I.D. (1992b). 'Radionuclides in the coastal region of south west Scotland: dispersion, distribution and geochemistry.' Analytical proceedings (In Press).

McKinley, I.G. and Hadderman, J. (1984). 'Radionuclide sorption database for Swiss safety assessment.' NAGRA Technical report 84-40, NAGRA, Baden, Switzerland.

McGee, E.J., Colgan, P.A., Dawson, D.E. and Rafferty, B. (1992). 'Effects of topography on caesium-137 in montane peat soils and vegetation.' Analyst, 117(3), 461-464.

Mitchell, B.D. and Jarvis, R.A. (1956). 'The Soils of the Country Round Kilmarnock'. 'Memoirs of the Soil Survey of Great Britain.' Department of Agriculture for Scotland. HMSO, Edinburgh.

Mytenaere, C. (1983). 'Behaviour and control of radionuclides in the environment: present state of knowledge and future needs'. In 'Ecological aspects of radionuclide release' - special publications series of the British Ecological Society, Number 3. 19-29 Ed. P.J. Coughtry.

Ohnuki, T. and Tanaka, T. (1989). 'Migration of radionuclides controlled by several different migration mechanisms through a sandy soil layer.' Health Physics, 56(1), 47-53.

Ohtsuki, Y. and Takebe, S. (1990). 'Migration behaviour of radionuclides (^{60}Co , ^{85}Sr and ^{137}Cs) in aerated sandy soil layer - differences of migration behaviour and desorption processes for radionuclides.' Journal of Nuclear Science and Technology, 27(8), 750-755.

Oldfield, F., Appleby, P.G. and Batterbee, R.W. (1978). 'Alternative ^{210}Pb dating: results from the New Guinea Highlands and Lough Erne.' Nature, 271, 339-342.

Oldfield, F., Appleby, P.G, Cambray, R.S., Eakins, J.D., Barber, K.E., Batterbee, R.W., Pearson, G.R. and Williams, J.R. (1979). '²¹⁰Pb, ¹³⁷Cs and ²³⁹Pu profiles in ombrotrophic peat.' *Oikos*, 33, 40-45.

Pakarinen, P. and Tolonen, K. (1977). 'Distribution of lead in Sphagnum fuscum profiles in Finland.' *Oikos*, 28, 69-73.

Peirson, D.H., Cambray, R.S., Cawse, P.A., Eakins, J.D. and Pattenden, N.J. (1982). 'Environmental radioactivity in Cumbria.' *Nature*, 300, 27-31.

Pentreath, R.J. (1980), 'Nuclear Power, Man and the Environment.' Wykenham Science Series no.51. London.

Pentreath, R.J., Harvey, B.R., Lovett, M.B. and Ibbett, R.D. (1985). 'Chemical separation of long lived radionuclides discharged into the marine environment.' in Proceedings of the seminar on Speciation of Fission and Activation Products in the Environment, 16-19 April 1985, Oxford.

Piccolo, A. and F.J. Stevenson. (1981). 'Infra-red spectra of Cu^{2+} , Pb_2^+ and Ca^{2+} complexes of soil humic substances.' *Geoderma*, 27, 195-208.

Polyakov, Y.A., Kader, G.M. and Kritskii, V.V. (1973). 'Behaviour of Sr-90 and Cs-137 in soils.' In Radio-ecology, 78-102 Eds. V.M. Klechovskii, C.G. Polikarpov and R.M. Aleksakhin, Wiley New York.

Posner, A.M. (1964). 'Titration curves of humic acid.' International Congress of Soil Science Trans. 8th (Bucharest, Romania) II; 161-174.

Robbins, J.A. and Edgington, D.N. (1975). 'Determination of recent sedimentation rates in Lake Michigan using ^{210}Pb and ^{137}Cs .' Geochimica Cosmochimica Acta, 39, 285-304.

Saar, R.A. and Weber, J.H. (1980). 'Lead(II)- fulvic acid complexes. Conditional stability constants, solubility and indications for lead(II) mobility.' Environmental Science and Technology, 14(7), 877-880.

Santschi, P.H. and Honeyman, B.D. (1989). 'Radionuclides in Aquatic Environments'. Radiation Physical Chemistry, 34(2), 213 - 240.

Sawhney, B.L. (1966). 'Kinetics of cesium sorption by clay minerals.' Soil Science Society of America Proceedings, 30, 565-569.

Schell, W.R., Tobin, M.J. and Massey, C.D. (1989). 'Evaluation of trace metal deposition history and potential element mobility in selected cores from peat and wetland ecosystems.' *The Science of the Total Environment*, 87/88, 19-42.

Schell, W.R. and Tobin, M.J. (1990). 'Deposition and mobility of chemical elements in forest and wetland environments.' In 'Transfer of Radionuclides in the Natural and Semi-Natural Environment.' 118-128 Eds. G. Desmet, P. Nassimbeni and M. Belli, Elsevier Applied Science, London.

Schnitzer, M. and Skinner, S.I.M. (1966). 'Organo-metallic interactions in soils: 7, Stability constants of Pb^{2+} , Ni^{2+} , Mn^{2+} , Co^{2+} , Ca^{2+} and Mg^{2+} - fulvic acid complexes.' *Soil Science*, 103, 247-252.

Schnitzer, M. and Kodama, K. (1967). 'The dissolution of micas by fulvic acid.' *Geoderma*, 15, 381-391.

Schnitzer, M. and Hanson, E.H. (1970). 'Organo-metallic interactions in soils: 8. An evaluation of methods for the determination of stability constants of metal-fulvic acid-complexes.' *Soil Science* 109, 333-340

Schultz, R.K., Overstreet, R. and Barshad, I. (1960). 'On the soil chemistry of ^{137}Cs .' *Soil Science*, 89, 16-27.

Scott, R.D., MacKenzie, A.B., Ben Shaban, Y.A., Hooker, P.J. and Houston, C.M. (1991). 'Uranium transport and retardation at the Needle's Eye Natural Analogue Site, South West Scotland.' *Radiochimica Acta*, 52/53, 357-365.

Smith, B., Higgo, J.J.W., Moody, J.R., Davis, J.R., Williams, G.M. and Warwick, P. (1990). 'Comparative Study of Humic Substances in Groundwaters:1. The Extraction of Humic Material from Drigg Groundwater and a Study of its Ability to Form Complexes with Cobalt and Nickel.' BGS Technical Report WE/90/43. British Geological Survey, Keyworth.

Smith, F.B and Clark, M.J. (1986). 'Radionuclide deposition from the Chernobyl cloud.' *Nature*, 322, 690 - 691.

Sposito, G. and Mattigod, S.V. (1979). 'GEOCHEM: a complete program for the calculation of chemical equilibria in soil solution and other natural water systems.' Kearney Foundation of Soil Science, University of California, Riverside.

Sposito, G. (1989). 'The Chemistry of Soils.' Oxford University Press, New York.

Stevenson, F.J. and Goh, K.M. (1971). 'Infra-red spectra of humic acids and related substances.' *Geochemica et Cosmicha Acta*, 53, 471-483.

Stevenson, F.J. and Ardakani, M.S. (1972). 'Organic matter reactions involving micronutrients in soils.' in *Micronutrients in Agriculture*. 79-114 Soil Science Society of America. Madison, Wisconsin.

Stevenson, F.J. (1976a). 'Binding of metal ions by humic acids.' In *Environmental Geochemistry* 95-106 Ed. J.O Nriagu Ann Arbor Science Publishers Inc., Ann Arbor, Michigan.

Stevenson, F.J. (1976b). 'Stability constants of Cu^{2+} , Pb^{2+} and Cd^{2+} complexes with humic acid.' *Soil Science Society of America Journal*, 40, 665-672.

Stevenson, F.J. (1977). 'Nature of divalent transition metal complexes of humic acids as revealed by a modified potentiometric titration method.' *Soil Science*, 123, 10-17.

Stevenson, F.J. (1982). 'Humus Chemistry: Genesis, Composition, Reactions.' Wiley Interscience, New York.

Stone, C. and Walker, S. (1992). 'Environmental Assessment in the British Planning System'. European Environment, 2(1), 10 - 13.

Sugden, C.L., Farmer, J.G. and MacKenzie, A.B. (1991). 'Lead and $^{206}\text{Pb}/^{207}\text{Pb}$ profiles in ^{210}Pb dated ombrotrophic peat cores from Scotland.' In Proceedings of the 8th International Conference on Heavy Metals in the Environment, p90-93, CEP Consultants, Edinburgh.

Sumner, D. (1987). 'Radiation risks - an evaluation.' The Tarragon Press, Glasgow.

Swan, D.S, Baxter, M.S., McKinley, I.G. and Jack, W. (1982). 'Radiocaesium and ^{210}Pb in Clyde sea loch sediments.' Estuarine Coastal Shelf Science, 15, 515-536.

Takamatsu, T. and Yoshida, T.(1978). 'Determination of constants of metal-humic acid complexes by potentiometric titration and ion selective electrodes.' Soil Science 125, 377-386.

Tamura, T. and Jacobs, D.G. (1960). 'Structural implications in cesium sorption.' *Health Physics*, 2, 391-398.

Tan. K.H. and McCreery, R.A. (1975). 'Humic acid complex formation and intermicellar adsorption by bentonite.' In *Proceedings of the International Clay Minerals Conference, Mexico City*, 629-641.

Theng, B.K.G. (1976). 'Interactions between montmorillonite and fulvic acid.' *Geoderma*, 15, 243-251.

Theng, B.K.G. (1979). 'Formation and properties of clay-polymer complexes.' Elsevier Science Publishing Company, New York.

Thompson, P. (1988). 'The reduction of germanium gamma spectrometer background in a radiochemistry section at AWRE.' *Science of the Total Environment*, 69, 93-105.

Torstenfelt, B., Andersson, K. and Allard, B. (1982). 'Sorptions of strontium and cesium on rocks and minerals.' *Chemical Geology*, 36, 123-137.

Tyler, G. (1981). 'Leaching of metals from the A-horizon of a spruce forest soil.' *Water, Air and Soil Pollution*, 15, 353-369.

U.K Parliament (1990). ' This Common Inheritance - Britain's Environmental Strategy.' London HMSO.

Urban, N.R., Eisenreich, S.J., Grigal, D.F. and Schurr, K.T. (1990). 'Mobility and diagenesis of Pb and ^{210}Pb in peat.' *Geochimica Cosmochimica Acta*, 54, 3329-3346.

van Dijk, H. (1971). 'Cation binding of humic acids.' *Geoderma* 5, 53-67.

Vennart, J. (1983). 'The recommendations of the International Commission on Radiological Protection'. In 'Ecological aspects of radionuclide release' - special publications series of the British Ecological Society, Number 3. 1-12 Ed. P.J. Coughtry.

Wild, A. (1988). 'Russell's Soil Conditions and Plant Growth.' 11th edition. Ed. Alan Wild, Longmans Scientific and Technical.

Xu, H., Ephraim, J., Ledin, A. and Allard, B. (1989). 'Effects of fulvic acid on the adsorption of

cadmium(II) on alumina.' Science of the Total Environment, 81/82, 653-660.

Zoltai, S.C. (1988). 'Distribution of base metals in peat near a smelter at Flin Flon, Manitoba.' Water, Air and Soil Pollution, 37, 217-228.

